Trinity College Dublin
Coláiste na Tríonóide, Baile Átha Cliath
The University of Dublin

Investigating the role of mechanosensitive channel Piezo1 in the CNS.

Thesis submitted to University of Dublin, Trinity College
for the degree of
Doctor of Philosophy

María Velasco-Estévez
2019

Supervisor: Prof. Kumlesh K. Dev
Co-supervisor: Dr. Graham K. Sheridan (University of Brighton)

Drug Development Group
Discipline of Physiology, School of Medicine
Trinity College Dublin, Ireland

Declaration and Statement of Plagiarism

I declare that this thesis has not been submitted as an exercise for a degree at this or any other university and it is entirely my own work.

I agree to deposit this thesis in the University's open access institutional repository or allow the library to do so on my behalf, subject to Irish Copyright Legislation and Trinity College Library conditions of use and acknowledgement.

Signed _____ Date _____

Acknowledgments

First and foremost, I would like to thank my supervisors Prof. Kumlesh Dev and Dr. Graham Sheridan for the opportunity and trust they gave me, and for their invaluable support and advice during all this time. Their patient and work through this time of my PhD have made this experience the most enjoyable one.

I would also like to thank everyone I have worked with in the lab: Chloe Hall, Myrthe Mampay and Helena Isla from University of Brighton; and Dr. Sinéad O'Sullivan, Dr. Steven Fagan, Dr. Justin Yssel, Mr Cedric Misslin, Ms Danae Stefanaki, Mr Luke Davison, Ms Trisha Ang, Dr Kapil Sharma and foremost, Ms Sibylle Béchet. Thank you for your work and help, and for making this group feel like a family to me. A special thank you to Dr. Stuart Cobb and Dr. Kamal Gadalla (University of Glasgow), for hosting me in their lab and helping me in the *in vivo* studies. I would like to thank Dr. Ana Rubio-Araiz (TCD), Dr. Ana Belén López (TCD) and Dr. Irene Llorente (RCSI) for their advices both in and outside the lab, and to Mr John-Mark Fitzpatrick for his invaluable support and friendship; to Ms Christine Monahan for her tireless and invaluable help and work in the department, to Mr Quentin Comerford for all his work in IT and Dr. Gavin McManus for his help with confocal microscopy. I'm also grateful to my funding body, the Irish Research Council, for making this project possible.

Finally, I would like to give a huge thank you to my family and friends, especially to my mum and dad, and to Marta and Jorge, for their endless patience and support through this time of my PhD. None of this would have been possible without you. Thank you.

Table of Contents

List of Tables and Figures

Chapter 1: Introduction

Chapter 2: Materials and Methods

Chapter 3: Piezo1 in mouse astrocytes and its role in neuroinflammation of CNS

Chapter 4: Astrocytic expression of Piezo1 in Alzheimer's disease

Chapter 5: Role of Piezo1 in regulation of myelination

Chapter 6: Discussion

List of Abbreviations

Aβ42	Amyloid-β 1-42 peptide
A.f.u.	Arbitrary fluorescence units
AD	Alzheimer's Disease
AFM	Atomic Force Microscopy
APP	Amyloid Precursor Protein
ATP	Adenosine Triphosphate
AUC	Area under the curve
BSA	Bovine serum albumin
CA	Cornus amonis
Ca^{2+}	Calcium cation
CMM	Conditioned Microglial Media
CMT	Charcot-Marie Tooth
CNS	Central Nervous System
CSF	Cerebrospinal Fluid
DHS	Dehydrated hereditary stomacytosis
DG	Dentate Gyrus
DIV	Day *in vitro*
DMEM	Dulbecco's Modified Eagle's Medium
DMSO	Dimethyl sulfoxide
EAE	Experimental Allergic Encephalomyelitis
ECM	Extracellular Matrix
EM	Electron microscopy
eNOS	endothelial Nitric Oxide synthase
ER	Endoplasmic reticulum
FAD	Familial Alzheimer's Disease
FBS	Fetal Bovine Serum
GALC	Galactosylceramidase
GBM	Glioblastoma Multiforme
GFAP	Glial fibrillary acidic protein
GLD	Generalized lymphatic dysplasia
HBSS	Hanks' buffered salt solution
H_2O_2	Hydrogen peroxide
HRP	Horseradish peroxidase
Iba-1	Ionised calcium binding adapter molecule 1
ICK	Inhibitory cysteine knot
IF	Intermediate Filaments
IFNγ	Interferon gamma
IL	Interleukin
KD	Krabbe's Disease
LPC	Lisophosphatidylcholine
LPS	Lipopolysaccharide
MA	Mouse astrocytes
MBP	Myelin basic protein
MOG	Myelin Oligodendrocyte Glycoprotein
MRE	Magnetic Resonance Elastography
MS	Multiple Sclerosis
MSC	Mechanosensitive cation channel
NaCl	sodium chloride
NFH	Neurofilament H
NFT	Neurofibrillary tangles
NO	Nitric oxide
NSCs	Neural Stem Cells
OCS	Organotypic Slice Culture
OECs	Olfatory Ensheathing Cells
OPC	Oligodendrocyte precursor cell
P1/10	Postnatal day 1/10
P/S	Penicillin/Streptomycin
Pa	Pascal
PBS	Phosphate buffer solution
PFA	Paraformaldehide
PI	phosphoinositide
PLP	Proteolipid protein
PSEN1/2	Presenilin 1/2

PSY	Psychosine
PVDF	Polyvinylidene difluoride
RBC	Red blood cell
RIPA	Radioimmunoprecipitation assay buffer
ROS	Reactive Oxygen Species
RT	Room Temperature
S1P	Sphingosine-1-phosphate
SACs	Stretch-activated cation channels
SC	Schwann Cell
SD	Standard deviation
SDS	Sodium dodecylsulphate
SEM	Standard error of mean
TFF	Trefoil Factor Family
TG	Transgenic
TLR4	Toll-like receptor 4
TNF-α	Tumour Necrosis Factor α
UTI	Urinary Tract Infection
WT	Wild-type
YAP	Yes-associated Protein

Scientific Abstract

All cells in the organism are able to sense changes in the mechanical properties of their environment, translating them into chemical intracellular signals through a process termed mechanotransduction, mostly via mechanoreceptors. **Piezo1** (Fam38A, Mib) is a mechanosensitive channel from the PIEZO family. It is one of the largest protein described so far, consisting of more than 2,500 amino acids and forming a 900kDa each monomer. Piezo1 associates in homotrimers and allows rapidly inactivated currents upon membrane stretch activation. It is largely conserved among species and its expression has been studied in lung, kidney, bladder, skin, endothelium, red blood cells and retinal ganglia cells; but little is known about Piezo1 in the CNS. Studies in the literature have reported that Piezo1 is expressed in the basal membrane of neurons under physiological conditions, but absent in astrocytes. In this study, we show that the expression of Piezo1 in astrocytes can be induced under certain inflammatory stimuli such as LPS, psychosine and amyloid-β42 treatment. Piezo1 is located in the endoplasmic reticulum of astrocytes in such conditions, and its modulation by the activator Yoda-1 or inhibitor GsMTx4 regulates the levels of proinflammatory cytokines, astrocytic migration and Ca^{2+} signalling. Furthermore, we show that Piezo1 is induced in the astrocytes around the amyloid plaques of the Alzheimer's rat model TgF344-AD, in the same subcellular expression to what observed *in vitro*, supporting our previous findings. In addition, previous studies in our group have shown that Piezo1 is expressed on the highly myelinated tracts of the CNS, i.e. corpus callosum, arbor vitae and optic tract, suggesting that Piezo1 may somehow be implicated in the regulation of myelination. Here, we investigated the effects of modulating Piezo1 in the myelin state using both an *ex vivo* model with organotypic slice culture and an *in vivo* model of LPC-induced focal demyelination in mice. We demonstrate that activation of Piezo1 induces demyelination in slices, while inhibition with GsMTx4 leads to the opposite effect. Interestingly, GsMTx4 prevents the LPC-induced demyelination *in vivo* as well as preventing microglia reactivity and astrocytic death. Altogether, our results suggest a novel role of Piezo1 in the CNS, regulating astrocytic reactivity in inflammatory and/or toxic conditions, as well as in regulating the myelin state of the CNS.

Lay Abstract

Cells in the organism can sense the mechanical properties of their environment by certain proteins called mechanoreceptors, making them able to respond to those changes. One of those mechanoreceptors is **Piezo1**. Piezo1 is a large protein expressed by most cells in our body and conserved in all organisms, from protozoa to human. In this project, we show how Piezo1 is expressed by a brain cell called astrocytes, that support neurons, maintain homeostasis of the brain and help in the brain defence. We demonstrate that Piezo1 is only expressed in astrocytes under certain conditions, like inflammation or in Alzheimer's disease, and how it regulates the astrocytic capacity to respond to these insults in the brain. We also investigated the role of Piezo1 in a brain process termed myelination. The neurons in the brain are protected by a sheath called myelin, which allows neurons to communicate between each other fast enough to make our brain work. The cells that wrap the neurons in the brain are called oligodendrocytes. When this myelin is broken, it gives rise to pathologies such as Multiple Sclerosis or Amyotrophic Lateral Sclerosis. How this process is regulated is not fully understood yet, due to its complexity. We hypothesize that myelination might be regulated, in part, by Piezo1. In this study, we prove that blocking or activating Piezo1 can alter the myelination state of the brain. More specifically, we show that the Piezo1 blocker, namely GsMTx4, prevents demyelination caused by toxins which are used in the lab to model demyelinating conditions. Based upon our findings, we suggest the novel role of Piezo1 in regulating cell activation to fight insults and in mediating the process of myelination, which may position Piezo1 as an interesting target for drug development in important pathologies such as Multiple Sclerosis, Krabbe's disease or neuroinflammation.

Hypothesis

Based upon previous studies from our lab, as well as studies in the literature showing an upregulation of Piezo1 in astrocytes associated to amyloid plaques in Alzheimer's disease (Satoh et al., 2006), we hypothesize that Piezo1 is expressed in astrocytes under certain inflammatory and pathological conditions, likely playing a role as modulator of the astrocytic inflammatory response. We also hypothesize that Piezo1 participates in the regulation of the myelination and remyelination processes, probably acting as a mechanotransductor between oligodendrocytes and neurons, as it has been observed that physical properties of the extracellular matrix are critical for the differentiation (Jagielska et al., 2012), proliferation (Jagielska et al., 2017), maturation (Urbanski et al., 2016) and regulation of myelination in oligodendrocytes (S. Lee et al., 2012).

Aims

The specific aims of this research project were to:

- Study the expression of Piezo1 in mouse astrocytes under certain inflammatory stimuli, i.e. LPS, psychosine, TNF-α/IL17a, H_2O_2 and amyloid-β42 treatment **(Chapter 3)**
- Assess the subcellular localization of Piezo1 in astrocytes **(Chapter 3)**
- Investigate the role of Piezo1 as modulator of astrocytic reactivity **(Chapter 3)**
- Study the calcium signalling through Piezo1 in presence or absence of extracellular calcium in primary mouse astrocytes **(Chapter 3)**
- Characterise the amyloid plaque formation, astrocyte reactivity and myelination state of the Alzheimer's rat model TgF344-AD **(Chapter 4)**
- Analyse the expression of Piezo1 in TgF344-AD rats **(Chapter 4)**
- Assess the effects of *E.coli* peripheral infection in TgF344-AD rats **(Chapter 4)**
- Study the effects of modulating Piezo1 on the expression levels of myelin markers using mouse cerebellar slice culture **(Chapter 5)**
- Examine the effects of inhibiting or activating Piezo1 in glial cells in mouse cerebellar slice culture **(Chapter 5)**
- Investigate the protective effects of GsMTx4 in focal demyelination using LPC with stereotaxic surgery in adult mice **(Chapter 5)**
- Assess the reactivity of astrocytes and microglia in adult mice with LPC-induced focal demyelination **(Chapter 5)**

Value of Research

Piezo1 is a novel mechanoreceptor expressed in most cell types, that seems to be involved in vital cellular processes such as migration, apoptosis and cell differentiation amongst others. In this study, we have demonstrated that Piezo1 can be induced in astrocytes under certain pathological conditions such as infection or amyloid plaque deposition, regulating the astrocytic reactivity *in vitro*. These findings suggest that Piezo1 might play a role in the modulation of the astrocytic inflammatory response, which is an interesting target in the treatment of many neurological conditions, as neuroinflammation is a common feature of most neuropathologies. Furthermore, we also proved that modulating Piezo1 with its chemical activator Yoda-1 or its inhibitor GsMTx4, modifies the myelin state in the *ex vivo* organotypic slice cultures, as well as preventing the demyelination induced by the toxin psychosine *ex vivo* and more interestingly, the LPC-induced demyelination *in vivo*. Currently, there is no curative treatment for demyelinating pathologies such as Multiple Sclerosis or Krabbe's disease, as only palliative treatments are available. This is partly due because the myelination and remyelination processes are not fully understood yet. In the present study, we proposed Piezo1 as a regulator of myelination, suggesting it can constitute a potential target for drug development in the treatment of demyelinating conditions.

Outputs

Manuscripts

- **Velasco-Estevez, M**; […] & Sheridan, GK (2019). *Piezo1 regulates calcium oscillations and cytokine release from astrocytes*. Manuscript under peer-review in GLIA.
- **Velasco-Estevez, M***; Mampay, M*, […] & Sheridan, GK (2019). *Changes in fractalkine expression and neuroinflammatory state of glia in Alzheimer's disease*. Manuscript under preparation. *Authors contributed equally.
- **Velasco-Estevez, M**; […] & Sheridan, GK (2019). *Inhibition of Piezo1 attenuates demyelination in the central nervous system*. Manuscript under peer-review in GLIA.
- **Velasco-Estevez, M**; […] & Sheridan, GK (2018). *Infection augments expression of mechanosensing Piezo1 channels in amyloid-plaque reactive astrocytes*. Frontiers in ageing neuroscience. DOI: 10.3389/fnagi.2018.00332
- Misslin, C; **Velasco-Estevez, M**; […] & Dev, KK (2017). *Phospholipase A2 is involved in galactosylsphingosine-induced astrocyte toxicity, neuronal damage and demyelination*. PLoS One 12(11). DOI: 10.1371/journal.pone.0187217
- O'Sullivan, S; **Velasco-Estevez, M** & Dev KK (2017). *Demyelination induced by oxidative stress is regulated by sphingosine-1-phosphate receptors*. GLIA 65(7). DOI:10.1002/glia.23148

Presented posters

Participation in over 15 national and international meetings and symposia in the last 4 years, presenting data as first author in multiple posters including:

- *Amyloid plaque pathology triggers expression of mechanosensing Piezo1 in astrocytes*. FENS 2018 **[Poster; First author]**
- *Mechanosensation: new component for the modulation of neuroinflammation?*. BraYn 2018 **[Poster; First author] [Chair of Neuroinflammation session]**
- *Inhibition of Piezo1 attenuates psychosine-induced demyelination ex vivo*. FIN7 2017 **[Poster; First author]**
- *Astrocytic expression of Piezo1 under LPS and psychosine treatment*. GLIA Meeting 2017 **[Poster; First author]**
- *Expression of the mechanoreceptor Piezo1 in the rodent brain*. FIN6 2016 **[Poster; First author]**
- *Changes in expression of FAM38A in rodent brain with age*. FENS 2016 **[Poster; First author]**
- *Expression of FAM38A in mouse astrocytes in stress and other stimuli*. Physiology Friday 2016. **[Oral presentation]**
- *Sphingosine 1-phosphate Reeptor-1 (S1PR1) distribution in the young and aged rat brain*. BNA 2015. **[Poster; First author]**

Awards and honours

- **Three-minute thesis in Spanish Competition** – First prize (expenses covered for GLIA 2019)
- **BNA travel award 2019** – awarded to attend BNA2019 in Dublin (2019)
- **FENS-IBRO/PERC travel award** (€750) - awarded to attend FENS18 in Berlin (2018)
- **Guarantors of Brain travel award** (£450) – to attend FENS18 in Berlin (2018)
- **HelloBio Travel Award** ($500) – to attend BraYn conference in Genoa, Italy (2018)
- **Abcam immunofluorescence competition** (£1,000) – Third prize (2017)
- **Trinity College Dublin travel award** (€200) – to attend GLIA17 in Edinburgh (2017)
- **Chem-Bio Collaborative research fund** (£3,7000) – in collaboration with Dr. Steward and Dr. Sheridan, University of Brighton (2017)
- **Irish Research Council Image Showcase** (€50) (2017)
- **Multidisciplinary Research Showcase, TCD** (€200) – Best poster (audience award) (2017)
- **TBSI-TCD Image Competition** – First prize (2016)
- **IRC Postgraduate Scholarship** – 3-years PhD scholarship (2015)

Chapter 1:
Introduction

1. Mechanobiology of cell membranes.

Mechanotransduction refers to the process by which mechanical cues or stimuli are converted into chemical signals inside the living cell. Mechanosensation is implicated in multiple physiological processes such as pain and sensation (Kocer, 2015), hearing (Eijkelkamp, Quick, & Wood, 2013; Zanini & Gopfert, 2014), blood pressure (Mohieldin et al., 2016; Tarbell, Simon, & Curry, 2014) and axon guidance (Koser et al., 2016). In order for a protein to be a mechanosensitive component, such protein must be sensitive to changes in a membrane property (curvature, thickness or tension); or by direct interaction with extracellular and cytoskeletal tethers (Hamill & Martinac, 2001). This means that the mechanical stress need to change the equilibrium of the open and close state of a mechanosensing channel (Beedle, Williams, Relat-Goberna, & Garcia-Manyes, 2015). Furthermore, the loss of its gene should abolish the capacity of mechanosensation without affecting the development of the cell (Ranade, Syeda, & Patapoutian, 2015).

There are four possible deformations in the mechanobiology of the membranes: compression, expansion/thinning, bending and shear stress **(Figure 1.1)**.

A. Compression

It has been shown that hydrostatic pressures of $1*10^7$ N/m^2 -corresponding to 100 atm- do not cause any alteration of the lipid density of the membrane bilayers (Srinivasan, Kay, & Nagle, 1974). Based on this, it can be estimated that the compressibility modulus –i.e. resistance to this type of deformation- is between 10^9 and 10^{10} N/m^2, such as most "incompressible" fluids (McIntosh & Simon, 1986). Therefore, it can be said that the cell membrane is volumetrically incompressible and maintains a constant volume of lipids, thus this parameter has no effect on the mechanosensing of the cells.

B. Expansion/thinning

The close association of lipids in the cell membrane is maintain by Van der Waals hydrophobic forces which leads to a low ion and water permeability. As a cell membrane is incompressible, any change in the area has to be accompanied by a change in thickness -the bigger the area, the thinner the bilayer should be. Following a mathematical analysis (Hamill & Martinac, 2001), at near lytic tensions the membrane area may increase up to ~4% while thickness may increase up to 3.6%. Membranes will disrupt above these lytic tensions as a consequence of the entry of water molecules between the separation of the lipid head groups, causing a destabilization of the hydrophobic cohesion structure of the membrane (McIntosh & Simon, 1986).

C. Bending

Resistance to bending is directly related to the coupling between the two monolayers of the cell membrane. The lesser the coupling, the lesser the resistance to bending. Bending is also influenced by spontaneous curvature of the membrane, which largely depends on the lipid composition (Hamill & Martinac, 2001) and the cytoskeleton association (Discher, Mohandas, & Evans, 1994).

D. Shear stress

At ambient temperatures, the membrane flows like a fluid under shear stress (Hamill & Martinac, 2001). Heterogenicity in the lipid composition –such as formation of lipid rafts or different lipid composition depending on the type of membrane- can lead to different responses to shear stress. Furthermore, the cytoskeleton attachment to the membrane can also increase the shear rigidity of the cell (Hamill & Martinac, 2001).

Therefore, changes in expansion, bending and shear stress in the lipid membrane would activate mechanosensing proteins and cause a downstream cascade leading to the corresponding responses or adaptations of the cell to the environment.

1.1. Mechanosensing effectors: mechanosensitive ion channels

From single-cell bacteria to multicellular organisms, cells can sense not only their external mechanical stimuli, but their internal as well –i.e. osmotic pressure and membrane deformation-. The mechanobiology has been a rather unknown field for a long time, due to the difficulties to empirically study mechanosensing effectors. Their low abundance and their association to auxiliary proteins have delayed the identification of these receptors. However, in the recent years, mechanobiology has gained more and more importance, and the mechanosensing proteins –mostly involving mechanosensitive ion channels- have started to be identified and studied.

Mechanotransduction involves three major classes of sensors: mechanosensitive cation (MSC) channels, elements of the cytoskeleton and intracellular matrix, and components of adhesion complexes and extracellular matrix (ECM) (Bavi et al., 2017; Hung et al., 2016). Amongst them, MSC ion channels are the fastest in responding to mechanical stimuli, by transducing the mechanical signal in less than millisecond time scale (Bavi et al., 2017; Cox et al., 2016). In order

to be considered a mechanosensing molecule, the protein of interest has to fulfil four criteria (Arnadottir & Chalfie, 2010; Ernstrom & Chalfie, 2002):

1. The protein must be expressed by the mechanosensory cells
2. The lack of this protein in the cell should abolish the response to the mechanical stimuli without altering other cell functions
3. Alterations in the protein should alter the properties of the mechanical response
4. Heterologous expression of the protein in other cells or in a lipid bilayer should allow them to respond to the mechanical stimuli.

The first evidence of MSC channel emerged from the intracellular ion recordings of vertebrate inner ear hair cells when mechanically stimulated in 1979 (Corey & Hudspeth, 1979). MS channels are pore-forming membrane units that open in response to a mechanical stimulus, allowing an influx of ions inside the cell. In prokaryotes, based on their conductance and sensitivity, we can distinguish three types of MSC channels: MscM (for Mini), MscS (for Small) and MscL (for Large) (Hamill & Martinac, 2001). The higher the conductance, the higher the activation pressure. MscM channels open at low membrane tension of ~1 mN/m (Nourse & Pathak, 2017) and have a conductance of ~200-370 pS, being cation selective (Bavi et al., 2017); MscS channels open at moderate tensions of ~5 mN/m, with conductance of ~1 nS and are weakly anion selective; MscL open at just under lytic tensions of 10-12 mN/m, with conductance of ~3 nS and nonselective. On the other hand, there are four families identified in animals: transient receptor potential (TRP), 2 pore domain K^+ (K_{2P}), the epithelial Na^+ (DEG/ENaC) and Piezo channels (Bavi et al., 2017; Chalfie, 2009; Cox et al., 2016; Martinac, 2004). MS channels are very diverse and there is little to no structural domain identities across families (Bavi et al., 2017). Likewise, they also have different sensitivities (Cox et al., 2016). We can classify the MSC channels in a '*mechanical continuum*' spectrum depending on their sensitivity to open **(Figure 1.2)**.

1.2. Mechanobiology of the brain

Floating in the cerebrospinal fluid, protected by the skull, our brain is perfectly isolated from the outer mechanical cues. Most of the neuroscience research throughout history has been focused mainly on the electrical and biochemical aspects of the brain. However, our brain is a mechanically sensitive organ, which can respond to different mechanical cues to regulate its endogenous activities. For instance, action potentials are accompanied by propagating

membrane deformations (Tasaki, Kusano, & Byrne, 1989), and deformation of the membrane influence synaptic vesicle clustering (B. M. Chen & Grinnell, 1995; Siechen, Yang, Chiba, & Saif, 2009).

Young's modulus (E) –or elastic modulus- describes the tendency of a substance to deform, and it is measured in units of force/area (N/m^2) or Pascals. It is, therefore, a measure for stiffness. The brain is the softest tissue in the organism, with a Young's modulus of 0.1-1 kPa (Barnes, Przybyla, & Weaver, 2017; Leipzig & Shoichet, 2009), although there are some controversies surrounding the specific values of the brain Young's modulus as it seems to vary with model, method of detection and brain region (Chatelin, Constantinesco, & Willinger, 2010). Overall, the stiffness of the human CNS seems to reach the maximum peak at adolescence/young adulthood and then followed by a decline with age (Sack, Streitberger, Krefting, Paul, & Braun, 2011). Due to its soft nature, even the smallest change in the extracellular matrix stiffness or in fluid pressure in the brain would lead to a dramatic increase in the Young's modulus, changing the intrinsic mechanical properties of the brain. The adult brain ECM –which determines the intrinsic stiffness of the tissue- is unique in terms of composition: it is mostly form by glycosaminoglycans (GAGs) such as hyaluronic acid; proteoglycans such as lecticans; and glycoproteins such as tenascin (Zimmermann & Dours-Zimmermann, 2008). This non-fibrillary nature of the brain ECM contributes to the low Young's modulus. The synthesis and deposition of the proteins forming the brain ECM is carried out by all types of brain cells, leading to a participation of the whole brain network to maintain the ECM homeostasis (Barnes et al., 2017). The stiffness of the brain ECM is vital for neuronal and glial cell function and growth, as it may strongly regulate many processes such as axonal growth and direction (Koser et al., 2016), hippocampal neurite length (Koch, Rosoff, Jiang, Geller, & Urbach, 2012), neural stem cell differentiation into neurons or glia (Lourenco et al., 2016; Pathak et al., 2014), branching and maturation of oligodendrocyte precursor cells (OPC) (Jagielska et al., 2017; Urbanski et al., 2016) or microglial activation (Moshayedi et al., 2014) amongst many others, proving how mechanosensitive brain cells are, and how important the mechanical contribution is to regulation of vital cell processes.

1.2.1. Mechanosensitive channels in the brain

MSCs represent a class of ion channels that gate upon mechanical force stimulation translating those mechanical cues into intracellular biochemical signals. They are functionally conserved, from prokaryotic to eukaryotic and play a role in multiple organism processes such as pain, hearing, blood pressure or osmoregulation (Chalfie, 2009; Nilius & Honore, 2012; Ranade et al., 2015). Most of the changes in pressure, tension and mechanical stress in the plasma membrane of cells are sense by mechanically activated ion channels. Eukaryotic MSC channels can be distributed in two categories: Piezo- and TRP channels that causes depolarization, and the K^+-selective channels of the 2P domain family that are hyperpolarizing (Gnanasambandam et al., 2017). The brain expresses a high variety of MSC inside these families **(Figure 1.2)** and mutation or dysfunction of such channels can lead to pathology. For instance, Transient Receptor Potential Vanilloid 4 (TRPV4) –the most studied channel from the TRP family- is highly expressed in the DRG neurons (Gu & Gu, 2014; Venkatachalam & Montell, 2007) and astrocytes (Benfenati et al., 2011; Salman et al., 2017). TRPV4 mutations –R269C, R232C and R269H- are involved in the Charcot-Marie-Tooth disease 2C (CMT2C), which is an autosomal dominant neuropathy characterized by limb, diaphragm and laryngeal muscle weakness (Koutsis et al., 2015; Landoure et al., 2010). From this same family, TRPV1 and TRPV2 are expressed in distinct dorsal root ganglia neurons of different sizes (Venkatachalam & Montell, 2007)

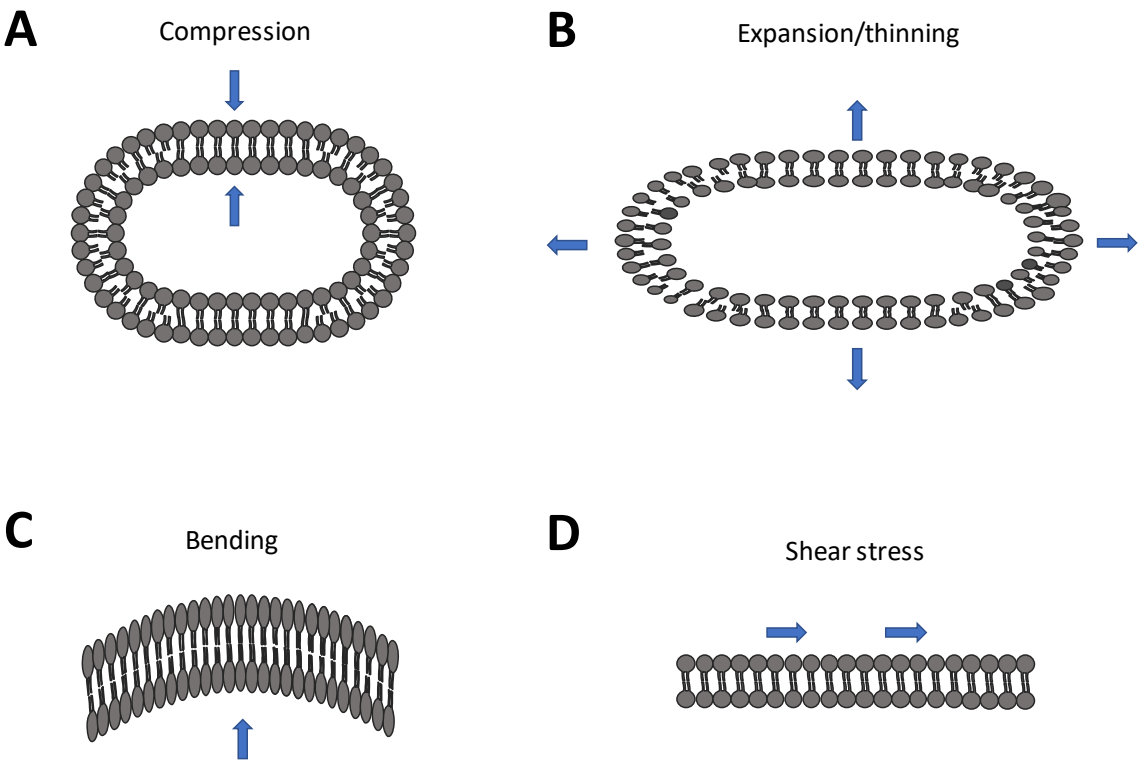

Figure 1. 1: Possible deformation of the cell membranes

There are four possible deformations of a membrane, compression, expansion, bending or shear stress.

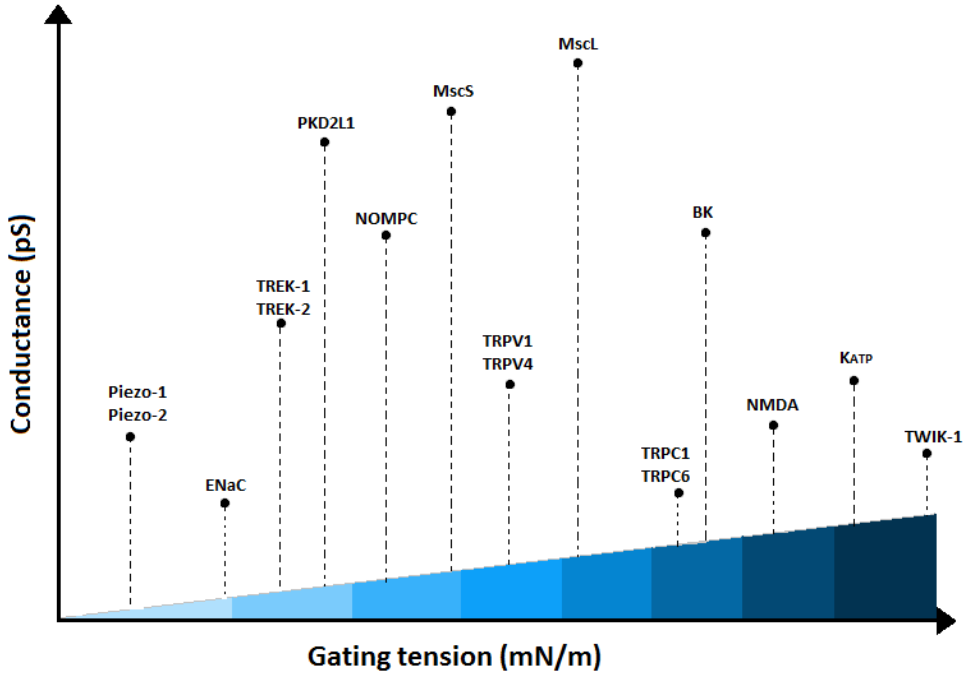

Figure 1. 2: Mechanical sensitivity or 'continuum spectrum' of mechanosensitive ion channels.

2. Piezo1: a novel mechanosensitive ion channel

Piezo1 (Mib, FAM38A) is a mechanosensitive receptor firstly reported in the mouse neuroblastoma cell line Neuro2A in 2010 (Coste et al., 2010). Its activation by mechanical stretch and other forms of mechanical stimulation like shear strain, suction and slow-induced shear stress, lead to an influx of Ca^{2+} in the cell causing rapidly inactivated currents (Gnanasambandam, Bae, Gottlieb, & Sachs, 2015; Gnanasambandam et al., 2017). This mechanoreceptor forms part of the evolutionary conserved PIEZO family, comprising Piezo1 and Piezo2, two essential components of mammalian MSC channels (Coste et al., 2012), which are highly conserved among species, with homologues in invertebrates, plants and protozoa, suggesting their important role in the physiology of the organisms **(Figure 1.3; Figure 1.4)**. Piezo1 is one of the largest mechanoreceptor described so far, with more than 2,500 amino acids and 38 transmembrane domains with each subunit having 12 parallel pairs of 24 peripheral transmembrane helices, forming a level-like structure that allows the cation-selective permeation upon mechanically-induced conformational change of the blades **(Figure 1.5A)** (Coste et al., 2010; Ge et al., 2015; Q. Zhao et al., 2018). Well-designed studies of cryo-electron microscopy of the structure of Piezo1 revealed that it forms a homotrimer of about 900 kDa with the extracellular domains resembling three distal blades and a central cap. These three segments, leading to a lever-like three-bladed, propeller-shaped structure, form a central pore module that encloses the ion-conducting pore and comprises the other helix, a C-terminal extracellular domain, an inner helix and an intracellular C-terminal domain **(Figure 1.5B)** (Ge et al., 2015). Piezo1 is a sophisticated mechanosensitive channel with distinct modules for the ion conduction and mechanical force sensing (residues 2,189-2,547, forming the pore module) and for mechanotransduction (residues 1-2,190, forming the peripheral helices) (Q. Zhao et al., 2016).

Patch clamp studies performed by Papapoutian's group have revealed that activation of Piezo1 leads to a quick response upon the stress activation and a slow inactivation, in a linear 3-state model of closed, opened and inactivated with a pressure dependent rate (Coste et al., 2010; Gottlieb & Sachs, 2012). Interestingly, repeated stimulation of Piezo1 led to an irreversible transition to non-inactivated currents, for reasons yet unclear (Gottlieb & Sachs, 2012). Probably, that inactivation involved interaction of Piezo1 with the cytoskeleton of the cell and the irreversible non-inactivated transition is due to a cytoskeletal breakdown, both inactivating and non-inactivating channels have similar kinetics in patch-clamp recording, suggesting that this difference is not because of channel reorganization and move across the seal (Bae, Sachs,

& Gottlieb, 2011; Suchyna et al., 2004).For instance, deletion of the cytoskeletal element filamin A in smooth-muscle cells did not alter Piezo1 mRNA levels but led to an increase in the amplitude of the currents and an increase in the cytosolic Ca^{2+} levels, without altering the single-channel current amplitude nor the current kinetics, therefore suggesting that absence of Filamin A increases the number of active Piezo1 channels (Retailleau et al., 2015). In an attempt to identify the specific interactions of Piezo1 with other proteins, Papapoutian's group studied its interaction with integrin, as it has been seen that Piezo1 is associated to integrin activation (McHugh et al., 2010). However, disruption of the integrin function did not suppress the MA Piezo1 channels (Coste et al., 2010), therefore suggesting that it is the mechanical activation of Piezo1 that leads to integrin activation, and not the opposite way. Despite the modulation of Piezo1 activity by other cytoskeletal or associated proteins, Piezo1 channels are inherently mechanosensitive and do not require any other cellular component to respond to mechanical forces, as Piezo1 expression in empty droplet bilayers responded to tension forces in the lipid bilayer alone (Syeda et al., 2016). In addition to activation by mechanical pressure, Piezo1 was found to respond to lateral membrane tension with great sensitivity compared to other MA channels (Lewis & Grandl, 2015) with T_{50} = 1.4 ± 0.1 mN/m; compared to average T_{50} of MscL and MscS of 5-10 mN/m (Lewis & Grandl, 2015; Nomura et al., 2012).

How Piezo1 functions and the pathways downstream of its activation are not fully understood yet. However, studies of general MSC channels have shown that channel opening must involve conformational changes, probably produced by stress of the bilayer membrane, and this would allow the influx of ions through the channel (Moe & Blount, 2005; Sukharev & Anishkin, 2004; Wiggins & Phillips, 2004). As any other MSC channel, Piezo1 is a cation channel. Studies about the ionic selectivity show that Piezo1 is permeable for Na^+, K^+, Ca^{2+} and Mg^{2+}, with a slight preference for Ca^{2+} (Coste et al., 2010).

2.1. Pharmacology of Piezo1

2.1.1. GsMTx4 as unspecific blocker of Piezo1

Similar to other MSC channels, previous studies have reported the non-specific blockage of Piezo1 by blockers such as ruthenium red (Q. Zhao et al., 2016), gadolinium (Coste et al., 2010) and streptomycin (Bae et al., 2011). The first specific inhibitor for mechanosensitive channels is the peptide GsMTx4 (Suchyna et al., 2000). GsMTx4 is a small peptide of 4kDa that was isolated from the venom of a tarantula, *Grammostola spatulata* (Bowman, Gottlieb, Suchyna, Murphy,

& Sachs, 2007). The peptide is first synthesized in a proform, with the first 21 amino acids in the C-terminal cleaved by an arginase, leading to the active 34 amino acids peptide **(Figure 1.6A)** (Bowman et al., 2007). Its structure follows the Inhibitory Cysteine Knot (ICK) motif – as many other peptides in spider venoms - and it is amphipathic (Oswald, Suchyna, McFeeters, Gottlieb, & Sachs, 2002). However, unlike the rest of ICK peptides, GsMTx4 is unique because of its high potency as inhibitor of MSC channels and the lack of stereospecificity, which is not a common feature of ICK peptides (Bosmans & Swartz, 2010). There are two main mechanisms of channel inhibition: gating modifiers and pore blocking (Suchyna et al., 2004). When inhibition is caused by pore blockers, the current is reduced but the time course and dose-response relationship are maintained; contrary to this, when inhibition occurs by gating modifiers, the time course is changed, and the dose-response relationship is shift to the right. Studies on the effects of GsMTx4 on stretch-activated ion channels in astrocytes showed that the activation curved was shifted to the right, proving that GsMTx4 inhibits MSC as a gating modifier (Bae et al., 2011; Bowman et al., 2007). GsMTx4 lacks stereochemical specificity and it acts by avidly binding to lipid bilayers at an approximate ratio of 1:300, meaning that the mechanical properties of the bilayer are altered, and therefore, the MSC activation is inhibited. It is a small peptide, of approximately $4nm^2$, but analysis of the expulsion areas suggests that there is a peptide dimerization that increases the buffering capacity: dimers of GsMTx4 can form when the membrane is stable for more than 300ns, where the fist molecule of GsMTx4 is inserted into the bilayer and the second molecule binds to this first one (Nishizawa et al., 2015). Simulation studies with analogues of GsMTx4 with single lysine-to-glutamate substitutions show that GsMTx4 is placed in the surface area of the outer monolayer in unstressed membranes, but when tension is applied to the membrane, GsMTx4 lays deeper in the interface of both monolayers acting as a clamp for tension and thus reducing the pressure effect on the MSC, inhibiting their gating (Gnanasambandam et al., 2017; Nishizawa et al., 2015). This mechanism of action could also explain the dual effect of GsMTx4 on Piezo and TREK channels, as when GsMTx4 lays on the outer monolayer blocking Piezo1, this tension change is transferred to the inner monolayer -as both monolayers are coupled- increasing the tension applied to this side and activating TREK potentiation (Gnanasambandam et al., 2017). This inhibition of MSC by GsMTx4 can be overcome by a stronger mechanical stimulus, which confirms the mechanism of action of GsMTx4 as a gating modifier (Suchyna et al., 2004) instead of pore blocker. GsMTx4 inhibition is specific for some MSC, not affecting rat astrocytes or rabbit heart cells (Bowman et al., 2007) but patch-clamp studies have shown that it does inhibit the activation of the mechanosensitive channel Piezo1 in mouse and human (Bae et al., 2011).

2.1.2. Chemical activators of Piezo1

MSC channels are naturally activated by mechanical cues, thus making difficult the study of the biology of these channels, due to a lack of possible pharmacological modulation. However, in 2015 the first chemical activator of Piezo1 was synthesize as a low molecular weight synthetic compound, named Yoda-1 **(Figure 1.6A)** (Syeda et al., 2015). At micromolar concentrations, Yoda-1 induces Ca^{2+} responses in HEK cells transfected with human or mouse Piezo1, but not in Piezo2 transfected cells, showing specificity for Piezo1. These studies carried out by Syeda and colleagues on the mechanisms of action of Yoda-1 suggest that it affects the sensitivity of the channel and stabilises the open state of Piezo1, reducing the mechanical threshold for activation and slowing down its inactivation kinetics (Syeda et al., 2015). Because of its specific effect on Piezo1 and not on Piezo2, chimeras of Piezo1 with Yoda-1-insensitive units of Piezo2 was designed to study the mechanisms of action of Yoda-1 (Lacroix, Botello-Smith, & Luo, 2018). These experiments by Luo's group shows that Piezo1 possesses three regions for interaction with Yoda-1, being the region 1961-2063 named Agonist Transduction Motif (ATM), one of each subunit of the blade. Interestingly, hybrid channels show sensitivity for Yoda-1 with only one Yoda-1-sensitive subunit, proving that Piezo1 only requires one subunit to interact with Yoda-1 producing similar activated currents than WT Piezo1 (Lacroix et al., 2018). In contrast with the Piezo1 blocker, GsMTx4, Yoda-1 directly interacts with Piezo1 domains, instead of acting through the lipid environment of the channel, as Piezo2 -which shares 50% homology with Piezo1- is insensitive to this activator (Syeda et al., 2015). Moreover, Yoda-1 analogues with small chemical changes are ineffective Piezo1 agonists (Syeda et al., 2015). Interestingly, the Yoda-1 analogue Dooku1 inhibits the effects of Yoda-1 on Piezo1, suggesting that Dooku1 can compete with Yoda-1 for the binding regions of Piezo1 thus inhibiting its agonists effects (Evans et al., 2018).

Very recently, another set of chemical Piezo1 activators were discovered this year, termed Jedi (Y. Wang et al., 2018). These two chemicals (Jedi1/2) were discovered by high-throughput screening of over 3000 compounds in HEK293T cells co-transfected with mPiezo1. Both Jedi 1 and Jedi2 are small molecules, of 202 Da, that share a 3-carboxylic acid methylfuran motif, implicated in the activation of Piezo1 **(Figure 1.6C-D)**. Inside-out patch-clamp recordings show that all Jedi1, Jedi 2 and Yoda-1 have agonistic effects on Piezo1 independently of any intracellular mediators, in accordance with previous studies showing the inherently mechanosensitive capacity of Piezo1 (Lewis & Grandl, 2015; Syeda et al., 2015; Y. Wang et al.,

2018). While Yoda-1 binds to the ATM regions of the blade, exerting its action on Piezo1 both from the inner and the outer side of the membrane (Syeda et al., 2015; Y. Wang et al., 2018), Jedi1/2 interact with only with extracellular loops of the blade, as they had no effect on Piezo1 when applied in the inside of the cell (Y. Wang et al., 2018).

The discovery of chemical structures that can both activate and inhibit MSC such as Piezo1 is of great impact on the field of mechanosensitive channels, specifically in the research of Piezo1, as these eases in great manner the study of these receptors by allowing pharmacological modulation of their activity.

2.2. Putative roles of Piezo1

Expression of Piezo1 has been reported in most tissues across the organism such as the lung (McHugh, Murdoch, Haslett, & Sethi, 2012), bladder (T. Miyamoto et al., 2014), kidney (Peyronnet et al., 2013), skin (Eisenhoffer et al., 2012), endothelium (S. Wang et al., 2016) and RBCs (Albuisson et al., 2013; Cahalan et al., 2015; Cinar et al., 2015; Faucherre, Kissa, Nargeot, Mangoni, & Jopling, 2014) and therefore it has been suggested to play many different roles. However, the specific mechanism of action and the downstream pathways of Piezo1 remain yet unclear. It has been suggested that Piezo1 can somehow activate the sphingosine-1-phosphate (S1P) signalling cascade, as the knockdown of Piezo1 blocks the capacity of extrusion of epithelial cells (Eisenhoffer et al., 2012) and this apical extrusion requires S1P signalling through the $S1PR_2$ (Gudipaty & Rosenblatt, 2016). It has also been observed that, despite the lack of need of any other cell component to open and create a current, Piezo1 can be modulated by cytoskeletal protein such as FlnA (Gottlieb & Sachs, 2012; Retailleau et al., 2015) and phosphoinositide, as both PI(4)P and $PI(4,5)P_2$ are required to maintain Piezo1 currents (Borbiro, Badheka, & Rohacs, 2015). Furthermore, it has been shown that activation of Piezo1 leads to a release of ATP in both urothelial (T. Miyamoto et al., 2014) and endothelial cells, as well as downstream NO formation by association of Piezo1 with eNOS in endothelial cells (S. Wang et al., 2016). Lastly, it has also been observed that Piezo1 interacts with the pump SERCA1-3 in endothelial cells (T. Zhang, Chi, Jiang, Zhao, & Xiao, 2017), although no clear binding partners have been associated to Piezo1 to our knowledge.

The first time a physiological role for Piezo1 was reported, was a knockout of the nociceptive response in *Drosophila melanogaster* larvae, in which the Piezo1-knockout larvae lost their rollover behaviour in response to physical poking (Kim, Coste, Chadha, Cook, & Patapoutian,

2012). It has also been proven the role of Piezo1 in the mitosis and extrusion of cells in skin, sensing both stretch and mechanical crowing, thus affecting two opposing functions depending on its subcellular location and subsequent activation. For instance, in areas of low epithelial cell concentration where epithelial cells are dividing, Piezo1 is expressed in the plasm membrane and cytoplasm; whilst in areas with high density of cells, Piezo1 forms large cytoplasmic aggregates triggering extrusion or apoptosis of cells (Eisenhoffer et al., 2012; Gudipaty & Rosenblatt, 2016). Previous studies have also shown a putative role of Piezo1 in modulating the integrin activation (McHugh et al., 2012), in which when Piezo1 is expressed at the endoplasmic reticulum (ER) of lung cells, its activation allows the influx of Ca^{2+} from the ER to the cytoplasm, activating calpain and initiating the cascade for integrin activation. The knockdown of Piezo1 led to cell detachment and an increment in cell mobility in small lung cancer cells, which might have implications in cell migration and metastasis (McHugh et al., 2012). Furthermore, expression of Piezo1 in the kidney might be associated with the detection of intraluminal pressure changes and urine flow sensing (Peyronnet et al., 2013) and it has been shown that Piezo1 is critical in the regulation of urine dilution and urea concentration on the collective ducts of the kidney (Martins et al., 2016). In the bladder, Piezo1 has been suggested to regulate the bladder extension sensing by the ATP release upon mechanical stretch stimuli, regulating bladder function (T. Miyamoto et al., 2014). Importantly, Piezo1 plays a critical role in the vascular system, as endothelial Piezo1 controls blood pressure through its activation by shear stress and later ATP release (S. Wang et al., 2016). Through a similar mechanism of action, Piezo regulates the release of ATP from human red blood cells (RBCs) therefore modulating the RBCs deformation and the control of the microvascular tone (Cahalan et al., 2015; Cinar et al., 2015). Finally, related to the CNS, it has been suggested that Piezo1 modulates the axon growth in the developing brain, showing that axons sensed the stiffness of the brain through Piezo1 and grew toward the soft areas (Koser et al., 2016).

2.3. Pathologies associated to Piezo1

Both gain-of-function and loss-of-function mutations of Piezo1 have been associated to pathological states (Alper, 2017). The most studied pathology associated to Piezo1 is the dehydrated hereditary stomatocytosis (DHS), also known as hereditary xerocytosis. It is an inherited autosomal dominant condition caused by a gain-of-function mutation in the *Piezo1* gen, in which RBCs show increased cation permeability, leading to RBC osmotic fragility and haemolytic anaemia (Andolfo et al., 2013; Archer et al., 2014). Patients with DHS show mild to

moderate haemolysis, elevated mean corpuscular haemoglobin concentration, decreased osmotic fragility, erythrocyte dehydration, splenomegaly, and perinatal oedema with hydrops (Alper, 2017; Martin-Almedina, Mansour, & Ostergaard, 2018). DHS is considered a rare disease, with a prevalence of 1 in 50,000 (Andolfo, Russo, Gambale, & Iolascon, 2016). Most cases of DHS involve mutations in *Piezo1,* all of them altering its mechanosensing properties and leading to an increase cation transport inside the RBCs, but also mutations in the porpyrin transporter *ABCB6* (Andolfo et al., 2013) and the Ca^{2+}-activated K^+ channel *KCNN4* could cause DHS (Zarychanski et al., 2012). Piezo1 gain-of-function alters the erythrocytes' volume regulation and those red blood cells in DHS have similar characteristics as erythrocyte dehydration (Alper, 2017; Demolombe, Duprat, Honore, & Patel, 2013). Mechanistically, gain-of-function of Piezo1 causes an excessive influx of Ca^{2+} in the erythrocyte, which leads to the efflux of K^+ through KCa3.1 channels and subsequent osmotic efflux of water and dehydration (Cahalan et al., 2015). Similarly, erythrocytes treated with Yoda-1, Piezo1 activator, showed the same phenotype as DHS (Cahalan et al., 2015), proving the specific role of Piezo1 in the regulation of DHS red blood cells volume.

Piezo1 loss-of-function mutations have shown to cause autosomal recessive generalized lymphatic dysplasia (GLD) (Fotiou et al., 2015; Lukacs et al., 2015). This condition is characterised by a widespread lymphoedema affecting all segments of the body and accompanied by hydrops (Fotiou et al., 2015), as well as facial swelling with mild dysmorphic features, and mild changes on their blood film but with no history of haemolytic anaemia (Martin-Almedina et al., 2018). Together with mutations on *CCBE1* and *FAT4*, loss-of-function mutations in *Piezo1* are associated to GLD (Fotiou et al., 2015; Lukacs et al., 2015). Mechanistically, these *Piezo1* mutations lead to a decreased function of Piezo1 with no calcium influx, and thus subsequent fluid retention in the erythrocyte causing hyper-hydration (Cahalan et al., 2015). One interesting feature of both DHS and GLD, is that both pathologies present some similar phenotypic characteristic, mainly perinatal oedema and foetal hydrops, despite having opposite mechanisms underlying (Martin-Almedina et al., 2018).

Only those two pathologies have been reported in the clinic to be associated with human mutation in *Piezo1* gene. However, despite *Piezo1* heterozygous mutations have not seen to be pathogenic in human patients, it may constitute a risk to many other disorders, as Piezo1 has been seen to be implicated in many vital processes such as migration. For instance, downregulation in *Piezo1* in small cell lung cancer, gastric cancer and colorectal cancer cell lines, increase cell migration and invasiveness (McHugh et al., 2012; X. N. Yang et al., 2014); whilst

being upregulated in breast cancer cell line MCF-7 and blocking with GsMTx4 led to a decrease in migration (C. Li et al., 2015). Lastly, despite not being studied in depth, genomic database of gliomas shows a general upregulation of *Piezo1* in glioblastoma multiforme (GBM) (gliovis.bioinfo.cnio.com). Interestingly, Piezo1-deficient mice die midgestation, being a lethal deficiency (Ranade et al., 2015). Only tissue-specific knockouts or knockdowns are viable (Faucherre et al., 2014; Ranade et al., 2014; Shmukler et al., 2015). Altogether, these studies show the polyvalent aspects of Piezo1 and its contribution to multiple cellular processes.

2.4. Piezo1 in the CNS

Despite the broad expression of Piezo1 in organisms and the extensive research of the involvement of Piezo1 in the vascular system, very little is known about Piezo1 in the nervous system. It has been suggested that astrocytes do not express Piezo1 under physiological conditions, but its expression is induced in the ER of senile-plaque associated astrocytes and amyloid-β42 treated astrocytes (Satoh et al., 2006). However, astrocytes of the optic nerve head do express Piezo1 in control conditions (Choi, Sun, & Jakobs, 2015). Piezo1 seems to be mainly distributed along the neuronal axons, and expression on the growth cones of *Xenopus'* retinal ganglion cells has also been reported (Koser et al., 2016). Moreover, expression of Piezo1 mRNA has been measured by *in situ* hybridisation in neurons in the cerebral cortex and substantia nigra of human brain samples (Satoh et al., 2006). Finally, in previous studies in our lab we have characterised the expression of Piezo1 at the protein levels in highly myelinated tracts of the CNS, i.e. corpus callosum, arbour vitae and optic tract (*unpublished data*).

The first report of a putative role of Piezo1 was regulating nociception in *Drosophila melanogaster*, where behavioural responses to noxious mechanical stimuli were reduced in knockout larvae for d*Piezo1* (Kim et al., 2012). Since then, Piezo1 has been attributed different roles depending on the tissue, as already mentioned above. However, the only role of Piezo1 in the brain proposed so far is its role in the axon growth of retinal ganglia cells (Koser et al., 2016). This elegant study shows that Piezo1 modulates the direction of the axon growth directing it to the softer areas of the brain and how inhibition with GxMTx4 blocks the axonal growth (Koser et al., 2016). Additionally, there are other studies reporting the importance of the physical properties of the extracellular matrix of the brain in the nervous cells. For instance, some studies have shown the inability of oligodendrocytes to differentiate and maturate in rigid, lesion-like matrix (Urbanski et al., 2016). OPCs are also highly mechanosensitive, as stiffness of their environment regulate cell survival, proliferation, migration and differentiation capacity

(Jagielska et al., 2017; Jagielska et al., 2012). Additionally, other studies supporting the idea of the importance of mechanotransduction in the brain have shown that oligodendrocytes can myelinate electro-spun nanofibers of a diameter similar to axons in a similar way they would do *in vivo* (S. Lee et al., 2012) and it has also been shown how the different component of the ECM can alter the morphological changes of oligodendrocytes, regulating their capacity to myelinate (Kippert, Fitzner, Helenius, & Simons, 2009). Importantly, it has also been shown that mechanosensation is crucial for neural stem cells (NSC) differentiation, and that Piezo1 activity influences whether NSC differentiate towards a neural -if in soft environment- or astrocytic -if in stiff- lineage (Pathak et al., 2014).

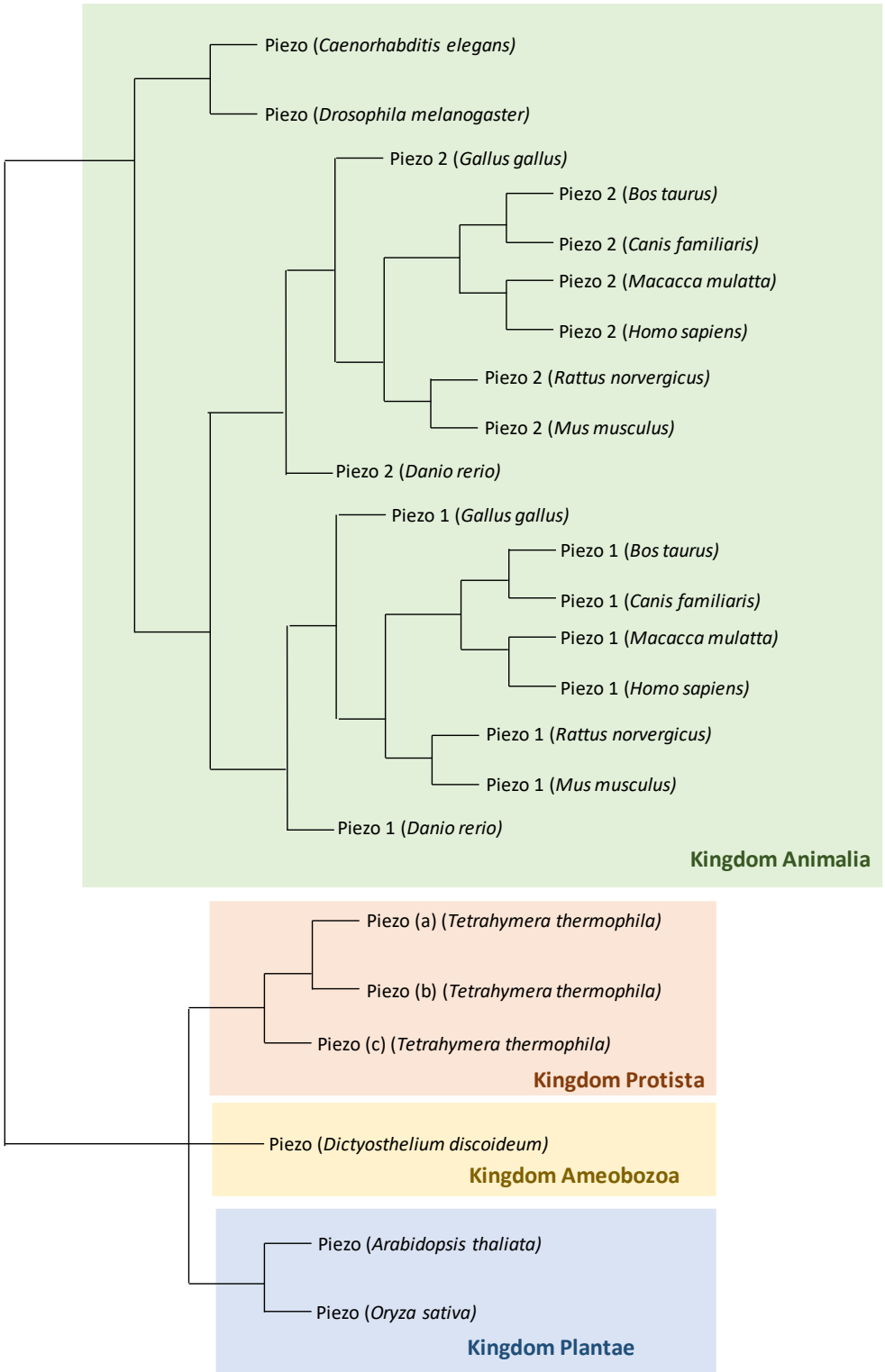

Figure 1. 3: Phylogenetic tree of PIEZO proteins
A single Piezo protein is expressed in lower organisms (Kingdom Protista and Ameobozoa) as well as Plantae and *C.elegans* and *D.melanogaster* from the Kingdom Animalia. Superior organisms from the Kingdom Animalia present two Piezo proteins: Piezo1 and Piezo2, suggesting that these Piezo proteins have acquired additional functions.

<u>Figure 1. 4</u>: CLUSTAL alignment of N-terminal sequence of Piezo1 in human, rat and mouse. Alignment showing the similarities in sequence of the N-terminal of Piezo1 from mouse (*Mus musculus*), rat *(Rattus norvergicus*) and human (*Homo sapiens*). Most changes can be seen in the N-terminal while the rest of the sequence is more conserved.

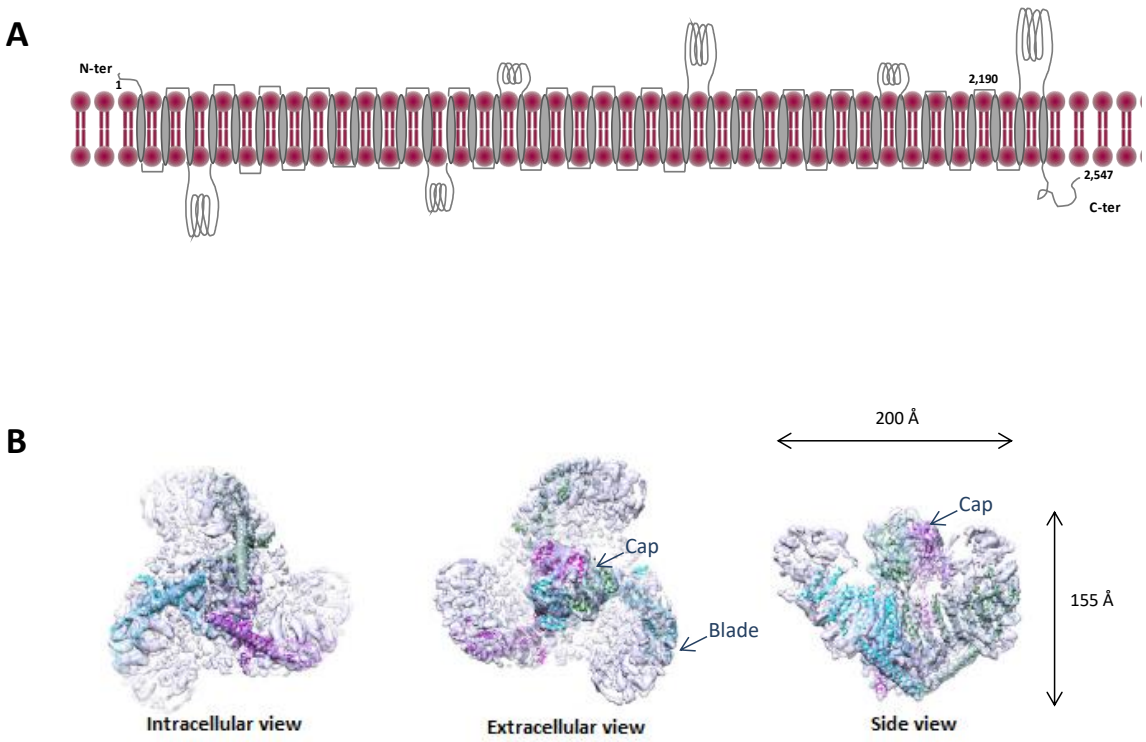

Figure 1. 5: Putative structure of Piezo1

(A) Schematic structure of the 38 transmembrane domains of Piezo1. **(B)** Cryo-electron microscopy image of the 3D structure of Piezo1 (modified from(X. Z. Xu, 2016).

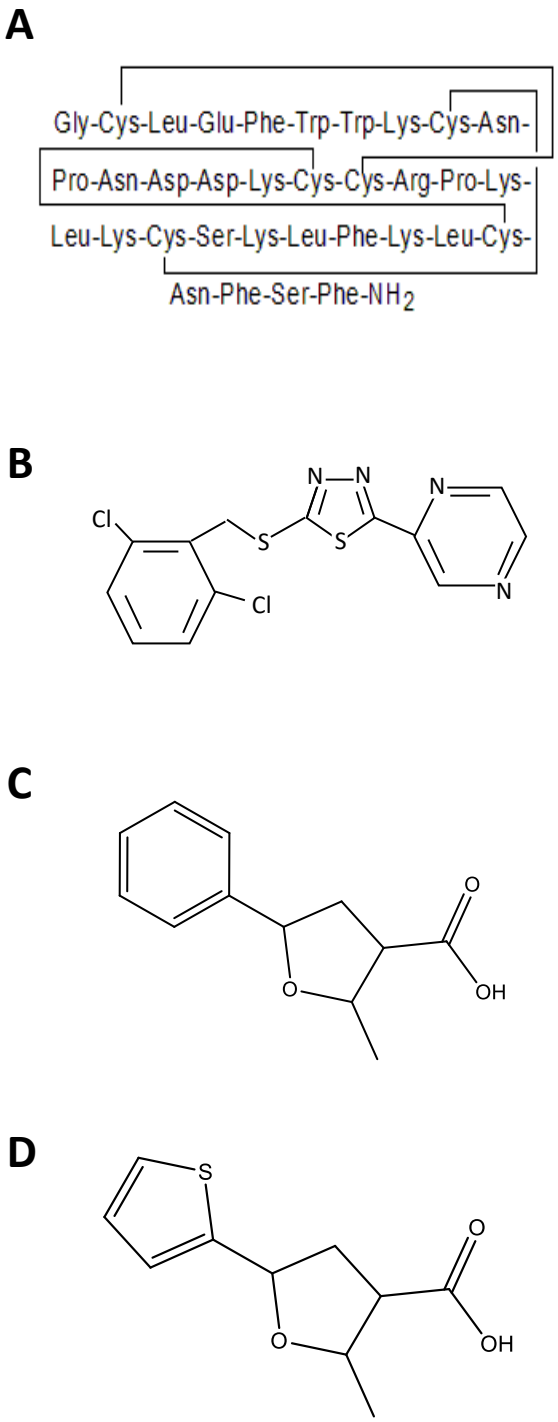

Figure 1. 6: Chemical structure of GsMTx4 and Yoda-1

(A) Chemical structure of the inhibitor of Piezo1, GsMTx4 and **(B)** their synthetic chemical activator, Yoda-1 **(C)** Jedi-1 and **(D)** Jedi-2.

3. Mechanobiology of CNS pathologies

Mechanical properties of the extracellular and intracellular environment are powerful modulators of cell responses. As previously stated, the brain is the softest tissue in the organism, with stiffness ranging from 0.1 to 1 kPa (Barnes et al., 2017; Leipzig & Shoichet, 2009) and therefore the slightest change could have big implications. The mechanobiology of the brain is starting to gain more importance in the field of neuroscience and being taken into account in the different pathological states of the CNS. Not surprisingly, many studies have suggested that changes in the mechanical properties of the brain is not a consequence of a pathology, but that abnormal stiffness actively contributes to disease progression (Schrader et al., 2011). Changes in the brain stiffness and mechanical properties of the matrix have been associated to different neuropathological conditions, including Alzheimer's disease, Multiple Sclerosis, Huntington's disease or Amyloid Lateral Sclerosis (Nagarajan et al., 2014). In this chapter, we will discuss further the mechanobiology underlying two pathologies: Alzheimer's disease and demyelinating conditions.

3.1. Neurodegenerative pathologies: Alzheimer's disease

Alzheimer's disease (AD) is the most common cause of dementia, affecting over 47 million people in the world, expected to increase up to 115 million by 2050 (www.alzheimers.org.uk). Dementia is characterized by a loss or decline in memory and other cognitive abilities. Despite not being the only cause of dementia in the elderly, AD is the most common, and as such it begins with memory loss of recent events (short-term memory impairment) and as dementia progresses, it causes language dysfunction, visuospatial alterations, impairment to execute daily activities, and even depression and personality changes (Holtzman, Morris, & Goate, 2011).

3.1.1. Etiopathology of Alzheimer's disease

The neuropathology of AD was first described by Alois Alzheimer in 1906 (Vishal, Sourabh, & Harkirat, 2011). At macroscopic level, it is characterised by gross atrophy of the brain and loss of neural tissue (Anandh, Sujatha, & Ramakrishnan, 2014; Perl, 2010) whilst at microscopic level the hallmarks are senile amyloid-β (Aβ) plaques, neurofibrillary tangles (NFT) and extensive neuronal loss (Perl, 2010; Selkoe & Schenk, 2003). Despite the extensive research in AD, the etiopathology of the disease is not fully clear. Historically, most researchers focused on the 'amyloid cascade hypothesis', which states that is the deposition of Aβ peptide in the brain, first

forming soluble oligomers and then fibrillary amyloid plaques, which originates and causes AD (Amemori, Jendelova, Ruzicka, Urdzikova, & Sykova, 2015; Lukiw, 2012). Aβ oligomers are formed by a miscleavage of the amyloid precursor protein (APP). APP is a large, transmembrane protein with a role in neural development and neurogenesis (Amemori et al., 2015). To be functional, APP undergoes cleavage by two possible ways: if cleaved by α-secretases, it produces the neuroprotective sAPPα fragment, preventing formation of Aβ; if cleave by β- and γ-secretases, Aβ and AICD are formed (De Strooper, 2010; Pearson & Peers, 2006; Selkoe & Schenk, 2003). Although usually being regarded as a trigger of AD, Aβ peptides hold a physiological function, and only when they are produced in excess and in an aberrant form, they are pathological (Pearson & Peers, 2006). Thus, it has been observed that Aβ regulates the synaptic activity, probably guarding against excessive glutamate release (Kamenetz et al., 2003; Lesne et al., 2005); neurotrophic and neurotropic effects with axonal sprouting *in vitro* (Phinney et al., 1999; Wujek, Dority, Frederickson, & Brunden, 1996); antioxidant effects by inhibiting the auto-oxidation of CSF and plasma lipoproteins (Kontush, 2001) as well as metal oxidation (Garzon-Rodriguez, Yatsimirsky, & Glabe, 1999); or antimicrobial properties (Licastro & Porcellini, 2016).

The second microscopic hallmark of AD is the hyperphosphorylation of Tau proteins, leading to the formation of NFTs (Perl, 2010). Tau is a microtubule-associated protein, required for the cytoskeleton stabilization and neurite outgrowth. Physiological Tau interacts with tubulin, facilitating the assembly of microtubules and stabilizing the cytoskeleton (Lindwall & Cole, 1984). Tau needs to undergo phosphorylation by different kinases in other to interact with tubulin; however, when hyperphosphorylation of Tau happens, it aggregates into helical filaments leading to a subsequent formation of NFTs and dissociating from microtubules, producing cytoskeletal disruption (Garcia & Cleveland, 2001). Both the amount of amyloid plaque burden and the quantity of NFTs correlate with the extent of the disease, but do not properly correlate with the cognitive decline or neuronal loss (Amemori et al., 2015).

Recent research has coined the 'inflammation hypothesis of AD', which supports the idea of chronic inflammation and neuronal ageing as causes for cellular stress and triggers for the onset of AD (Krstic & Knuesel, 2013). Neuroinflammation has proven to have a dual role in the pathology of AD. Inflammation is a protective mechanism of the organism to repair, regenerate or removed the damaged tissue or infective agents from the body (Kulkarni, Lichtnekert, Anders, & Mulay, 2016). However, when this inflammatory response persists, it leads to chronic inflammation and it has been shown to be generally detrimental to the progression of many

pathologies, including AD (W. W. Chen, Zhang, & Huang, 2016). Initial neuroinflammation in AD is beneficial, as it activates the glial responses of astrocytes and microglia and contributes to the clearance of Aβ deposits and neuronal regrowth (Akiyama et al., 1996; C. Liu, Cui, Zhu, Kang, & Guo, 2014). However, a chronic and exacerbated inflammatory response contributes to the progression of AD by producing ROS, priming of microglia, synaptic dysfunction, contributing to NFTs formation and release of pro-inflammatory and apoptotic mediators (Lim, Rodriguez-Ortiz, & Kitazawa, 2015); Liu et al., 2014). There are many clinical studies showing a relationship between infection and clinical AD, where systemic inflammation is associated to an exacerbated progression of AD (Holmes et al., 2009), as well as showing the link between chronic inflammatory conditions -such as obesity, depression or diabetes- and AD (Biessels & Kappelle, 2005; Casserly & Topol, 2004; Johnson et al., 2015). Bacterial and viral infections have also been linked to onset of AD (Bibi et al., 2014). Infections should be considered in AD research, as this pathology mostly affects the elderly, and they are prone to infections such as urinary tract infections (UTI) and other comorbidities (Rowe & Juthani-Mehta, 2013). Moreover, it has been shown than AD patients have more additional medical conditions than non-AD patients (Clodomiro et al., 2013; Duthie, Chew, & Soiza, 2011).

3.1.2. Role of glia in AD

It is well known the importance of the glia in the homeostasis and well-functioning of the brain. Thus, dysfunction of glial cells ultimately results in failure of CNS homeostasis and compromises its general health, leading to different neuropathies. Likewise, most pathologies have a glial contribution, and so happens too in AD.

Microglia are usually regarded as the resident macrophages of the brain (Thomas, 1992), exerting both pro- and anti-inflammatory effects. Microglia plays a role in AD in terms of phagocytosis of amyloid plaques as well as mediating inflammatory responses in AD progression. Activated microglia have been observed in AD brains, characterized by short, thickened and less ramified processes (Amemori et al., 2015). Their clearing capacity of amyloid plaques is important in the early stages of AD, as microglia have been seen to be able to phagocytose Aβ via different receptors, such as scavenger receptors or complement receptors (Doens & Fernandez, 2014); and also able to degrade Aβ by enzymes like neprilysin or metalloproteases (Carson & Turner, 2002; Qiu, Ye, Kholodenko, Seubert, & Selkoe, 1997). Furthermore, the hyperreactive state of microglia in AD and the increased secretion of

proinflammatory factors may contribute to the progression of AD producing a neurotoxic environment for the surrounding neurons (Krstic & Knuesel, 2013).

Astrocytes are the most abundant cell in the nervous system and the key player in CNS homeostasis, performing multiple functions such as biochemical support, homeostasis of blood-brain barrier, maintenance of ion balance, repair of injuries and participation in the synaptic transmission (C. Liu et al., 2014). Reactive astrocytes have also been found around the amyloid plaques in AD brain (Rodriguez-Arellano, Parpura, Zorec, & Verkhratsky, 2016). Despite its less common correlation with inflammatory responses, some studies suggest that astrocytes have a more important and sustained role than microglia in enduring neuroinflammation (C. Li et al., 2011; Savchenko, McKanna, Nikonenko, & Skibo, 2000) as they can also release pro- and anti-inflammatory cytokines, and, unlike microglia, they do not require other mediators to phagocytose or degrade Aβ (Wyss-Coray et al., 2003). Thus, it seems that in an early stage of AD, activation of astrocytes is beneficial to try resolve the plaque deposition and NFT formation; however, as this pathological state is not completely resolve, astrocytes undergo a chronic inflammatory state and contribute to the progression of AD. Reactive astrocytes in AD are also involved in the formation of ROS, contributing to the tauopathy, triggering neuronal apoptosis via death-receptor 5, generating more Aβ and providing a pro-inflammatory environment (Leyns & Holtzman, 2017; C. Li et al., 2011; C. Liu et al., 2014). How glial cells can be modulated as a possible treatment for AD is yet unexplored, but many studies have started to focus on understanding the role of microglia and astrocytes in the development of AD and how they can constitute a new target for clinical treatment.

3.1.3. Risk factors in AD

As most many other neuropathologies, AD is a complex condition with both genetic and environmental factors. The genetic contribution to AD has been greatly investigated. Early onset of AD comprises only 10% of the total cases, but it has a big genetic contribution, referred to as familial AD. Most cases of familial AD are linked to mutations in the *App*, *Psen1* and *Psen2* genes, all of them associated to the miscleavage and formation of Aβ peptides. The remaining 90% of the AD cases are late-onset or sporadic (non-familial) AD. Linked to these cases, there is a gene commonly associated to AD, the *ApoE* (Saunders, 2001). *ApoE* have four alleles, and the allele ε4 (*APOE4)* has been associated to an increased likelihood of developing AD (Selkoe & Schenk, 2003). More than 22 other genes have been associated to some form of AD, however, mutations in these genes only account for a small percentage of the AD cases, and should be regarded as

only a risk factor alongside many others such as the environment, infections, intellectual activity of the individual or life-style (Amemori et al., 2015).

3.1.4. Mechanical properties of the AD brains

The interaction of the Aβ peptide with the cells is very complex and depends on the chemical and physical properties of the environment, including the cell membrane (M. Yang & Teplow, 2008). These changes in the cellular membrane are age-dependent and seem to be important for the Aβ production and neurotoxicity (Abad-Rodriguez et al., 2004). Interestingly, sophisticated studies using atomic force microscope (AFM) to measure the mechanical properties of hippocampal neurons showed that Aβ oligomers induce changes in the elasticity of the neuronal membrane, reducing its stiffness, and being the aged neurons the most susceptible to the binding and subsequent change (Ungureanu et al., 2016). Furthermore, the insertion of Aβ in N2A and HT22 neuronal cell lines also caused changes in cellular stiffness (Lulevich, Zimmer, Hong, Jin, & Liu, 2010). Mechanical properties of the cellular membrane define how a cell can respond to external mechanical cues; therefore, altered membrane composition and physical properties might directly induce functional changes in the cell, regardless of the mechanism of action.

Several studies in Ehman's lab have shown that the overall brain stiffness of AD patients and AD mouse model change with the pathology (Murphy et al., 2012; Murphy et al., 2011; Murphy et al., 2016). By using magnetic resonance elastography (MRE), these studies show a decrease in stiffness in AD patients (Murphy et al., 2012; Murphy et al., 2011; Murphy et al., 2016) and the APP-PS1 mouse model (Murphy et al., 2012; Murphy et al., 2011; Murphy et al., 2016). Moreover, these stiff changes occurred mostly in the frontal, parietal and temporal lobes, in agreement with the topology of AD development. This research proves the component of mechanical changes in the pathophysiology of AD.

3.1.5. Animal models in AD: the TgF344-AD rat model

Most animal models for AD incorporate mutations for *App* or *Psen1/2* **(Table 1.1)**. However, all of them are models of overexpressing Aβ to initiate the pathology, and it has been proven that the animals do not show the full spectrum of AD hallmarks, unless it is combined with other human mutations (Holcomb et al., 1998; Jankowsky et al., 2001). Furthermore, it should be kept in mind that these mutations constitute less than 1% of the human cases for AD and that the mechanisms of action of familial AD (mimicked by mouse models) may differ from sporadic AD (Amemori et al., 2015). For instance, the 5xFAD transgenic (Tg) mouse model co-expresses five

familial AD mutations (*App* swedish, Florida and London mutations, and *Psen1* M146L and L286V). This animal model develops cerebral amyloid plaques and gliosis at 2 months old, and achieve $A\beta_{42}$ burdens, neuron loss and memory impairment in Y-maze (Oakley et al., 2006). Another common AD model is the triple transgenic (3xTg-AD) mouse model of AD, generated with App_{SWE}, *Psen1* M146L and *Tau* P301L mutations. This model shows Aβ deposition in cortex at 6 months old and in hippocampus at 12-months old, but no neuronal loss is observed (Oddo, Caccamo, Kitazawa, Tseng, & LaFerla, 2003; Rohn et al., 2008). Less common is a model of senescence, the senescence accelerated mouse prone 8 (SEMP8), which is a non-genetically modified mouse that express accelerated ageing, and displays the hallmarks of AD such as amyloid plaques, tau phosphorylation and oxidative stress (Alvarez-Garcia et al., 2006; Morley, Farr, Kumar, & Armbrecht, 2012; Takeda, 2009).

Because most animal models overproducing Aβ do not demonstrate robust tauopathy and neuronal loss unless associated with other mutation (Holcomb et al., 1998; Jankowsky et al., 2001) and as the inflammatory cascade hypothesis is not regarded in these models, the need of the generation of a new animal model that presents the full spectrum of age-dependent AD and cognitive impairment seems logical. Thus, the transgenic rat model TgF344-AD was developed (Cohen et al., 2013). TgF344-AD are generated on Fischer 344 rats with the App_{SWE} and *Psen1ΔE9*. These rats develop age-dependent typical hallmarks of AD such as accumulation of cerebral Aβ, hyperphosphorylation of Tau, cognitive impairment, apoptosis or neuronal loss (Cohen et al., 2013), as well as other symptoms of AD pathology like early vascular dysfunction (Joo et al., 2017), anxiety-like behaviour and memory impairment (Pentkowski et al., 2018) (Pentkowski 2017), and ocular dysfunction (Tsai et al., 2014). All these symptoms and hallmarks constitute a broad spectrum of AD symptoms, that is usually lacking in most mouse models for AD, making the TgF344-AD rat model a very suitable animal model for AD research.

Animal model	Species	Gene (Mutation)	Aβ plaques	Tau hyperphosphorylation	NFTs	Neuronal loss	Behavioural impairment	Vascular dysfunction
APP/PS1	Mouse	APP (K670N/M671L); PSEN1 (M146L)	Yes	Little	No	No	Yes	No
APP23	Mouse	APP (K670N/M671L)	Yes	Yes	No	Little	Little	Yes
PDAPP	Mouse	APP (V717F)	Yes	Yes	No	No	Yes	No
5xFAD	Mouse	APP (K670N/M671L, I716V, V717I); SEN1 (M146L/L286V)	Yes	Yes	No	Yes	Yes	No
3xTg	Mouse	APP (K670N/M671L); Tau (P301L); PSEN1 (M146V)	Yes	Yes	Yes	No	Yes	No
SEMP8	Mouse	/	Yes	Yes	No	Yes	Yes	No
TgAPPswe	Rat	APP (K670N/M671L)	Little	No	No	No	Better performance	No
PSAPP Tg	Rat	APP (K670N/M671L, I716V, V717I); SEN1 (M146L)	Yes	Yes	No	Little	Little	Yes
TgF344-AD	Rat	APP (K670N/M671L); PSEN1 (EΔ9)	Yes	Yes	Yes	Yes	Yes	Yes

Table 1. 1: Animal models for Alzheimer's disease

Common rodent animal models used in AD research, showing their mutation and main features.

3.2. Demyelinating conditions in the CNS

Myelin is a cholesterol rich extension of the plasma membrane of oligodendrocytes and Schwann cells, which is wrapped around the axons of neurons of the central and peripheral nervous system, respectively, allowing "saltatory conduction" of the action potential (Alizadeh, Dyck, & Karimi-Abdolrezaee, 2015; S. Lee et al., 2012; Simons & Nave, 2015). Myelination is a characteristic of the more evolved brains. The larger and more evolutionary complex a nervous system gets, the more myelinated it is. For instance, 40% of the human brain comprises of white matter, from which 60-70% of it is myelin (Morell & Norton, 1980). By being myelinated, those axons can greatly reduce their diameter without compromising the speed of signal transmission: a myelinated mammalian axon is only few micrometres (µm) thick, while the giant unmyelinated squid axon is 500 µm, using 5,000 times more energy to transmit at the same speed and constituting a spatial physical problem (Remahl & Hildebrand, 1982). Disruption of the myelin sheath is termed 'demyelination', and it is associated with a number of disorders in the CNS.

3.2.1. Normal molecular organization of myelin in the CNS

Myelin is a modified version of the plasma membrane of oligodendrocytes in the CNS, which allows these cells to enwrapped segments of the CNS axons in a spiral fashion, providing both a physical barrier against toxic agents and insulation of the axons, as well as providing trophic factors (Alizadeh et al., 2015; Irvine & Blakemore, 2008). Structurally, myelin is a packed, multi-layered membrane wrapped around the axons of some neurons. Myelin structure is tightly regulated, where a myelinated axon shows different domains such as the node of Ranvier, paranode, juxtaparanode, and internode (Ohno et al., 2014; Plemel et al., 2014). For the electric impulse to be quick in the myelinated axons, it is "saltatory", meaning that it flows in the node of Ranvier and depolarizes the axonal membrane at each node, resulting in saltatory conduction (Ohno et al., 2011). The node of Ranvier contains a high amount of voltage-dependent Na^+ channels on the axonal membrane, allowing this depolarization (Amor et al., 2014). The paranode is the adjacent segment to the node of Ranvier, where the myelin loops attach to the axonal membrane (Poliak et al., 1999). They are important in maintaining the segregation of Na^+ and K^+ channels in the different areas of the axonal membrane (Gard, Burrell, Pfeiffer, Rudge, & Williams, 1995). The juxtaparanode is the next region, playing a key role in restoring the membrane potential and thus expressing delayed-rectifier Kv^+ channels -such as Kv1.1 and Kv1.2 channels- and Na^+/K^+ ATPase channels for a rapid exchange of intracellular Na^+ for extracellular K^+ (Poliak et al., 2003). This process is energetically demanding but necessary for rapid and

repetitive firing of action potentials. The disruption of the normal nodal structure can lead to demyelinating conditions and result in neuronal death (Alizadeh et al., 2015).

In terms of composition, some specific proteins are highly abundant in myelin: Proteolipid protein (PLP) is the most abundant protein in myelin, followed by Myelin Basic Protein (MBP), Myelin Oligodendrial Glycoprotein (MOG) and 2'-3'-cyclic-nucleotide 3'-phosphodiesterase (CNP) (Boggs, 2006; Domingues et al., 2018; Sypecka & Domanska-Janik, 1995). The important role of these proteins mostly resides their capacity to augment the myelin adhesiveness and stability. For instance, MBP regulates the myelin stability, as it is rich in positively-charged residues, thus binding to the negatively-charged lipids of the axonal membrane by electrostatic interactions (D. W. Lee et al., 2014). Interestingly, while PLP and MBP contribute to myelin compaction, CNP delays it, suggesting an equilibrium between the different myelin proteins, like MBP and CNP, to prevent premature or excessive myelin compaction and dysfunction (Snaidero et al., 2014).

3.2.2. Demyelination and its consequences

The term 'demyelination' is referred to the damage or loss of myelin sheath around the axons, regardless of the nature of its aetiology. In the CNS, it is usually regarded as a consequence of the death of oligodendrocytes, which could happen due to injury, genetic mutations, infectious agents, autoimmune reactions, or any other unknown mechanism.

For example, several genetic disorders such as CMT (Koutsis et al., 2015), Alexander disease (L. Wang et al., 2018) or Krabbe's disease (KD) (Giri et al., 2002) are characterised by axonal demyelination. KD or Globoid Cell Leukodystrophy is an autosomal recessive pathology caused by genetic defects in the lysosomal enzyme galactosylceramidase (GALC) (Suzuki, 2003). This GALC deficiency results in the accumulation of the toxic intermediate metabolite galactosylsphingosine, or psychosine (Giri et al., 2002) causing demyelination and almost complete loss of the OLs in the white matter, alongside glial reactivity and infiltration of multinucleated macrophages called 'globoid cells' (Davenport, Williamson, & Taylor, 2011; Suzuki, 2003).This excess of psychosine leads to its leak from lysosomes, forming aggregates that have cytotoxic effects by various mechanisms such as mitochondrial dysfunction (Haq, Giri, Singh, & Singh, 2003), S1P signalling (C. O'Sullivan & Dev, 2015), PKC, JNK and NFκB signalling (Davenport et al., 2011; Haq et al., 2003) and inflammatory responses (Giri, Khan, Nath, Singh, & Singh, 2008). It has been shown that treatment of *ex vivo* models as organotypic slice culture with psychosine mimics the demyelination and oligodendrocytes death observed in KD (C. O'Sullivan & Dev, 2015). Moreover, the mouse model *twitcher* mouse is an authentic animal

model to study KD, extensively utilised for research in the field of myelination (Davenport et al., 2011).

Another mechanism underlying demyelination is immune-mediated reactions. Multiple Sclerosis (MS) is the classic example of demyelination caused by immune-reactivity in the CNS (Bitsch, Schuchardt, Bunkowski, Kuhlmann, & Bruck, 2000). Symptoms of MS range from weakness in limbs, sensory disturbance, visual loss to ataxia. Cognitive deficits are commons, especially in the latest stages of the diseases, where memory loss, impaired attention or difficulty in changing between cognitive tasks can be appreciated (Hauser & Oksenberg, 2006). MS affects twice more women than men (Harbo, Gold, & Tintore, 2013) and there are four clinical forms of MS: relapsing remitting (RRMS), secondary progressive (SPMS), primary progressive (PPMS) and progressive relapsing (PRMS) (Loma & Heyman, 2011; Sospedra & Martin, 2005). Inflammation of the CNS has always been regarded as the primary cause for MS, but studies have shown a clear contribution of genes, environment and external agents influencing the development of MS (Loma & Heyman, 2011). It is believed that the etiopathology of MS resides in autoreactive T cells that trigger an autoimmune response against the CNS myelin component, causing demyelination (Grigoriadis & Hadjigeorgiou, 2006). This specific recognition of myelin component as antigens is modulated by the adaptive immune response of the immune system. However, the innate immune response also plays a key role in the initiation and progression of MS: the innate response can regulate B and T cell effector function and is the one responsible to present new antigens and prime the naïve T-cells (Platt & Wetzler, 2013). It has been shown that the Toll-Like Receptors (TLR) play a key role in regulating the inflammatory response in MS and that modulation of the TLR can have positive results in animal models of demyelination such as the experimental autoimmune encephalomyelitis (EAE) or MS (O'Brien et al., 2008).

3.2.3. Current disease-modifying treatments (DMTs) for Multiple Sclerosis

Unfortunately, there is no cure for MS. Current treatments focus in speeding the recovery after the attacks, slowing progression of the pathology and managing the symptoms. Most of these therapies focus on immunosuppression and are unable to stop and reverse the progression of the disease.

Treatments for relapsing-remitting MS (RRMS) focus on slowing disease progression as measured by lesion formation and annual relapse rate (Loleit, Biberacher, & Hemmer, 2014) slowing. Amongst these range of treatments, we can find interferon-β1a/b (Jacobs et al., 1996; Z. Liu, Pelfrey, Cotleur, Lee, & Rudick, 2001; Patti et al., 2010) to prevent Th1 cell differentiation

and activity, Fingolimod (Brinkmann et al., 2010; Comi et al., 2010; Matloubian et al., 2004) to prevent lymphocyte egress from thymus, dimethyl fumarate (Schulze-Topphoff et al., 2016) to activate Th2 immunosuppression, and Natalizumab (Polman et al., 2006; Yednock et al., 1992) to prevent lymphocyte migration.

However, because of this need of effective disease-modifying treatments for MS and other demyelinating diseases, in the recent years glial cells have been found to be an interesting and potential target for new drug development in this area. Microglia, astrocytes and oligodendrocytes could constitute a pivotal target in the treatment of MS and demyelinating disorders. For instance, microglia is known to have a key role in remyelination, as clearance of myelin debris is indispensable for the remyelination of lesions (Gudi, Gingele, Skripuletz, & Stangel, 2014); thus, one proposed therapy is to stimulate the activation of microglia for a quick debris clearance around the lesions, as it has been observed with the recombinant antibody rHIgM22 which recruits microglia and enables phagocytosis of myelin debris, promoting remyelination in models of MS (Warrington et al., 2007).

As previously mentioned in Section 3.1.2, astrocytes are the most abundant glial cells and a key player in maintaining the CNS homeostasis. Many studies in the past decades have proven that astrocytes are implicated in the onset, progression and therapeutic of most CNS pathologies. In demyelinating diseases, the reactivity of astrocytes and glial scar formation seem to have an important dual role, as some studies have shown that the lack of reactivity and glial scar formation leads to an increased size and extension of the lesions (Y. Zhao & Rempe, 2010), but it has also been shown in the literature that glial scar can prevent from axonal regeneration and repair (Yuan & He, 2013). A second key function of astrocyte in these pathologies is the regulation of OPC formation and regulation via the production of different growth factors (Kiray, Lindsay, Hosseinzadeh, & Barnett, 2016). Astrocytes can produce platelet-derived growth factor (PDGF), FGF-2 or ciliary neurotrophic factor (CNT) which contribute to differentiation of OPC and protection of mature oligodendrocytes (Bogler, Wren, Barnett, Land, & Noble, 1990). Thus, potential therapies that target astrocytes would focus on regulating astrocyte reactivity, e.g. by targeting S1P signalling such as Fingolimod and Siponimod (Bryan & Del Poeta, 2018; Lublin et al., 2016), via NFkB inhibition such as Laquinimod (Thone & Linker, 2016) or via transcription factor Nrf2 with dimethyl fumarate (Strassburger-Krogias et al., 2014).

3.2.4. Mechanobiology of oligodendrocytes

OLs are the myelinating cells of the CNS and derive from OPCs. OPCs in the adult brain are abundant and widely distributed, constituting a self-renewing population glial cells that allows remyelination in the adult brain in case of injury or damage (Jagielska et al., 2012). Both during the initial myelination during development and during the regenerative process of remyelination, OPC undergo proliferation, migration and differentiation into OLs to ensure the correct myelin formation. Myelination and remyelination are very complex processes that have not been fully uncovered yet. Historically, myelination research has focused on the chemical aspects of this process, studying the biochemical pathways involved and their regulation. However, recent elegant studies have demonstrated the important contribution of the mechanical and physical components to the modulation of myelination. OPCs and oligodendrocytes are sensitive to mechanical changes. One of the first studies showing that oligodendrocytes are mechanosensitive cells was performed in 1995, using different synthetic topographical patterns to study the migration of oligodendrocytes, and showed that these cells underwent parallel alignment to these patterns, proving that they are topographically sensitive (Webb, Clark, Skepper, Compston, & Wood, 1995). More recently, an elegant study using electro-spun polystyrene nanofibers show how oligodendrocytes can myelinate those nanofibers of a similar diameter than the CNS myelinated axons, in a similar way that they would *in vivo* (S. Lee et al., 2012). It has been shown that the axon calibre modulates whether that axon gets myelinated or not (Friede, 1972). Furthermore, it has been demonstrated that oligodendrocytes can myelinate PFA-fixed axons, therefore not needing the axonal signals to start the process (S. S. Rosenberg, Kelland, Tokar, De la Torre, & Chan, 2008). These studies prove that, at least at the initial stages of myelin formation, mechanical cues are indispensable for the wrapping of myelin around the axons. But the mechanical properties of the environment not only regulate the initiation of myelination; it has also been shown that the decision of OPCs to whether continue as precursor cell or differentiate into a myelinating oligodendrocytes also depends on the physical properties of the environment (Lourenco et al., 2016; Urbanski et al., 2016). Thus, it has been proven that OPCs are respondent to changes in the stiffness of the environment and that cell survival, proliferation, migration and differentiation *in vitro* depend on the stiffness of the matrix, as growth of OPCs on gels with different stiffness (Jagielska et al., 2012) or mechanostimulation of the cells (Hernandez et al., 2016) regulated those processes. In this same line of research, several studies have shown that OPCs differentiation is inhibited with stiffness as well as oligodendrocytes branching and maturation, while promoted in soft substrates (Hernandez et al., 2016; Jagielska et al., 2017; Urbanski et al., 2016). This process is

likely due to nuclear and epigenetic changes, where mechanical cues stimulate changes in the nuclear shape, chromatin organization and histone deacetylation, leading to the induction or repression of different genes (Hernandez et al., 2016; Jagielska et al.,2017). It has usually been considered that oligodendrocytes were a homogeneous population in the CNS; however, it has recently been identified an unexpected oligodendrocyte transcriptional heterogenicity, with up to 12 individual populations in juvenile and adult mice samples (Marques et al., 2016), which suggests that mechanical properties of the CNS can alter the transcriptome of the OLs through epigenetic changes, modulating the myelination state of the brain.

Finally, it has been observed that OPCs and oligodendrocytes not only sense mechanical changes, but they also suffer mechanical changes on their membranes. Thus, it has been shown that OPCs stiffen upon differentiation, independently of the substrate *in vitro* (Jagielska et al., 2012), probably due to the rearrangement in their membrane lipid composition as well as their cytoskeleton stabilization. This is in agreement with the observations made on brain stiffness, showing that white matter is stiffer than grey matter (Budday et al., 2015; Weickenmeier et al., 2016), helping explain why immature, incompletely myelinated brain are softer that developed and myelinated brains, as well as more vulnerable to mechanical insults such as the shaken baby syndrome, suggesting that myelin also contributes to the physical protection of the brain, providing structural support as a whole.

4. Concluding remarks

In conclusion, all cells in the organism are sensitive to mechanical stimuli, and changes in the physical properties of the environment or the cells themselves can trigger a myriad of different cellular responses. The brain is the softest organ in the body, and thus, the slightest change on its mechanical properties and stiffness can have big consequences. These changes in the mechanical properties of the external environment are sense by cells mostly via mechanosensitive ion channels, which provide a quick response to mechanical cues translating those physical signals into chemical ones, by a process termed mechanotransduction. The mechanosensitive receptor Piezo1 is a recently described protein involved in many different processes among the different tissues. Its activation produces rapidly-inactivating currents in response to membrane-stretch, allowing an influx of cations, preferably Ca^{2+}, upon activation. Its expression in the CNS seems to be only in neurons under physiological conditions (Kim et al., 2012; Koser et al., 2016; Satoh et al., 2006), whilst also in astrocytes under certain pathological stimuli (Alzheimer's disease, Parkinson's disease) (Satoh et al., 2006). Based on this, we hypothesize that Piezo1 might be upregulated on astrocytes to modulate their reactivity -i.e., cytokine release, migration or Ca^{2+} signalling-. In addition, despite Piezo1 not being reported in oligodendrocytes or OPCs yet, it has been shown that myelinating cells and their precursors are highly sensitive to mechanical cues, and that the process of myelination in influence by the mechanical properties of the ECM. Based upon previous studies and our own results about the expression of Piezo1 in the myelinated tracts of the CNS, we also hypothesize that Piezo1 may be involved in neural processes such as myelination. Further research on both the mechanisms of action and Piezo1 roles in the CNS would be of great importance in the field to understand the process of mechanotransduction in the nervous system.

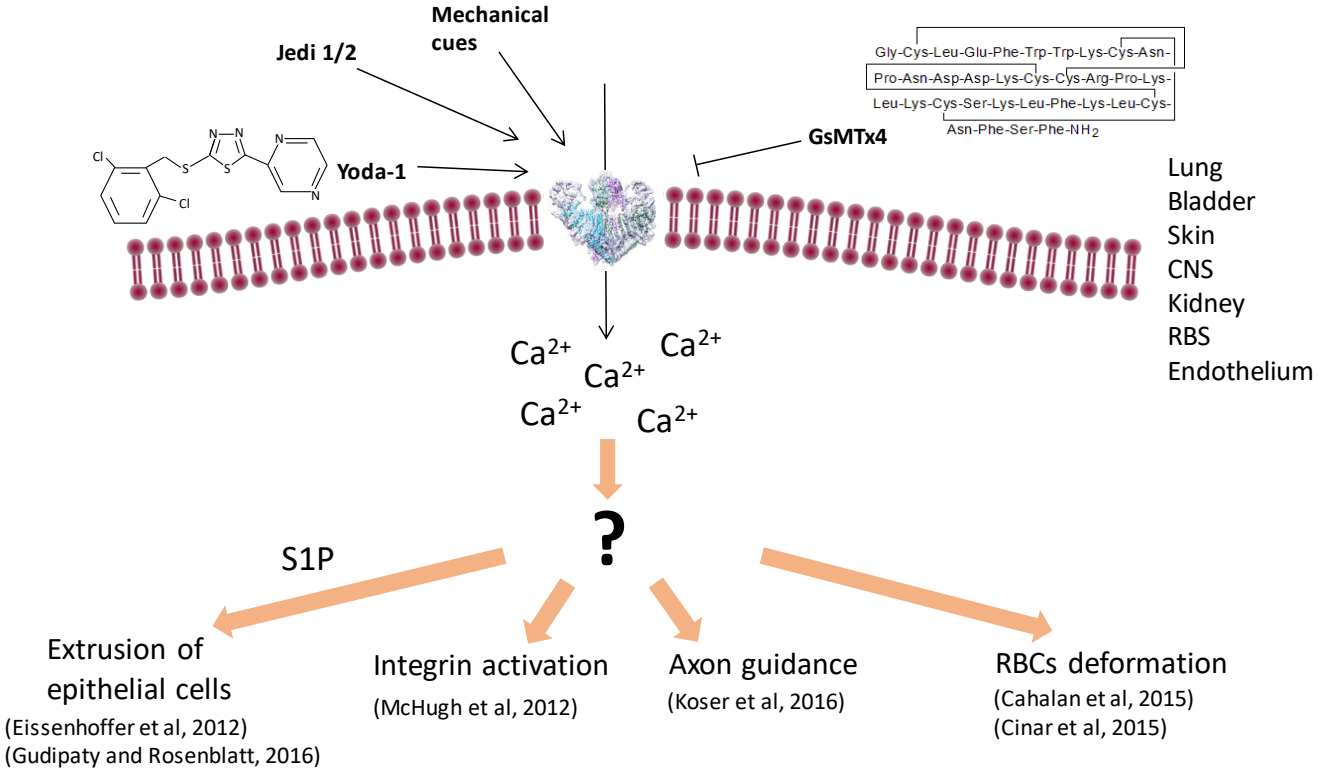

Figure 1. 7: Putative mechanisms of action of Piezo1 in different tissues

Chapter 2:
Materials and methods

1. Materials

1.1. Compounds

All compounds used are summarised in **Table 2.1**. Lysophosphatidylcholine (LPC) was prepared as 10% stock in PBS (Sigma, L4129). Lipopolysaccharide (LPS) was prepared as 1mg/ml stock in H_2O (Sigma, L4391, batch #036M4070V). Psychosine (PSY; Santa Cruz, sc-202781, batch #C2015) was prepared as 10mM stock solution in dimethyl sulfoxide (DMSO; Sigma, D8418). The cytokines IL17a and TNF-α, carrier free dissolved in PBS were purchased from R&D Systems (421-ML/CF and 410-MT/CF, respectively). $A\beta_{1-42}$-conditioned microglial medium (CMM) was obtained by treating primary microglia culture from postnatal day 1 (P1) C57BL/6 mice with 10µM amyloid-β_{1-42} peptide for 24 hours, and kindly provided by Dr. Karen Bryson. Hydrogen peroxidase (H_2O_2; Sigma, 216763) was prepared fresh for every treatment by diluting in serum free media. The activator of Piezo1, Yoda-1 (Tocris, 5586) was prepared as 50mM stock solution diluted in DMSO. The inhibitor of Piezo1, GsMTx4 (Alomone, STG-100) was prepared as 250µM stock solution diluted in dH_2O. Vehicle control using 0.02% DMSO (final concentration of DMSO in 10µM Yoda-1 and 100nM psychosine treatments) was done.

1.2. Antibodies

All antibodies used are summarised in **Table 2.2**. Primary antibodies used were: FAM38A (Abcam, ab128245; RRID: AB_11143245), Piezo-1 (N-15) (Santa Cruz, sc-164319; RRID: AB_10842990), vimentin (Santa Cruz, sc-373717; RRID: AB_10917747), myelin oligodendrocyte glycoprotein (MOG; Millipore, MAB5680; RRID: AB_1587278), neurofilament H (NFH; Millipore, AB5539; RRID: AB_177520), myelin basic protein (MBP; Abcam, ab40390; RRID: AB_1141521), myelin proteolipid protein (PLP; Millipore, MAB388; RRID: AB_177623), glial fibrillary acidic protein (GFAP; Abcam, ab7260; RRID:AB_305808), ionised calcium binding adapter molecule-1 (Iba-1; Wako, 019-19741; RRID: AB_839504), amyloid-β 1-42 (Aβ42; Abcam, ab201061; RRID: AB_2722492), oligodendrocyte marker O4 (O4; R&D systems, MAB1326; RRID: AB_357617) and actin (Abcam, ab3280; RRID: AB_303668). Secondary antibodies used were: HRP-conjugated anti-mouse (Sigma, A8924; RRID: AB_258426), HRP-conjugated anti-rabbit (GE Healthcare, NA934; RRID: AB_772206), HRP-conjugated anti-goat (Sigma, A4174; RRID: AB_258138), Alexa 488 anti-rabbit (Alexa, A11008; RRID: AB_143165), Alexa 488 anti-goat (Sigma, SAB4600032), Alexa 549 anti-mouse (Jackson ImmunoResearch, 115-506-068), Alexa 633 anti-chicken (Alexa, A21103; RRID: AB_2535756), biotinylated anti-rabbit (Thermofisher, A24535; RRID: AB_2536003), Avidin Alexa 488 conjugate (Thermofisher, A21370).

1.3. Stains

CytoPainter ER staining Kit (Abcam, ab139482) was used to stain ER in mouse astrocytes. Nuclear stain Hoechst 34580 (Invitrogen, H21486) to stain nuclei. MTT (3-(4,5-dimethylthiazon-2-yl)-2,5-diphenyltetrazolium bromide) to perform viability assay (Invitrogen, M6494). Cal-520 AM (Abcam, ab171868) was used to perform calcium imaging on primary astrocytes. JC-1 (Abcam, ab113850) was used to perform mitochondrial stress assay.

2. Cell Culture

2.1. Aseptic technique

All *in vitro* procedures were carried out in strictly aseptic techniques. All instruments were sterilised before and after use by autoclaving and sprayed with 70% ethanol before placing them back inside the laminar flow hood (Mason Technologies, Ireland). Cell laboratory coat and gloves sprayed with 70% ethanol were used at all times. The interior of the laminar flow hood with the instruments inside were exposed to germicidal UV lamp, emitting at 253.7nm to ensure sterility after use. Cell culture preparation and treatments were carried out under the laminar flood hood and cells were kept in an incubator, with temperature and CO_2 concentration stable at 37°C (in the case of mouse astrocytes) or 35.5°C (in the case of cerebellar slice culture) and 5% CO_2 concentration.

2.2. Mouse astrocyte cell culture.

Mixed glial cell cultures were prepared from cortical tissue from either male or female one day old wild type C57BL/6 mice provided by BioResources Unit Trinity College Dublin and University of Brighton, following the protocol previously described in (Sheridan & Dev, 2012) and (S. A. O'Sullivan, Velasco-Estevez, & Dev, 2017). All tissue was isolated in accordance with EU regulations and UK Animals (Scientific Procedures) Act 1986 Amendment Regulations (SI 2012/3039); as well as with local ethical approval (Trinity College Dublin and University of Brighton). Animals were sacrificed by decapitation, the skull removed, and cortical tissue detached with forceps and placed in Hanks' buffered salt solution (HBSS; Gibco, 14025-050). The cortical tissue was cross-chopped with a scalpel and gently triturated until a clear solution was obtained. The tube was then centrifuged at 1200 x g for four minutes at room temperature and the cell pellet was resuspended in pre-warmed Dulbecco's Modified Eagle's Medium/F12 (DMEM/F12; Hyclone, SH30023) supplemented with 10% Fetal Bovine Serum (FBS; Labtech, FB-1090) and 1% penicillin/streptomycin (P/S; Sigma, P4333). The solution was passed through a cell strainer (40µm) and then plated into a T75 flask. Cells were cultured at 37°C and 5% CO_2 in

a humidified incubator and grown in the supplemented DMEM/F12 media previously described for 14 days, changing media at Day *in vitro* (DIV) 1 and 8. At DIV 14 astrocytes were ready to be trypsinised with 0.5% trypsin and plated for the experiment. Mouse astrocyte purity was >95%, as previously described (Healy et al., 2013), and was checked by double staining of Iba-1 and GFAP by immunocytochemistry.

2.3. Mouse organotypic slice culture.

Cerebellar slices cultures were prepared from cerebellum isolated from male and female postnatal day 10 (P10) C57BL/6 mice. Mice were sacrificed by decapitation, the skull removed, and the cerebellum separated from the hindbrain. Cerebellum was cut into 400µm parasagittal sections using a McIlwan tissue chopper. Tissue was placed in a petri dish with Opti-MEM (Gibco, 31985) and separated into individual slices under a dissection microscope. Five slices were placed per cell culture insert (Millicell, PICMORG50). Slices were grown for the first four days in media containing 50% Opti-MEM, 25% HBSS, 25% heat inactivated horse serum (Gibco, 26050-088) supplemented with 2mM Glutamax (Gibco, 35050), 28mM D-Glucose (Sigma, G8769), 1% P/S and 10mM HEPES (Gibco, 15630-056), changing the media at DIV 1 and DIV 4. At DIV 7 media was changed to a serum-free media containing 96% Neurobasal-A (Gibco, 10888-022), 2% B-27 supplement (Gibco, 17504-044) supplemented with 1% P/S, 28nM D-glucose, 2mM Glutamax, 10mM HEPES. Media was changed at DIV 10 and treatment was done at DIV 12.

2.4. Migration assay

A 500µm wide strip of silicone (silicone sheet of 0.005'' NRV G/G 12''x12'', SM11074036) was placed down the middle of each well of a 12 well-plate. Primary astrocytes were then seeded in each well and grown in supplemented DMEM/F12 media until 85% confluent. Cells were then serum starved and treated with serum-free media or media with 100ng/ml LPS supplemented with 10µM Yoda-1 or 500nM GsMTx4 for 24h. The silicone strip was then carefully removed and the 500µm "wound area" was imaged over time using a Nikon Eclipse Ti-U microscope with 10X magnification objective and a Nikon digital sight camera connected to the NIS-Elements BR 3.2 software package (Nikon, Japan). The wound area was imaged at time points 0h, 4h, 24h and 48h, and the width was calculated using ImageJ software (http://imagej.nih.gov/ij).

2.5. Calcium imaging

Primary astrocytes were seeded in 25mm tissue culture plastic coverslip (Sarstedt, #83.1840) in a 6 well-plate and grown for 72h in supplemented DMEM/F12 media until 70% confluent. Cells were then serum-starved and treated with 100ng/ml LPS for 24h. After treatment, cells were

incubated with 3µM Cal-520 dye (Abcam, ab171868) in 1X HBSS (no phenol red) supplemented with 10mM glucose and 25mM HEPES for 90min at 37°C plus 30min at room temperature, protected from dark. Coverslips were then placed into an acquisition chamber Attofluor™ cell chamber (Invitrogen) with supplemented 1X HBSS -or 1X HBSS [- Ca^{2+}] [- Mg^{2+}] in case of intracellular calcium measurements-. Cells were stimulated with HBSS or 10µM Yoda-1 (at 30sec) and 50µM ATP (at 270sec) and were imaged on a Leica SP5 as *xyt*, using a 20X objective. Analysis of the recordings was performed using ImageJ software. Briefly, .lif files were exported as .tiff with no LUT. After adjusting threshold in an image with high intensity signal, file was made binary and watershed. Particles bigger than 150 $pixels^2$ were analysed and saved as ROI. The whole image sequence was opened, and all ROI mean intensity vales were analysed at all time-points. To quantify the difference in amplitude of Ca^{2+} transients, the ratio values were normalised according to the formula F/F_0, being F_0 the average of the baseline values. The cells with normalised ratio above 2 at any time point were considered as responders and used for further analysis.

3. *In vivo* techniques

3.1. TgF344-AD rat model

Housing and treatment of the wild-type and TgF344-AD rats were performed in Dr. Hervé Boutin laboratory, at University of Manchester. Initially, two male and female wild-type (WT) Fisher and TgF344-AD (Tg) rats with the APP_{SWE} and *PSEN1ΔE9* mutations were purchase from Prof. Town laboratory (University of Southern California, USA) by Dr. Boutin and set-up as breeding pairs in-house at the Biological Services Unit (BSU) of University of Manchester. Animals were randomly into four groups –i.e. WT and TG non-infected and WT and TG with infection. The number of rats per group were 12m WT (n=5), 18m WT (n=5), 12m TG (n=6), 18m TG (n=6), 12m iWT (n=5), 18m iWT (n=5), 12m iTG (n=6), 18m iTG (n=6). All animals were housed in groups of 2-4 in individually ventilated cages, with 12h dark/light cycles, environmental enrichment and given *ad libitum* access to food and water. All experiments were carried out in accordance with the Animal Scientific Procedures Act 1986 Amendment Regulations (SI 2012/3039), following internal ethical review at the University of Manchester.

3.2. Urinary Tract Infection

A urinary tract infection (UTI) was administered to the iWT and iTG groups at 7-8, 10-11, 13-14, and 16-17 months of age using *Escherichia coli* UTI89. For infections at 7-8 and 10-11 months of age, a concentration of 1.3 x 10^9 colony forming units/mL (cfu/mL) was used, and for infections

at 13-14 and 16-17 months of age, a concentration of 2.6 x 10^9 cfu/mL was used. Therefore, before sacrifice, 12-month rats received two round of infection and 18-month rats received four rounds. Prior to infection, stocks of *E. coli* were stored as 1.02 x 10^{11} cfu/mL in 15% glycerol and were rapidly thawed and brought to the correct concentration using sterile PBS. Rats were anesthetized and infected with 0.1 mL of *E. coli* UTI89 by inserting a catheter (polyethylene tubing covering 30-G hypodermic needles) into the urethra and injecting the inoculum into the bladder. Prior to infection, buprenorphine (0.03 mg/kg) was administered and the animals' bladders were emptied by gently pressing on the abdomen to release any bladder content. Infected animals were placed into clean cages and were monitored for 5 days post-infection to confirm infection levels. Urine was plated on CLED agar plates and incubated at 37°C for 18-24h after which colony forming unit counts were performed and scored according to the following classification system: 0 = Zero colonies; 0.5 = scanty growth (<5 cfu); 2 = scanty growth (<20 cfu); 3 = moderate growth (>20 cfu); 4 = confluent growth. Non-infected rats tested for infection all scored ≤0.5.

3.3. Stereotactic surgery

Ten male C57BL/6J mice (9-10 weeks old, 20-30 g; Envigo, United Kingdom) were randomly divided into three groups: PBS vs LPC (n=2), LPC vs GsMTx4+LPC (n=4) and PBS vs GsMTx4+LPC (n=4). All experiments followed the European Communities Council Directive (86/609/EEC) and UK Animal (Scientific Procedures) Act 1986 Amendmend Regulations (SI 2012/3039); as well as institutional guidelines for the care and use of laboratory animals of University of Glasgow. Animals were injected intraperitoneally with 1.25% Avertin (tribromoethanol, 0.02ml/g body weight) in PBS prior to anaesthesia under inhalation of 3% isoflurane, and eye drops were applied. Mice were maintained under 1.5% - 2% inhaled isoflurane during procedure and placed and stabilized in a small animal stereotactic frame (KOPF®; California, USA). Once stabilized, an incision on the skin over the skull was made, the area was cleaned with saline and 1% lidocaine was applied for 5 minutes. Area of interest is the posterior motor cortex (M2), coordinates: ML = ± 1mm, AP = 1mm, DV = 1.5mm **(Figure 2.1)**. Injections were performed using a Hamilton neurosyringe 1710RN, no needle (Esslab, 7656-01) and a Hamilton needle RN 336-A (Esslab, 65461-01). Once the coordinates are found, skull at this area of interest was drill until thin, and then lifted with forceps. Needle was inserted 1.5mm depth, at a speed of 0.5mm/min. Wound was left to heal for 2 minutes. Injection was made at a speed of 1µl over 6 minutes, with a pause of 5 minutes afterwards. Withdrawal speed of the needle was 0.5mm/min. Skin was sutured with Vicryl® 6-0 taperpoint curve needle (Ethicon, W9981). Animals were placed in recovery cages o/n with administration of painkillers if needed and were then housed individually.

Perfusion was performed at day 4 post-surgery. Animals were put to sleep with pentobarbital and then perfused with 4% PFA. Dissection of the whole brain was done and placed in 4% PFA for 4 hours, 4°C. Brains were then submerged in 30% sucrose for a week. Samples were then embedded in OCT and snap-frozen in liquid nitrogen, following storage at -80°C until cryosectioned.

4. Biochemistry

4.1. DS-PAGE and Western Blot

Mouse astrocyte samples were obtained by scrapping the cells in Radioimmunoprecipitation assay buffer (RIPA) containing 150mM sodium chloride (NaCl; Sigma, A3014), 1% Triton-X (Sigma, T8787), 0.1% sodium dodecylsulfate (SDS; Fisher, S/5200/53) and 50mM Tris pH 8.0 (Fisher, T/3710/60). Samples were sonicated three times for ten seconds at 20% amplitude using a vibracell VCX 130 (Sonics, USA). Samples from cerebellar slice cultures were obtained by dissolving the slice in RIPA buffer and sonicating as stated above. Samples were mixed in 1:1 dilution with Laemmli sample buffer 2X (BioRad, 161-0737) and boiled at 95°C for 5 minutes. Simultaneously, 15% or 6% poly-acrylamide separating gels with 4% stacking gels were prepared: 0.38M Tris, 15% or 6% and 4% acrylamide (Applichem Panreac, A1672) –respectively-, 0.1% SDS, 0.01% ammonium persulfate (APS; Sigma, A3678) and 0.01% N,N,N',N'-Tetramethylethane-1,2-diamine (TEMED; Sigma, A7024). Samples were loaded to have 6µg of total protein per condition. The gels were run in running buffer (25mM Tris, 0.2M Glycine, 0.1% SDS, pH 8.3) at constant voltage 120V in order to separate the proteins by their molecular weight. Wet transfer to a polyvinylidene difluoride membrane (PVDF; Millipore, IPVH00010) was done, prior activation of the PVDF membrane in methanol. 10X transfer buffer contains 25mM Tris, 192mM Glycine and 20% methanol (purchase in Solvent store in TBSI, TCD). Wet transfer was done on ice, at 75mA constant for 75 minutes. Blocking of the membrane was done with 5% bovine serum albumin (BSA; Santa Cruz, sc-2323) in PBS-Tween (0.05%) buffer for an hour at room temperature. Incubation with primary antibodies was done overnight at 4°C. Antibodies used are all described in **Table 2.2**. Membranes were washed with PBS-Tween (0.05%) for ten minutes, three times. Incubation with secondary antibodies was done at room temperature for 1.5 hours. Washes were done as before, and membranes were developed using chemiluminescent HRP substrate (Millipore, WBKLS0500).

4.2. Immunocytochemistry

After each pharmacological treatment, mouse astrocytes were fixed in 10% formalin solution (PFA; Sigma, F1635) for 5 minutes on ice. Cells were blocked over-night at 4°C in blocking solution 1% BSA + 0.1% Triton X-100. Primary antibodies were diluted in blocking solution and incubated over-night at 4°C. Cells were washed with PBS + 0.1% Triton X-100 for five minutes, three times. Incubation with secondary antibodies was done in the dark, at room temperature for an hour. If incubated with biotinylated anti-rabbit antibody, later step of avidin Alexa 488 conjugate is needed. After washes, cells coverslips were mounted on a microscope slide (Clarity, C361) with antifade reagent (ThermoFisher, S36936). For endoplasmic reticulum staining, CytoPainter ER staining kit (Abcam, ab139482) was used, following the manufacturer's instructions. Appropriate negative control was done, by preparing samples in absence of secondary antibody (autofluorescence control) and in absence of primary antibody (unspecific background control). Imaging was done using the Leica SP8 confocal microscope in TBSI, TCD.

4.3. Immunohistochemistry

After treatment of organotypic cerebellar slices (OCS), fixation was done by increasing concentrations of PFA (1%, 2%, 3% and 4%) for 5 minutes each. Blocking and permeabilization was performed over-night at 4°C in blocking solution 10% BSA + 0.5% Triton X-100. Primary antibodies were diluted in 2% BSA + 0.1% Triton X-100, incubating for 48h at 4°C. Slices were washed with PBS + 0.1% Triton X-100 buffer, three times for ten minutes. Incubation with secondary antibodies was done over-night at 4°C. Slices were washed again and mounted on microscope slides using ProLong® Gold antifade reagent.

Mice brain samples stored at -80°C were cryosectioned in a Leica cryostat at 12µm thickness slices. Tissue was placed into SuperFrost™ Plus adhesion slides (Fisher, #10149870) 3 sections per slide and stored at -80°C until stained and imaged. For staining, the slides were let air dry at room temperature for 20 minutes prior antigen retrieval in Tris-EDTA buffer (30 min at 95°C) when necessary. They were then permeabilized in 0.2% Triton-X in PBS for 30 mins, following washes with PBS. Next, they were blocked with 5% BSA/PBS for 3h at room temperature and incubated with the primary antibody in 2% BSA/PBS at 4°C overnight. Slides were washed again five times in PBS and incubated with the secondary antibody diluted in 2% BSA/PBS at 4°C overnight, protected from light. Finally, slides were washed, and coverslip placed with ProLong® Gold antifade reagent.

4.4. Image analysis

Images from OCS were done using a Leica SP8 confocal microscope in TBSI, TCD. Five slices per condition were grown and an average of 25-30 images per condition was captured at 20X magnification. The images were exported as 8-bit.tif files for analysis using the software package FIJI. For fluorescence intensity quantification, 10 regions of interest (ROI) were manually selected from each image and the average fluorescence intensity within each ROI was calculated. Intensity values were normalised to the average of control for each marker. To analyse the expression of SMI-32 in the white matter tracts, the software package Imaris® (http://www.bitplane.com/imaris/imaris) was used. Briefly, the white matter tracts on each image was selected manually and the area of SMI-32 immunoreactivity was measured.

The TgF344-AD rat section samples were imaged using an Axio Scan.Z1 slide scanner (Zeiss,Germany) with a 20X magnification objective (Plan-Apochromat). Individual images were montaged together automatically in ZEN software (Zeiss, Germany) to reconstruct a single image of the whole brain section. For quantitative fluorescence intensity analysis, all images were captured in a single uninterrupted run (~50 hours imaging time) and uniform microscope settings were maintained throughout the session. The images were exported as 8-bit .tif files for Piezo1 fluorescence intensity quantification. Image analysis was conducted using the software package FIJI as before. For morphological analysis of GFAP, BoneJ plug in in ImageJ was used. Briefly, after thresholding and selecting the hippocampal region of interest, the image was made binary and skeletonised 3D in order to analyse the skeletons. The number of skeletons (astrocytes) per area and the average branch length were measured. To analyse the Aβ morphological features, the particle analyser command of ImageJ was used. Briefly, images were threshold and made binary, holes filled, and particles were analysed showing the number of particles per area and the perimeter. Two or three brain sections from 5 or 6 different animals per age group/genotype were analysed (n = 5-6). More specifically, the number of rats per group were as follows: 12m WT (n = 5); 18m WT (n = 5); 12m TG (n = 6); 18m TG (n = 6); 12m iWT (n = 5); 18m iWT (n = 5); 12m iTG (n = 6); 18m iTG (n = 6). Therefore, 100-180 fluorescence intensity ROI measurements were captured depending on the age and genotype of the rat. Piezo1 fluorescence intensities were normalised to the 12m WT value for each region and the percentage (%) change relative to the 12m WT group is represented in each bar graph.

Mouse brain samples were imaged using a Leica SP5 confocal microscope in University of Brighton. Two or three brain sections from 2 or 4 different animals per group were analysed (n=8). For fluorescence analysis, the software package FIJI was used as before. Briefly, 10 ROI were manually selected of each image and fluorescence intensity was averaged. Fluorescence

intensity values are shown in arbitrary fluorescence units. For MBP and NFH co-localization analysis, ImageJ plug-in Coloc2 was used (https://imagej.net/Coloc_2), selecting the arbor vitae as ROI in case of organotypic slice cultures or whole image in case of mouse cortex in the *in vivo* studies. Values for thresholded Mander's tM2 (MBP channel over NFH channel overlap) were compared for statistical analysis amongst groups. For cell count and surface area analysis, software package FIJI was used with the particle analyser tool. Briefly, the images were converted form 8-bit to binary, and particles were analysed displaying the fluorescence intensity, number of particles and area. A value of 20 pixels was set as minimum particle size and an outline of particle was created and used to corroborate the detection of all correct particles with the original image.

4.5. MTT assay

Cells were seeded at a density of 15,000 cells/well in a 96 well plate (Cat No. 10687551, Corning) and grown for 48h to 72h until 70% confluent. They were serum-starved for 3h prior to treatment with LPS (100ng/ml) or PSY (5µM), alone or supplemented with GsMTx4 (500nM) or Yoda-1 (10µM), for 16h, 24h or 48h. After treatments, media was stored for ELISA and replaced with 100µl of fresh media supplemented with 10µl of 12mM MTT (Invitrogen, M6494) for 4h at 37°C. Next, 75µl were removed and 50µl of DMSO were added. Cells were incubated for 10 minutes at 37°C. The plate was then mixed, and the absorbance was read at 540nm.

4.6. Mitochondrial potential assay (JC-1) Assay

Changes in mitochondrial potential were measured using a commercially available JC-1 assay kit (Abcam, ab113850) following manufacturer's instructions. Briefly, cells were seeded in a 96 well-plate and treated as described above for MTT assay. Blank wells with no cells but compound were included. Half an hour prior completion of the treatment, 10µM JC-1 dye was added to the treatment (final working concentration 5µM). Once incubation was completed, wells were washed twice with 1X Dilution buffer. Aggregate emission was measure in a BioTek synergy HT microplate reader (BioTek, VT, USA) setting excitation wavelength at 535±17.5nm and emission at 590±17.5nm.

4.7. Enzyme Linked Immunosorbent Assay (ELISA)

Mouse cytokines IL-6, IL-1β and TNF-α supernatant level were measured using R&D systems ELISA kits. Mouse IL-6 ELISA kit (DY406) with a range of 15.60-1,000 pg/ml; mouse IL-1β/IL-1F2 Duo Set ELISA Kit (DY401) with a range of 15.60-1,000 pg/ml; and mouse TNF-α ELISA kit (DY410) with a range of 31.20-2,000 pg/ml were used according to manufacturer's instructions. Briefly, 96 well plates maxiabsorbant (Sigma, 442404) are coated with the capture antibody diluted in

PBS over-night at 4°C. Plates are washed in PBS + 0.5% Tween-20 and blocked with the appropriate Reagent Diluent (RD) at room temperature for a minimum of 1 hour. Plates are washed, and samples and standards diluted in RD are added. Plates are incubated for 2 hours at room temperature and then washed. Detection antibody diluted in RD is added and plates incubated for 2h at room temperature. Plates are washed and streptavidin-HRP solution added for 20 minutes in the dark. After another wash, substrate solution is added (R&D Systems, DY999) and incubated for 20 minutes. The reaction is stopped by adding 2N H_2SO_4 to the plate and absorbance is immediately read at 450nm with wavelength correction at 570nm.

4.8. Quantitative Reverse-transcription PCR (RT-qPCR)

RNA extraction

In order to quantify mRNA levels of Piezo1 in primary mouse astrocytes, RT-qPCR was performed. RNA extraction was performed using the RNeasy mini Kit (QIAGEN, #74104), following manufacturer's instructions. Briefly, cells were lysed and homogenized in buffer RLT with syringe and 25-gauge needle. One volume of 70% ethanol was added, and mix was transfer to an RNeasy spin column placed in a 2ml collection tube and centrifuged 15s at 8,000x g. Buffer RW1 was added to the column and centrifuged to wash the spin column membrane. Buffer RPE was added next to the column and centrifuged twice. RNeasy spin column was placed in a new collection tube and 30µl of RNase-free water was added to collect the RNA by centrifugation. The quantity and quality of mRNA was measured by spectrophotometric analysis using a nanodrop (ThermoFisher, NanoDrop™ One/One^C microvolume). The concentration of mRNA obtained was quantified by the OD at 260nm. The 260/280 ratios were used as a measure for contamination with protein in the sample; only samples with values between 1.8-2.0 were considered acceptable.

cDNA synthesis

Reverse transcription of the mRNA was performed using the QuantiNova Reverse Transcription Kit (QIAGEN, #205411), following manufacturer's instructions. Briefly, the genomic DNA removal was done by mixing the sample with gDNA removal mix and internal control RNA and incubated for 2 min at 45°C in a ^{3}Prime thermocycler (TECHNE, 3PRIMEG/02, serial no. *32288*). The reverse-transcription master mix was then added to the template RNA obtained and was incubated for 3 min at 25°C followed by 10 min at 45°C and last 5 min at 85°C.

RT qPCR reaction

The PCR master mix was obtained by mixing SYBR green dye (QIAGEN, #1054596), Quantitect® Primer of mouse Piezo1 (Mm_Piezo1_3_SG; QT01199142) or β-actin (Mm_Actb_1_SG; QT00095242) and the cDNA template. Reaction was performed in a Rotor-Gene Q 5plex

(QIAGEN, #90158). A PCR initial activation step of 95°C for 5 min was set up. PCR cycles were comprised of a first step of 95°C for 5 seconds (denaturation step) and a second step of 60°C for 10 seconds (annealing/extension step), acquiring on green and repeated for 40 times. After PCR is completed, melting curve analysis was performed to check the specificity of the reaction.

Analysis

Relative changes of Piezo1 mRNA was performed using β-actin as housekeeping protein. dCT, ddCT and fold-change values were calculated, and statistical analysis was performed on ddCT values using a one value t-test with theoretical mean of 0. Graphs show fold-change of LPS-treated astrocytes compared to control unstimulated astrocytes baseline.

4.9. Peptide synthesis

Peptide synthesis of the blocking peptide for the sc-164319 was performed by solid-phase synthesis. The peptide synthesized was Nter-M-E-P-H-V-L-G-A-V-L-Y-W-L-L-L-P-Cter. In order to prepare the solid-phase, TentaGel S-NH_2 resin (Iris Biotech GmbH, S30902) was pour into an empty syringe and swell with N, N-Dimethylformamide (DMF) for 15 min. DMF was removed and a mix of 0.4mmoles of Fmoc Rink Amide linker (Iris Biotech GmbH, #1450695.0005), 0.4 mmoles of HBTU (Millipore, #8510060100), 140µl of N,N-Diisopropylethylamine (DIPEA; Sigma-Aldrich #387649) and 3ml of DMF; and left reacting for 1h with occasional mixing. Then, resin was washed three times with 5ml DMF and deprotected adding 5ml of 20% piperidine (Sigma, #104094) in DMF to syringe for 2 min, three times. Resin was washed again with DMF. Coupling of the amino acids was performed by adding a mix of 0.4 mmoles of amino acid + 0.4 mmoles HBTU + 140µl DIPEA + 3ml DMF to the resin and leaving it react for 1h. Washing, deprotecting and coupling steps were repeating until all amino acids in the sequence were coupled. When all the sequence was completed, the syringe was washed eight times with dichloromethane (Sigma, #270997), following eight washes with methanol (Fisher Scientific, M/4056/17) and eight washes with diethylether (Fisher Scientific, D/2450/PB17). Resin was allowed to air dry o/n and cleavage of the peptide from the resin was performed the next day. In order to cleave the peptide, cleavage mix consisting of trifluoroacetic acid (TFA; Sigma, T6508-25MC), 1,4-dithiothreitol (DTT; Sigma, #10197777001) and Pierce water LC-MS grade (ThermoFisher, #51140) in a ratio 90:5:5 was added for 4h with occasional mixing. Then, the peptide/resin mixture was pass through a Pasteur pipette containing compacted glass wool and collected in ice-cold diethylether. The tube was centrifuged at 3500 rpm for 5 min, the diethylether decanted and the pellet re-dissolved in fresh diethylether. Washing in diethylether was repeated three more times. Peptide pellet was then allowed to air dry and stored at -20°C until used.

5. Statistical analysis

All statistical analysis was performed using GraphPad Prism 7 (GraphPad®, https://graphpad.com/scientific-software/prism/; RRID: SCR_015807). In order to calculate an estimate of the sample size needed to not underpower the experiments, we used the G*power software (Universitat Dusseldorf, http://www.gpower.hhu.de/; RRID: SCR_013726). Based on preliminary experiments and similar experiments found in the literature, for each set of experiments we set an α value of 0.05, a β value of 0.8 and an effect size ranging from 0.1 to 0.5 depending on the mean and standard deviation of the preliminary data. Assessment of the normality of data was carried out by column statistics with D'Agostino analysis before any further statistical test was performed. To analyse the expression of Piezo1 *in vitro*, repeated measures one-way analysis of variance (ANOVA) tests were performed, as data in every experiment was matched. Holm-Sidak multiple comparisons post-hoc test was run in conjunction with one-way ANOVAs and all groups were compared to control. When only two groups were compared, a paired Student t-test was performed, as several experiments were run with samples always prepared in parallel. In case three or more groups had to be compared and only one independent variable was involved, a repeated measures one-way ANOVA test was performed, because data on every experiment compared was matched and with a Gaussian distribution. Post-hoc test was run after one-way ANOVA in order to take into account the scatter of all groups and as an attempt to make the significance level apply to the entire family of comparisons. Newman-Keuls post-hoc test was done when all groups were compared between each other. This type of post-hoc test might not give confidence intervals, but it was performed after one-way ANOVA rather than the commonly run Tukey's post-hoc test as Newman-Keuls test has more power than the former one. When two independent variables were presented, two-way ANOVA test was performed, following Bonferroni's post-hoc test. When three independent variables were presented, a nested two-way ANOVA or a three-way ANOVA, following Bonferroni's post-hoc was performed. P values < 0.05 were considered statistically significant for *in vitro* and *ex vivo* experiments. To analyse the linear correlation between two different parameters, Pearson r values were calculated using the raw fluorescence intensity values. Changes in expression in *in vivo* experiments were considered significant when they passed two criteria, i.e. the relative percentage (%) change was >20% and the P value < 0.01. Data is presented as mean ± Standard Error of Mean (SEM). Further details of the statistical analysis performed are given in each figure legend and the results section.

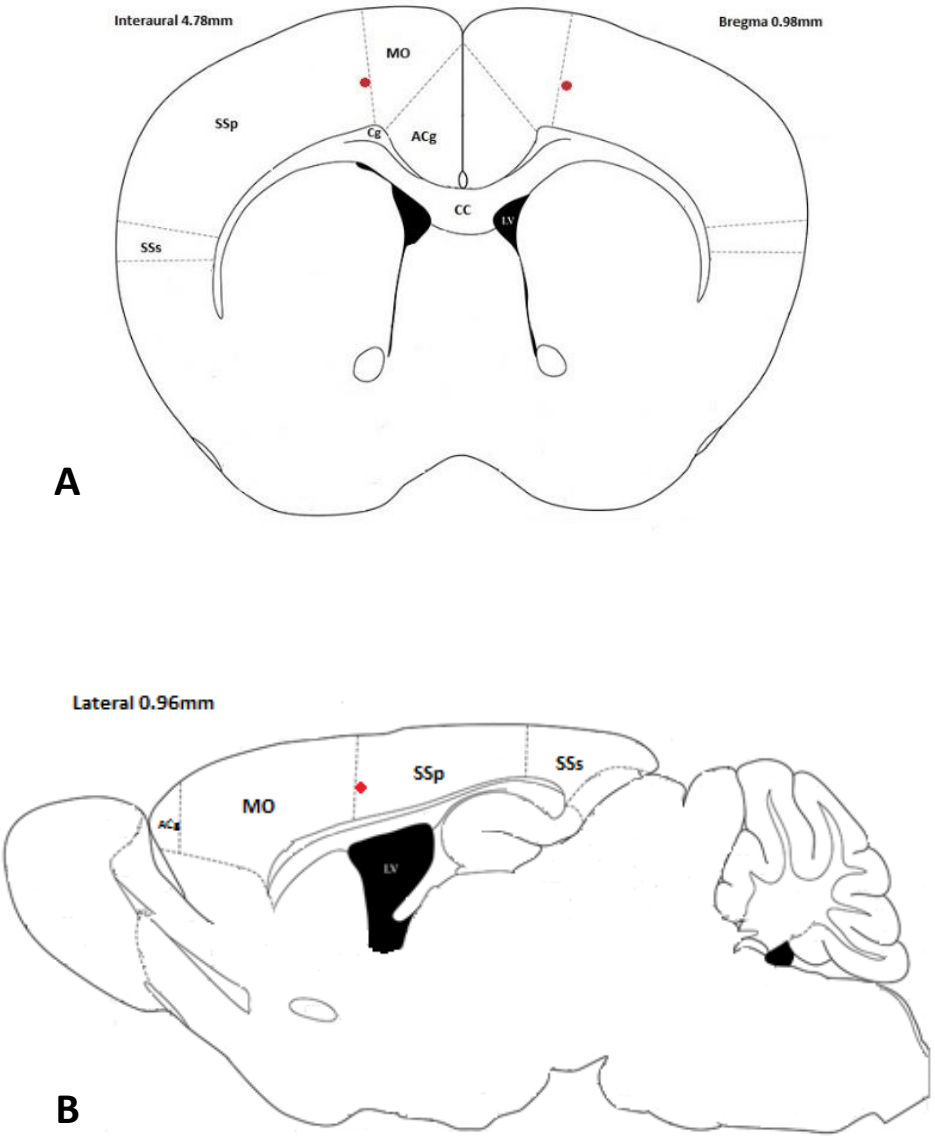

<u>Figure 2. 1</u>: Mouse brain atlas.

Area of injection in stereotactic surgery is marked with a red dot (ML = ± 1mm, AP = 1mm, DV = 1.5mm) on the motor cortex. Both coronal and sagittal views are shown.

Compound	Details	Working concentration	References
LPC	Sigma, L4129	1% (w/v)	Plemel et al., 2018
LPS	Sigma, L4391	100ng/ml	Preliminary data
Psychosine	Santa Cruz, sc-202781	100nM	O'Sullivan et al., 2015
IL17a	R&D system, 421-ML	250ng/ml	O'Sullivan et al., 2016
TNF-α	R&D system, 210-TA	10ng/ml	O'Sullivan et al., 2016
H_2O_2	Sigma, 216763	0.5mM	O'Sullivan et al., 2017
GsMTx4	Alomone, STG-100	500nM or 3µM	Preliminary data
Yoda-1	Tocris, 5586	10µM	Syeda et al., 2015

Table 2. 1: List of compounds used

PRIMARY ANTIBODIES						
Target	**Type**	**Host**	**Supplier**	**Cat No.**	**RRID**	**Dilution**
Piezo-1 (FAM38A)	Polyclonal	Rabbit	Abcam	ab128245	AB_11143245	1/200 IF; 1/500 WB
Piezo-1 (FAM38A)	Polyclonal	Goat	Santa Cruz	sc-164319	AB_10842990	1/200 IF; 1/500 WB
Vimentin	Polyclonal	Mouse	Santa Cruz	sc-373717	AB_10917747	1/1000
MOG	Monoclonal	Mouse	Millipore	MAB5680	AB_1587278	1/1000
MBP	Polyclonal	Rabbit	Abcam	ab40390	AB_1141521	1/1000
PLP	Polyclonal	Rabbit	Abcam	ab28486	AB_776593	1/1000
PLP	Monoclonal	Mouse	Millipore	MAB388	AB_177623	1/1000
Neurofilament H	Polyclonal	Chicken	Millipore	AB5539	AB_177520	1/2000
GFAP	Polyclonal	Rabbit	Abcam	ab7260	AB_305808	1/1000
Amyloid-β 1-42	Monoclonal	Rabbit	Abcam	ab201061	AB_2722492	1/1000
O4	Monoclonal	Mouse	Novus Bio	MAB1326	AB_357617	1/400
Iba-1	Polyclonal	Rabbit	Wako	19-19741	AB_839504	1/1000
Actin	Monoclonal	Mouse	Abcam	ab3280	AB_303668	1/3000

SECONDARY ANTIBODIES					
Target	**Host**	**Supplier**	**Cat No.**	**RRID**	**Dilution**
HRP-conjugated anti-mouse	Goat	Sigma	A8924	AB_258426	1/5000
HRP-conjugated anti-rabbit	Goat	GE Healthcare	NA934	AB_772206	1/5000
HRP-conjugated anti-goat	Rabbit	Sigma	A4174	AB_258138	1/5000
Alexa 488 anti-goat	Donkey	Sigma	SAB4600032		1/1000
Alexa 488 anti-rabbit	Donkey	Alexa	A11008	AB_143165	1/1000
Alexa 549 anti-mouse	Donkey	JIR	115-506-068		1/1000
Alexa 633 anti-chicken	Donkey	Alexa	A21103	AB_2535756	1/1000
Avidin Alexa 488 conjugated	N/A	Thermofisher	A21370		1/1000
Biotinylated anti-rabbit	Goat	Thermofisher	A24535	AB_2536003	1/1000

Table 2. 2: List of antibodies used

Chapter 3:
Astrocytic Piezo1 and its role in neuroinflammation of the Central Nervous System

Chapter aims

Based on the previous findings by Satoh and colleagues (2006), on the upregulation of Piezo1 mRNA in the astrocytes surrounding the amyloid plaques of post-mortem Alzheimer's brains, we hypothesized that the expression of the mechanoreceptor Piezo1 may be induced in astrocytes under certain pathological or inflammatory conditions, playing a role in the modulation of the reactive state of glia cells. To investigate so, we used primary mouse astrocyte culture and stimulate them with different insults, analysing the expression of Piezo1 and certain cellular responses under pharmacological modulation of Piezo1.

Thus, the specific aims of this chapter were:

- To study the expression of Piezo1 in mouse astrocytes under pathological stimuli, i.e. lipopolysaccharide (LPS), psychosine, amyloid-β and hydrogen peroxide (H_2O_2).
- To assess the subcellular localization of the expression of Piezo1 in astrocytes
- To investigate the role of Piezo1 in astrocyte cell survival, mitochondrial stress and cytokine release
- To analyse calcium signalling by activation of Piezo1 with Yoda-1
- To study the effects of blocking/activating Piezo1 in astrocytic migration

Abstract

Piezo1, also known as Mib (membrane protein induced by beta-amyloid-treatment) or FAM38A, was first described as a mechanosensitive protein in 2010. Since then, further research has been conducted investigating the Piezo family, although little is known about the specific role of Piezo1 in the brain. Studies have, however, reported the expression and function of Piezo1 in neurons and also demonstrated high mRNA levels of Piezo1 in astrocytes associated with senile amyloid plaques in *post-mortem* Alzheimer's brains. Here, we analysed the expression of Piezo1 in mouse astrocyte primary cultures under physiological and pathological stimuli, including LPS, psychosine, H_2O_2 and IL17a and TNF-α. While not expressed under control conditions, we found Piezo1 to be expressed in astrocytes under LPS or psychosine stimulation. Notably, this expression was co-localized with endoplasmic reticulum, suggesting that Piezo1 expression is not restricted to the outer membrane. Modulation of Piezo1 by the blocker GsMTx4 or the activator Yoda-1 did not alter astrocyte cell survival or mitochondrial stress in these cells. In contrast, we observed that activation of Piezo1 by Yoda-1 caused a decrease in the LPS-induced release of the proinflammatory cytokines TNF-α, IL1β and IL6, while blocking Piezo1 by GsMTx4 had the opposite effect. Modulation of Piezo1 also had an effect in astrocytic migration, causing an increase of the migrated distance when Piezo1 was blocked. We also showed that the Piezo1 activator, Yoda-1, induces the release of Ca^{2+} from intracellular stores and affects subsequent ATP-induced Ca^{2+} response. Taking these results together, we hypothesize that Piezo1 may play a role in the regulation of the reactive state of astrocytes when in pathological environment and in neuroinflammatory response, by attenuating astrocytic reactivity.

1. Introduction

Piezo1 was first reported as a mechanosensitive channel in mouse neuroblastoma cell lines (Neuro2A) in 2010 (Coste et al., 2010). Prior to this, mRNA for Piezo1 was detected in astrocytes associated to the senile plaques in *post-mortem* Alzheimer brains, receiving the name of Mib (membrane protein induced by beta-amyloid-treatment). However, at that time, Mib was not linked to the mechanosensitive channels family (Satoh et al., 2006). Currently, Piezo1 is known to be one of the largest receptors reported, with more than 2,500 amino acids and 30-40 transmembrane segments (Kamajaya, Kaiser, Lee, Reid, & Rees, 2014). It forms a homotrimer that is permeable to calcium (Ca^{2+}) in a non-selective manner (Gnanasambandam et al., 2015) allowing an cellular influx of Ca^{2+} when activated by mechanical cues (Coste et al., 2010). Expression of Piezo1 has been reported in the outer membrane of neurons (Koser et al., 2016) and in astrocytes in the optic nerve (Choi et al., 2015) although its expression in astrocytes of CNS under basal conditions appears to be absent. Despite its putative role in extrusion of cells in epithelia (Eisenhoffer et al., 2012; Gudipaty & Rosenblatt, 2016), modulation of integrin activation (McHugh et al., 2012) and modulation of red blood cells deformation (Cahalan et al., 2015; Cinar et al., 2015), little is known about Piezo1 role in the CNS. Studies have shown that stiffness of the environment modifies the length and direction of axonal growth cone through Piezo1 signalling (Koser et al., 2016), but no other role or implication of Piezo1 has been proposed so far.

Several studies have reported the mechanosensitive and responsive nature of neurons and glia to mechanical stimuli (Blumenthal, Hermanson, Heimrich, & Shastri, 2014; Previtera, Langhammer, Langrana, & Firestein, 2010). For instance, astrocytes change morphology depending on the stiffness of their environment, showing longer and thicker processes in stiff hydrogels, resembling a reactive phenotype (Bollmann et al., 2015). Astrocytes have been given increasing importance regarding their roles in health and disease states, with two different states of (re)activity being suggested, namely, A1 and A2 astrocytes (Liddelow et al., 2017). In brief, A1 astrocytes are rapidly formed in acute CNS injury and show a reduced phagocytic capacity, limit the differentiation of oligodendrocytes, and secrete some yet unknown molecules that results in neuronal death. Contrary to this, the A2 phenotype of astrocytes is observed under ischemia conditions, where this cell subtype is suggested to promote neuronal survival and tissue repair. Interestingly, LPS induces the A1 astrocyte phenotype however only in presence of microglia, as pure astrocyte cultures (cultured from *Csf1r*$^{-/-}$ mice, lacking microglia) cannot be differentiated into this phenotype. This new field of activated astrocytes

might have important implications in future research of different nervous system pathologies and its therapies.

In the present study, we chose an *in vitro* approach to analyse the expression of Piezo1 in primary mouse astrocytes following stimulation with inflammatory insults, including LPS sourced from *E.coli* and amyloid-β stimulated microglia media. Primary mouse astrocyte cultures from newborn C57Bl/6J mice were used as a model due to its ease of culture, reproducibility and technical needs of the experiments planned. We also show how certain stimuli such as LPS, psychosine or amyloid-β led to the expression of Piezo1 in the endoplasmic reticulum of astrocytes and how the modulation of Piezo1 affected the reactivity state of astrocytes in terms of proinflammatory cytokine release and migration rate. Moreover, we show how activation of Piezo1 by Yoda-1 caused the release of Ca^{2+} from intracellular stores and alters subsequent activation by ATP. Altogether, these results highlight a possible role of Piezo1 in astrocyte inflammatory activation of the CNS

2. Results

2.1. Piezo1 is expressed in primary neurons while absent in primary astrocytes under physiological conditions

Since its description in 2010 (Coste et al., 2010), expression of Piezo1 mRNA has been measured by *in situ* hybridisation in neurons in the cerebral cortex and substantia nigra of the human brain tissue samples (Satoh et al., 2006). To our knowledge, studies have not reported the protein expression of Piezo1 in neuronal or glia cells. Thus, in order to characterise firstly, the cellular expression of Piezo1 at the protein level, we performed mouse primary neuronal and astrocyte cultures and co-stained these cell cultures with Piezo1 and neurofilament-H (NFH) as a neuronal marker or vimentin as a marker of astrocytes. Expression of Piezo1 was observed in primary neuron culture **(Figure 3.1 A-D)**, but absent in primary mouse astrocyte culture under control conditions **(Figure 3.1. E-H)**, in agreement with human studies of Piezo1 mRNA (Satoh et al., 2006).

2.2. LPS increases expression of Piezo1 in a subset of primary mouse astrocytes

The Gram-negative bacterial endotoxin, LPS, is an agonist of the toll-like receptor 4 (TLR4) and induces a strong immune response. Once activated, TLR4 plays an important role in the defence against bacteria as well as inducing a range of inflammatory cell responses, such as induction of cytokines like IFN-β, IL18 or TNF-α (Palsson-McDermott & O'Neill, 2004). TLR4 is also expressed in rodent astrocytes (Nakano et al., 2015). Here we examined whether stimulation of mouse astrocytes with LPS can lead to the expression of Piezo1. Mouse astrocytes from prefrontal cortex of new-born wild type C57BL/6J mice were treated with 100ng/ml of LPS for 16h, 24h or 48h. After treatment, the cells were stained for vimentin, DAPI and Piezo1 (Abcam, ab128245). No expression of Piezo1 was observed under control conditions; however, expression of Piezo1 was detected under all time lapse images post-treatment with LPS, although the highest percentage of Piezo1-positive cells was observed 24h after LPS treatment (16h LPS: 15.5% ± 8.8%, **p<0.01; 24h LPS: 21.3% ± 7.9%, **p>0.001; 48h LPS: 13.7% ± 6.2%, **p<0.01; RM one-way ANOVA following Newman-Keuls post-hoc test, n=8, dF=3) **(Figure 3.2 G-I, M)**. In these experiments, we noted only a subset of astrocytes, for example 21.3% ± 7.9% (24h LPS) expressed Piezo1. These results were also supported by Western-blot analysis, where a band at 285kDa corresponding to Piezo1 can be observed under LPS treatment **(Figure 3.2 A)**. Other bands could be observed at 200, 175 and 150 kDa; however, these disappeared upon prior

incubation of the antibody with the control peptide **(Data not shown)**, leading to the hypothesis that these are unspecific bands probably due to similar regions of other receptors in the sample. Moreover, we analysed the levels of Piezo1 mRNA in astrocytes with qPCR, and observed that after 24h LPS-treatment, astrocytes expressed an increase in fold-change of Piezo1 mRNA of 2.226 ± 0.127, compared to control baseline. Thus, these data suggest that although Piezo1 is not expressed in astrocytes under physiological conditions, LPS stimulus can drive its expression, following a time-dependent trend, with peak at 24h stimulation.

2.3. Intracellular expression of Piezo1 in the endoplasmic reticulum

Piezo1 expression has been reported to be both in the plasma membrane (Coste et al., 2010) and the ER (McHugh et al., 2010; Satoh et al., 2006). It is conceivable that localization of this mechanoreceptor may affect its role and/or its protein half-life, where the ER located Piezo1 plays a differing role to the membrane expressed version. It is believed that when located in the ER, Piezo1 can modulate the function of integrin proteins (McHugh et al., 2012), whereas when activated in the plasma membrane the role of Piezo1 remains unclear. In order to study Piezo1 localisation under control and inflammatory conditions, mouse astrocytes treated with LPS (100ng/ml) were stained for Piezo1 and the cytoPainter® ER dye. Interestingly, LPS appeared to trigger expression of Piezo1 in astrocytes exclusively in the ER **(Figure 3.2 O-V)**, which contrasts with its expression in cortical neurons where it is also localised in the outer membrane **(Figure 3.1. A-D)**. As Piezo1 is a Ca^{2+} channel, its activation in the ER could suggest a role in intracellular Ca^{2+} signalling, leading to the activation of a myriad of biochemical pathways, perhaps such as apoptosis (A. Miyamoto et al., 2015), phagocytosis and cytokine release (Heo, Lim, Nam, Lee, & Kim, 2015).

2.4. Piezo1 is also expressed in astrocytes under psychosine and amyloid-β conditioned microglial media.

Psychosine (galactosylsphingosine, PSY) is a toxin that accumulates in Krabbe's disease brains due to the deficit of the enzyme galactosylceramidase (Davenport et al., 2011). When accumulated in the brain, psychosine potentiates the cytokine-mediated induction of iNOS (Giri et al., 2002) and it is believed to play a major role in the degeneration or dysfunction of myelin-forming cells (Taniike & Suzuki, 1995). Based upon our previous results in which LPS induced the expression of Piezo1 in mouse astrocytes, we tested whether this expression could also be induced by other cell stressors. Thus, mouse astrocytes were stimulated with psychosine (5µM), H_2O_2 (5µM), TNF-α/IL17a cocktail, and amyloid-β conditioned microglial media (CMM) at 16h, 24h and 48h. Neither H_2O_2 nor TNF-α/IL17a induced the expression of Piezo1 in astrocytes at

any time-point (H_2O_2: 1.86% ± 1.33%, n.s. p>0.99; TNF-α/IL17a: 3.19% ± 0.89%, n.s. p>0.99; RM one-way ANOVA following Newman-Keuls post-hoc test; n=8, dF=5) **(Figure 3.3 A)**. However, expression of Piezo1 was detected in 30-40% of astrocytes stimulated with both psychosine (29.34% ± 1.62%, ***p<0.001) and Aβ CMM (37.37% ± 4.99%, ***p<0.001) at 24h **(Figure 3.3 B, C)**. These results suggest that an increase in astrocytic Piezo1 expression may be an event specific to certain neurodegenerative diseases.

2.5. Yoda-1 activates the intracellular release of Ca^{2+} in LPS-treated astrocytes

Astrocytes are sensors of neuronal activity and they integrate this information through Ca^{2+} signalling by oscillations and transitions (Pfrieger & Barres, 1996; Smith, 1994). Given Piezo1 is a Ca^{2+} channel and the observed localization in the ER in astrocytes under inflammation stimuli, we investigated whether activation of Piezo1 by Yoda-1 could lead to Ca^{2+} signalling from internal ER stores of the astrocytes. Here, we analysed Ca^{2+} levels using the dye Cal520 (Abcam, ab171868) in the presence or absence of Ca^{2+} in the culture media. A baseline of 30 sec (23 frames) was allowed before washing on HBSS or 20µM Yoda-1 and the signal was recorded for 4 min (185 frames) until 50µM ATP was washed on and recorded for further 3 mins (140 frames) **(Figure 3.4; Figure 3.5)**. In complete media (containing extracellular Ca^{2+}, thus were the signal observed could be due to both extracellular and intracellular Ca^{2+} storage movement), Yoda-1 had no significant effect compared to astrocytes where HBSS was applied under physiologic conditions (HBSS: 104 ± 10.14 vs Yoda1: 116.6 ± 10.24, n.s. p=0.48; two-way ANOVA following Holm-Sidak post-hoc test, n=6, dF=1). However, LPS caused an enhanced Ca^{2+} response to ATP (154.0 ± 13.46 vs 104 ± 10.14, *p=0.02), and Yoda-1 further contributed to this stimulation (216.4 ± 13.58 vs 104 ± 10.14, ***p<0.001) **(Figure 3.4)**. In contrast, when extracellular Ca^{2+} was omitted from the culture media (thus, all Ca^{2+} transients observed were due to release from intracellular stores), neither HBSS or Yoda-1 triggered a response in control astrocytes while ATP induced a transient Ca^{2+} signal **(Figure 3.5 A-B)**. In LPS-treated astrocytes, Yoda-1 triggered a small transient Ca^{2+} signal (5.52 ± 2.02 vs 0.00 ± 0.0; **p=0.0058; two-way ANOVA following Holm-Sidak post-hoc test, n=6, dF=1). In addition, Yoda-1 modified the subsequent ATP response, which reached a similar intensity but was longer lasting **(Figure 3.5 D)**, as measured by a significantly larger area under the curve (AUC) (157.2 ± 8.2 vs 122.5 ± 6.4; **p<0.0022) compared to control **(Figure 3.5 E-G)**. This functional data supports the expression data, showing that the specific activator of Piezo1, Yoda-1, triggers a response in LPS-treated astrocytes leading to Ca^{2+} release from the internal ER stores, while not inducing a response in non-stimulated astrocytes.

2.6. Activation of Piezo1 decreases the release of proinflammatory cytokines IL-6, IL-1β and TNF-α

It has been suggested that Piezo1 is involved in the modulation of integrin adhesion (McHugh et al., 2010; McHugh et al., 2012), cell extrusion from epithelia (Gudipaty & Rosenblatt, 2016) and axon guidance (Koser et al., 2016). As we observed a Ca^{2+} release from intracellular stores and since LPS is known to trigger inflammation and cytokine release from astrocytes (Liddelow et al., 2017), we next investigated if modulating Piezo1 activity in astrocytes alters cell viability and/or the release of pro-inflammatory cytokines. Mouse astrocytes were stimulated with LPS plus the Piezo1 activator (Yoda-1) or the non-specific inhibitor (GsMTx4). We observed no significant differences in astrocyte cell viability in any of the conditions tested, as determined by MTT assay (RM two-way ANOVA following Holm-Sidak post-hoc test, n=5, dF=6) **(Figure 3.6 A)**. Furthermore, no differences were noted in mitochondrial potential, as measured by JC-1 analysis (RM two-way ANOVA following Holm-Sidak post-hoc test, n=6, dF=6) **(Figure 3.6 B)**. In contrast, Piezo1 altered the levels of proinflammatory cytokines IL-6, IL-1β and TNF-α in astrocytes. Specifically, LPS increased the release of TNF-α at all treatment time-points (16h LPS: 2688.0pg/ml ± 564.4pg/ml, ***p<0.001; 24h LPS: 2380.0pg/ml ± 702.4pg/ml, ***p<0.001; 48h LPS: 2046.0pg/ml ± 917.0pg/ml vs control: 19.19pg/ml ± 6.7pg/ml, ***p<0.001; RM two-way ANOVA following Holm-Sidak post-hoc test, n=5, dF=6), but treating the astrocytes with Yoda-1 significantly decreased the levels of TNF-α at 16h (754.1pg/ml ± 648.8pg/ml vs 2688.0pg/ml ± 564.4pg/ml, ***p<0.001); at 24h (684.3pg/ml ± 682.1pg/ml vs 2380.0pg/ml ± 702.4pg/ml, ***p<0.001) and at 48h LPS treatment (483.9pg/ml ± 350.2pg/ml vs 2046.0pg/ml ± 917.0pg/ml, ***p<0.001) **(Figure 3.6 C)**. Similarly, treatment with Yoda-1 decreased the levels of IL-6 at 48h (3741.0pg/ml ± 715.8pg/ml vs 5347.0pg/ml ± 1122.0pg/ml, ***p<0.01) and IL-1β at 48h (110.8 pg/ml ± 27.72 pg/ml vs 514.8 pg/ml ± 273.3 pg/ml, ***p<.001) **(Figure 3.6 D, E)**. In contrast, GsMTx4 increased the levels of both IL-6 (7206.0pg/ml ± 962.0pg/ml vs 5347.0pg/ml ± 1122pg/ml; ***p<0.001) and IL-1β (687.1pg/ml ±277.8pg/ml vs 514.8pg/ml ± 273.3pg/ml; **p<0.001) **(Figure 3.6 D, E)**. These results show that Piezo1 plays a role in regulating pro-inflammatory cytokines in astrocytes by down-regulating proinflammatory cytokine release upon Piezo1 activation under inflammatory stimulus.

2.7. Inhibition of Piezo1 enhances migration of LPS-stimulated astrocytes

While controversial, astrocytes have been suggested to migrate under neuroinflammatory conditions and contribute to glial scar formation after traumatic CNS injury (Buffo, Rolando, & Ceruti, 2010). Given we observed Yoda-1 to activate transient intracellular Ca^{2+} signalling, and that previous studies that have shown Piezo1 as having a role in endothelial cell migration (Eisenhoffer et al., 2012), we next examined the role of Piezo1 in regulating astrocyte cell migration, in a cell wound assay. Under non-inflammatory conditions, the incubation of control astrocytes with either Yoda-1 (10µM) or GsMTx4 (500nM) did not alter migration velocity (Yoda-1: 2.95 ± 1.0 µm/h vs 2.74 ± 1.0 µm/h, n.s. p>0.99; GsMTx4: 3.35 ± 0.85 µm/h vs 2.74 ± 1.0 µm/h, n.s. p>0.99; RM two-way ANOVA following Holm-Sidak post-hoc test, n=5, dF=20) **(Figure 3.7 A-C, G)**. However, in inflammatory conditions, the inhibition of Piezo1 by treatment with 500nM GsMTx4 significantly enhanced motility in LPS-activated astrocytes compared to LPS alone (5.00 ± 0.9 µm/h vs 2.98 ± 0.1 µm/h; ***p<0.001; RM two-way ANOVA following Holm-Sidak post-hoc test, n=5, dF=20) **(Figure 3.7 D, E, H)**. In contrast, activation of Piezo1 with 10µM Yoda-1 reduced this cell migration (2.12 ± 0.7 vs 2.98 ± 0.1 µm/h; **p<0.01) **(Figure 3.7 D, F, H)**. This data suggests that Piezo1 channel activity down-regulate astrocytic migration under neuroinflammatory conditions.

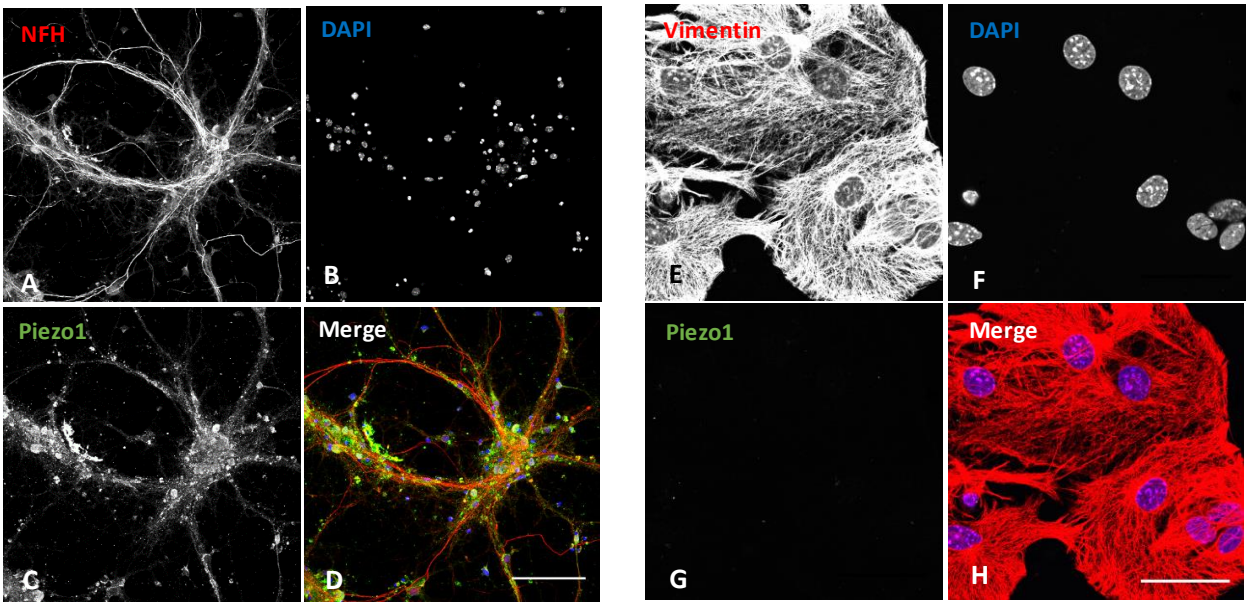

Figure 3. 1: Cellular location of Piezo1

(A-D) Immunocytochemistry of primary neuron culture in control conditions, showing expression of Piezo1. Red, NFH; green, Piezo1 (ab128245); blue, DAPI. *Courtesy of Miss Myrthe Mampay, University of Brighton*. **(E-H)** Immunocytochemistry of primary astrocyte culture in control conditions, showing absence of Piezo1 signal. Red, Vimentin; green, Piezo1 (ab128245); blue, DAPI. Scale bar = 20µm.

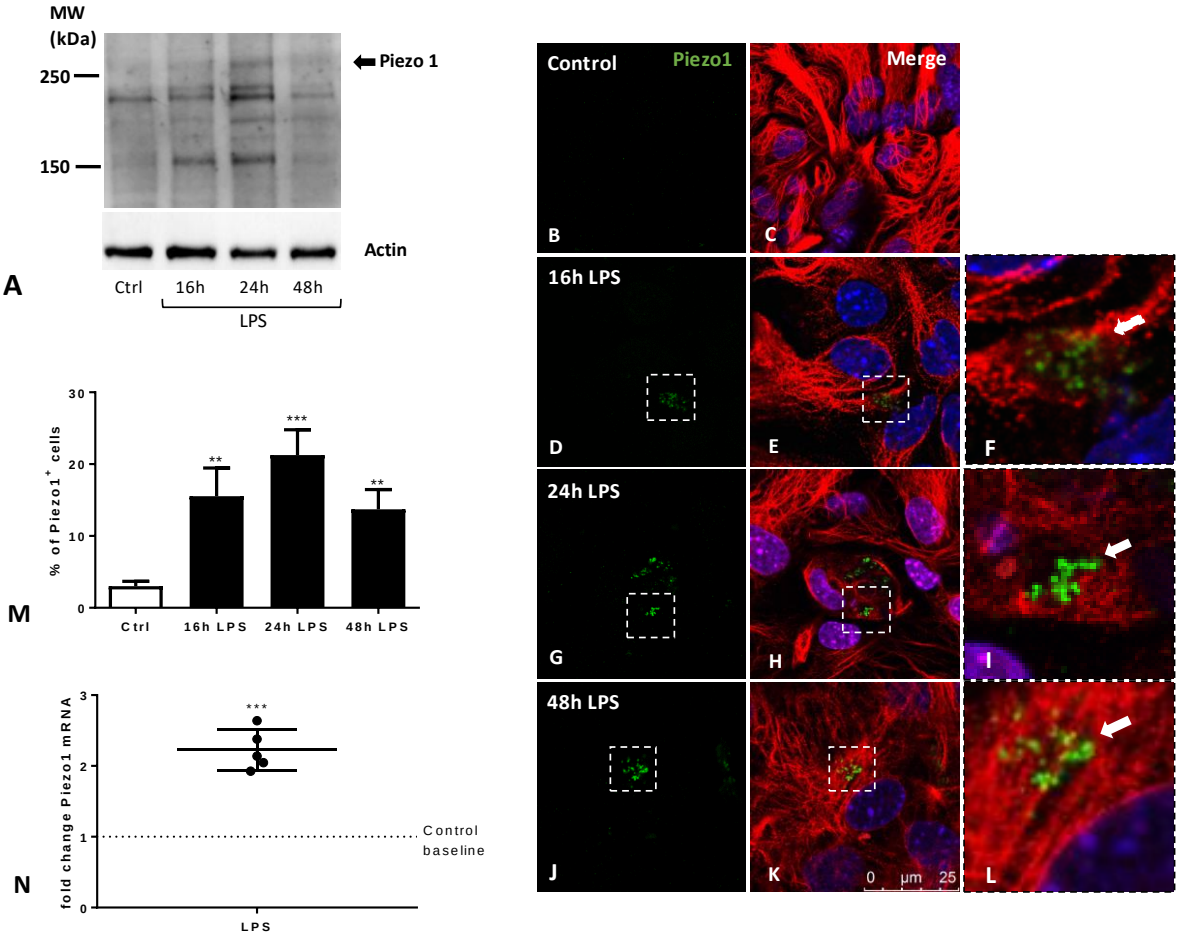
MW
(kDa)
250
150
Piezo 1
Actin
Ctrl
16h
24h
48h
LPS
A
% of Piezo1+ cells
Ctrl
16h LPS
24h LPS
48h LPS
M
fold change Piezo1 mRNA
Control
baseline
LPS
N
Control
Piezo1
Merge
B
C
16h LPS
D
E
F
24h LPS
G
H
I
48h LPS
J
K
L
0 µm 25

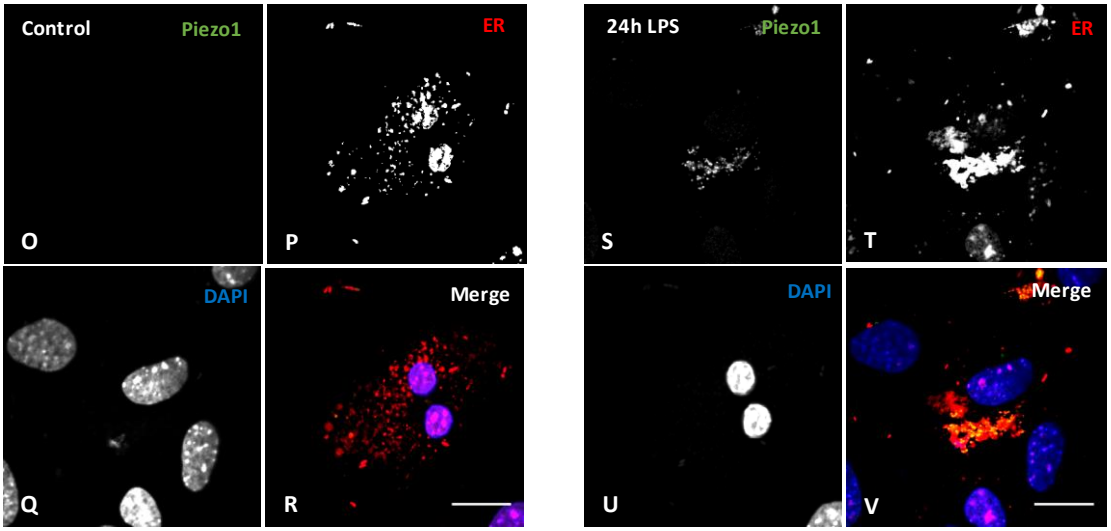
Control
Piezo1
ER
O
P
DAPI
Merge
Q
R
24h LPS
Piezo1
ER
S
T
DAPI
Merge
U
V

Figure 3. 2: LPS increases expression of Piezo1 in mouse astrocytes

(A) Expression of Piezo1 (ab128245) in mouse astrocytes (MA) stimulated with LPS (100ng/ml) for 16h, 24h and 48h by Western-Blot. A 285kDa band corresponding to Piezo1 can be seen in the 24h LPS-stimulated sample, while in 16h and 48h LPS treatment the band was seen at a lower intensity. No band was observed in the control sample. Loading control actin, 42kDa band. **(B-L)** Immunocytochemistry of MA in control and LPS treatment for 16h, 24h and 48h. Red, vimentin; green, Piezo1; blue, DAPI. An increase in the expression of Piezo1 under 24h LPS treatment can be observed. Treatment with LPS for 16h and 48h led to a lower expression of Piezo1. **(M)** Statistical analysis of the increase in percentage of Piezo1-positive cells under different conditions. Repeated measures one-way ANOVA, Newman-Keuls post-hoc test used. Data shown as mean ± SEM, n=8, dF=3; being each experimental unit cells from the same flask and passage. **(N)** RT qPCR analysis of the mRNA levels of Piezo1. LPS-treated astrocytes showed a 2.226 ± 0.127 fold-change in the mRNA levels of Piezo1 compared to control baseline of 1. Quantification Piezo1 mRNA levels was performed using β-actin mRNA levels as housekeeping protein. Statistical analysis was performed on ddCT values, using a one sample t-test with theoretical mean of 0. Graph represents fold-change Piezo1 mRNA of LPS-treated astrocytes compared to control astrocytes, mean ± SEM, n = 5, dF=4; being each experimental unit cells from the same flask and passage **(O-V)** Immunocytochemistry of MA shows co-localization of Piezo1 in the endoplasmic reticulum (ER) in LPS-treated astrocytes. Green, Piezo1; red, ER (CytoPainter®, Abcam); yellow, co-localization between Piezo1 and ER staining). Scale bar = 20µm.

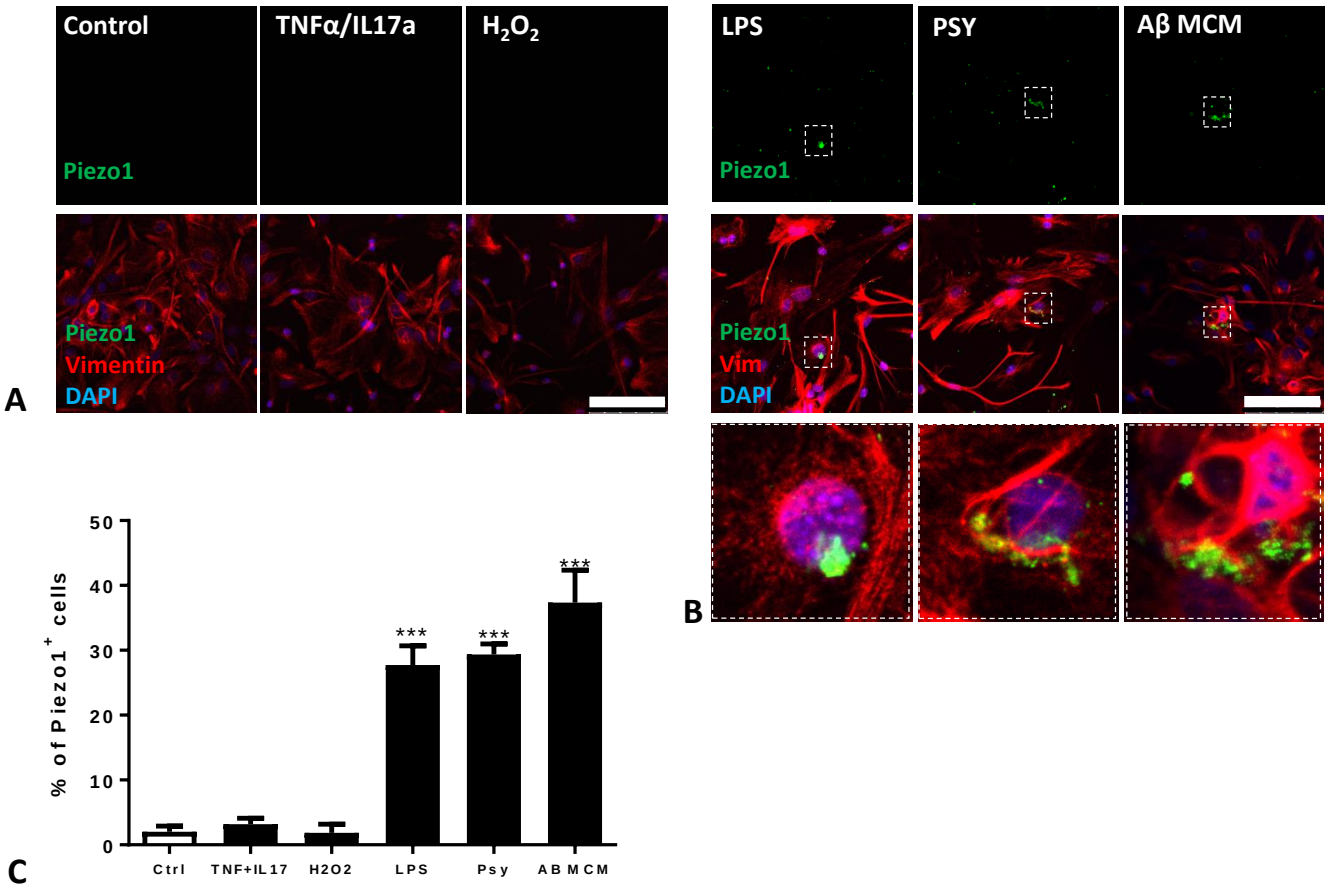

Figure 3. 3: LPS, PSY and amyloid-β_{1-42} increase the expression of Piezo1 in mouse astrocytes

(A) Immunocytochemistry of MA in control, cytokine cocktail and H_2O_2-treated conditions at 18h time-point. Red, vimentin; green, Piezo1; blue, DAPI. There is no expression of Piezo1 in MA under treatment with cytokines TNF-α/IL17a or H_2O_2. **(B)** However, immunocytochemistry of MA under LPS, PSY or CMM treatment showed an increase in Piezo1 expression. **(C)** Statistical analysis of the percentage of Piezo1-positive cells show a significant increase in the number of cells expressing Piezo1 under LPS, PSY or CMM treatment compared to control. Repeated measures one-way ANOVA, with Newman-Keuls post-hoc test was performed. Data presented as mean ± SEM, n=8, dF=5; being each experimental unit cells from the same flask and passage. Scale bar = 100µm.

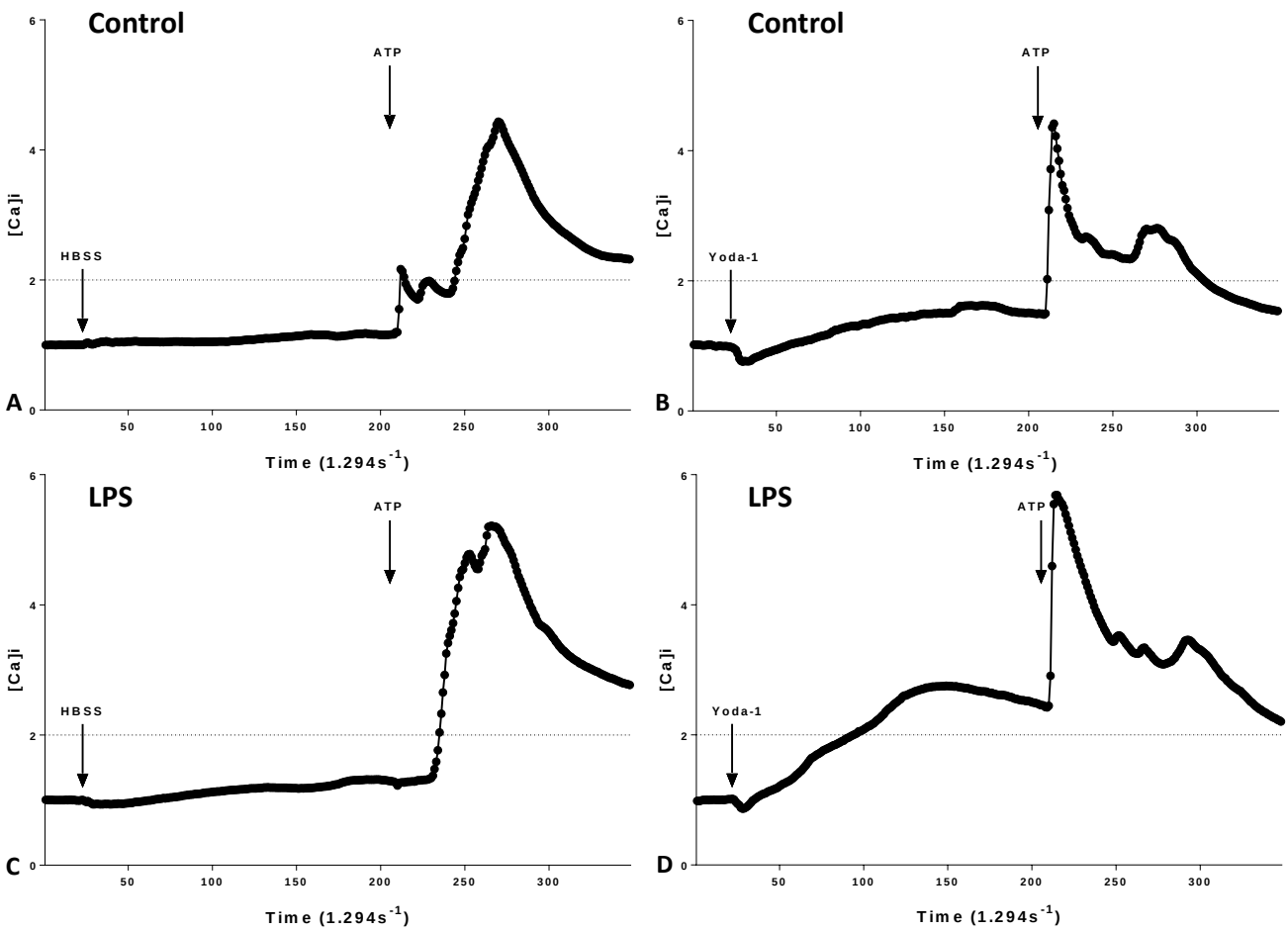

	Control + HBSS	Control + Yoda-1	LPS + HBSS	LPS + Yoda-1
No. of Peaks	1	1	1	1
Peak X (time)	270	215	266	215
Peak Y ([Ca]i)	4.434	4.414	5.215	5.686
AUC	104.4	116.6	154.2	216.4

E

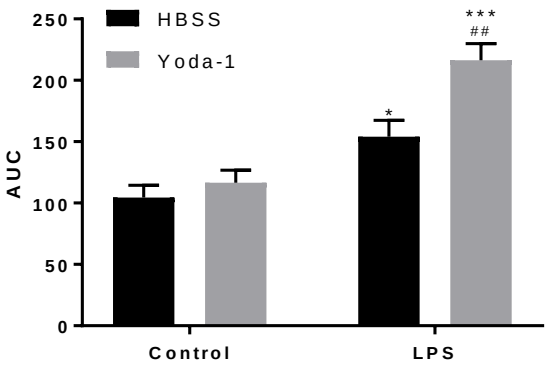

F

* compared to Control/HBSS
\# compared to LPS/HBSS

Figure 3. 4: Live calcium imaging of MA in presence of extracellular Ca^{2+} and Mg^{2+}

(A, B) Control astrocytes were stimulated with HBSS or Yoda-1 after 30sec baseline, followed by ATP stimulation at 4.5 min. Neither HBSS or Yoda-1 had a significant effect on calcium release, and ATP stimulation had similar Ca^{2+} peak times and intensities **(C, D)** Same experimental protocol was done in 24h LPS-stimulated astrocytes. HBSS had no effect on Ca^{2+} release but Yoda-1 led to an increase in Ca^{2+} signals, although statistically not significant. **(E-F)** Analysis of the Ca^{2+} signals reveal an increase in the Ca^{2+} response after ATP stimulation in LPS-stimulated astrocytes, compared to physiological conditions. Moreover, Yoda-1 intensified this increase in response. Statistical analysis was performed by two-way ANOVA with Holm-Sidak post-hoc test. Data shown as mean ± SEM, n = 6, dF=1; being each experimental unit cells from the same flask and passage.

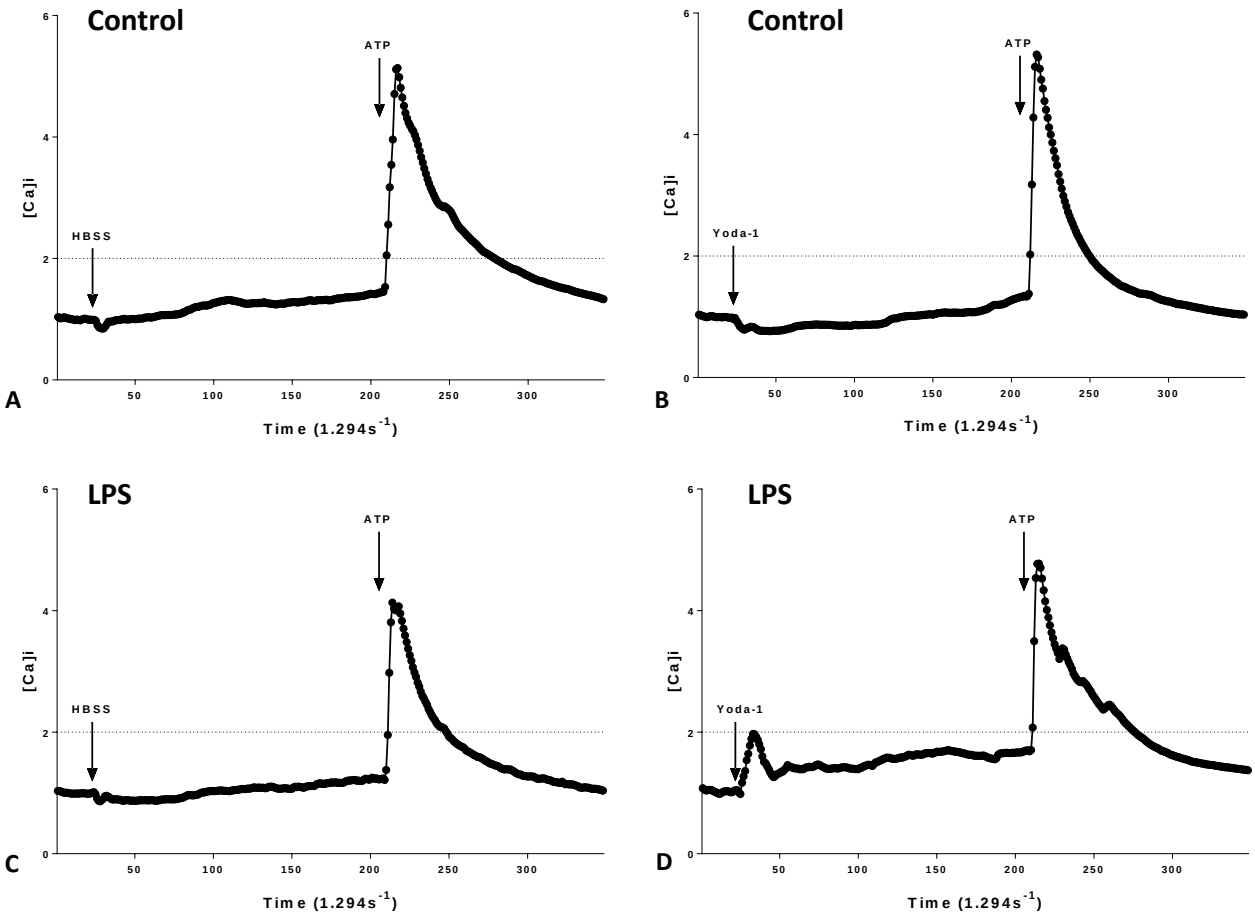

	Control + HBSS	Control + Yoda-1	LPS + HBSS	LPS + Yoda-1
No. of Peaks	1	1	1	2
Peak X (time)				33
Peak Y ([Ca]i)				0.6365
AUC				5.523
Peak X (time)	217	216	218	215
Peak Y ([Ca]i)	3.092	4.229	2.561	3.438
AUC	122.5	114.2	114.5	157.2

E

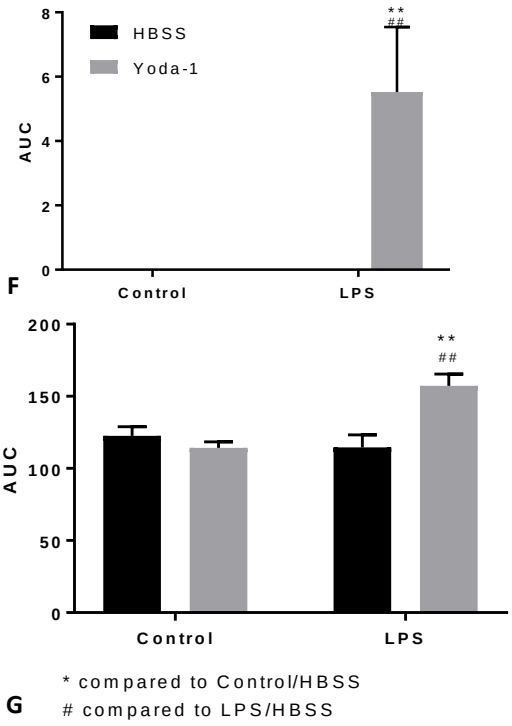

Figure 3. 5: Live intracellular calcium imaging of MA in absence of extracellular Ca^{2+} and Mg^{2+} **(A, B)** Control astrocytes were stimulated with HBSS or Yoda-1 after 30sec baseline, followed by ATP stimulation at 4.5 min. Neither HBSS or Yoda-1 had an effect on calcium release, and ATP stimulation had similar Ca^{2+} peak times and intensities **(C, D)** Same procedure was done in 24h LPS-stimulated astrocytes. HBSS had no effect on Ca^{2+} release but Yoda-1 led to a peak in Ca^{2+} signals from intracellular stores. **(E-G)** Analysis of the Ca^{2+} signals reveal a release of Ca^{2+} from intracellular stores in LPS-treated astrocytes after Yoda-1 stimulation. Subsequent stimulation with ATP led to a more sustained signal, with higher AUC but similar intensity peak and time peak than the rest of the groups. Statistical analysis was performed by two-way ANOVA with Holm-Sidak post-hoc test. Data shown as mean ± SEM, n=6, dF=1; being each experimental unit cells from the same flask and passage.

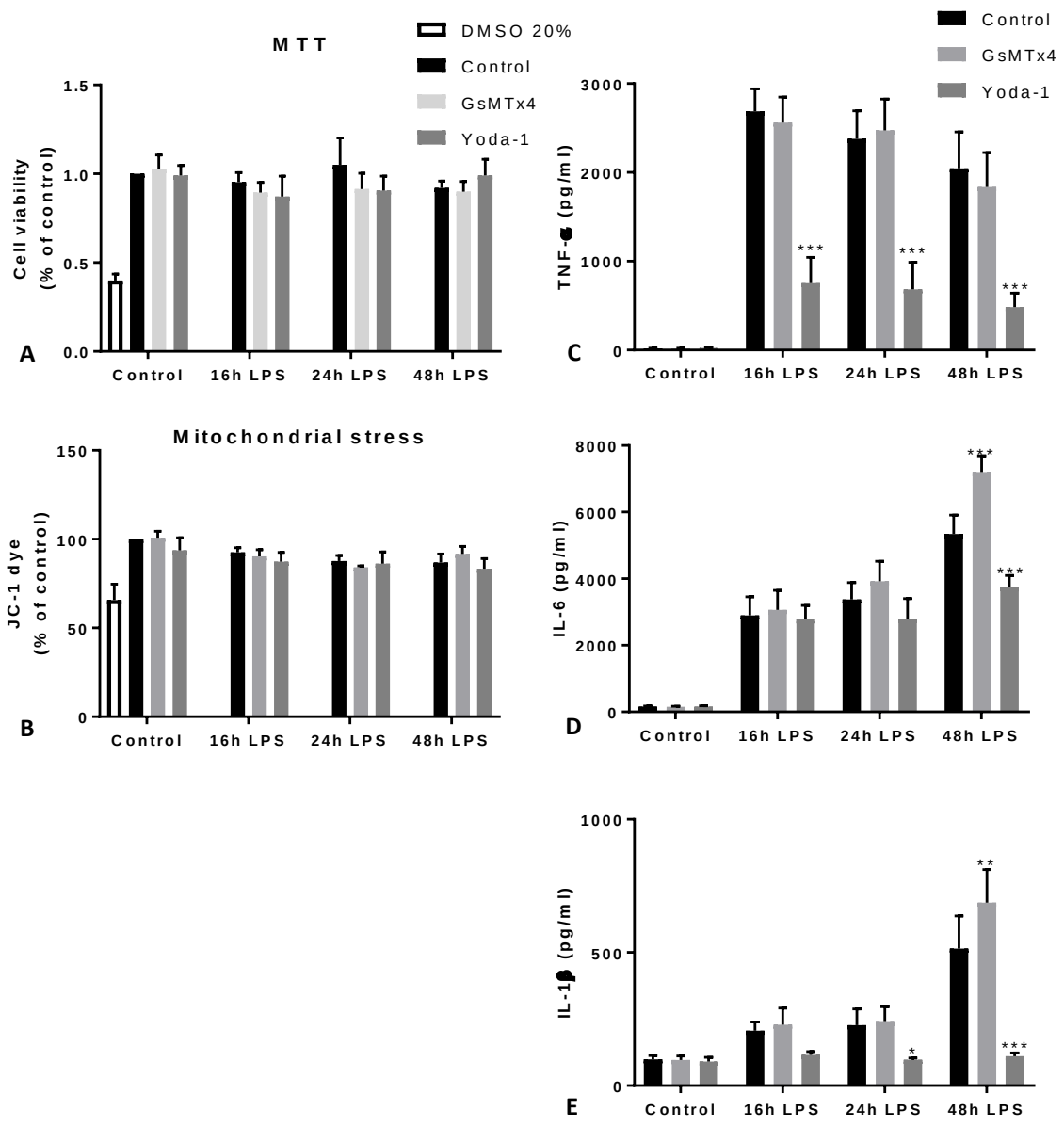

<u>Figure 3. 6</u>: Activation of Piezo1 by Yoda-1 decreases the release of proinflammatory cytokines TNF-α, IL-1β and IL-6 without affecting cell viability

(A) MTT assays of MA astrocytes under different treatments showed that activation or inhibition of Piezo1 by Yoda-1 or the Piezo1 inhibitor GsMTx4 had no effect on the cell viability of MA or **(B)** mitochondrial stress by the JC-1 assay. **(C)** However, activation of Piezo1 with Yoda-1 significantly attenuated the release of TNF-α under LPS treatment, whereas its inhibition with GsMTx4 had no effect on the levels of TNF-α. **(C, D)** Yoda-1 also diminished the levels of IL-6 and IL-1β under 24h and 48h LPS treatment in MA, while GsMTx4 significantly increased the levels of IL-6 and IL-1β, compared to control 48h LPS treatment. Repeated measures one-way ANOVA, Newman-Keuls post-hoc test was used. Data shown as mean ± SEM, n=5, dF=6; being each experimental unit cells from the same flask and passage.

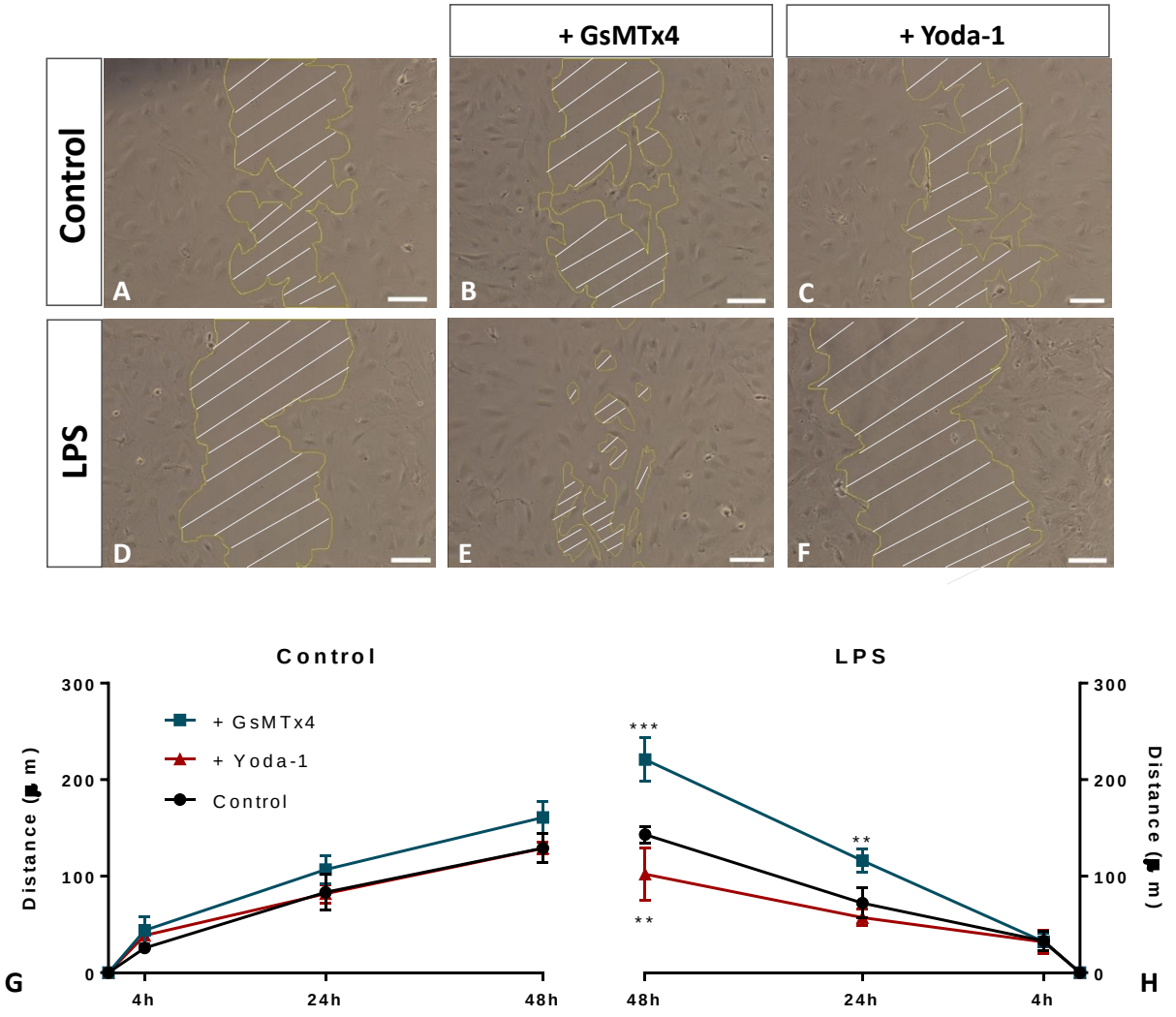

Figure 3. 7: GsMTx4 accelerates astrocytic migration in LPS-stimulated astrocytes

(A-F) Wound-healing assay was used to measure the astrocytic migration rate in both control and 24h LPS-treated astrocytes, with or without SAC blocker GsMTx4 or the Piezo1 activator Yoda-1. **(G)** Migrated distance of unstimulated astrocytes and **(H)** LPS-stimulated astrocytes with or without GsMTx4 or Yoda-1. Statistical analysis performed with two-way ANOVA, Dunnet's post-hoc test. Data shown as mean ± SEM, n=5, dF=20; being each experimental unit cells from the same flask and passage. Scale bar = 50μm.

3. Discussion

3.1. Summary of findings

The mechanosensitive channel, Piezo1, was described in the mouse neuroblastoma cell line Neuro2A, in 2010 (Coste et al., 2010). Since then, its expression has also been reported and studied in the bladder (T. Miyamoto et al., 2014), kidney (Peyronnet et al., 2013), skin (Eisenhoffer et al., 2012), lungs (McHugh et al., 2012) and red blood cells (Albuisson et al., 2013; Faucherre et al., 2014). In the current study, we showed that expression of Piezo1 in mouse astrocytes can be induced by toxic and inflammatory stimuli such as LPS, psychosine or amyloid-β42 microglial conditioned media, while it is absent under physiological conditions. We also showed that the expression of Piezo1, under these toxic and inflammatory stimuli, is located in the ER. We observed that activation of Piezo1 by the specific agonist Yoda-1 caused the release of Ca^{2+} from intracellular stores as well as a longer subsequent ATP response, where the intracellular Ca^{2+} levels were maintained following stimulation with ATP. Moreover, the pharmacological modulation of Piezo1 altered the reactive state of astrocytes in terms of cytokine release and migration rate without altering the cell viability or mitochondrial stress **(Supplemental Figure 3.1)**.

Collectively, our results suggest that astrocytes are cells highly sensitive to mechanical cues, with capacity to overexpress Piezo1 in the endoplasmic reticulum under certain pathological stimuli. Mechanical changes both in the cytoskeleton and in the extracellular matrix may lead to activation of these mechanical receptors, such as Piezo1, modulating the Ca^{2+} signalling cascades and reactive state of astrocytes. Further research needs to be done in order to assess the specific mechanism of action by which Piezo1 may modulate astrocytic responses, as well as to further understand the role of Piezo1 as a promising target for regulating and treating neuroinflammation in the progression of certain pathologies.

3.2. Expression of Piezo1 in astrocytes is only induced under certain inflammatory stimuli

It has been shown that Piezo1 is expressed in multiple tissues in the organisms (Albuisson et al., 2013; Coste et al., 2010; Eisenhoffer et al., 2012; McHugh et al., 2012), including neuronal expression in physiological conditions (Koser et al., 2016). However, expression of Piezo1 has not been found in astrocytes under physiological conditions (Satoh et al., 2006). Here, we show that mouse astrocytes express Piezo1 under LPS, psychosine and amyloid-β CMM treatments. These inflammatory stimuli induced the expression of Piezo1 in the endoplasmic reticulum, but not on the plasma membrane. LPS is an activator of the TLR4 that is activated in bacterial infection. Upon activation, TLR4 modulates the expression of several inflammatory genes that play a central role in the innate immune response (Akira & Takeda, 2004). Psychosine is a toxin that accumulates in the brain in Krabbe's disease, due to the lack of the enzyme galactosylceramidase (Davenport et al., 2011). Although psychosine has not been reported as a proinflammatory stimulus, it potentiates the release of LPS-induced cytokines and nitric oxide (NO) in rat astrocytes (Giri et al., 2002). Based upon all these results, we suggest that Piezo1 expression in astrocytes is induced under such conditions in order to regulate the production of proinflammatory cytokines and to modulate the migration capacity of the astrocytes, two of the main features of reactivity in astrocytes in the CNS (Y. Su et al., 2017). Our results are in agreement with the literature, where previous studies have suggested that activation of Piezo1 in the ER leads to an activation of the cell-to-cell adhesion mediated by integrins, and that Piezo1 knock-down leads to cell detachment and higher mobility in lung cells (McHugh et al., 2012). Under TNF-α/IL17a or H_2O_2 treatment, mouse astrocytes did not express Piezo1, which suggests that not all inflammatory or damaging stimuli induce the expression of the mechanoreceptor, therefore inferring that Piezo1 contribution to reactivity and astrocytic responses modulation may somehow be specific to certain pathological states.

3.3. Activation of Piezo1 with Yoda-1 causes release of Ca^{2+} from intracellular stores

The subcellular location of Piezo1 in differing cell compartments is likely linked to its functional roles. According to the literature, activation of Piezo1 in the ER alters integrin signalling (McHugh et al., 2012). In addition, modulation of Piezo1 expressed at the basal membrane regulates certain functions such as durotaxis (Koser et al., 2016). In the present study, we found that the activation of Piezo1 with Yoda-1, under inflammatory conditions (LPS treatment) and in the absence of extracellular Ca^{2+} and Mg^{2+}, led to intracellular Ca^{2+} signalling, which we hypothesise this was likely due to the release of Ca^{2+} from intracellular stores. Of interest, in

these inflammatory conditions (LPS treatment), activation of Piezo1 by Yoda-1 induced a longer Ca^{2+} response to ATP stimulation, maintaining oscillating intracellular levels of Ca^{2+} following ATP stimulation, while just one peak of Ca^{2+} released from intracellular stores following ATP stimulation happened in control astrocytes or LPS astrocytes with no Yoda-1. In agreement that Piezo1 regulated ATP signalling, it has been shown that activation of Piezo1 increases the levels of endogenous ATP (Cinar et al., 2015; T. Miyamoto et al., 2014; S. Wang et al., 2016), which in turn could activate receptors such as inositol-3-phosphate receptor (IP3) causing an enhanced release of Ca^{2+} from intracellular stores like ER. This putative mechanism could explain the effects we observed of Yoda-1 on ATP-induced Ca^{2+} signalling in astrocytes.

3.4. Pharmacological modulation of Piezo1 alters the release of proinflammatory cytokines upon LPS treatment

Tumour Necrosis Factor alpha (TNF-α) is a proinflammatory cytokine, considered one of the main mediators of neuroinflammation leading to multiple biochemical cascades that eventually culminates in cell death in CNS disease (Haile et al., 2010; Potrovita et al., 2004; Wen et al., 2015). Interleukin-6 (IL-6) is a pleiotropic cytokine that plays a key role in the interaction between the immune and the nervous system. Interleukin-1β (IL-1β) is a pro-inflammatory cytokine from the IL-1 family, involved in neuroinflammation and host defence (Allan, Tyrrell, & Rothwell, 2005). The levels of IL-1β are upregulated in the CNS under conditions of stress, damage and disease such as Alzheimer's disease (Xuan et al., 2015), acute brain injury (Murray, Parry-Jones, & Allan, 2015), Parkinson's disease (Q. S. Zhang, Heng, Yuan, & Chen, 2017) or ischaemia (Denes et al., 2013). LPS acts as a trigger to these three proinflammatory cytokines, amongst others (Allan et al., 2005; Van Wagoner & Benveniste, 1999). Here we have shown that LPS-induced production of TNF-α, IL-6 and IL-1β increases with time and that it can be significantly reduced by activation of Piezo1 using its specific activator Yoda-1. Contrarily to this, inhibition of Piezo1 by GsMTx4 did not lead to any change in the levels of TNF-α but increased the levels of IL-6 and IL-1β, compared to the LPS treatment alone. These results indicate that Piezo1 plays, a role in proinflammatory response by altering the levels of cytokines by downregulating cytokine production upon activation.

3.5. Piezo1 plays a role in the modulation of astrocytic migration

Astrocytes are sensitive to changes in their environment and tissue or cellular damage, responding to insults in order to modify the brain response. The reactive state of astrocytes can be assessed by their morphological change, cytokine release and astrocytic migration rate. In this study we have shown how pharmacological modulation of Piezo1 under LPS stimulation not only alters the release of proinflammatory cytokines, but it also modifies the migrating capacity of the astrocytes. One of the regulators of cell migration is Ca^{2+}. Previous studies in the literature have shown that Piezo1 can regulate durotaxis of the neuronal growth cone (Koser et al., 2016) and migration of lung cancer cells (McHugh et al., 2012). Here, we show how modulation of Piezo1 can also alter the migration of astrocytes under LPS stimulation. Under inflammatory conditions, such as LPS, in which Piezo1 is overexpressed in the ER of astrocytes the inhibition of Piezo1 by GsMTx4 led to an increase in the migrated distance, while activation with Yoda1 had the opposite effect. These results are in line with our previous experiments in cytokine release, suggesting that activation of Piezo1 in astrocytes under presence of certain stimuli drive the cells into a non-reactive state, where proinflammatory cytokines and migration capacity are reduced. On the contrary, inhibition of stretch activated channels (SACs) by GsMtx4 causes a stronger inflammatory response of astrocytes, promoting the release of cytokines and migration velocity. This is the first time that Piezo1 has been reported as a modulator of the inflammatory response of astrocytes. Further research such as investigating whether astrocytic Piezo1 is differentially expressed depending on astrocytic phenotype A1 or A2, as well as studying in depth the biochemical cascades involved in these processes need to be done in order to fully understand the mechanisms of action underlying this regulation, as further discussed in **Chapter 6, heading 13**.

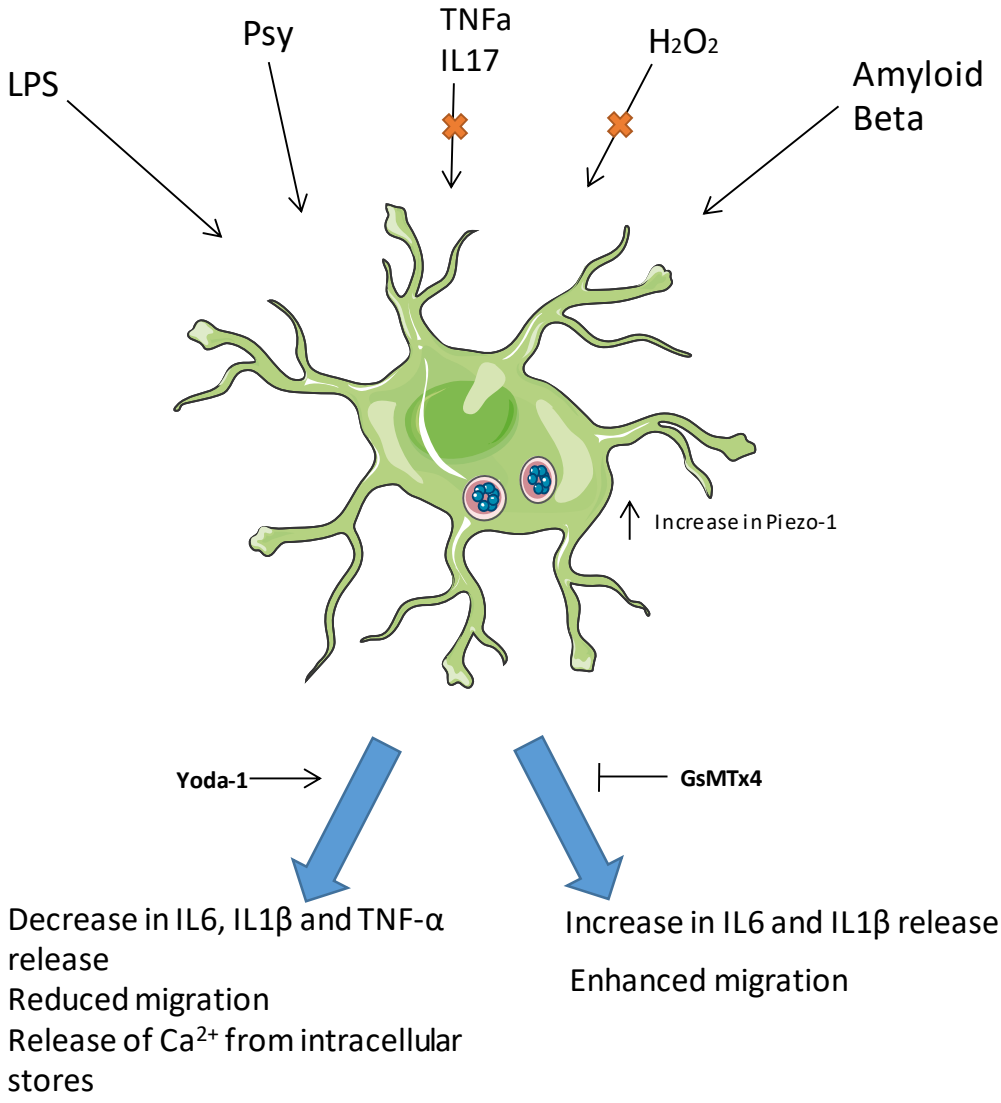

<u>Supplemental Figure 3. 1</u>: Expression of Piezo1 in astrocytes under LPS, PSY and Aβ42 treatment and its role in cytokine release modulation

Expression of Piezo1 was increased in mouse astrocytes after treatment with the stimuli LPS, PSY and Aβ42 MCM. No expression of Piezo1 was seen under TNF-α/IL-17a or H_2O_2 treatment, which suggests that only certain conditions allow the expression of Piezo1 in astrocytes. Pharmacological modulation of Piezo1 had effects on the inflammatory response of astrocytes: activation of Piezo1 by Yoda-1 led to a decrease in the release of TNF-α, IL-1β and IL-6 and decreased migration rate, whereas inhibition with GsMTx4 increased the levels of IL-6 and IL-1β and migrating velocity under LPS treatment. Furthermore, activation of Piezo1 by Yoda-1 caused a release of Ca^{2+} form intracellular stores and altered the subsequent responses of astrocytes to ATP stimulation.

Chapter 4:
Role of Piezo1 in pathology: astrocytic expression in Alzheimer's disease

Chapter aims

It has been shown in the literature (Satoh et al., 2006) that mRNA of Piezo1 seems to be upregulated in the astrocytes associated to senile plaques of human *post-mortem* Alzheimer's brains; however, it has never been studied whether this increment of astrocytic Piezo1 happens at a protein level. Based upon our findings *in vitro,* we hypothesize that Piezo1 expression may be induced in the astrocytes associated to the amyloid plaques *in vivo*. Thus, here we used the Alzheimer's rat model TgF344-AD, with or without repeated peripheral infections with *E.coli*, to analyse the astrocytic expression of Piezo1 in this pathology.

The specific aims of this chapter were:

- To characterise β-amyloid plaque load, glial cell reactivity and myelination phenotypes in the TgF344-AD Alzheimer's rat model.
- To study the effects of *E.coli* urinary tract infection (UTI) of TgF344-AD rats in the development of the pathology.
- To analyse the correlation of an increment in expression of Piezo1 and the levels of glial cell markers.
- To assess the effects of *E. Coli* UTI on the levels of Piezo1 expression.

Abstract

Amyloid plaque formation and deposition is one of the pathophysiological hallmarks of Alzheimer's disease. These are hard, brittle structures scattered throughout the brain that are thought to cause neurodegeneration, neurofibrillary tangles and tau hyperphosphorylation. Since recent years, the neuroinflammatory component in the etiopathology of Alzheimer's disease has gained more weight and it has been shown that reactive glia associate to these plaques having a dual effect: a beneficial initial inflammatory response, while prejudicial if chronic. Glial cells are highly mechanosensitive cells that can sense changes of the extracellular matrix stiffness in health and disease, through mechanically activated ion channels. Piezo1, a stretch-activated cation channel, can sense these external mechanical cues and translate them into chemical ones through a process termed '*mechanotransduction*'. In previous studies in our lab, we have shown how Piezo1 can be upregulated in primary astrocytes under pathological stimuli and modulate the reactivity of these cells, suggesting that Piezo1 is a regulator of the inflammatory response of astrocytes. Here, we used the transgenic Alzheimer's rat model TgF344-AD at 12- and 18-months old. We characterised the amyloid plaque load, astrocyte reactivity and myelin state of the model to assess the fitness of the TgF344-AD rats as an animal model for Alzheimer's disease. Furthermore, repeated urinary tract infections with *E.coli* were used to assess the contribution of infection to the pathology of Alzheimer's disease, as UTIs are the most common co-morbidity in the elder population affected with Alzheimer's disease. Interestingly, we found that infection enhanced the amyloid plaque deposition in cortex and hippocampus, as well as the reactive state of astrocytes and demyelination state. Moreover, we assessed the levels of Piezo1 and we observed that Piezo1 was upregulated in the astrocytes around the amyloid plaques, and that repeated infections further enhanced this upregulation. Altogether, these results suggest that ageing and peripheral infection increase the inflammatory response of astrocytes around the plaques and the expression of mechanosensors such as Piezo1. Further research needs to be done to assess the specific role of Piezo1 in the astrocytic response of Alzheimer's disease, and whether Piezo1 could prove to be a novel drug target for dementia.

1. Introduction

Alzheimer's disease (AD) is the most common form of dementia in the elderly population nowadays, with an estimation of over 47 million people affected around the world in 2017 according the UK Alzheimer's society (www.alzheimers.org.uk). Pathological hallmarks of AD are a progressive deposition of amyloid-β plaques (Aβ), formation of neurofibrillary tangles (NFTs), chronic neuroinflammation and neuronal loss (Amemori et al., 2015; Holtzman et al., 2011; Selkoe & Schenk, 2003). To date, there is no effective treatment for AD, and this could be due to a poorly understanding of AD etiopathology. The main hypothesis is the 'amyloid-β cascade hypothesis', which maintains that Aβ on its own is the primary trigger for AD. However, it has been observed that overproduction of Aβ on its own is not enough to develop a proper phenotype in animal models, unless it is combined with other AD-linked genes (Holcomb et al., 1998; Jankowsky et al., 2001). Recently, the importance of neuroinflammation in AD coined the term 'inflammation hypothesis of AD'. This hypothesis supports the idea that chronic inflammation alongside neuronal ageing leads into cellular stress and impairment of neuronal function, triggering the pathology of AD (Krstic & Knuesel, 2013).

Neuroinflammation plays a dual role in the progression of AD: initial inflammation, in terms of reactive glia, is beneficial for the degradation of Aβ plaques (Akiyama et al., 1996; C. Liu et al., 2014), but a chronic inflammatory state has a detrimental effect in the progression of AD (C. Liu et al., 2014). It has been shown that both acute and chronic systemic inflammation in AD patients is associated to an increased cognitive decline (Holmes et al., 2009). Not only that, but chronic inflammatory conditions such as obesity, depression or diabetes represent a risk factor for developing AD (Casserly & Topol, 2004; Cunningham & Hennessy, 2015; Johnson et al., 2015). As this pathology mostly affects the elderly, AD research should take into account the general health of these patients and how comorbidities could affect the progression of the condition. These factors are getting increasing attention, as it has been shown that AD patients have more additional medical conditions than patients with no AD (Clodomiro et al., 2013; Duthie et al., 2011). The neuroinflammation state of the AD brain results in the activation of microglia and astrocytes, which release different cytokines and contribute to the chronic immune response (C. Liu et al., 2014). Deposits of Aβ cause astrogliosis in the damaged areas (Johnstone, Gearing, & Miller, 1999) and the reactive astrocytes can migrate to the Aβ aggregates and degrade them, helping clear these deposits (Wyss-Coray et al., 2003). As a tool for studying AD *in vivo*, a transgenic rat carrying the 'Swedish' mutant human APP (APP_{SWE}) and mutant human presenilin-1 (*PS1ΔE9*), denominated TgF344-AD rats, was developed in 2013

(Cohen et al., 2013). This model expresses accumulation of Aβ oligomers as well as tauopathy (Cohen et al., 2013; Tsai et al., 2014). Importantly, the TgF344-AD rat model also presents other symptoms typical from AD which are usually absent in most models, such as early vascular dysfunction (Joo et al., 2017), anxiety-like behaviour and memory impairment (Pentkowski et al., 2018) or ocular dysfunction (Tsai et al., 2014); making the TgF344-AD rat model a more translatable animal model to human Alzheimer's disease. Furthermore, we aimed to mimic one of the most common co-morbidities in AD patients, urinary tract infections (UTI). As AD mostly affects the elderly, UTI are fairly common and have been observed to exacerbate the progression of the disease probably by enhancing the inflammatory conditions of the organism.

An implication of the deposition of Aβ in the AD brain is the change in the tissue stiffness around the plaques. Despite amyloid fibrils are significantly stiffer than the neuropil of neurons and glia (Y. B. Lu et al., 2006), it has been shown that brain stiffness decreases in AD both in patients (Murphy et al., 2011) and mouse model (Murphy et al., 2012) and correlates with the severity of the cognitive impairment of the pathology (Murphy et al., 2016). Astrocytes, as any other cell, sense changes in stiffness and develop a response to it. For example, changes in ECM stiffness of the brain cause astrocyte activation in rat tissue (Moshayedi et al., 2014). Changes in the mechanical properties of the tissue are detected mostly by mechanosensitive receptors, which transduce mechanical signals into chemical ones in less than millisecond timescale (Bavi et al., 2017; Cox et al., 2016). Thus, mechanosensitive receptors involved in the progression of different pathologies may be a new interesting target.

Studies on post-mortem analysis of AD brains revealed that Piezo1 mRNA was down-regulated in neurons and up-regulated in astrocytes associated to the Aβ plaques (Satoh et al., 2006). In previous studies in our lab, we have shown how astrocytes under different stimuli, such as LPS or Aβ CMM, can start expressing Piezo1 in the ER, while it is absent in physiological conditions **(Chapter 3)**. In this study, we used the AD rat model TgF344-AD to analyse the expression of Piezo1 in two of the areas most affected by Aβ deposition: cortex and hippocampus. We also characterised the phenotype of the TgF344-AD model in terms of Aβ deposition and size, astrogliosis and myelination state; and how UTI with *E.coli*, one of the most likely causes of infection in elderly people with dementia, affected the development of the pathology. Our results suggest that restoring homeostatic mechanotransduction pathways and neuron/glial crosstalk around amyloid plaques may lead to the discovery of novel drug targets for neurodegeneration and AD treatment.

2. Results

2.1. Peripheral infection of TgF344-AD rats triggers the Aβ deposition and plaque size

TgF344-AD rats are a transgenic model expressing the APP_{SWE} and *PSEN1ΔE9* mutations. APP_{SWE} mutation is responsible for an increased abnormal cleavage of cellular APP by β-secretases; while *PSEN1ΔE9* encodes a mutated form lacking the exon 9 of presenilin-1, which is the catalytic of γ-secretases, also responsible for the cleavage of APP. The combination of both mutations leads to a hereditary and quickly developed form of AD in animal models. In order to assess this AD model and how the UTI infection with *E.coli* could affect the development of the pathology, we first studied the Aβ deposition, fluorescence intensity and plaque size in the hippocampus, in 12 and 18 months old wild-type (WT) and transgenic (TG) rats, with or without the peripheral infection using immunohistochemistry of 12µm sagittal sections of the rat brains **(Figure 4.1)**. It can be observed that, as expected, all TG rats showed plaque deposition, while this pathological hallmark was absent in WT rats **(Figure 4.2 A-D)**. Interestingly, we observed that the number of plaques (0.29 ± 0.11 plaques/pixel^2 vs 0.48 ± 0.05 plaques/pixel^2, $^{###}$p<0.001; three-way ANOVA following Holm-Sidak post-hoc test; n=6, dF=1) **(Figure 4.2G)** and their fluorescence intensity in the hippocampus of TG rats increased with age (37.35 ± 2.83 vs 63.44 ± 2.54, $^{###}$p<0.001; three-way ANOVA following Holm-Sidak post-hoc test; n=6, dF=1) **(Figure 4.2F)**, while the plaque size decreased (0.22 ± 0.03 vs 0.17 ± 0.02, $^{\#}$p=0.02; three-way ANOVA following Holm-Sidak post-hoc test; n=6, dF=1) **(Figure 4.2E)**. This decrease in size could be due to an initial attempt from microglia and astrocytes to clear the Aβ deposits (Jones, Minogue, Connor, & Lynch, 2013; Ries & Sastre, 2016) which nevertheless, is not enough to stop the Aβ production in the pathology. Furthermore, peripheral infection caused a further increase in the number (12m.o.: 0.43 ± 0.05 vs 0.29 ± 0.11 plaques/pixel^2, $^{\$\$\$}$p<0.001 and 18m.o.: 0.58 ± 0.04 plaques/pixel^2, $^{\$}$p=0.01) **(Figure 4.2G)** and the fluorescence intensity of plaques (12m.o: 48.75 ± 3.3 vs 37.35 ±2.83, $^{\$\$}$p=0.003 and 18m.o.: 66.46 ± 3.0 vs 63.44 ± 2.54, n.s. p=0.89) **(Figure 4.2F)** as well as bigger size of the plaques (12m.o: 0.27 ± 0.05 vs 0.22 ± 0.03, $^{\$}$p=0.024 and 18m.o:0.22 ± 0.04 vs 0.17 ± 0.02, $^{\$}$p=0.013) **(Figure 4.2E)** compared to their non-infected age and genotype match group, suggesting that peripheral infection contributes to a more aggressive phenotype of AD at least partly due to an increase in Aβ deposition.

2.2. Astrogliosis in AD increases with age and peripheral infection

The contribution of neuroinflammation to the development of AD has gained increasing importance over recent years. It has been shown that initial inflammation has a beneficial role for the restrain of the pathology, by activating both astrocytes and microglia which try to clear the new Aβ deposits in the brain (Ries & Sastre, 2016). However, this clearance is not enough, and the persistent activation of glia leads to chronic neuroinflammation, which then has a detrimental effect. Here, we analysed the reactivity of astrocytes by analysing the number, GFAP intensity and morphology of astrocytes in the hippocampus **(Figure 4.3 A-D)**. We observed that the number of astrocytes increased with age (12mo WT: 3.392 ± 0.04 vs 18mo WT: 7.56 ± 1.65, $^{\#\#}$p=0.0036; three-way ANOVA following Holm-Sidak post-hoc test, n=6, dF=1) **(Figure 4.3E)**, and that it was further increased by both AD pathology (12mo TG: 5.51 ± 1.95 vs 3.392 ± 0.04, n.s. p=0.28 and 18mo TG: 9.14 ± 1.7 vs 7.56 ± 1.65, n.s. p=0.40) **(Figure 4.3F)** and infection (12mo iTG: 6.037 ± 2.32 vs 5.51 ± 1.95, n.s. p=0.7 and 18mo iTG: 16.81 ± 3.4 vs 9.14 ± 1.7, $^{\$\$\$}$p<0.001) **(Figure 4.3G)**, in a concomitant manner. More interestingly, when analysing the morphology of the astrocytes, we observed that both age (WT: 0.076 ± 0.004 vs 0.067 ± 0.003, $^{\#}$p=0.03; TG: 0.0697 ± 0.008 vs 0.0593 ± 0.003, $^{\#\#}$p=0.005; three-way ANOVA following Holm-Sidak post-hoc test, n=6, dF=1) and infection (12mo WT: 0.068 ± 0.005 vs 0.076 ± 0.004, $^{\$}$p=0.03; 18mo WT: 0.0598 ± 0.004 vs 0.067 ± 0.003, $^{\$}$p=0.03) diminish the branch length, leading to a bigger and more globular phenotypic morphology of the astrocytes **(Figure 4.3 J)**. Additionally, the GFAP fluorescence intensity was found to increase in TG rats with age (5.85 ± 2.71 vs 26.58 ± 3.29, $^{\#\#\#}$p<0.001; three-way ANOVA following Holm-Sidak post-hoc test, n=6, dF=1) and infection (12mo: 36.16 ± 4.19 vs 5.85 ± 2.71, $^{\$\$\$}$p<0.001 and 18mo: 61.18 ± 4.55 vs 26.58 ± 3.29, $^{\$\$\$}$p<0.001) **(Figure 4.3 I)**. These two parameters can be used as markers for astrocyte reactivity, as it has been shown that GFAP increases in astrogliosis (Mucke & Eddleston, 1993; Sofroniew, 2009) and that astrocytes undergo changes in morphology leading to hypertrophy (Sofroniew & Vinters, 2010). Furthermore, we observed that the peripheral infection with *E.coli* triggered a stronger astrogliosis, leading to higher number of astrocytes, higher expression of GFAP fluorescence intensity and smaller bodies with smaller branch length **(Figure 4.3 E-G)**. These results support the role of astrocytes contributing to the neuroinflammation state of the brain in AD and show how pathology not only has a detrimental effect on the onset and development of AD because of the Aβ plaque deposition, but also by worsening the chronic neuroinflammatory state of the astrocytes.

2.3. Ageing and amyloid plaque pathology trigger the expression of Piezo1.

It is believed that Piezo1 is absent in astrocytes, at least under physiological conditions (Coste et al., 2010) and we find that certain pathological or inflammatory stimuli, such as LPS or psychosine, can trigger the expression of Piezo1 in the ER of astrocytes *in vitro* **(Chapter 3)**. Therefore, we investigated if upregulation of Piezo1 in astrocytes was also evident *in vivo* using the TgF344-AD rat model. With this in mind, we triple stained 18-months old TgF344-AD rat brain for Piezo1, Aβ and GFAP. High magnification (100X) Z-stack projections demonstrated an upregulation of Piezo1 in reactive astrocytes surrounding the amyloid plaques in prefrontal cortex **(Figure 4.4 A-G)**. We observed there was a three-fold upregulation of Piezo1 on the astrocytes surrounding the plaques (290.1% ± 13.9% vs 100.0% ± 7.1%; ***p<0.001; unpaired t-test with Welch's correction, n=25, dF=24) compared to those located at least 200µm away from any plaque **(Figure 4.4 B).** Interestingly, the expression of Piezo1 *in vivo* closely resembled the pattern observed *in vitro* as seen in **Chapter 3**, showing expression in circa 30% of the astrocytes around the plaques. This expression was found to be perinuclear, indicating that Piezo1 likely co-localizes with the endoplasmic reticulum. To assess whether the levels of Piezo1 changed in AD *in vivo*, we then characterised the spatiotemporal fluorescence changes of Piezo1 in the different areas of hippocampus and cortex in 12- and 18-months old WT and TgF344-AD rats **(Figure 4.4 H-O)**. It can be observed, in all cases (CA1, CA3, Dentate gyrus and cortex), that both age and pathology caused an increase in the levels of Piezo1. More specifically, there was an average increase of Piezo1 of 74.7% normalized to control in 12-months old (CA1: 68% ± 4.8%; CA3: 58% ± 6.5%; DG: 98% ± 2.0%; ***p<0.001; three-way ANOVA following Holm-Sidak's post-hoc test, n=10, dF=1) and of 101% in 18-months old TgF344-AD rats compared to age-matched WT rats (CA1: 89% ± 5.4%; CA3: 79% ± 5.3%; DG: 135% ± 2.3%; ***p<0.001) **(Figure 4.4 L-N)**. This increase was similar in cortical areas, where Piezo1 levels were higher in 12- (2.5% ± 1.3%; *p<0.05) and 18-months old (29.0% ± 1.0%; ***p<0.001) TgF344-AD rats compared to age-matched WT **(Figure 4.4 O)**. Furthermore, in WT rats, an increased expression of Piezo1 was evident during ageing in specific hippocampal areas of the CA1 (34% ± 4.23%; $^{###}$p<0.001) and DG (22% ± 1.0%; $^{###}$p<0.001), as well as the cortex (14% ± 1.5%; $^{###}$p<0.001) **(Figure 4.4 L-O)**. Taken together, both ageing and amyloid plaque pathology trigger the increase in expression of Piezo1 channel on cortical and hippocampal areas of TgF344-AD rats.

2.4. Piezo1 expression is upregulated by peripheral bacterial infection

To investigate the effects of peripheral bacterial infection in the development of pathology and Piezo1 expression, 12-months old rats were exposed to a urinary tract infection (UTI) with *E.coli* at 8 and 11 months of age; while 18-months old rats had two more infections at 14 and 17 months of age (iTG). This peripheral infection enhanced the expression of Piezo1 in 12- and 18-months TgF344-AD rats compared to their age-matched non-infected TgF344-AD rats in hippocampal but mostly cortical areas **(Figure 4.4 L-O)**. Moreover, peripheral infection also upregulated the levels of Piezo1 in cortical areas in WT rats at 12-months (13.6% ± 1.5%; $^{\$\$\$}$p<0.001; three-way ANOVA following Holm-Sidak's post-hoc test, n=10, dF=1) and 18-months old (25.0% ± 2.0%; $^{\$\$\$}$p<0.001), showing that the upregulation induced by infection is not fully dependant on the age or amyloid plaque pathology. These results indicate that repeated UTI enhances Piezo1 expression in the cerebral cortex of WT rats and it also causes a further and above increase in the expression of Piezo1 compared to that seen in response to amyloid plaques alone. To demonstrate the specificity of the polyclonal antibody sc-1643419 used against Piezo1, we synthesized the antigen against this specific antibody by solid-phase synthesis and confirmed its synthesis with MicroTOF mass spectrometry **(Supplemental Figure 4.1 A-B)**. Once we had successfully synthesize the antigen for the antibody, we then confirmed that incubation of Piezo1 antibody with the synthesized control peptide led to a blocking of the signal in immunohistochemistry compared to standard immunohistochemistry, validating our immunolabelling technique for Piezo1 **(Supplemental Figure 4.1 C-H).**

2.5. Myelin state is altered in amyloid-plaque pathology.

Amyloid plaque deposition is not the only hallmark of AD, which also comprises neurodegeneration, neuroinflammation and taupathy. Additional to this, it has been observed a disruption and degradation of myelin sheath in AD patients (X. Zhan et al., 2014; X. Zhan et al., 2015). There are some studies that lead to the hypothesis that the myelin injury is involved in the early stages of the AD onset, as initial amyloid-β deposits are developed in the poorly myelinated gray matter areas of the brain (Braak & Braak, 1997; Braak, Braak, & Kalus, 1989) and myelin breakdown is observed at the earliest stages of the AD onset (Bartzokis, Lu, & Mintz, 2007; de la Monte, 1989). Hence, we characterised the levels of the myelin component proteolipid protein (PLP) in hippocampus and cortical areas **(Figure 4.5)**. We noted that TgF344-AD rats expressed lower levels of PLP in all areas at 12- (Hipp: 55.22 ± 1.51 vs 65.46 ± 2.00, ***p<0.001; PFC: 28.49 ± 1.21 vs 40.76 ± 1.64, ***p<0.001; FPC: 29.89 ± 1.07 vs 39.17 ± 1.06,

***p<0.001; AVC: 37.71 ± 1.06 vs 47.09 ± 1.61 a.f.u., ***p=0.0002; three-way ANOVA following Holm-Sidak's post-hoc test, n=6, dF=1) and 18-months old (Hipp: 52.31 ± 2.16 vs 60.28 ± 1.75, *p=0.01; PFC: 33.29 ± 1.27 vs 42.91 ± 1.61, ***p<0.001; FPC: 40.49 ± 1.32 vs 47.34 ± 1.91, **p=0.0011; AVC: 46.60 ± 1.512 vs 59.24 ± 2.28, ***p<0.001) compared to their age-matched controls **(Figure 4.5 E-H)**, showing that amyloid pathology leads to a decrease in the myelin protein levels. Furthermore, we noted that peripheral infection with *E.coli* enhanced this demyelination, both in WT and TgF344-AD rats compared to their age- and genotype-matched non-infected counterparts **(Figure 4.5 E-H)**. Interestingly, we found a linear correlation between the fluorescence intensity levels of Piezo1 and PLP in both overall cortex (y=0.5542x+17.42; r=0.5715, ***p<0.001; Pearson r correlation analysis, number of XY pairs=720) and hippocampus (y=0.1164x+13.95; r=0.3362, ***p<0.001; Pearson r correlation analysis, number of XY pairs = 720) **(Figure 4.5 I-J)**, in agreement with our previous observations of expression of Piezo1 in highly myelinated areas of the brain *(unpublished data)* and leading to the hypothesis that Piezo1 may play a role in axonal stability and/or myelin state.

2.6. Piezo1 expression strongly correlates with amyloid plaque deposition in the hippocampal dentate gyrus

We observed from our immunohistochemistry analysis that both GFAP and Piezo1 expression were higher around the amyloid plaques, especially in hippocampus, which was also found to be an area with high plaque deposition. To assess the relationship between GFAP, Piezo1 and $A\beta_{1\text{-}42}$ expression, we correlated their intensity values in the dentate gyrus of the hippocampus of all groups **(Figure 4.6)**. As expected, and in agreement with our previous *in vitro* studies (non-stimulated conditions) in **Chapter 3**, we did not observe a linear relationship between GFAP and Piezo1 in 12- and 18-months old WT rats (12mo: r=0.02795, n.s. p=0.52; 18mo: r=0.2681; n.s. p=0.51; Pearson r correlation, number of XY pairs = 540 and 960, respectively). However, under infection and/or amyloid plaque deposition, there was a linear correlation between the expression of GFAP and Piezo1, mostly in TgF344-AD with peripheral infection animals (12mo iTG: r=0.3216, ***p<0.001; 18mo iTG: r=0.5119, ****p<0.001; Pearson r correlation, number of XY pairs = 580 and 720, respectively) **(Figure 4.6 A-H)**. This supports our previous results showing that expression of Piezo1 in astrocytes is enhanced in amyloid pathology and under infection, both of which also lead to an increase of astrocyte reactivity and GFAP expression. Moreover, we noted a linear correlation between GFAP and $A\beta_{1\text{-}42}$ in both 12- (r=0.5425, ***p<0.001; Pearson r correlation analysis, number of XY pairs = 720) and 18- (r=0.6482, ***p<0.001;

Pearson r correlation analysis, number of XY pairs = 720) months old TgF344-AD, which was further accentuated in those animals with peripheral infection (12mo iTG: r=0.648, ***p<0.001; 18mo iTG: r=0.734, ***p<0.001; Pearson r correlation analysis, number of XY pairs = 580 and 720, respectively) **(Figure 4.6 I-L)**, supporting our previous data, noting that plaque deposition leads to an increase of astrocyte reactivity, which is enhanced by peripheral infection with *E.coli*. Finally, we observed a linear correlation between Piezo1 and $A\beta_{1-42}$ in 12- and 18-months old TgF344-AD rats with or without peripheral infection **(Figure 4.6 M-P)**, suggesting that Piezo1 is overexpressed around the plaques, in accordance with our previous analysis. Altogether, these results suggest that both peripheral infection with *E.coli* and deposition of amyloid plaques are concomitant triggers for the expression of mechanosensing Piezo1 channel in reactive astrocytes *in vivo*.

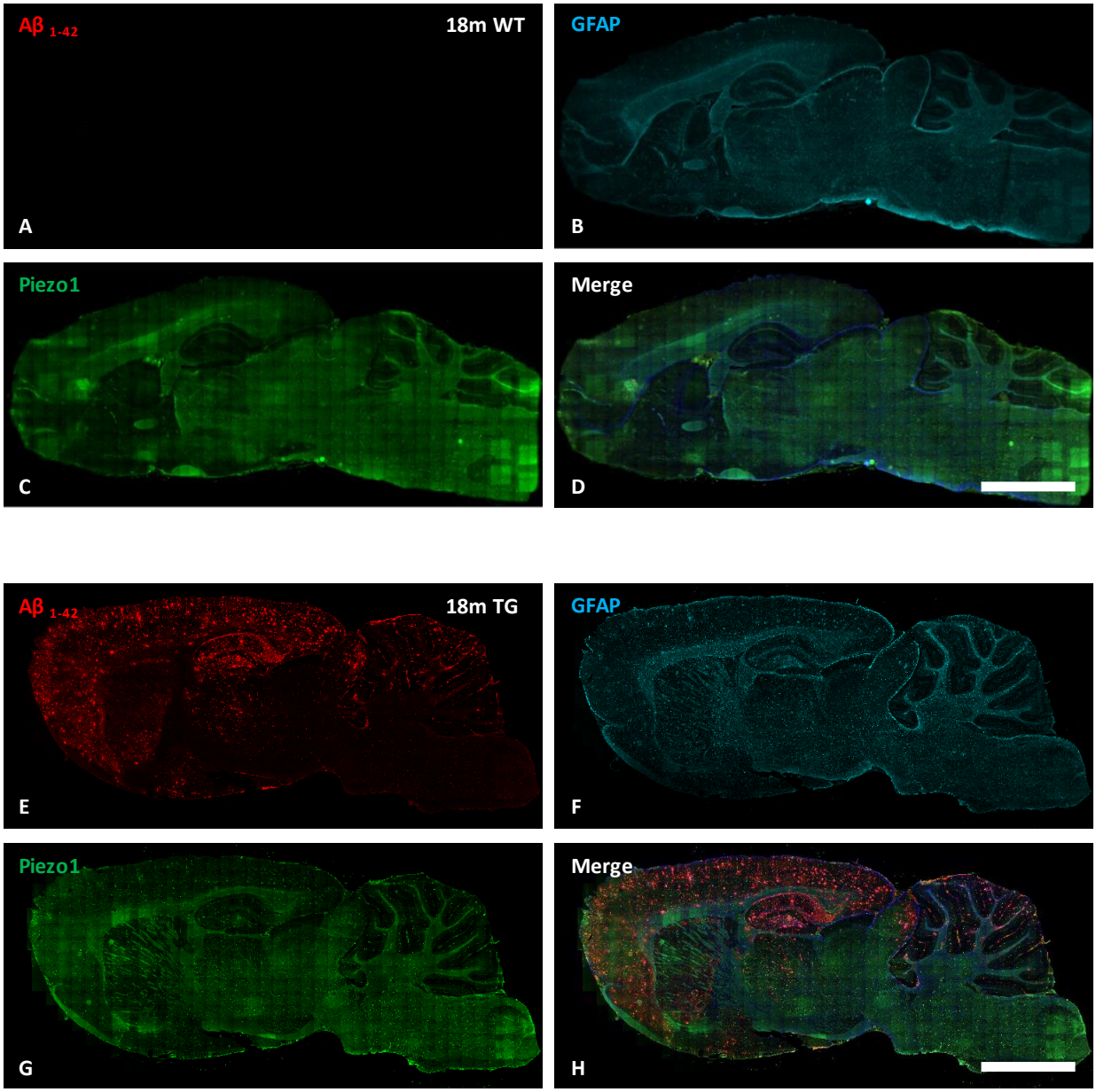

Figure 4. 1: Piezo1 expression in the TgF344-AD rat model of Alzheimer's disease

(A-D) Immunohistochemical staining of 18-months old wildtype rat brain and **(E-H)** transgenic TgF344-AD rat brain were stained for **(A, E)** $A\beta_{1-42}$ plaques, **(B, F)** astrocytic GFAP and **(C, G)** mechanosensitive channel Piezo1, showing their distribution on a sagittal plane of the rat brain. Scale bar = 300µm.

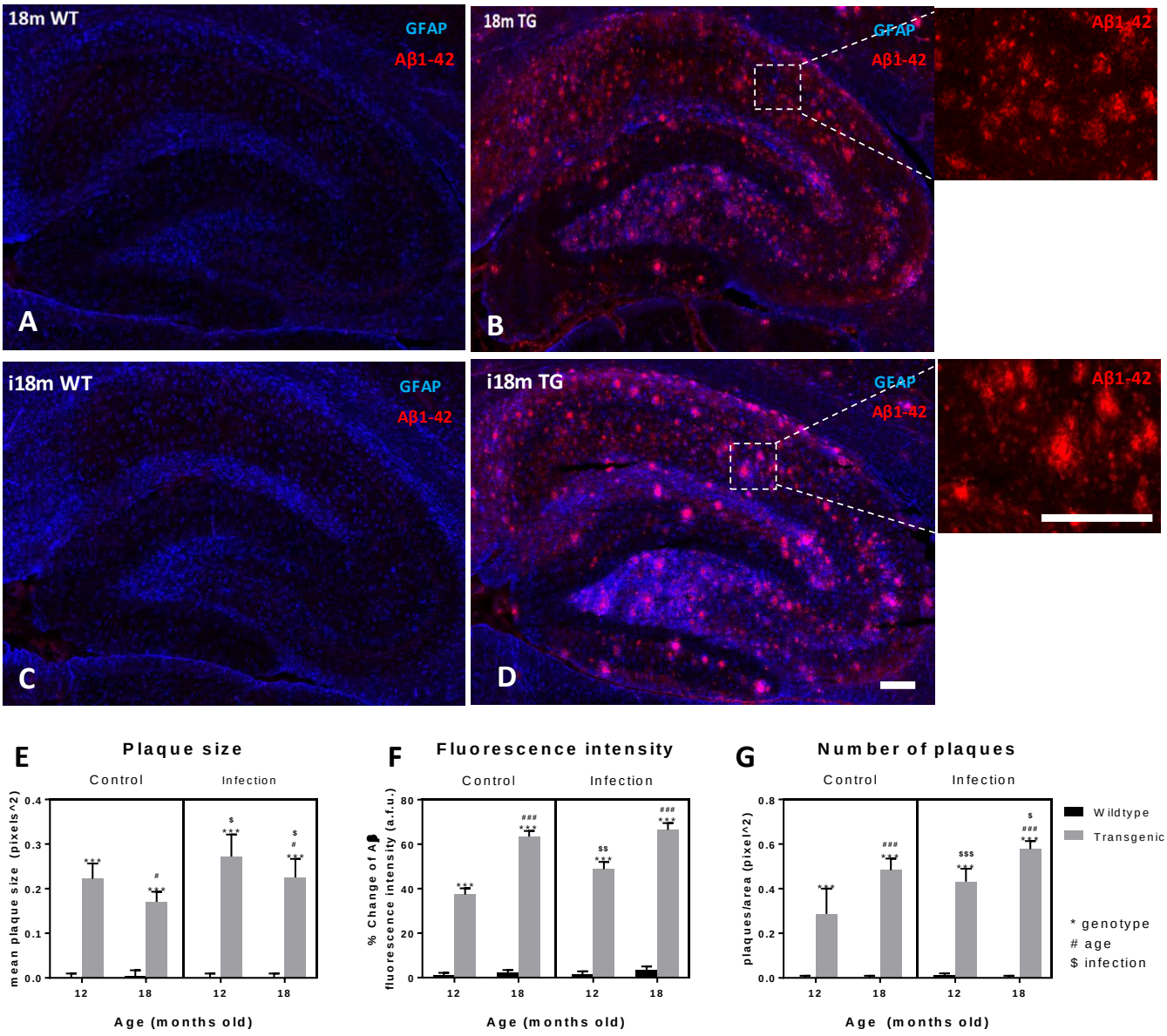

Figure 4. 2: Plaque deposition in TG rats is enhanced by peripheral infection

(A-D) Sagittal planes of 18-months old WT and TgF344-AD rats with or without peripheral infection were stained for astrocytic GFAP and $A\beta_{1-42}$ plaques. **(E)** Plaque size, **(F)** fluorescence intensity and **(G)** number of plaques were analysed and it was observed that these values were enhanced in TgF344-AD rats with peripheral infection compared to their non-infected age-matched counterparts. Statistical analysis was performed using a three-way ANOVA following Holm Sidak's multiple comparison post-hoc test. Data is shown as mean ± SEM. N=5-6, being each n a different animal per group, dF= 1. *p compared to age-matched WT group, $^{\#}$p compared to phenotype-matched 12-month old group, $^{\$}$p compared to age- and genotype-matched non-infected group. Scale bar = 40µm.

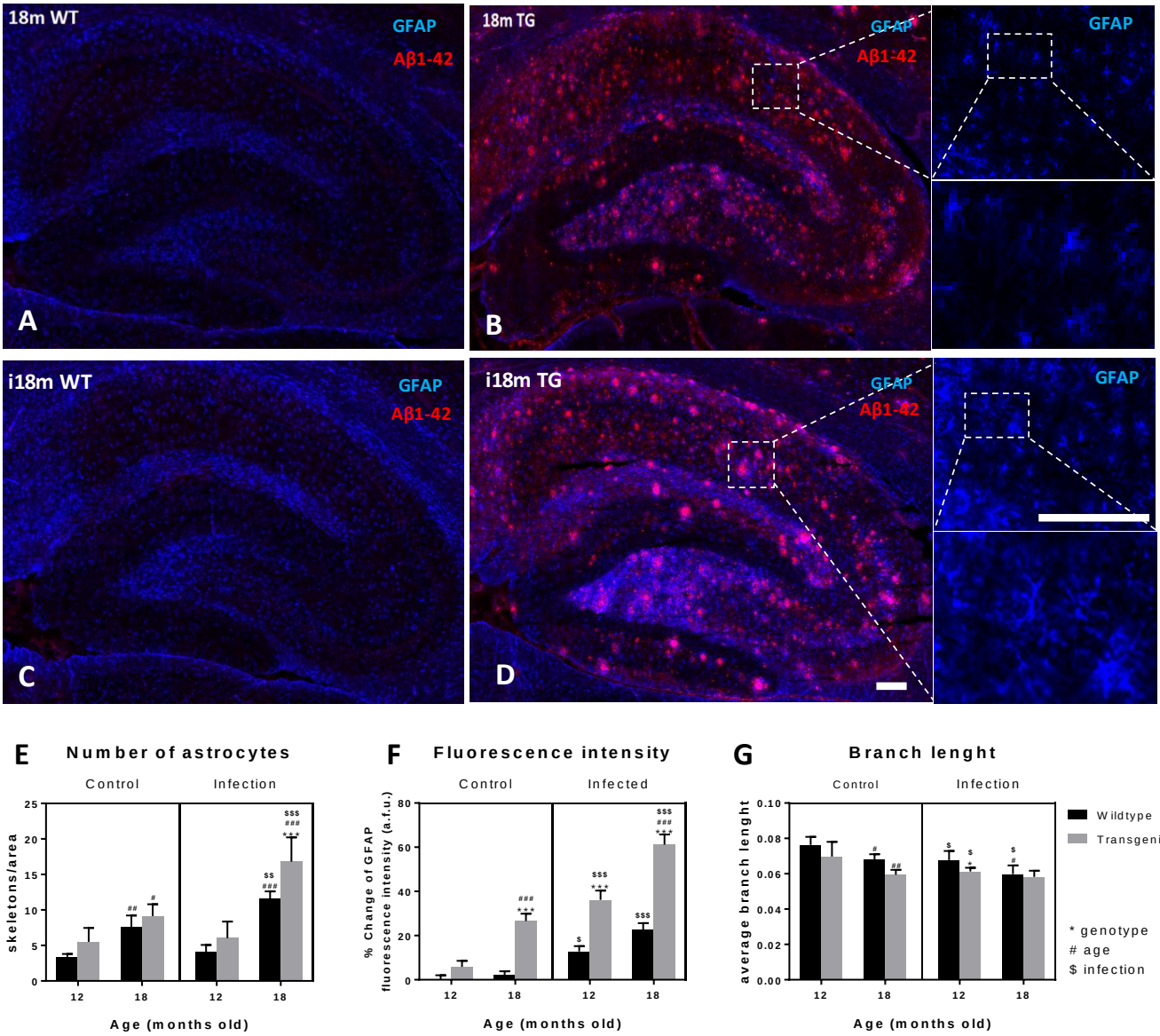

Figure 4. 3: Astrogliosis is increased in TG rats by peripheral infection.

(A-D) Sagittal planes of 18-months old WT and TgF344-AD rats with or without peripheral infection were stained for astrocytic GFAP and $A\beta_{1\text{-}42}$ plaques. **(E)** Number of astrocytes, **(F)** fluorescence intensity and **(G)** branch length of astrocytes were analysed, showing that TG rats presented and increase of the reactive state of astrocytes, which was further increased by peripheral infection. Statistical analysis performed using three-way ANOVA following Holm-Sidak's post-hoc test. Data is shown as mean ± SEM. N=5-6, being each n number an animal per group; dF=1. *p compared to age-matched WT group, $^{\#}$p compared to phenotype-matched 12-month old group, $^{\$}$p compared to age- and genotype-matched non-infected group. Scale bar = 40µm.

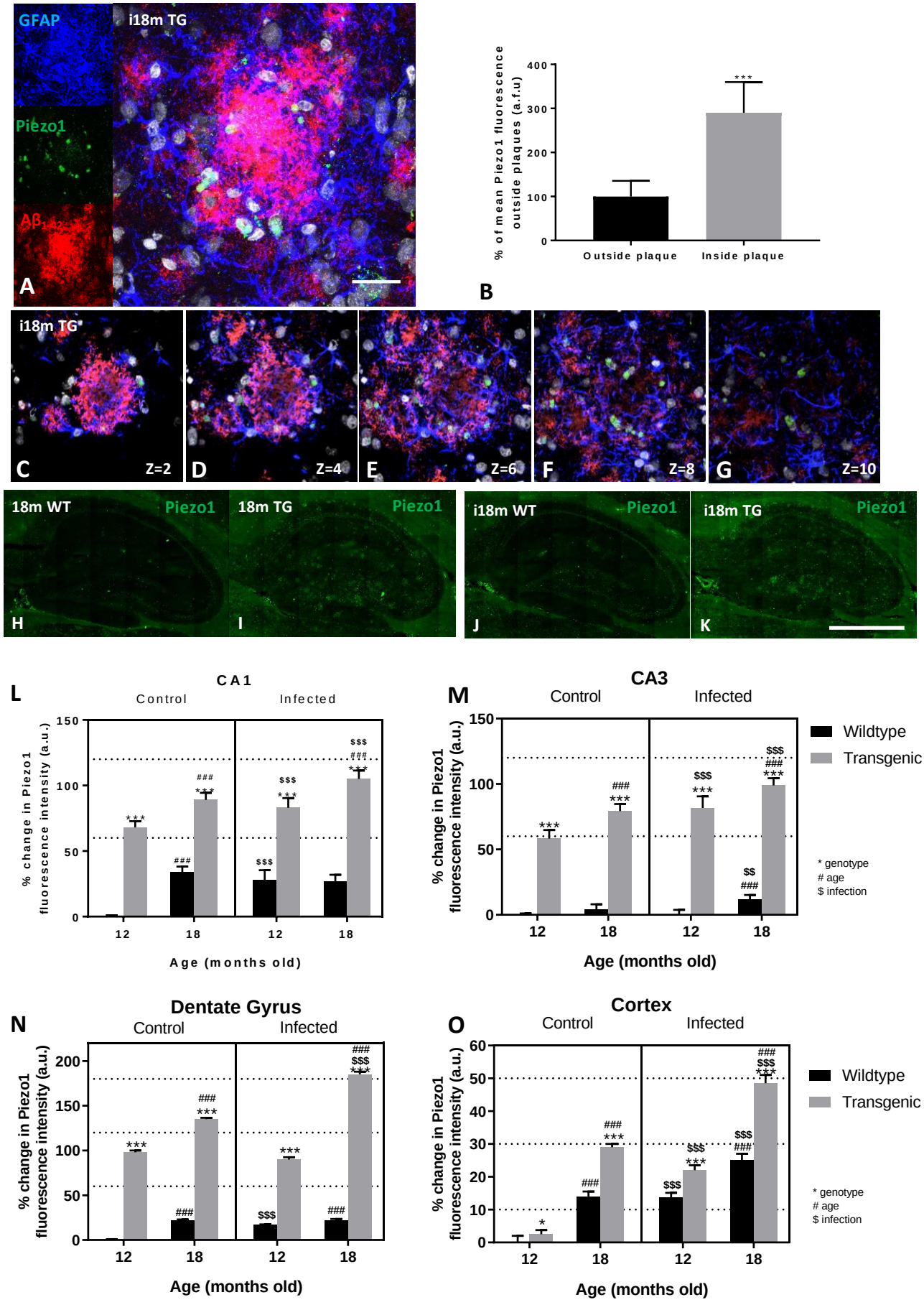
GFAP
Piezo1
Aβ1-42
i18m TG
A
% of mean Piezo1 fluorescence outside plaques (a.f.u)
Outside plaque
Inside plaque
B
i18m TG
C Z=2
D Z=4
E Z=6
F Z=8
G Z=10
18m WT Piezo1
18m TG Piezo1
i18m WT Piezo1
i18m TG Piezo1
H
I
J
K
CA1
Control
Infected
% change in Piezo1 fluorescence intensity (a.u.)
Age (months old)
L
CA3
M
Wildtype
Transgenic
* genotype
# age
$ infection
Dentate Gyrus
N
Cortex
O

Figure 4. 4: Piezo1 is upregulated with age, infection and amyloid plaque pathology in astrocytes

(A) High magnification (100x) Z-stack of a cortical plaque, showing the perinuclear pattern of expression of Piezo on astrocytes. **(B)** There is a three-fold upregulation of Piezo1 expression inside the plaques, compared to at least 200µm away from any plaque, which shows that Piezo1 expression is triggered in the astrocytes around the amyloid plaques, whilst absent outside. **(C-G)** Snapshot of the Z-stack projection of a cortical plaque, showing the perinuclear location of Piezo1 on the astrocytes surrounding the amyloid plaque. **(H-K)** Immunolabelling of Piezo1 in hippocampus of 18-months old WT and TgF344-AD rats, with or without peripheral infection. **(G-J)** There is an increase of Piezo1 expression with age, amyloid pathology and infection in all hippocampal areas and cortex, as measured as a normalized percentage of the 12-months old non-infected WT group. Statistical analysis was performed using a three-way ANOVA with Holm-Sidak's multiple comparison post-hoc test. Data is shown as mean ± SEM. N=5-6, being each n number an animal per group; dF=1. *p compared to age-matched WT group, $^{\#}$p compared to phenotype-matched 12-month old group, $^{\$}$p compared to age- and genotype-matched non-infected group. Scale bar of **(A-G)** = 10 µm. Scale bar of **(H-K)** = 300µm.

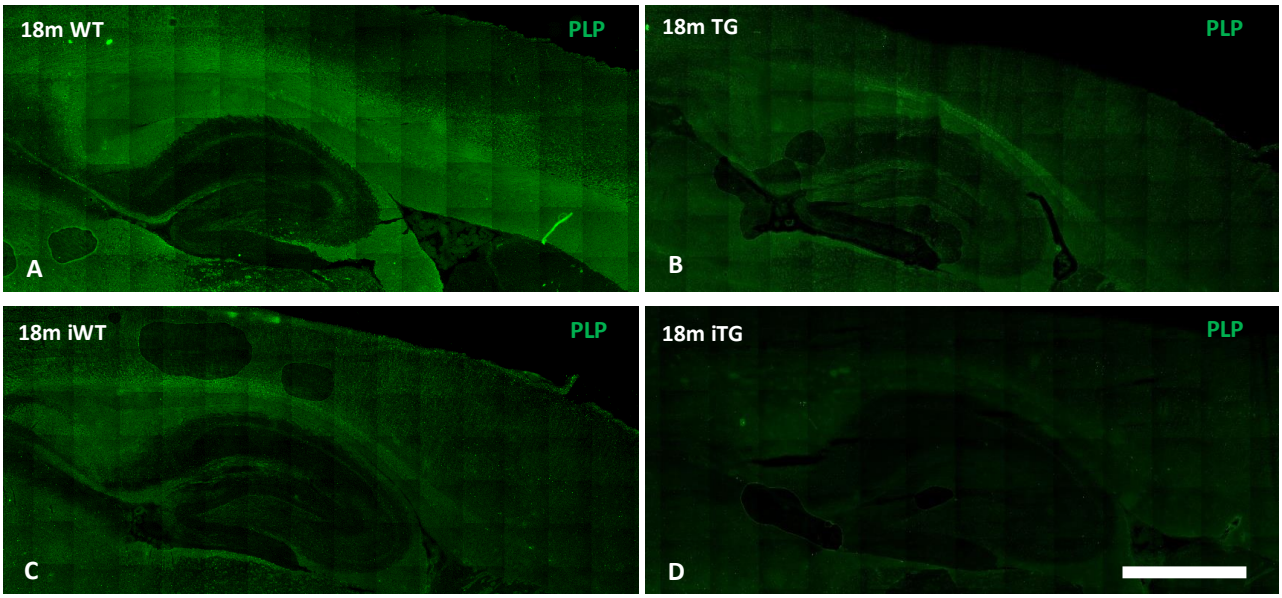
18m WT
PLP
A
18m TG
PLP
B
18m iWT
PLP
C
18m iTG
PLP
D

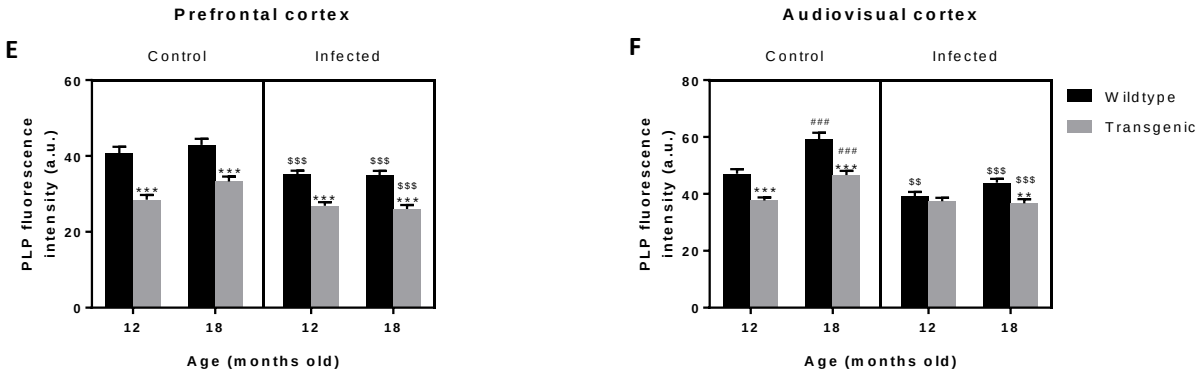
Prefrontal cortex
E
Control
Infected
PLP fluorescence intensity (a.u.)
Age (months old)
Audiovisual cortex
F
Wildtype
Transgenic

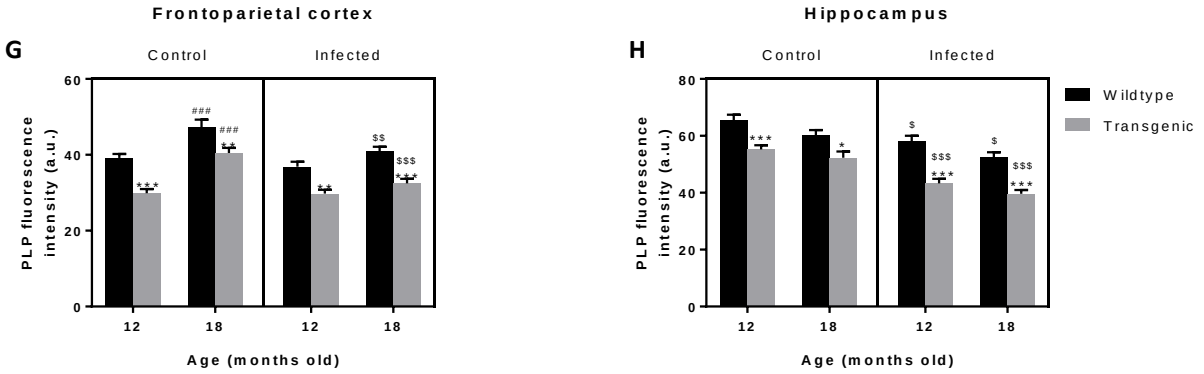
Frontoparietal cortex
G
Hippocampus
H

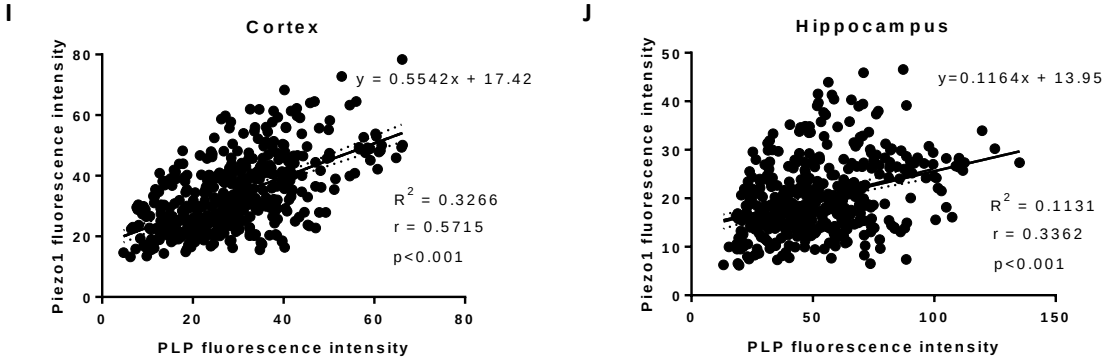
I
Cortex
y = 0.5542x + 17.42
R2 = 0.3266
r = 0.5715
p<0.001
Piezo1 fluorescence intensity
PLP fluorescence intensity
J
Hippocampus
y=0.1164x + 13.95
R2 = 0.1131
r = 0.3362
p<0.001

Figure 4. 5: Amyloid deposition and peripheral infection leads to a decrease in the levels of myelin in hippocampus and cortical areas.

(A-D) Immunohistochemistry of 18-months old WT and TgF344-AD rats with or without peripheral infection, showing expression of myelin protein PLP. **(E-H)** Statistical analysis of the fluorescence intensity of PLP reveals that TgF344-AD rat have lower levels of PLP than age-matched WT, and that peripheral infection leads to a decrease in the levels of myelin protein in both WT and TgF344-AD rats in hippocampus and cortex. Statistical analysis performed using a three-way ANOVA with Holm-Sidak's multiple comparisons post-hoc test. Data shown as mean ± SEM; n = 5-6, being each n number an animal per group; dF=1. *p compared to age-matched WT group, $^{\#}$p compared to phenotype-matched 12-month old group, $^{\$}$p compared to age- and genotype-matched non-infected group. Scale bar = 500µm. **(I-J)** Linear correlation between Piezo1 and PLP intensity values in cortex and hippocampus shows a relationship between them, in agreement with previous experiments showing expression of Piezo1 in the high myelinated areas of the brain. Statistical analysis performed using a Pearson r correlation, n = 450 values, being each n number a XY pair.

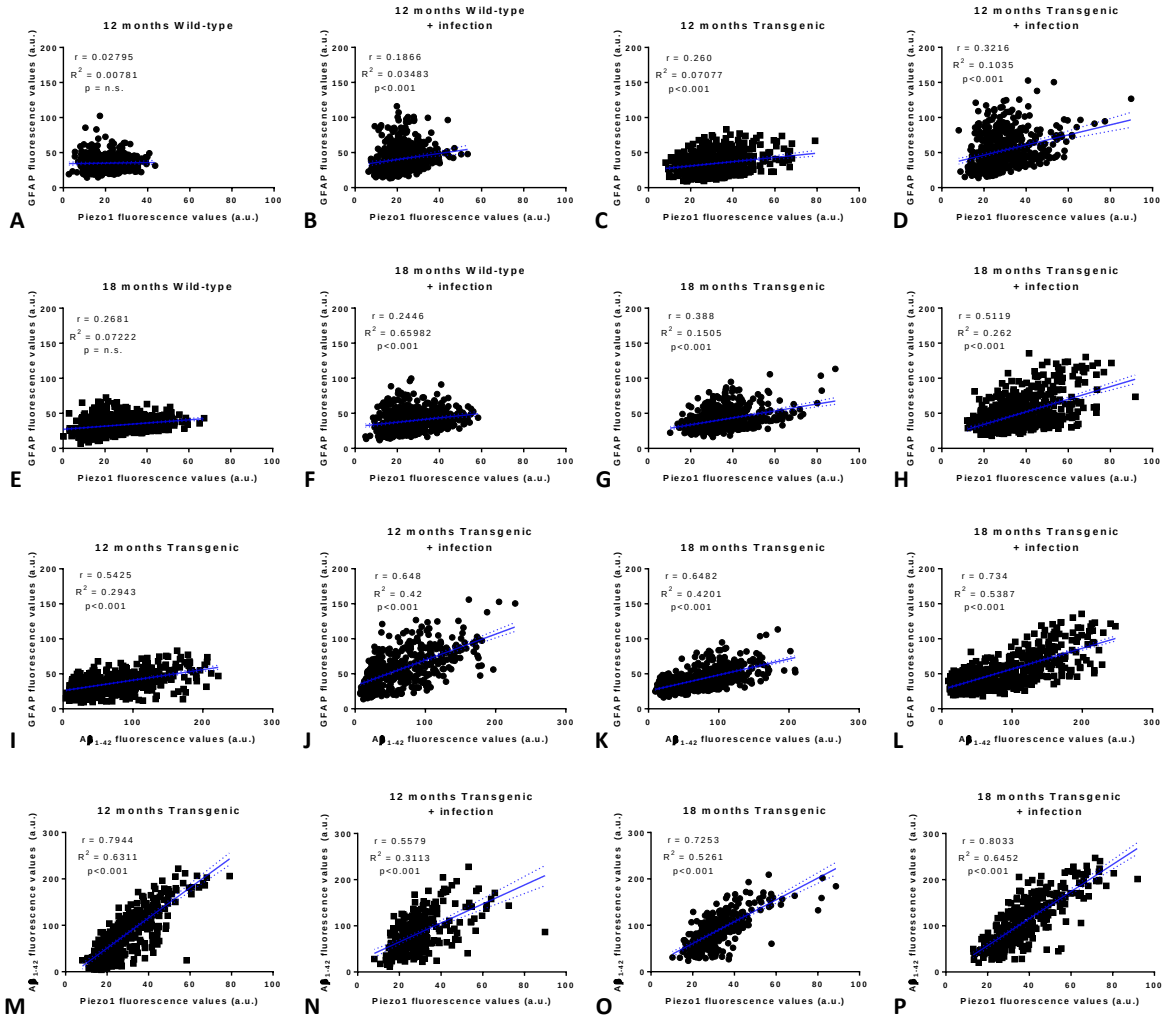

<u>Figure 4. 6</u>: Piezo1 expression in the hippocampal dentate gyrus correlates with GFAP and amyloid-β in TgF344-AD rats.

(A-H) Pearson correlations between GFAP and Piezo1 in WT and TgF344-AD rats with or without infection showed no correlation in WT without infection. There was a linear correlation in infection as well as non-infected TgF344-AD rats, suggesting that expression of GFAP and Piezo1 are only related under astrocyte reactivity. Moreover, we note that R^2 values are relatively low for all groups, indicating that despite there is an association between GFAP and Piezo1 expression, GFAP may not be the best predictor for Piezo1 expression. **(I-L)** We also correlated GFAP and $A\beta_{1-42}$ values in TgF344-AD with and without infection, showing a linear regression between values, in accordance with our previous observations were GFAP is enhanced around the plaques. **(M-P)** Piezo1 and $A\beta_{1-42}$ values in TgF344-AD with and without infection were correlated, showing that a strong correlation between these values, suggesting that $A\beta_{1-42}$ fluorescence is a good predictor of Piezo1 channel expression in the hippocampus. Statistical analysis performed using a Pearson r correlation, n = 450 values, being each n number a XY pair.

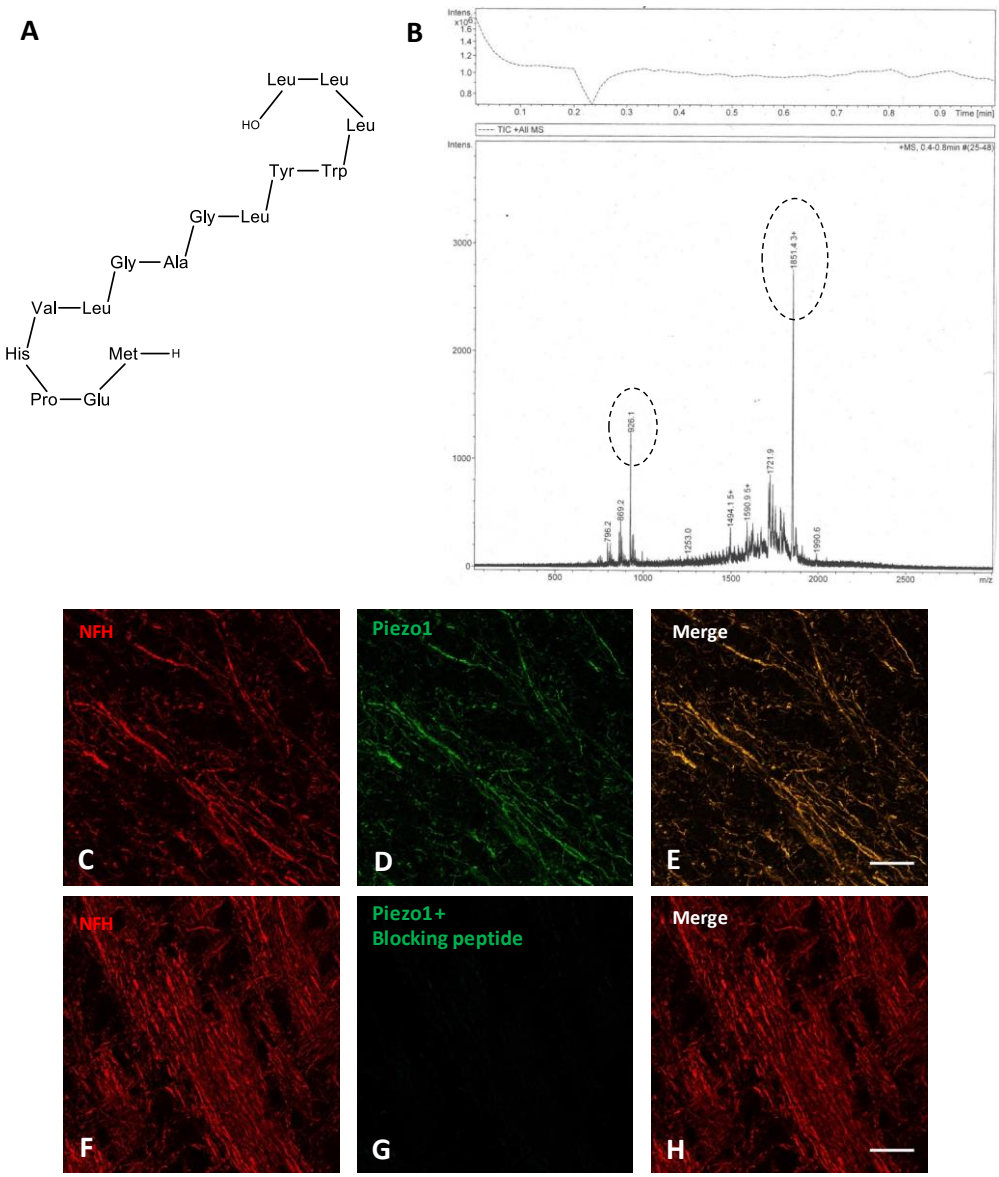

<u>Supplemental Figure 4. 1</u>: Synthesis of blocking peptide for sc-164319 and validation of antibody

(A) Synthesis of the control peptide (Nter-MEPHVLGAGLYWLLL-Cter) by solid-phase synthesis. **(B)** MicroTOF mass spectrometry to confirm the synthesis of the desired peptide. Two peaks at 926.1 and 1851.4 (3+) m/z confirm the presence of the 5741.94 g/mol peptide. **(C-E)** Immunohistochemistry of rat cortex, labelled for NFH and Piezo1, showing expression of Piezo1 in the axons of cortical areas. **(F-H)** After incubation of the Piezo1 antibody with the synthesized peptide for 5h RT prior staining, immunohistochemistry of rat brain tissue reveals no signal of Piezo1+blocking peptide, corroborating the specificity of the Piezo1 antibody used and validating the specific signal of our experiments.

3. Discussion

3.1. Summary of findings.

Most of the AD research utilises transgenic mice models overexpressing amyloid-β, however, it has been observed that they do not expressed the full array of AD hallmarks. The TgF344-AD rats combines the human mutation APP_{SWE} and overexpression of human *PSEN1ΔE9*, with the intention of creating an improved animal model for AD that recapitulates a broader spectrum of neuropathological features seen in the human AD brain. This model shows age-dependent amyloid deposition, tau hyperphosphorylation and cognitive dysfunction (Cohen et al., 2013). Here, by combining this model with repeated urinary infections with *E.coli*, we model a common co-morbidity that occurs in the elderly with AD, and prove how this model mimics the systemic inflammation and the spatiotemporal deposition of plaques observed in the hippocampus and cortex of human patients with AD.

We have characterised the plaque deposition, myelin state and reactivity of glia in this model. Firstly, we showed that TgF344-AD rats present an age-dependent deposition of plaques across the cortex and hippocampus. Secondly, we noted that TgF344-AD present activated astrogliosis in an age-dependent manner, where the number of cells and GFAP expression was higher in the transgenic rats, as well as a switched to an ameboid morphology type, correlating to reactive state of astrocytes. Finally, we assessed the myelin state of the model, finding that TgF344-AD rats present reduced levels of PLP expression in cortex and hippocampus, also in an age-dependent manner. Interestingly, peripheral infection enhanced all the pathological parameters, leading to higher load of plaques, increased astrocyte reactivity, and lower levels of myelin.

In this study, we prove how levels of Piezo1 are increased in the TgF344-AD model, and how astrocytes surrounding the amyloid plaques perinuclearly upregulate this mechanoreceptor in a similar pattern to what observed in our previous studies *in vitro* **(Chapter 3)**. Age-dependant increases in the levels of Piezo1 in cortex and hippocampus of WT rats appear to be mainly neuronal, whilst in TgF344-AD appear to be expressed perinuclear in the astrocytes associated to plaques, although concomitant increases in neurons and microglia are likely and not excluded. This is interesting because the role of Piezo1 in neurons is very likely to be different to its role in astrocytes, as both the subcellular location and conditions under which it is expressed are different.

Our results suggest that Piezo1 channels regulate glial mechanosensation and may trigger astrogliosis under pathological conditions such as infection and AD, in a concomitant manner. Further research needs to be done in order to address the specific role of Piezo1 in reactive astrocytes and whether it plays a regulatory role in neuroprotection or neurodegeneration, maybe proving to be an interesting drug target for neurodegenerative pathologies.

3.2. Characterisation of amyloid plaque load and glial reactivity of TgF344-AD rats

One of the main hallmarks of AD pathology is the deposition of amyloid plaques. This is called the amyloid cascade hypothesis of AD (Hardy & Allsop, 1991) and states that aberrant cleavage of APP by γ-secretases results in the accumulation of cytotoxic oligomeric amyloid-$\beta_{1\text{-}42}$ peptide, which aggregates and forms these fibrillar structures that then clump together and generate amyloid plaques (Morris, Clark, & Vissel, 2014). Whilst amyloid plaques contribute to the neurodegeneration and neuroinflammation associated to AD (Dansokho & Heneka, 2018), the sole expression of plaques is not enough to explain the etiopathology of AD and is not necessarily a good clinical indicator of dementia (Hyman, Marzloff, & Arriagada, 1993). For instance, Aβ-overproducing mouse models have not demonstrated robust taupathy and neuronal loss unless other human genes not related to AD were included (Holcomb et al., 1998; Jankowsky et al., 2001), proving the need for better and more representative animal models for AD research. In this study, we show how the rat model TgF344-AD presents an age-dependent deposition of amyloid plaques, and how number, size and fluorescence intensity of plaques correlates with the state of the pathology. Moreover, peripheral infection -a common co-morbidity in human AD patients- enhances the formation and deposition of these plaques, contributing to the further progression of the pathology.

It has been largely shown in the literature the role of glia in the neuroinflammatory state of AD (Akiyama et al., 1996; Krstic & Knuesel, 2013; C. Liu et al., 2014). Studies in the field show that reactive glia are beneficial in the early stages of the pathology, contributing to plaque clearance by astrocytes and microglia, but when this neuroinflammation becomes chronic, it has a detrimental effect in the progression of AD (C. Liu et al., 2014). In this study, we show how TgF344-AD rats present astrogliosis and morphology changes into a more reactive phenotype in an age-dependent manner. Furthermore, we prove the contribution of the peripheral infection to enhance the neuroinflammatory state of astrocytes in pathology, in accordance with our results of amyloid plaque formation. Altogether, we demonstrate that the TgF344-AD rat model

with peripheral infection with *E.coli* is a reliable model that mimics the hallmarks observed in human AD patients, therefore constituting a good tool to study AD *in vivo.*

3.3. Amyloid pathology present lower levels of myelin components in cortical and hippocampal regions

Demyelination is not usually regarded in literature as one of the hallmarks of AD. However, it has been proven that there is myelin disruption and oligodendrocyte alteration in this pathology (Horiuchi et al., 2012; Schmued, Raymick, Paule, Dumas, & Sarkar, 2013; X. Zhan et al., 2014). It is believed that myelin breakdown contributes to neurodegeneration and dementia associated with AD (Cai & Xiao, 2016). Whether this myelin disruption is caused by neuroinflammation, oxidative stress or apoptosis of oligodendrocytes, is yet unclear. In this study, we have shown TgF344-AD rats present reduced levels of the myelin protein PLP in hippocampal and cortical areas, compared to their age-matched WT counterparts. Similar to what observed in the analysis of plaque load and astrocyte reactivity, peripheral infection worsened the myelin breakdown, causing a further decrease in the levels of myelin measured by PLP expression. Of interest, we noted that myelin disruption did not follow an age-dependent manner in the cortex, which suggest that it may not be the cause of initial neurodegeneration, but a consequence of plaque formation and neuroinflammation. Furthermore, we acknowledge that a more extensive analysis of the structure and state of the myelin sheath would be required to claim demyelination in this AD model. Thus, analysis of the co-localization between the expression of myelin markers and neuronal markers could be done, as well as electron microscopy to assess the thickness and state of the myelin.

3.4. Astrocytic expression of Piezo1 in Alzheimer's disease

Utilizing the TgF344-AD rat model we here showed that Piezo1 protein expression increases in several key brain structures in response to ageing, peripheral infection and amyloid plaque pathology. Piezo1 channels increase in the prefrontal cortex and hippocampal CA1 and DG with normal ageing. These brain regions are particularly important for processing salient sensory information (Barbas and Zikopoulos, 2007; Lester et al., 2017), for learning and memory (Kaneand Engle, 2002; Guo et al., 2018) and for higher executive functions (Arnsten and Li, 2005; Suwabe et al., 2017), all of which deteriorate in the elderly (Zimprich and Kurtz, 2013; Thomé et al., 2016). Despite ours is the first study showing the increment of Piezo1 expression at protein level, in 2006, Satoh and colleagues reported the expression of Mib mRNA in the astrocytes

associated to amyloid plaques, in post-mortem AD brains (Satoh et al., 2006). Four years later, in 2010, Coste and colleagues described the mechanosensitive channel Piezo1 in the neuroblastoma cell line Neuro2A, and the previously called Mib protein was renamed as Piezo1 (Coste et al., 2010). Astrocytes are very sensitive to changes in their local environment, sensing changes in the stiffness (Blumenthal et al., 2014; Leipzig & Shoichet, 2009), and our data suggests that under pathological conditions such as AD or inflammation, certain mechanosensors such as Piezo1 channels are upregulated in a sub-population of astrocytes. Interestingly, we found that Piezo1 is upregulated in a perinuclear manner of mostly a subset of astrocytes around the amyloid plaque. This is in accordance to our previous studies *in vitro* **(Chapter 3)** showing that Piezo1 is expressed in the endoplasmic reticulum of primary mouse astrocytes when stimulated with LPS, PSY or amyloid-β CMM. The fact that Piezo1 is subcellularly located in the endoplasmic reticulum, in contrast with the expression in neurons in the basal membrane, suggests that its role in astrocytes differs to that in neurons. Piezo1 in neurons is involved in the durotaxis of the axonal growth cone (Koser et al., 2016) whilst it has been shown that when located in the endoplasmic reticulum, Piezo1 is involved in integrin signalling in small lung cancer cells (McHugh et al., 2012) and we have shown that pharmacological modulation of Piezo1 leads to a regulation of the astrogliosis and reactive responses of astrocytes. Which the specific function of Piezo1 is in the astrocytes around the amyloid plaques and why it is upregulated only in a subset of cells, is yet unknown. However, given that both the amyloid plaque deposition and the peripheral infection leads to an increase in the levels of Piezo1, in a concomitant manner, lead us to hypothesize a potential role for pro-inflammatory glia in regulating astrocytic Piezo1 levels. Future studies will focus on the signalling cascades triggered by Piezo1 in astrocytes and Piezo1 as a potential therapeutic target for amyloid plaque-induced neurodegeneration in Alzheimer's disease, as further discussed in **Chapter 6**.

.

Chapter 5:
Role of Piezo1 in the regulation of myelination

Chapter aims

Many research studies from the past years have shown that myelinating cells –oligodendrocytes and Schwan cells- are mechanosensitive, sensing the changes in the matrix stiffness and this in turn has a role in cell differentiation (Jagielska et al., 2012; Jagielska et al., 2017), proliferation (Jagielska et al., 2017), maturation (Urbanski et al., 2016) and myelination (S. Lee et al., 2012; S.S. Rosenberg et al., 2008). Based on our previous findings of Piezo1 expression in the highly myelinated areas of the brain, we hypothesize that Piezo1 might be one of the mechanosensing proteins that regulate the myelin state in the CNS, probably acting as the linker in the crosstalk of neurons and glia.

The specific aims of this chapter were:

- To examine the effects of the activation of Piezo1, by Yoda-1, on myelin protein expression using cerebellar organotypic slice culture.
- To investigate whether the Piezo1 blocker, GsMTx4, alters the expression of myelin proteins and glial cell activation in brain slices.
- To assess if activation/inhibition of Piezo1 prevents loss of myelin proteins caused by psychosine.
- To evaluate the effects of activation/inhibition of Piezo1 on glial cells *ex vivo*.
- To investigate the effects of GsMTx4 in myelin protein levels *in vivo* using a focal demyelination injury mouse model by stereotaxic injection of LPC.
- To analyse the effects of GsMTx4 in neuronal death and levels of oligodendrocyte precursors in the LPC-focal demyelination model.
- To assess the glial cell reactivity in the LPC-focal demyelination adult mouse model.

Abstract

Myelination is a complex process, yet not fully understood. Most research focuses purely on the biochemical signalling pathways that regulates myelination. However, in the recent years there has been evidence that suggest a physical contribution to myelination initiation and repair. Here, we hypothesized that Piezo1 –a mechanosensitive cation channel- may play a role in communicating mechanical and chemical signals to regulate myelination. We show, for the first time, that Piezo1 is expressed in the highly myelinated areas of the rodent brain; and that activation of Piezo1 by the specific activator Yoda-1 leads to demyelination in the *ex vivo* cerebellar slice culture model. On the contrary, blocking Piezo1 by the peptide GsMTx4 (an inhibitor of stretch-activated cation channels, in which Piezo1 belongs) caused increased myelination and prevented the psychosine-induced demyelination *ex vivo*. Furthermore, using the *in vivo* focal demyelination mouse model by stereotaxic injection of 0.1% LPC, we showed that GsMTx4 prevented the LPC-induced demyelination, axonal damage, and glial activation *in vivo*, leading to similar levels to control. Based on these current observations and in line with previous studies, we propose these effects may be due to a regulation in the excitotoxicity caused by Ca^{2+} in the axons, as well as through a downstream modulation of integrin signalling between axons and oligodendrocytes and the activation of calpain and $sPLA_2$ that leads to lipid degradation in oligodendrocytes. In conclusion, our findings strongly suggest a new role of Piezo1 and stretch-activated cation channels in regulating myelination as blockage of these type of channels upregulated the expression of myelin components and prevented toxin-induced demyelination. This knowledge is important for better understanding the myelin formation and regulation process as well as being a key concept that can lead Piezo1 to be a novel drug target for illnesses where myelin is dysregulated.

1. Introduction

Historically, research into the processes of myelination has focused on the biochemical and signalling pathways. In contrast, the role of physical mechanics in myelination is less well studied. Notwithstanding, recent research has shown a mechanical component in the modulation of myelination. For instance, OPCs have shown to myelinate electro-spun polystyrene nanofibers of a similar diameter to neural axons, showing that myelination can occur without dynamic axonal signalling, although admittedly not as per *in vivo*, suggesting chemical signals are also needed (S. Lee et al., 2012). To clarify the contribution of mechanical cues such as stretch to the myelinating capacity of oligodendrocytes, studies have modelled TBI using stretch-injury to optic nerve fibres. These studies have shown that such stretch-injury induces an increase in waves of free Ca^{2+} in oligodendrocytes that is a distance away from the initial locus of the injury and contributes to the posterior demyelination (Maxwell, 2013).

Piezo1 is known to be expressed on neurons (Koser et al., 2016) and we have shown in previous studies that Piezo1 is expressed at relatively high levels in myelinated areas of the brain, such as corpus callosum, arbor vitae and optic tract *(unpublished data)*. It has been observed that Piezo1 is involved in the durotaxis of the axonal growth cone (Koser et al., 2016), but there are no studies determining its possible role in myelination or axonal stability. Demyelinating disorders and neuropathies are often associated with disrupted axonal Ca^{2+} homeostasis (Baloh, 2008), where sustained elevations of intracellular Ca^{2+} can lead to pathological levels of ROS, excitotoxicity, cytoskeletal instability and activation of apoptotic cascades, resulting in irreversible neurodegeneration (Barsukova, Forte, & Bourdette, 2012; Frati et al., 2017). Many SACs like Piezo1 care Ca^{2+} ion channels and their dysregulation may lead to a disruption of intracellular Ca^{2+} homeostasis in the cells. Thus, we suggested that Piezo1 may be a target for protection of neurodegeneration in demyelinating conditions. Furthermore, several studies have shown that neural stem and progenitor cells differentiation is influenced by mechanotransduction (Arulmoli et al., 2015) and more specifically, that Piezo1 is involved in the lineage choice of these neural stem and progenitor cells (Pathak et al., 2014).

In this study, we have used both a specific activator of Piezo1, namely Yoda-1, and an inhibitor of SACs like Piezo1, namely GsMTx4, to investigate the effects of pharmacological modulation of Piezo1 in the myelin-state and axonal stability. Yoda-1 was developed in 2015 as a selective Piezo1 agonist (Syeda et al., 2015), while GsMTx4 is a 34 amino acids peptide found in the venom of the tarantula *Grammostola spatulate* (Suchyna et al., 2000). GsMTx4 acts as a gating modifier

by sitting into lipid membranes close to ion channels, such as Piezo1, making it more difficult for pores to open in response to membrane stretch (Gnanasambandam et al., 2017). We postulated that this mechanism of action could be therapeutically beneficial in CNS demyelinating diseases. Indeed, many SACs like Piezo1 are Ca^{2+} permeable ion channels and dysregulations in SAC opening probability can lead to a disruption of intracellular Ca^{2+} homeostasis (Naruse and Sokabe, 1993; Yeung et al., 2005). The D and L enantiomers of GsMTx4 have almost identical activity (Wang et al., 2016) which suggests that its mechanism is not reliant on direct stereo-chemical interactions, i.e. GsMTx5 does not conform to the standard 'lock and key' model of traditional ligand/receptor pharmacology (Gnanasambandam et al., 2017). GsMTx4 (AT-300) has been designated an orphan drug by the US Food and Drug Administration (FDA) and counteracts cellular Ca^{2+} dysregulations in preclinical models of muscular dystrophy (Ward et al., 2018); a genetic condition characterised by disrupted Ca^{2+} homeostasis in muscle cells and eventual muscle wasting (Johnstone et al., 2017).

In this study, we first used an *ex vivo* approach using organotypic cerebellar slice cultures. This model allows the study of pharmacological treatment on the levels of different myelin and glial markers, while reducing the time, suffering and number of animals. We then used an *in vivo* model of LPC-focal demyelination in adult mice by stereotaxic injection, at a concentration of LPC 0.1%, which shows demyelination and cell death. Here, we present evidence that blocking SACs with GsMTx4 can protect both neurons and oligodendrocytes from demyelination caused by chemical insults such as psychosine or LPC both *ex vivo* and *in vivo*. We also show how Piezo1 is involved in this process, as activation with the specific agonist Yoda-1 contributed to demyelination in the *ex vivo* brain slices.

2. Results

2.1. Expression of Piezo1 channels in myelin-rich areas of the brain

Previous studies have demonstrated that Piezo1 is expressed by neurons, and possibly in highly myelinated areas of the brain. To further corroborate this possibility, we firstly examined expression of Piezo1 in rodent mouse and rat brains. Data showed that Piezo1 was expressed in highly myelinated areas in the brain, including arbor vitae of cerebellum, corpus callosum and optic tract **(Supplemental Figure 5. 1)**. To investigate further the expression of Piezo1, we next examined its expression in cerebellar organotypic slice cultures from postnatal day 10 (P10) mice. While generating immunocytochemical data using the Piezo1 antibody in slice cultures remains challenging (primarily due to slice culture thickness), we observed Piezo1 expression in the arbor vitae of the cerebellum, in agreement with our *in vivo* observations **(Fig 5.1)**. Based on this expression data, we hypothesized that the mechanoreceptor Piezo1 is closely associated with myelin-rich regions of the brain and could play a role in regulating mechanical and biochemical stimuli during myelination.

2.2. Piezo1 regulates myelin protein levels in cerebellar slice cultures

Having examined the expression of Piezo1 in white matter areas such as the arbor vitae of cerebellum, we next used cerebellar organotypic slice cultures to examine its role in regulating myelination. To assess the effects of activating Piezo1 on myelination, DIV 12 slice cultures were treated with 10µM Yoda-1, a specific activator of Piezo1, for 48h. Slices were then stained for myelin markers myelin-oligodendrocyte glycoprotein (MOG) **(Fig 5.2 A)**, myelin proteolipid protein (PLP) **(Fig 5.2 C)** and myelin basic protein (MBP) **(Fig 5.2 E)**. Statistical analysis showed that Yoda-1 caused a decrease in the levels of MOG (68.67% ± 9.02 vs 99.32% ± 5.42; *p=0.045; RM one-way ANOVA following Holm-Sidak post-hoc test, n=6, dF=4), PLP (56.47% ± 9.79% vs 81.34% ± 15.27%, **p=0.0072; RM one-way ANOVA following Holm-Sidak post-hoc test, n=6, dF=4) and MBP (72.24% ± 8.04% vs 100.0% ± 9.62%, *p=0.05; RM one-way ANOVA following Holm-Sidak post-hoc test, n=6, dF=4) compared to control **(Fig 5.2 A-F)**. Next, we aimed to examine the effects of blocking Piezo1 on myelination. GsMTx4 is 34 amino acids peptide that acts as a blocker of SACs, to which Piezo1 belongs (Bae et al., 2011; Suchyna et al., 2000). In contrast to the specific Piezo1 activator Yoda-1, the treatment of slice cultures with GsMTx4 statistically increased the levels of MOG (127.80% ± 11.82% vs 99.32% ± 5.42; *p=0.05), PLP (106.10% ± 12.97% vs 81.34% ± 15.27%; **p=0.0072) and MBP (124.90% ± 11.49% vs 100.0% ± 9.62%, *p=0.05) compared to control. In order to determine the role of Piezo1 on remyelination,

we examined these effects of GsMTx4 in a slice culture demyelinating model. Galactosylsphingosine (psychosine, PSY) is a toxic metabolite that accumulates in the brain of patients with Krabbe's Disease (Giri et al., 2002), and that has been demonstrated cause demyelination (Misslin, Velasco-Estevez, Albert, O'Sullivan, & Dev, 2017; C. O'Sullivan & Dev, 2015). As previously observed 100µM psychosine led to a decrease in the levels of myelin markers MOG (71.19% ± 5.97% vs 99.32% ± 5.42; *p=0.05), MBP (62.03% ± 6.88% vs 100.0% ± 9.62%, **p=0.0069) and PLP(44.95% ± 12.64% vs 81.34% ± 15.27%; ***p=0.0003) **(Fig 5.2 A-F)**. More importantly, GsMTx4 prevented this psychosine-induced demyelination, leading to similar levels of myelin markers as control, and significantly higher than PSY-treated conditions in all markers (MOG: 114.7% ± 6.96% vs 71.19% ± 5.97%, $^{\#\#}$p=0.0037; PLP: 78.61% ± 12.51% vs 44.95% ± 12.64%, $^{\#\#\#}$p=0.0006; MBP: 100.1% ± 13.67% vs 62.03% ± 6.88%, $^{\#\#}$p=0.0062) **(Fig 5.2 A-F)**.

We note that these values represent the expression of myelin components, however they cannot clarify whether this expression is found in the myelin sheath around the axons rather than part of the non-myelinating OLs or as myelin debris. Thus, we analysed the co-localization of axonal NFH fluorescence and myelin marker MBP to assess whether this changes in the expression of myelin markers were also reflected in the amount of myelin protein MBP localised around the axons. In line with the fluorescence analysis, we found a decrease in the levels of co-localization between NFH and MBP with Yoda-1 (0.1396 ± 0.018 vs 0.2783 ±0.022, ***p<0.001; RM one-way ANOVA following Holm-Sidak post-hoc test, n=8, dF=4) and psychosine (0.0999 ±0.01 vs 0.2783 ±0.022, ***p<0.001) **(Figure 5.2G)**. Interestingly, while GsMTx4 causes a significant increase in the expression of myelin proteins, there is no apparent increment in the levels of co-localization between NFH and MBP (0.3168 ± 0.028 vs 0.2783 ±0.022, n.s. p=0.45), but it did prevent the effects of psychosine, leading to similar levels of co-localization as control conditions (0.2979 ± 0.044 vs control 0.2783 ±0.022, n.s. p=0.7; vs PSY 0.0999 ±0.01, $^{\#\#\#}$p<0.001)

The levels of expression of myelin proteins were also investigated by Western-Blot analysis, showing a decrease in the levels of MOG **(Fig 5.2 H)** and MBP **(fig 5.2 I)** when slices were treated with Yoda-1 (MOG: 84.31% ± 4.59% vs 102.6% ± 8.22%; *p=0.044; MBP: 78.02% ± 0.89% vs 99.8% ± 1.72%, *p=0.024; RM one-way ANOVA following Holm-Sidak post-hoc test, n=5, dF=4) or psychosine (MOG: 82.61% ± 5.12%, *p=0.044; MBP: 74.32% ± 5.34%; *p=0.012) that was augmented by treatment with GsMTx4. Of note, we observed no significant differences amongst treatments between slices obtained from male and female animals (*data not shown*). Overall this data suggests that Piezo1 activation downregulates the levels of myelin protein expression in organotypic slice culture studies while its blockage augments it and even prevents from demyelination associated to psychosine.

2.3. Axonal damage induced by demyelination is attenuated by GsMTx4 treatment in organotypic slice culture.

Neurofilament H (NFH) is a structural cytoskeletal protein specific to neurons (Rudrabhatla, 2014) comprising both phosphorylated and non-phosphorylated epitopes of NFH (Louis et al., 2012). In previous studies, we have utilised the non-phosphorylated NFH epitope SMI-32 as a marker for neuronal damage, in particular monitoring its expression in axons (as a marker of neuronal damage) compared to expression in the soma of neurons (physiological state) (Misslin et al., 2017; S. A. O'Sullivan et al., 2017). Here, we analysed whether demyelinating effects of psychosine and Yoda-1 led to axonal damage by measuring SMI-32 expression in the white matter tracts of slice cultures, as well as if GsMTx4 could prevent this damage. It can be observed that both Yoda-1 (Yoda-1: 329.0% ± 29.5% vs 109.1% ± 13.93%, ***p<0.001; RM one-way ANOVA following Holm-Sidak post-hoc test, n=5, dF=4) and psychosine (386.5% ± 38.58% vs 109.1% ± 13.93%, ***p<0.001) led to expression of SMI-32 in the arbor vitae of organotypic brain slices **(Fig 5.3 A, white arrows)**, while GsMTx4 prevented this axonal expression in PSY+GsMTx4 treated slices (150.6% ± 10.15% vs 386.5% ± 38.58%, $^{###}$p<0.001) **(Fig 5.3 A-B)**. Furthermore, it was noted that psychosine (94.98% ± 5.12% vs 102.1% ± 3.7%, n.s. p=0.82; RM one-way ANOVA following Holm-Sidak post-hoc test, n=10, dF=4) or Yoda-1 (92.68% ± 3.95% vs 102.1% ± 3.7%, n.s. p=0.76) did not cause a decrease on NFH **(Fig 5.3 C-D)**, supporting our hypothesis that the decrease in myelin markers observed previously are due to demyelination that likely precedes neuronal damage and thereafter neuronal death. In these set of studies, we also noted that GsMTx4 alone caused an increase in the levels of NFH (122.2% ± 7.73 vs 102.1% ± 3.7%, *p=0.05) **(Fig 5.3 C-D)**, where we hypothesise that GsMTx4-induced increase in levels of myelin may promote neuronal stabilization in addition to a direct effect on oligodendrocytes.

2.4. The effects of GsMTx4 on glial activation or viability

As previously reported, psychosine has a cytotoxic effect on astrocytes in a concentration- and time-dependent manner (Misslin et al., 2017; C. O'Sullivan & Dev, 2015). Here, we next examined whether GsMTx4 or Yoda-1 regulated astrocyte or microglia cell activity or viability by analysing the expression of astrocytic marker vimentin and microglial Iba-1. Neither Yoda-1 (117.50% ± 35.82% vs 109.1% ± 7.51%, n.s. p=0.9745; RM one-way ANOVA following Holm-Sidak post-hoc test, n=6, dF=4)), GsMTx4 (96.37% ± 12.98% vs 109.1% ± 7.51%, n.s. p=0.9745), psychosine (92.46% ± 25.66% vs 109.1% ± 7.51%, n.s. p=0.9745) nor psychosine + GsMTx4 (74.13% ± 21.23% vs 109.1% ± 7.51%, n.s. p=0.8634) had an effect on the expression of Iba-1 in slice culture compared to control **(Fig 5.4 A-B)**. On the contrary, and in agreement with previous

studies, we observed an expected decrease in the levels of vimentin caused by psychosine (75.79% ± 5.93% vs 101.3% ± 2.44%, *p=0.0256; RM one-way ANOVA following Holm-Sidak post-hoc test, n=6, dF=4), which was not attenuated by psychosine + GsMTx4 treatment (77.79% ± 2.97% vs 101.3% ± 2.44%, *p=0.0355). Furthermore, neither Yoda-1 (101.20% ± 9.04% vs 101.3% ± 2.44%, n.s. p=0.9892) nor GsMTx4 (95.19% ± 6.63% vs 101.3% ± 2.44%, n.s. p=0.8418) alone had any effect on vimentin compared to control conditions **(Fig 5.4 D-E)**. These results were also supported by Western-Blot analysis **(Fig 5.4 C, F)**. These results suggest that the effects of Piezo1 modulation on myelination state in organotypic slice culture are independent from glial cell viability and activation.

2.5. GsMTx4 attenuates LPC-induced demyelination in the cerebral cortex *in vivo*

Having demonstrated the effects of GsMTx4 in preventing psychosine -induced demyelination in an *ex vivo* model using organotypic slice culture, we aimed to assess these effects *in vivo*. To do this, we investigated the effects of GsMTx4 in a focal demyelination model using LPC, a toxin that has widely been used to cause focal demyelination *in vivo* (Jarjour, Zhang, Bauer, Ffrench-Constant, & Williams, 2012; Luo et al., 2018; Plemel et al., 2018). Stereotaxic injections of LPC with or without GsMTx4 were performed in the cortex of adult male C57BL/6 mice aged 9-10 weeks (25-30g weight). LPC was injected in the border of the somatosensory and motor cortex, specifically at the coordinates ML = ± 1mm, AP = 1mm, DV = 1.5mm **(Fig 5.5 A-B)**. Mice were randomly distributed in three groups in which we compared: LPC 0.1% vs PBS (group A, n= 2), LPC 0.1% vs LPC 0.1% + GsMTx4 3µM (group B, n = 4) or PBS vs LPC 0.1% + GsMTx4 3µM (group C, n = 4) **(Fig 5.5 C-E)**. As positive control, we observed LPC 0.1% injections caused a decrease in the levels of MBP compared to control in group A (18.28 ± 2.17 vs 50.25 ± 5.18, n=2, qualitative description) **(Fig 5.5 F, I)** and lower levels of colocalization of MBP over NFP staining (0.6133 ± 0.1390 vs 0.9751 ± 0.02, n=2, qualitative description) **(Fig 5.5 L)**. Importantly, GsMTx4 prevented this LPC-induced loss of myelin, leading to similar levels of MBP as control (Group C: 35.98 ± 2.99 vs 40.36 ± 3.51, n.s. p=0.4081; ordinary two-way ANOVA following Holm-Sidak post-hoc test, n=4, dF=16), and significantly higher levels compared to LPC injection (Group B: 38.48 ± 14.79 vs 20.19 ± 6.00, **p=0.0015) **(Fig 5.5 F, J)**, as well as higher level of MBP:NFH colocalization, which were similar to PBS injections (Group B: 0.9377 ± 0.013 vs 0.58 ± 024, ***p<0.001; Group C: 0.9450 ± 0.018 vs 0.9500 ± 0.014, n.s. p=0.84; Unpaired t-test with Welsch's correction, n=4, dF=3) **(Fig 5.5 M, N)**. Notably, the levels of NFH decreased in LPC injected hemisphere compared to PBS injection, probably due to the neuron loss after demyelination (18.28 ± 2.16 vs 50.25 ± 5.18, n=2, qualitative analysis). This loss of NFH labelling

was also prevented in GsMTx4 treated hemispheres (40.66 ± 3.86 vs 21.52 ± 1.39, **p=0.0041; ordinary two-way ANOVA following Holm-Sidak post-hoc test, n=4, dF=16), with similar intensity values to PBS-injected controls (42.43 ± 7.55 vs 40.39 ± 2.05, n.s. p=0.73) **(Fig 5.5 G, J)**. To assess whether GsMTx4 could protect oligodendrocytes after LPC-induced injury by having an effect on the proliferation of OPCs, we analysed the expression of the oligodendrocyte marker O4, which is expressed in precursors and immature oligodendrocytes (Bansal, Warrington, Gard, Ranscht, & Pfeiffer, 1989). We observed no significant differences in the expression of O4 marker in between hemispheres across the three groups (Group A: 26.69 ± 2.32 vs 29.71 ± 0.63, n.s. p=0.83; Group B: 37.23 ± 3.52 vs 33.30 ± 1.87, n.s. p=0.58; Group C: 23.25 ± 2.47 vs 24.97 ± 1.95, n.s. p=0.83; ordinary two-way ANOVA following Holm-Sidak post-hoc test, n=4, dF=16) **(Fig 5.5 H-K)**. Taken together, these data led us to hypothesize that GsMTx4 prevents LPC-induced demyelination *in vivo*, rather than causing remyelination after the damage.

2.6. GsMTx4 modulates astrocytic cell viability and glial reactivity

The effects of LPC on glia reactivity are controversial, as it has been previously reported that LPC cause astrocytic reactivity after 7 days post-surgery in rat brain (Sheikh et al., 2009), while it has also been shown that LPC injection in spinal cord causes astrocytic death at 72h of surgery (Plemel et al., 2018) at the same 1%LPC concentration. However, here we found that LPC 0.1% injections had a cytotoxic effect on astrocytes, leading to lower levels of GFAP intensity (34.69 ± 2.07 vs 74.49 ± 9.76 a.f.u., n=2, qualitative analysis), cell count (28.83 ± 3.19 vs 65.33 ± 5.60 cells/ROI, n=2, qualitative analysis) and surface area (78.43 ± 6.37 vs 116.8 ± 14.9 μm^2, n=2, qualitative analysis) compared to control (Group A) **(Fig 5.6 A-D)**. Notably, GsMTx4 had a positive effect protecting the number of astrocytes on LPC 0.1% + GsMTx4 3µM injected hemispheres (78.75 ± 4.51 vs 46.81 ± 3.80 cells/ROI, ***p<0.001; ordinary two-way ANOVA following Holm-Sidak post-hoc test, n=4, dF=16) (Group B), leading to similar results on cell count compared to control (58.5 ± 3.04 vs 57.0 ± 4.36 cells/ROI, n.s. p=0.78) **(Fig 5.6 A, C)**. Interestingly, GsMTx4 seems to not only protect astrocytes from cell death, but to also trigger activation of the astrocytes at the wound area, leading to a slight increase in GFAP intensity compared to control (69.94 ± 4.73 vs 62.97 ± 2.29 a.f.u., n.s. p=0.2) and to a significantly higher surface area (132.7 ± 5.38 vs 94.68 ± 3.87 μm^2, **p=0.0021), which has been associated to a more reactive phenotype **(Fig 5.6 B, D)**. When analysing the microglial staining Iba-1, we observed a strong response to LPC from Iba-1 stained microglia. It can be noted that microglia acquired a more reactive phenotype, morphing into larger cells and retracting their processes

(Fig 5.6 E). Quantification showed a higher intensity of Iba-1 fluorescence (70.12 ± 1.37 vs 36.03 ± 4.48 a.f.u., n=2, qualitative analysis), higher number of cell count (79.72 ± 4.31 vs 65.33 ± 5.60 cells/ROI, n=2, qualitative analysis) and a higher surface area (135.40 ± 10.38 vs 85.63 ± 8.42 μm^2, n=2, qualitative analysis) in LPC-injected hemispheres compared to control (group A) **(Fig 5.6 F-H)**. Notably, this reactivity was prevented in LPC 0.1% + GsMTx4 3µM injected hemispheres, where Iba-1 fluorescence intensity (Group B: 41.91 ± 1.98 vs 73.58 ± 5.03, ***p<0.001; Group C: 41.98 ± 2.53 vs 43.79 ± 2.21 a.f.u., n.s. p=0.67; ordinary two-way ANOVA following Holm-Sidak post-hoc test, n=4, dF=16), cell count (Group B: 57.74 ± 1.18 vs 74.26 ± 2.55 cells/ROI, ***p<0.001; Group C: 52.12 ± 1.93 vs 55.73 ± 4.48 cells/ROI, n.s. p=0.7845) and surface area (Group B: 79.33 ± 4.42 vs 126.4 ± 7.78 μm^2, ***p<0.001; Group C: 79.87 ± 5.98 vs 76.97 ± 4.20 μm^2, n.s. p=0.72) were similar to PBS (Group C) and significantly lower than in LPC 0.1% injected hemispheres (Group C) **(Fig 5.6 F-H)**. Under this treatment, microglia maintained a resting morphology, showing smaller bodies with longer processes **(Fig 5.6 E)**. These results match the literature showing that LPC induces reactivity in microglia in the grey matter and change of morphology in LPC injected rat brain tissue (Baradaran, Hajizadeh Moghaddam, & Ghasemi-Kasman, 2018; Ousman & David, 2000; Sheikh et al., 2009). This set of data demonstrates that SACs play a role in glial activation, turning astrocytes to what seems a more reactive state, while maintaining microglia in a resting state.

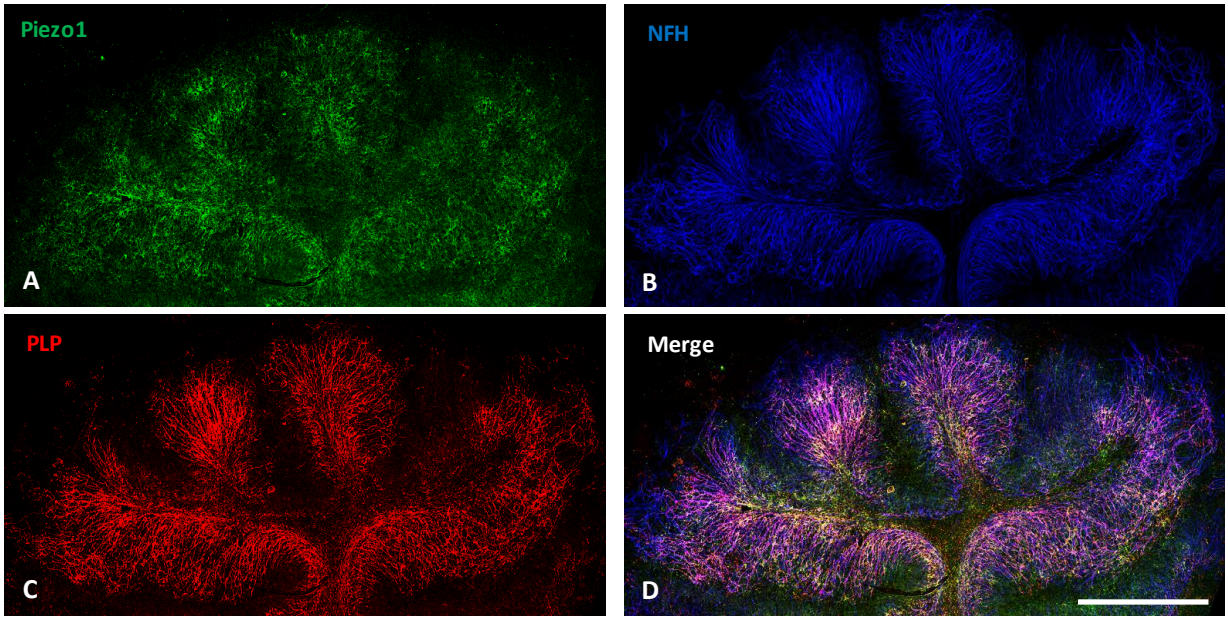

<u>Figure 5. 1</u>: Piezo1 is expressed in the myelinated areas of the cerebellum in organotypic slice culture.

Cerebellar slices were obtained from P10 mice and cultured *in vitro* for 12 days. Fluorescence staining was performed to confirm the expression of **(A)** Piezo1, alongside with **(B)** NFH and **(C)** PLP. Scale bar = 500 µm.

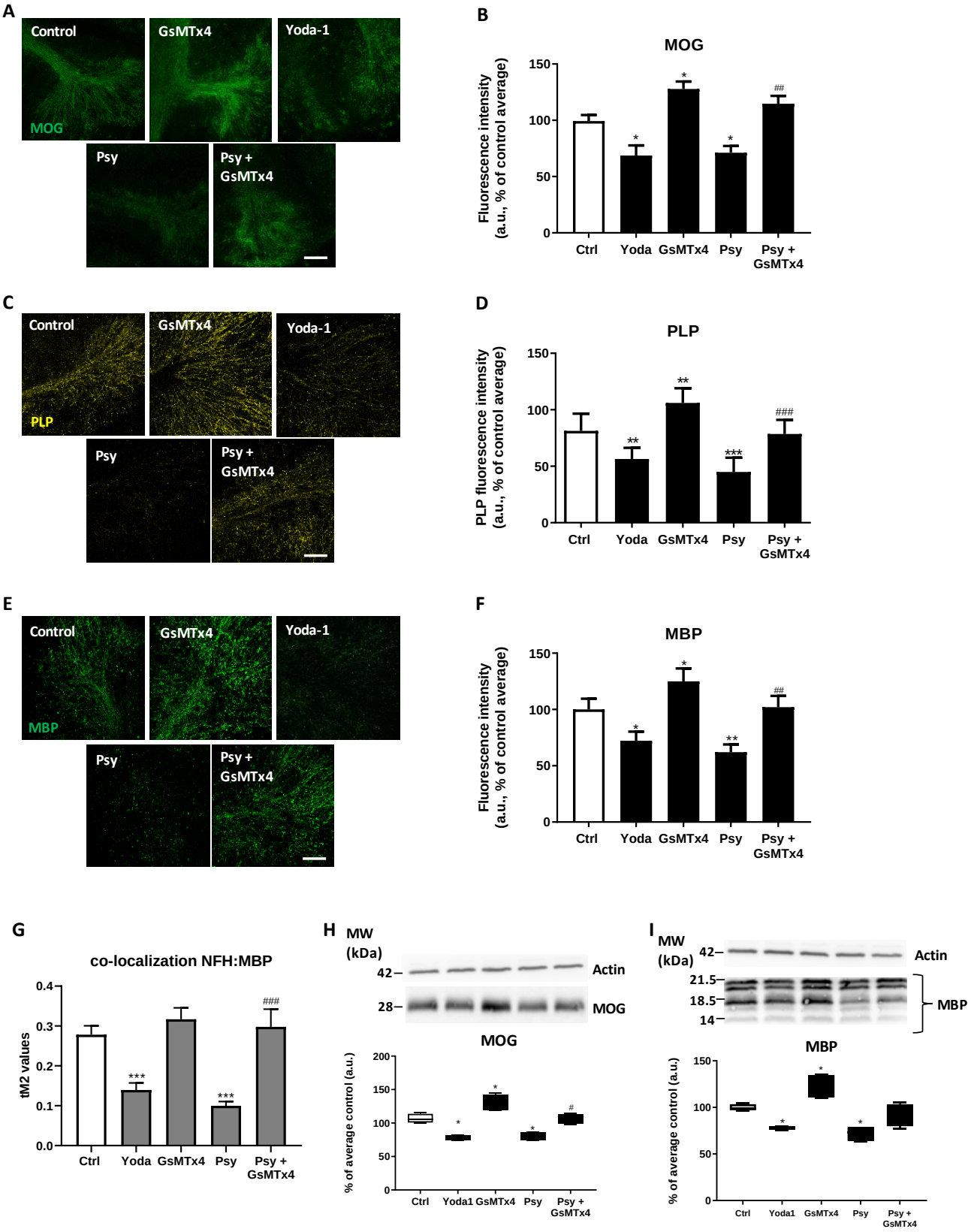
A
Control
GsMTx4
Yoda-1
MOG
Psy
Psy + GsMTx4
B
MOG
Fluorescence intensity (a.u., % of control average)
Ctrl
Yoda
GsMTx4
Psy
Psy + GsMTx4
C
PLP
D
PLP
PLP fluorescence intensity (a.u., % of control average)
E
MBP
F
MBP
G
co-localization NFH:MBP
tM2 values
H
MW (kDa)
Actin
MOG
% of average control (a.u.)
I
MBP
Yoda1

Figure 5. 2: The modulation of Piezo1 alters the myelin state of OCS and blockage of SACs by GsMTx4 prevents the PSY-induced demyelination.

Yoda-1 (10µM) induced demyelination as assessed by **(A, B)** MOG, **(C, D)** PLP and **(E, F)** MBP fluorescence intensity. On the contrary, treatment of slices with GsMTx4 (500nM) promoted the expression of the three myelin markers. As described in Misslin et al, 2017, 18h exposure to PSY (100nM) induced demyelination. However, co-treatment of PSY + GsMTx4 prevented this demyelination. **(B, D, F)** Quantification of fluorescence intensity of MOG, PLP and MBP. Repeated measures one-way ANOVA with Holm-Sidak post-hoc test was performed. Data shown as mean ± SEM, n=6, dF=4. **(G)** Colocalization analysis of MBP over NFH, as measured by thresholded Mander's values (tM2). Repeated measures one-way ANOVA with Holm-Sidak post-hoc test was performed. Data shown as mean ± SEM, n=6, dF=4 **(H-I)** Fluorescence results were corroborated with Western-Blot analysis for MOG and MBP. Repeated measures one-way ANOVA with Holm-Sidak post-hoc test was performed. Data shown as mean ± SEM, n=4, dF=4.

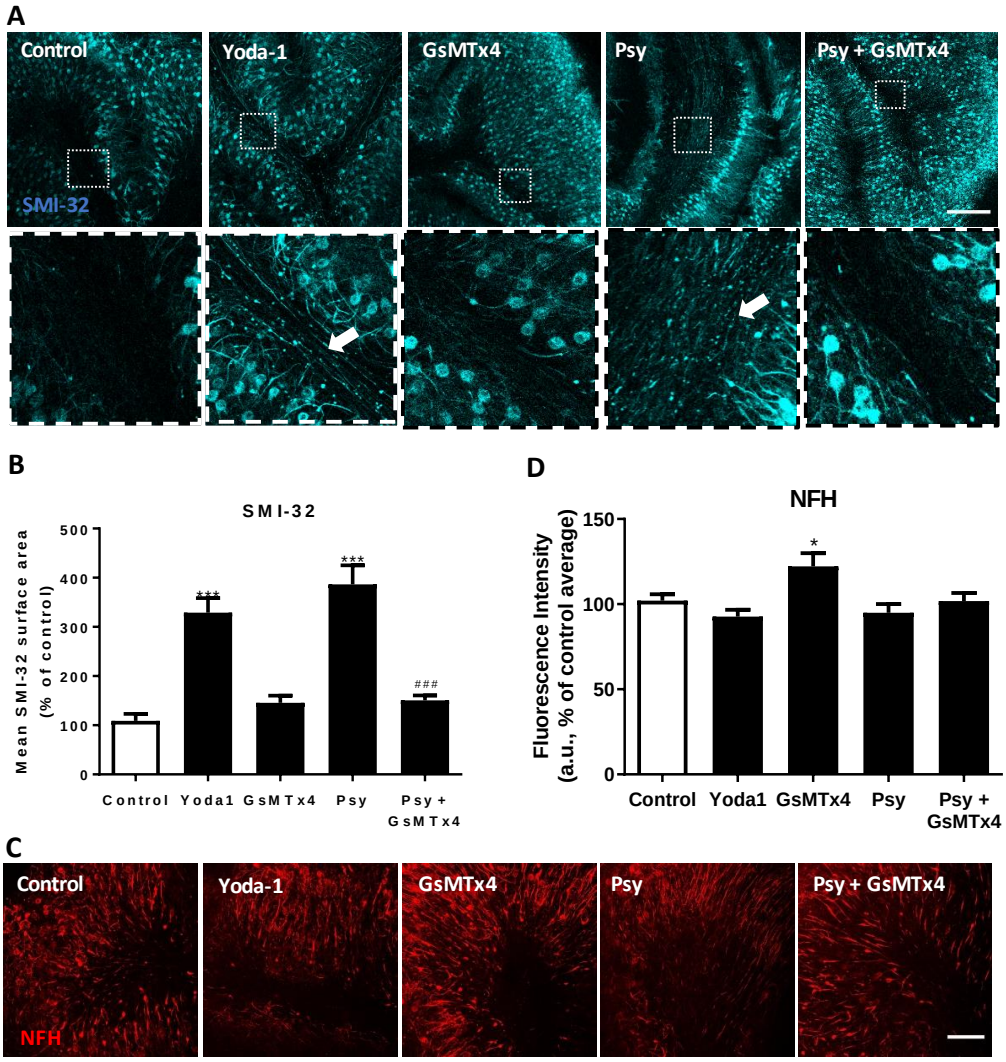

Figure 5. 3: GsMTx4 prevents PSY-mediated axonal injury in OCS.

(A) Immunofluorescence of slices showing the expression of axonal damage marker SMI-32 was done. Expression is constitutive in the soma of neurons, but expression of SMI-32 in the axons is observed only under damage situation (white arrows). Scale bar = 200µm **(B)** Statistical analysis of SMI-32 surface expression reveals an increase in the expression of SMI-32 in the white matter tracts under PSY and Yoda-1 treatment. However, PSY + GsMTx4 attenuated the effect of PSY and expression of SMI-32 is barely observed. Repeated measures one-way ANOVA with Holm-Sidak post-hoc test performed. Data is presented as mean ± SEM, n=5, dF=4. **(C)** Neurons were staining using NFH labelling. Scale bar = 100 µm. **(D)** Statistical analysis of NFH intensity values shows no variation under demyelination with PSY or Yoda-1 treatment. GsMTx4, on the contrary, caused an increase in the levels of NFH fluorescence intensity. Repeated measures one-way ANOVA with Holm-Sidak post-hoc test performed. Data is presented as mean ± SEM, n=10, dF=4.

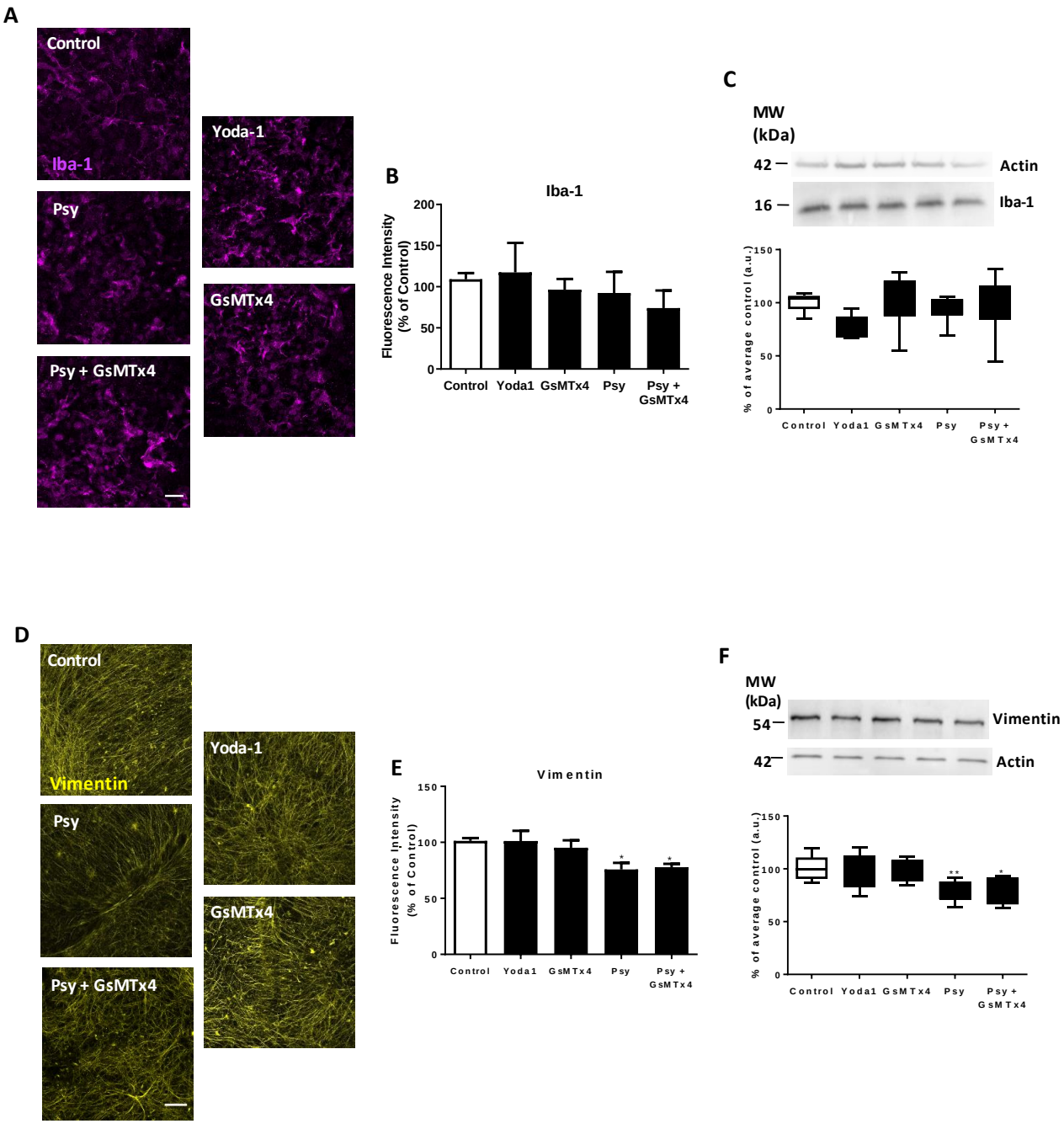
A
Control
Iba-1
Psy
Psy + GsMTx4
Yoda-1
GsMTx4
B
Iba-1
Fluorescence Intensity (% of Control)
200
150
100
50
0
Control
Yoda1
GsMTx4
Psy
Psy + GsMTx4
C
MW (kDa)
42
Actin
16
Iba-1
% of average control (a.u.)
150
100
50
0
Control
Yoda1
GsMTx4
Psy
Psy + GsMTx4
D
Control
Vimentin
Psy
Psy + GsMTx4
Yoda-1
GsMTx4
E
Vimentin
Fluorescence Intensity (% of Control)
150
100
50
0
Control
Yoda1
GsMTx4
Psy
Psy + GsMTx4
F
MW (kDa)
54
Vimentin
42
Actin
% of average control (a.u.)
150
100
50
0
Control
Yoda1
GsMTx4
Psy
Psy + GsMTx4

Figure 5. 4: GsMTx4 does not prevent PSY-mediated astrocyte toxicity in OCS.

(A-B) Immunofluorescence of microglial marker Iba-1 shows no apparent difference in morphology or fluorescence intensity amongst the treatment groups. Scale bar = 25 µm. Statistical analysis on fluorescence intensity values performed using repeated measures one-way ANOVA with Holm-Sidak post-hoc test. Data is shown as mean ± SEM, n= 6, dF=4. **(D-E)** Immunofluorescence of astrocytic marker vimentin shows a cytotoxic effect of PSY, which was not reverted by PSY + GsMTx4 treatment. Scale bar = 50 µm. Statistical analysis on fluorescence intensity values performed using repeated measures one-way ANOVA with Holm-Sidak post-hoc test. Data is shown as mean ± SEM, n=6, dF=4. **(C, F)** Western-Blot analysis for Iba-1 and vimentin corroborated the results observed by immunofluorescence. Statistical analysis on fluorescence intensity values performed using repeated measures one-way ANOVA with Holm-Sidak post-hoc test. Data is shown as mean ± SEM, n=7, dF=24 for Iba-1 and n=5, dF=20 for vimentin.

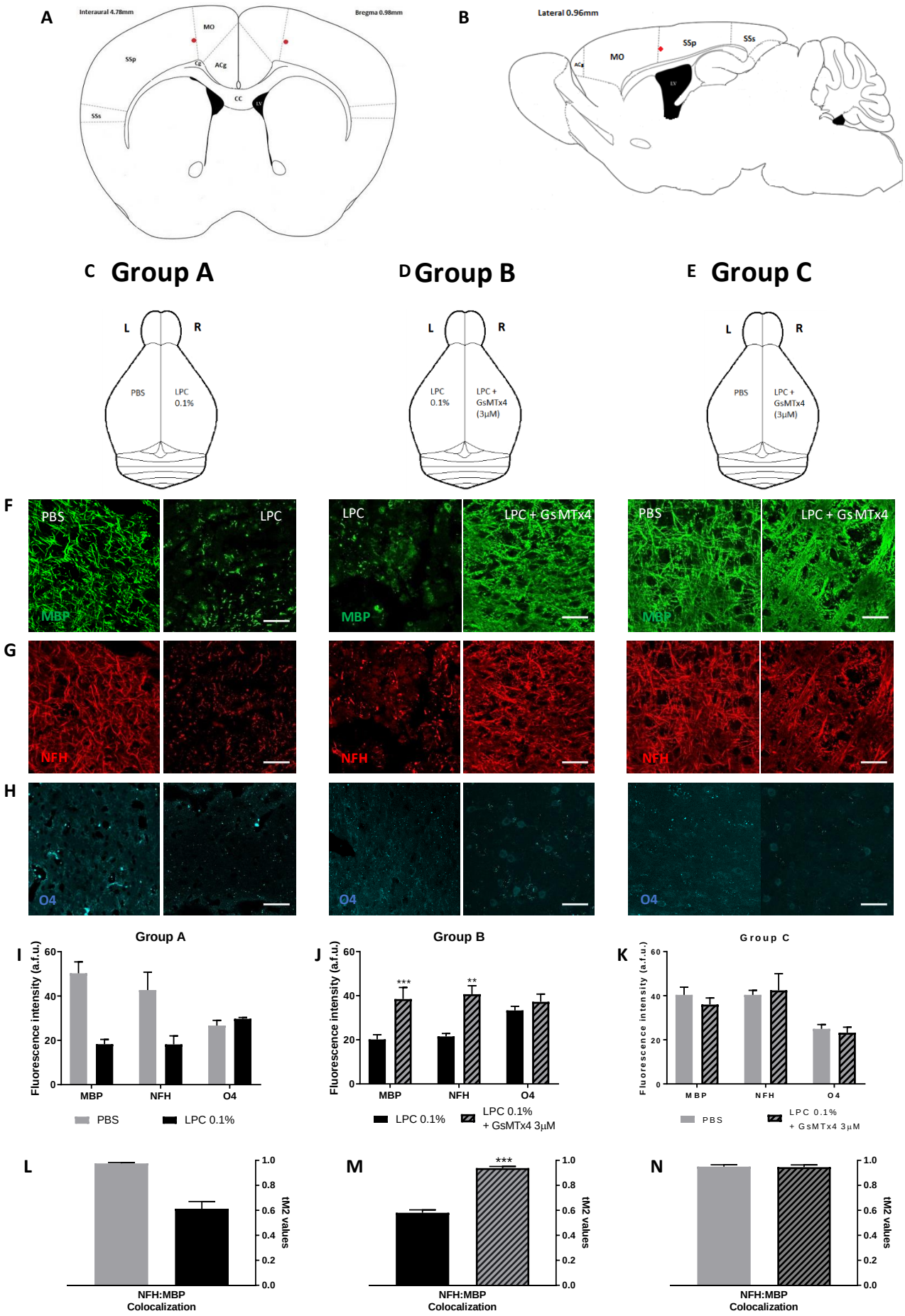
A
Interaural 4.78mm
Bregma 0.98mm
MO
SSp
ACg
CC
LV
SSs
B
Lateral 0.96mm
MO
SSp
SSs
ACg
LV
C Group A
D Group B
E Group C
L
R
PBS
LPC 0.1%
LPC
LPC + GsMTx4 (3μM)
F
G
H
MBP
NFH
O4
I
J
K
Group A
Group B
Group C
Fluorescence intensity (a.f.u.)
MBP
NFH
O4
PBS
LPC 0.1%
LPC 0.1% + GsMTx4 3μM
***
**
L
M
N
tM2 values
NFH:MBP Colocalization

Figure 5. 5: GsMTx4 protects from LPC-induced demyelination *in vivo*.

(A, B) Stereotaxic surgery in adult mice (9-10 weeks old) was performed in the border between somatosensory and motor cortex. Mice were randomly distributed in three groups: **(C)** PBS vs LPC 0.1%, **(D)** LPC 0.1% vs LPC 0.1% + GsMTx4 3µM, and **(E)** PBS vs LPC 0.1% + GsMTx4 3µM. **(F)** Immunohistochemistry of 12µm brain slices was performed to analyse the levels of MBP, **(G)** NFH and **(H)** oligodendrocyte marker O4. **(I-K)** Statistical analysis of MBP, NFH and O4 fluorescence across groups A to C. Statistical analysis performed using an ordinary two-way ANOVA following Holm-Sidak post-hoc test comparing left vs right hemisphere for groups B and C. Data is shown as mean ± SEM, n=4, dF=16; being each n number a different animal within the group. Group A had n=2, therefore no statistical analysis was performed but qualitative analysis was reported. **(L-N)** Analysis of the colocalization of MBP over NFH expression was performed, using thresholded Mander's values (tM2). **(L)** Qualitative analysis of tM2 in both hemispheres of group A is reported (n=2). **(M, N)** Statistical analysis of colocalization values between both hemispheres in groups B and C was performed using unpaired t-test with Welsch's correction, n=4, dF=3; being each n number a different animal within the group.

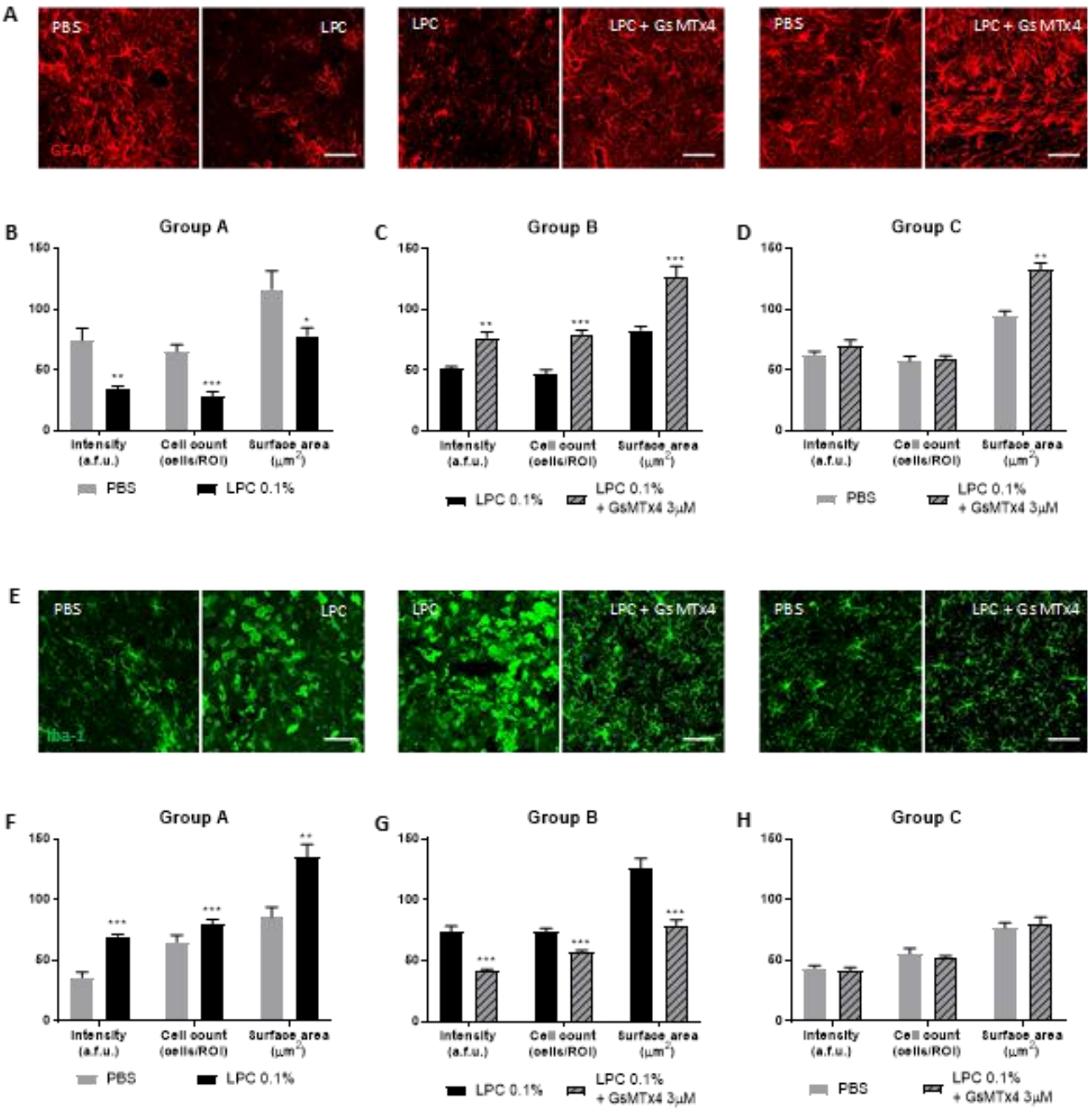
A
PBS
LPC
GFAP
LPC
LPC + Gs MTx4
PBS
LPC + Gs MTx4
B
Group A
Intensity (a.f.u.)
Cell count (cells/ROI)
Surface area (µm²)
PBS
LPC 0.1%
C
Group B
LPC 0.1%
LPC 0.1% + GsMTx4 3µM
D
Group C
PBS
LPC 0.1% + GsMTx4 3µM
E
PBS
LPC
Iba-1
LPC
LPC + Gs MTx4
PBS
LPC + Gs MTx4
F
Group A
G
Group B
H
Group C

Figure 5. 6: GsMTx4 attenuates the astrocyte death and microglial reactivity caused by LPC **(A-C)** Immunofluorescence of astrocytic marker GFAP shows the cytotoxic effects of LPC injection, causing a decrease in the fluorescence intensity values and cell count. It can be observed that co-treatment with GsMTx4 attenuates this cytotoxicity on astrocytes. **(D)** Furthermore, surface area analysis of GFAP shows an increase in the immunolabelled area of LPC + GsMTx4 compared to LPC or PBS injected hemispheres, showing a change in morphology associated with astrocyte reactivity. **(E-G)** Analysis of the microglial Iba-1 marker shows higher intensity and cell count of Iba-1 positive cells in LPC injected hemispheres, compared to PBS control or co-treatment with LPC + GsMTx4. **(H)** Morphological analysis of the surface area of Iba-1 expression reveals higher surface area in LPC injected hemispheres and it can be observed that Iba-1 positive cells adopt an ameboid-like morphology, while PBS and LPC + GsMTx4 injected hemispheres showed a thinner and ramified morphology. All statistical analysis was performed using a two-way ANOVA with Holm-Sidak post-hoc test comparing left vs right hemisphere on each group. Data shown as mean ± SEM.

3. Discussion

3.1. Summary of findings.

This is the first time reported that Piezo1 has a role in myelination in the brain. Myelination is a complex process involving oligodendrocytes in the CNS and Schwann cells in the PNS insulating the neuron's axons with myelin sheath. Regulation of myelination and remyelination is usually seen as a crosstalk process between cells or oligodendrocytes maturation and differentiation through different biochemical pathways, e.g. ERK/MAPK (Ishii, Furusho, Dupree, & Bansal, 2014), wnt/β-catenin (Fancy et al., 2009), PI3K/AKT/mTOR (Hu, Schlanger, He, Macklin, & Yan, 2013). However, in the recent years mechanotransduction – conversion of the mechanical stimuli into chemical signalling - has gained more weight and importance in this field. It has been shown that stiffness of the substrate affects OPCs differentiation and oligodendrocytes maturation, as the former could not properly differentiate in a rigid, lesion-like matrix (Urbanski et al., 2016). Furthermore, electro-spun polystyrene nanofibers of a similar diameter to neuron's axons can be myelinated by oligodendrocytes (S. Lee et al., 2012), suggesting that myelination has a mechanical component that needs to be led by biochemical signals. In addition to this, we have previously shown that Piezo1 is greatly expressed in the highly myelinated areas of the brain, leading to our hypothesis that this mechanosensitive receptor can have a role in the regulation of myelination through mechanotransduction **(Supplemental Figure 5.1)**. In this study, we have shown how activation of Piezo1 by specific activator Yoda-1 cause demyelination in *ex vivo* model organotypic slice culture, while the inhibition of SACs signalling by the tarantula-venom peptide GsMTx4 leads to higher levels of myelin markers MBP, PLP, and MOG. Not only that, but the demyelinating effect caused by psychosine on these slices was reverted by co-treatment with GsMTx4. These effects were corroborated *in vivo* by a focal demyelinating model using stereotaxic injection of LPC 0.1% as demyelinating agent in one hemisphere, while injecting co-treatment of LPC 0.1% + GsMTx4 3µM in the other hemisphere. The effects of GsMTx4 were independent from changes in the oligodendrocyte marker O4, which supports the hypothesis that GsMTx4 acts preventing this demyelination instead of promoting remyelination. These novel results support the idea of Piezo1 as a key target for the regulation of myelination, where a better understanding of its functionality might help to understand the myelination process, and maybe even turning Piezo1 into a therapeutic target for demyelinating pathologies.

3.2. Role of Piezo1 in the regulation of myelination

Here we have shown that activation of Piezo1 by the specific activator Yoda-1 led to a decrease in levels of MOG, MBP and PLP with no differences in the levels of NFH that could indicate death of neurons; suggesting demyelination of the axons with no neuronal death involved. Moreover, inhibition of SACs -where Piezo1 belongs to- through the peptide GsMTx4 led to an increase in levels of MBP, PLP, MOG and even NFH. This suggests that blocking SACs, and therefore blocking the influx of Ca^{2+} had an effect not only in the myelin sheath and myelinating process, as it happened with Yoda-1, but also has an effect on the neuronal axons. In accordance with previous studies performed in our lab, when OCS were treated with psychosine, this toxin caused demyelination (C. O'Sullivan & Dev, 2015); but interestingly, inhibition of SACs by co-treatment of psychosine plus GsMTx4 reverted this demyelinating effect of psychosine, leading to similar levels to control. Not only that, but when analysing the axonal damage marker SMI-32, it can be observed that demyelination, whether caused by Yoda-1 or psychosine, leads to axonal damage and subsequent expression of SMI-32 in the white matter tracts of organotypic slices. However, when slices were treated with GsMTx4, the psychosine-induced axonal damage was prevented and barely no expression of SMI-32 can be observed in the axons.

The organotypic slice cultures are a useful tool to study myelination *ex vivo*. However, in order to assess these effects *in vivo*, we used a focal demyelinating model by stereotaxic injections in young male adult C57BL/6 mice (9-10 weeks old). There were three different treatments injected: LPC 0.1%, PBS or LPC 0.1% + GsMTx4 3µM. Animals were randomly distributed in three groups, in which left and right hemisphere were injected with different treatments. This approach allows us to reduce the interindividual variations and reduce the animals needed, in accordance with the 3Rs. Group A was injected with LPC 0.1% in the left hemisphere vs PBS in the right hemisphere to make sure our technique was valid and LPC 0.1% showed demyelination. Group B was injected with LPC 0.1% in the left hemisphere and LPC 0.1% + GsMTx4 3µM in the right hemisphere to analyse if GsMTx4 attenuated the effects of LPC in the cortex. Finally, group C was injected with PBS in the left hemisphere and LPC 0.1% + GsMTx4 3µM in the right hemisphere to assess if the preventive effect of GsMTx4 was enough to maintain the levels of myelin similar to control levels. Interestingly, here we have shown how co-injection of LPC 0.1% + GsMTx4 3µM did lead to a prevention of the LPC-induced demyelination and maintain the levels of myelin similar to control. Furthermore, it attenuated the neuronal death caused by LPC and measured by the levels of NFH. By analysing the precursor and immature oligodendrocytic marker O4, we observed that none of the treatments caused

any effects on O4 expression, suggesting that the observed effects are indeed due to prevention of demyelination and not because of a promotion in remyelination.

3.3. Effects of GsMTx4 in glial cells

It can be found in the literature that Piezo1 is not expressed in healthy astrocytes, but it has been reported to be expressed on the senile astrocytes associated to amyloid plaques in post-mortem Alzheimer's disease brains (Satoh et al., 2006). Piezo1 is also expressed in the astrocytes in the optic nerve (Choi et al., 2015) and we have previously shown that astrocytes under certain stimuli – i.e. LPS or psychosine - also express this mechanosensitive ion channel. Activation or inhibition of Piezo1 in healthy cerebellar slices did not show any effect on the levels of astrocytic marker vimentin. This could be due to the fact that Piezo1 is not expressed on astrocytes under such conditions. Additionally, psychosine treatment produced a decrease in the levels of vimentin, and this reduction in vimentin was not reverted under psychosine plus GsMTx4 treatment. These results match our previous *in vitro* studies, showing that modulation of Piezo1 in LPS or psychosine treated astrocytes –which show expression of Piezo1 in the ER-, had no effect on the cell viability of primary mouse astrocyte culture **(Chapter 3, Figure 3.4).** On the second stage of this study, we analysed the expression of astrocytic GFAP marker and microglial Iba-1 *in vivo*. In this case, we observed that LPC had a cytotoxic effect on astrocytes, leading to lower levels of GFAP expression and cell count of GFAP-positive cells. However, in this occasion, co-treatment with GsMTx4 prevented this cytotoxicity and the number of GFAP-positive cells were similar to control. This could be due not to a direct effect of GsMTx4 in astrocytes, but because of a different microenvironment in which the astrocytes are: as GsMTx4 seems to prevent demyelination, astrocytes around the wound area are not exposed to myelin debris and subsequent inflammation and microglial activation, which can then lead to astrocyte death. On the other hand, it can be observed that GsMTx4 caused a slight increase in the levels of GFAP intensity and a significant increase in the surface area of GFAP labelling compared to control. These two markers are indicative of astrocyte reactivity, suggesting that blockage of SACs leads to a more reactive phenotype in astrocytes. These results are in accordance to what we observed previously in our studies *in vitro*, in which treatment with GsMTx4 in LPS-stimulated astrocytes, led to higher levels of proinflammatory cytokines release and astrocytic migration **(Chapter 3, Figure 3.4, Figure 3.5)**.

When studying the effects of Yoda-1 or GsMTx4 in microglia, there was no effect observed in the levels of microglial Iba-1 marker in slices under any treatment. There are no previous studies in the literature reporting the expression of Piezo1 in microglia. However, primary culture of mouse microglia seems to express Piezo1 in the outer membrane as well as cytoplasm *(personal communication from Miss Myrthe Mampay*). In addition to this, RNA sequencing shows higher load of Piezo1 mRNA in microglia (around 30 FPKM) than in any other brain cell type such as neurons (3 FPKM) or astrocytes (4 FPKM), according to the database created by groups from Stanford University (http://web.stanford.edu/group/barres_lab/brain_rnaseq.html). We note that Iba-1 is not a specific marker to measure microglial reactivity, and therefore we cannot conclude that modulation of Piezo1 in cerebellar slices had no effect in changing microglia to a more reactive phenotype just by analysing Iba-1 levels. However, when analysing expression of Iba-1 *in vivo* at the second stage of this study, it can be noted that LPC causes an increase in Iba-1 fluorescence intensity, cell count of positive cells and higher surface area, with a bigger, more rounded and retracted projections phenotype. It has been previously stated in the literature that resting microglia has a short, with fine and ramified processes shape, whereas activated microglia lack these processes, having a spherical and amoeboid shape, also described as 'macrophage-like' shape (Boche, Perry, & Nicoll, 2013).

3.4. Putative mechanisms for Piezo1 regulation of myelination

It is known that Piezo1 activation leads to an increase of Ca^{2+} influx inside the cell (Coste et al., 2010). However, the biochemical pathways downstream of this influx of Ca^{2+} remain yet unknown, and therefore more research should be performed in order to assess the actual mechanism by which Piezo1 is able to regulate myelination in the CNS. Nevertheless, it has been suggested that when the epithelial barrier is too crowded, activation of Piezo1 in epithelial cells activated the live cell extrusion from the epithelial barrier by S1P cascade (Gudipaty & Rosenblatt, 2016). Previous studies in this lab have shown how antagonists of S1P-receptors (S1PR) such as FTY720 (antagonist of all five S1PR) or BAF312 (antagonist of S1PR1 and S1PR5) have positive effects on myelination in mouse cerebellar slice culture (C. O'Sullivan & Dev, 2015), thus indicating that this might be a pathway through which Piezo1 can exert its effects on the regulation of myelination.

As we have shown in this study, Yoda-1 caused demyelination of organotypic slice cultures in absence of any other demyelinating agent, while GsMTx4 caused an increase in the myelination

and an increase in the levels of NFH. We hypothesize that these effects may be mediated through the activation/inhibition of Piezo1 in the axons. Piezo1 is expressed in the outer membrane of neurons (Koser et al., 2016). Its activation with Yoda-1 causes an influx of Ca^{2+} inside the axon, which can be further increase with the release of Ca^{2+} from intracellular stores by the activation of Piezo1 in the ER. It has been shown in the literature that activation of Piezo1 leads to production of adenosine tri-phosphate (ATP) (Cinar et al., 2015; S. Wang et al., 2016) and ATP is an allosteric activator of IP3 receptors in the ER (Tu, Wang, Nosyreva, De Smedt, & Bezprozvanny, 2005), leading to a further release of Ca^{2+} from intracellular stores to the cytoplasm. This high increase in Ca^{2+} in the axons, could activate calpain (Azuma & Shearer, 2008), which would disrupt the integrin association to the actin cytoskeleton via talin and vinculin. This disruption in the integrin signalling between oligodendrocytes and axons would cause the association of the myelin sheath to the axon to stop and could lead to demyelination. On the contrary, GsMTx4 could block this Ca^{2+} influx in the outer membrane and ER through Piezo1, inhibiting this excitotoxic effect and disruption of the integrin signalling. Also, it has been shown that an influx of Ca^{2+} due to stretch or mechanical insults, such as in traumatic brain injury, causes the activation of calpain, which can mediate the proteolysis of spectrin (a major constituent of the axonal cytoskeleton) leading to cytoskeletal instability and neuronal death (Buki & Povlishock, 2006). Thus, we propose GsMTx4 could have such protective effects in axons by blocking Piezo1 and other SACs in the neurons, therefore inhibiting calpain activation and leading to stronger stabilization of cytoskeleton, as observed in cerebellar slices. In addition to this effect, GsMTx4 seems to have a protecting effect to demyelination, possibly acting through SACs in the oligodendrocytes. It has been previously shown that Ca^{2+} regulates myelination in oligodendrocytes (Fu, Wang, Huff, Shi, & Cheng, 2007). By blocking SACs with GsMTx4 in the myelinating oligodendrocytes, the influx of Ca^{2+} is being blocked, and thus the activation of calpain and PLA_2 that causes lipid degradation **(Supplemental Figure 6.3).**

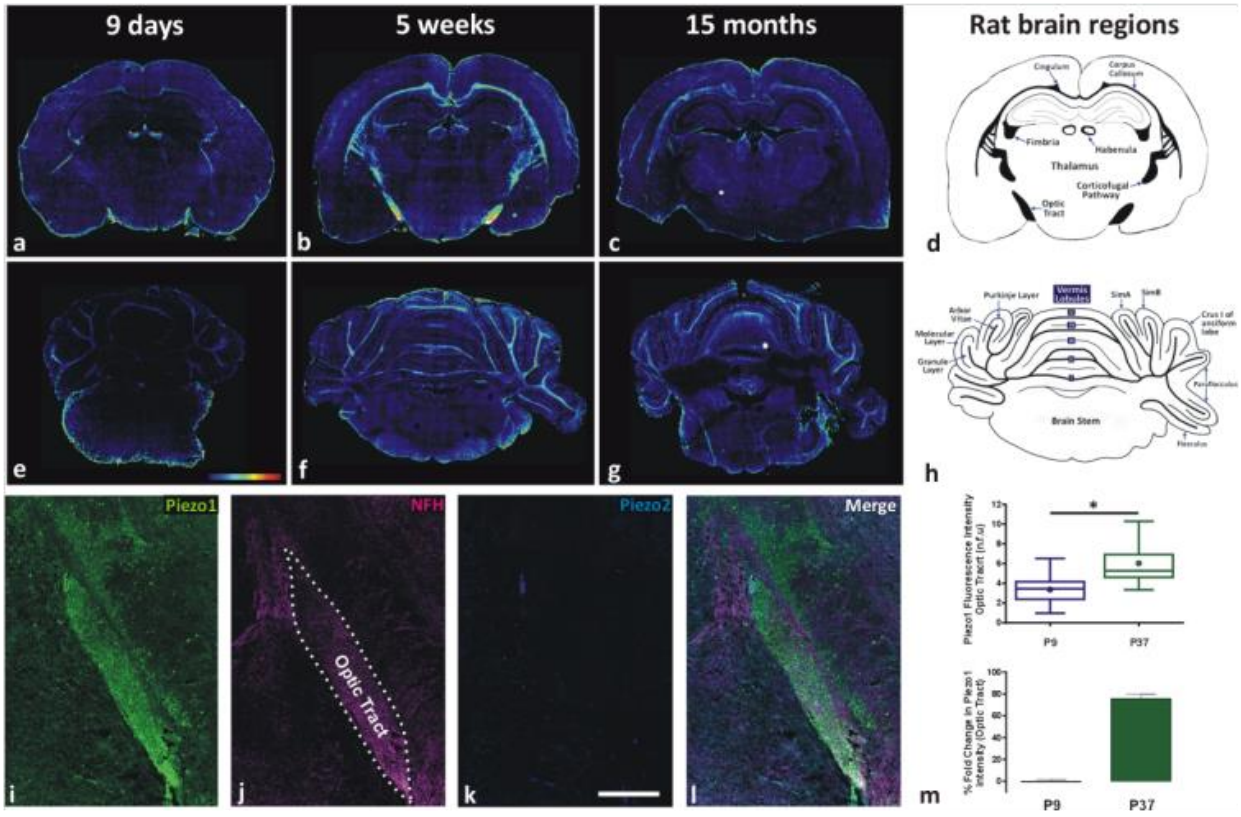

Supplemental Figure 5. 1: Piezo1 expression in rat brain at postnatal day 9, 5 weeks old and 15 months old.

(A-L) Piezo1 is greatly expressed on the highly myelinated areas of the brain in the rodent brain, i.e. arbour vitae of the cerebellum, optic tract and corpus callosum. Its expression also varies with age, peak expression of Piezo1 observed at 5 weeks old (young adult rat), also when there is a peak in the myelination state. **(D)** Schematic figure of the areas in the rat brain and **(H)** cerebellum.

Chapter 6:
Discussion

1. Summary of findings

Piezo1 was discovered to be expressed in the mouse neuroblastoma cell line Neuro2A almost a decade ago (Coste et al., 2010) and has since been found in many other tissue cell types, such as lung (McHugh et al., 2012), skin (Eisenhoffer et al., 2012), bladder (T. Miyamoto et al., 2014), kidney (Peyronnet et al., 2013), endothelium (S. Wang et al., 2016) and RBCs (Albuisson et al., 2013; Cahalan et al., 2015; Cinar et al., 2015; Faucherre et al., 2014). This mechanosensitive channel mediates several different vital cell functions including cell apoptosis, migration and differentiation. However, the expression and function of Piezo1 in the CNS has remained relatively unclear. Piezo1 is reported to be expressed in the basal membrane of neurons (Koser et al., 2016) whilst being absent in astrocytes, with no studies reporting its expression in other type of brain cell like microglia or oligodendrocytes. Here, we aimed to investigate the role of Piezo1 as follow:

- We first investigated the role of Piezo1 in astrocytes and showed it to be absent in physiological conditions. We found, however, Piezo1 expression could be induced in the endoplasmic reticulum of astrocytes under certain inflammatory and toxic stimuli, such as LPS, psychosine or Aβ. We also demonstrated that pharmacological modulation of Piezo1, by its activator Yoda-1 or its inhibitor GsMTx4, regulated the reactive state of astrocytes by (I) mediating the levels of proinflammatory cytokines IL6, IL1β and TNF-α in astrocytes, (II) regulating astrocyte migration, and (III) altering Ca^{2+} signalling response upon Piezo1 activation *in vitro* **(Chapter 3)**.
- Next, we investigated astrocytic Piezo1 *in vivo*, using the transgenic TgF344-AD Alzheimer's rat model, in presence or absence of repeated peripheral infections with *E.coli*. Corroborating our *in vitro* data, we observed that Piezo1 expression was induced in the endoplasmic reticulum of the astrocytes around the amyloid plaques, and that peripheral infection further enhanced this expression *in vivo*. We also validated the amyloidosis, astrocyte reactivity and myelin state of this rat model, observing that the TgF344-AD rat models displays many of the AD characteristics and hallmarks of this disease **(Chapter 4).**
- Lastly, based upon our previous studies showing Piezo1 is expressed in highly myelinated tracts of the optic tract, corpus callosum and arbor vitae of the cerebellum (*unpublished data*) and the numerous studies proving a contribution of mechanical stimuli in the initiation and progression of myelination (Jagielska et al., 2012; S. Lee et al., 2012; Lourenco & Graos, 2016; Urbanski et al., 2016), we hypothesized and examined a potential role for Piezo1 in the regulation of myelination in the CNS.

In this study, using an organotypic cerebellum slice culture *ex vivo* model, we showed that activation of Piezo1 with Yoda-1 induced demyelination, whilst blocking with GsMTx4 had the opposite effect on the white matter tracts of these slices. Moreover, GsMTx4 attenuated the psychosine-induced demyelination effect *ex vivo*. Importantly, we demonstrated that GsMTx4 had a protective effect on myelination *in vivo* using an LPC-induced focal demyelination mouse model. We showed that co-injection with GsMTx4 inhibited the LPC-induced demyelination, and also attenuated microglia reactivity and neuron loss. In agreement with our *in vitro* studies on astrocytes, we observed that GsMTx4 caused an increase in the reactive state of the astrocytes around the wound **(Chapter 5).**

These findings report, for the first time, a role for the mechanoreceptor Piezo1 in the modulation of the astrocytic reactivity upon inflammatory or pathological conditions. Furthermore, we suggest Piezo1 as a regulator of myelination, likely playing a role as modulator in the crosstalk between oligodendrocytes and neurons.

2. Piezo1 regulates levels of cytokine in astrocytes

It has been shown that healthy astrocytes do not express Piezo1, which under physiological conditions, is only expressed in neurons (Satoh et al., 2006). Here we showed Piezo1 is expressed in pathological conditions both in cultured astrocytes and in an *in vivo* model of Alzheimer's disease. Thus, we suggest that Piezo1 may act as a regulator of the astrocytic reactivity response to insults. To support this idea, we have shown that the specific activation of Piezo1 by Yoda-1 led to decreased levels of IL-6, IL-1β and TNF-α under LPS treatment compared to LPS treatment alone, in astrocytes. TNF-α is a pleiotropic mediator of physiological and neurological functions including thermoregulation, regulation of sleep and regulation of cell fate (Perry, Dewhurst, Bellizzi, & Gelbard, 2002). High levels of TNF-α have been associated to pathological conditions such as bacterial infection (Barichello et al., 2009), Multiple Sclerosis (Obradovic, Kataranovski, Dincic, Obradovic, & Colic, 2012), Parkinson's disease (Boka et al., 1994; Mogi et al., 1994) or Alzheimer's disease (Bruunsgaard et al., 1999). There are several mechanisms by which TNF-α exerts its neurotoxic effects in the CNS, including disruption of the integrity of the blood-brain barrier (G. A. Rosenberg, Estrada, Dencoff, & Stetler-Stevenson, 1995), activation of microglial cells and potentiation of the glutamate-mediated toxicity by preventing glutamate uptake (Chao & Hu, 1994). Previous studies have shown that neutralizing TNF-α or antagonizing its receptors, attenuates its neurotoxic effects in the CNS (Sriram &

O'Callaghan, 2007). Similarly, IL-6 is released in high concentrations under certain pathologies such as AD (Swardfager et al., 2010), and schizophrenia (Sasayama et al., 2013). Blockade or neutralization of proinflammatory cytokines such as TNF-α and IL-6 has beneficial effects in the evolution of many conditions such as Rheumatoid Arthritis. Here we have shown that activation of Piezo1 can be a new approach to reduce the levels of both cytokines at least under those conditions that induce the expression of Piezo1 in astrocytes. The mechanisms underlying this modulatory effect are yet to be found, as well as whether activation of Piezo1 is also involved in the release of other pleiotropic proinflammatory cytokines such interferon-γ (IFN-γ), IL-1 or IL-12.

Of interest, studies in the literature show that LPS induces the production of proinflammatory cytokines via NFκB (Lilienbaum & Israel, 2003). Historically, it has been regarded that the activation of NFκB is positively regulated by intracellular Ca^{2+} signals, where an increase of the levels of internal Ca^{2+} activate Ras, which leads to the activation of the ERK/MAPK cascades. MAPK can then phosphorylate the inhibitory subunit IκB, directing it to the proteasome and activating NFκB (Schulze-Osthoff, Ferrari, Riehemann, & Wesselborg, 1997). NFκB can then act as a transcription factor and induce the production of proinflammatory cytokines (Han & Logsdon, 2000; Hsuan et al., 1999; Morita et al., 2003; Pahl & Baeuerle, 1996). However, Ca^{2+} regulation of the activation of Ras is complex and dependent on time, amplitude, duration and frequency of the Ca^{2+} signal, this ion activates or inhibits Ras (Cullen & Lockyer, 2002). For instance, the Ca^{2+}-promoted Ras Inactivator (CAPRI) is a cytosolic Ras GTPase-activator protein (GAP) that is inactive in unstimulated cells; however, when intracellular Ca^{2+} is elevated in the cell, CAPRI is recruited to the plasma membrane switching on its Ras GAP activity, inactivating Ras and subsequently inactivating the ERK/MAPK signalling cascade (Lockyer, Kupzig, & Cullen, 2001). Thus, we suggest that activation of Piezo1 by Yoda-1 could cause the Ca^{2+}-induced activation of CAPRI, inhibiting the ERK/MAPK cascades and activation of NFκB as transcription factor for proinflammatory cytokine production, supporting our findings on the levels of cytokine release in stimulated astrocytes following modulation of Piezo1 by Yoda-1 or GsMTx4.

3. Piezo1 mediates intracellular calcium signalling in astrocytes

Supporting the idea that Piezo1 may alter levels of cytokines via a Ca^{2+}-dependent mechanism, we have demonstrated this mechanoreceptor can alter Ca^{2+} signalling in astrocytes. The endoplasmic reticulum is an intracellular Ca^{2+} store, essential in the regulation of Ca^{2+} homeostasis as well as in the role of Ca^{2+} as second messenger at an intra- and intercellular level (Beck, Nieden, Schneider, & Deitmer, 2004). The levels of intracellular Ca^{2+} are around 10^{-4} mM, approximately four times less than the extracellular concentration, where small changes in the Ca^{2+} homeostasis can activate/deactivate a myriad of biochemical pathways, such as MAPK, ERK or JNK (Kant, Bhandakkar, & Medhekar, 2017). The importance of Ca^{2+} homeostasis is also central in disease, where despite specific etiopathology and progression, most neurological conditions including Parkinson's disease, AD, MS, Huntington's disease or amyotrophic lateral sclerosis, have Ca^{2+} dysregulation as a common feature (Nagarajan et al., 2014). Therefore, we hypothesized that Piezo1 may modulate the internal Ca^{2+} levels. When analysing the levels of intracellular Ca^{2+} in astrocytes, we observed Yoda-1 did not regulate Ca^{2+} levels in astrocytes under basal conditions, in agreement with our previous findings showing Piezo1 is not expressed in unstimulated astrocytes. However, we showed that stimulated astrocytes responded to Yoda-1 with a transient peak in internal Ca^{2+} levels. We showed also that Yoda-1 altered subsequent ATP-mediated Ca^{2+} signalling, leading to a smaller maximal magnitude, but longer lasting Ca^{2+} signalling. We hypothesize that due to three potential mechanisms: (I) firstly, that Yoda-1 diminished Ca^{2+} from internal stores and thus alters subsequent ATP-mediated Ca^{2+} signalling; (II) secondly, Yoda-1 induced ATP production via activation of Piezo1; and (III) thirdly, the sarcoplasmic/endoplasmic reticulum Ca^{2+}ATPase (SERCA) pump can act as a binding partner of Piezo1, supporting the hypothesis of Piezo1 as a regulator of the Ca^{2+} homeostasis of the cell (T. Zhang et al., 2017). In support of Piezo1 regulating Ca^{2+} signalling via an ATP-dependent mechanism, studies have shown that activation of Piezo1 produces internal ATP release (Friedrich et al., 2017; T. Miyamoto et al., 2014). ATP is known to mediate calcium waves in astrocytes (Guthrie et al., 1999), by activating the purinergic receptors, which release inositol-3-phosphate (IP3) and subsequent activation of the IP3R in the ER (S. Y. Lee & O'Grady, 2003). It can be observed that the transient peak of Ca^{2+} influx with Yoda-1 is relatively small compared to ATP. We propose this is because Yoda-1 not acting as a normal agonist following a lock-key mechanism. Instead, Yoda-1 binds to certain regions of Piezo1 lowering the mechanical threshold for activation allowing Piezo1 to enter an open state for a significant fraction of time

in absence of mechanical stimuli. Such temporal stimulation of Piezo1 may allow the Ca^{2+} signalling we observed induced by Yoda-1 (Syeda et al., 2015).

4. Piezo1 as modulator of astrocyte cell migration

Previous studies have suggested that Piezo1 plays a role in modulating integrin signalling, where knockdown of Piezo1 in small lung cancer cells led to cell detachment and increased migration (McHugh et al., 2012). Given that activated astrocytes have enhanced migration, which is suggested to enable these cells to reach the site of injury (Y. Zhang et al., 2015), we investigated if Piezo1 regulates astrocyte migration. As expected, we found that neither Yoda-1 nor GsMTx4 altered migration in control unstimulated astrocytes. Interestingly, LPS-stimulated astrocytes presented higher migration rates when Piezo1 was blocked with GsMTx4, while activation with Yoda-1 had the opposite effect.

Migration is a biological feature of many cells, such as lymphocytes, macrophages, myofibroblast, microglia and astrocytes amongst others. There are two basic phenotypes of migration: ameboid-like migration (integrin-independent) and mesenchymal-type migration (integrin-dependent) (Friedl & Brocker, 2000; Nourse & Pathak, 2017; Shi, Badri, Choudhury, & Schuger, 2006). The ameboid-like migration is utilized by, for example leukocytes, and is driven by short-lived and weak interactions between the cell and the matrix, therefore independent of integrin signalling cascades, enabling rapid cell movement (Shi et al., 2006). On the other hand, mesenchymal-type migration depends on integrin signalling and cytoskeletal contractibility, and it is observed in cells such as fibroblasts or endothelial cells (Friedl & Brocker, 2000). The migration capacity of astrocytes is somewhat controversial, but both radial glia (astrocyte progenitors) (Goldman, Zerlin, Newman, Zhang, & Gensert, 1997) and reactive astrocytes, are migratory in the CNS (J. S. Zhan et al., 2017). During CNS damage, the ECM and integrin network suffers rearrangements and altered signalling, which can influence the migratory and proliferative capacities of reactive glial cells (Wagner, Tagaya, Koziol, Quaranta, & del Zoppo, 1997). The mechanisms underlying the migration of reactive astrocytes remain still unclear. Here, we hypothesize that Piezo1 can modulate the migratory capacity of reactive astrocytes by modulating the calcium signalling, integrin cascades, cytoskeletal rearrangement, shifting the cells to an ameboid-like migration state.

Contact inhibition between astrocytes limits their migration (Wagner et al., 1997). This cell contact is regulated by integrin receptors, where down-regulation of integrin signalling enhances the migratory capacity of astrocytes: for instance, conditional deletion of integrin β1

in astrocytes would enhance glial migration (Robel et al., 2009). Integrins can regulate migration causing a rearrangement of the cytoskeletal proteins, such as the intermediate filaments (J. S. Zhan et al., 2017). Interestingly, it has been observed that intermediate filament-deficient astrocytes present impaired migration (Lepekhin et al., 2001), thus proving a vital role of intermediate filaments in astrocyte migration. Reactive astrocytes overexpress one of their filaments, GFAP (Sofroniew & Vinters, 2010), which can help to explain why astrocytes that present a reactive phenotype show an increased migration, while astrocytes under physiological conditions seem to lack this capacity. As previously stated, Piezo1 modulates the integrin signalling (McHugh et al., 2010; McHugh et al., 2012). Of interest, knockdown of Piezo1 in epithelial cells inactivates the endogenous integrin β1, reducing cell adhesion. This process occurs presumably via activation of calpain with the release of Ca^{2+} from the ER intracellular stores by activation of Piezo1 (McHugh et al., 2010). Reduced calpain activity has been associated to a switch to ameboid-like migration in some cancer cell types (Carragher et al., 2006; Storr, Carragher, Frame, Parr, & Martin, 2011). Interestingly, Piezo1 knockdown in small lung cancer cells resulted in a decrease in calpain activity, integrin signalling, cell adhesion and a switch to ameboid-like migration, with enhanced migrating capacity (McHugh et al., 2012). Recently, it has been reported that Piezo1 is a binding protein for the trefoil factor family-1 peptide (TFF1), playing a role in gastric cancer motility (X. N. Yang et al., 2014). TFF1 is a small peptide involved in epithelial restitution and cell motility by modifications in the cytoskeleton and modulation of Aquaporins (Marchbank & Playford, 2018; Taupin & Podolsky, 2003). TFF1 is upregulated in mouse astrocytes in response to inflammatory stimuli, proinflammatory cytokines such as IL6 or TNF-α, and brain damage (Hinz et al., 2004). Altogether, based upon the findings in the literature and our own studies, we suggest that induced Piezo1 in astrocytes may play a role in modulating the migratory capacity of reactive astrocytes via calpain and integrin signalling. Thus, the inhibition of Piezo1 by GsMTx4 would lead to a decrease in the intracellular calcium signalling on astrocytes, with subsequent low calpain and integrin activation, which would cause a decrease in cell adhesion and a switch to an ameboid-like migration. These findings may be translated to the field of cancer, as well as in pathologies characterised by formation of chronic glial scar or astrocytic reactivity.

5. Could Piezo1 provide a mechanical contribution in development of astrocyte glioma?

Glioma is a broad category of brain tumours characterised by uncontrolled proliferation of glial cells. The most common types are those derived from astrocytes, including glioblastoma multiforme (GBM), which is a grade IV glioma and the most malignant subtype of brain tumour in adults, with an incidence of 2-3 per 100,000 adults per year (Reilly, 2009). Some of the key players involved in the development of GBM include mutations in *pten, idh1* or *tp53*; but there are more than 75 genes shown to have a role in the onset of this condition (Backes et al., 2015). While mutations in *piezo1* have not been found associated with GBM, the contribution of mechanical properties in these cancers is well accepted. The physical stiffening of tumours during cancer progression is observed and is the basis for palpation-based detection. Physical changes on the tumour environment can come due to fluid pressure by oedema (X. Wang et al., 2015), differential secretion of ECM protein (Haseley et al., 2012; Nakagawa, Kubota, Kabuto, Fujimoto, & Okada, 1996), cell compression and changes in cell membrane (Barnes et al., 2017). Particularly in brain tumours, investigations on the tissue stiffness are controversial, as studies using elastography to measure the stiffness in patient brains show that tumours are stiffer than normal brain (Chauvet et al., 2016; L. Xu et al., 2007) but others show the opposite (Reiss-Zimmermann et al., 2015). This controversy might arise from the observation that glioma biopsies per se are softer that glial tissue, however, under compression, glioma stiffening can become higher (Pogoda et al., 2014), a situation that can happen *in vivo* due to the abnormal vascularization of tumours and oedema. Overall, the stiffening of the brain tumours is generally accepted as consistently measured and supported by techniques such as MRI and AFM (Barnes et al., 2017; Pope et al., 2012). Furthermore, it has been shown that the ECM stiffness influences GBM migration by facilitating CD44 and hyaluronic acid interaction (Knupfer et al., 1999; Lamontagne & Grandbois, 2008). Interestingly, elevated shear forces also induce the GBM migrating capacity, at least partially through a CXCR4-dependent mechanism (Munson, Bellamkonda, & Swartz, 2013), Altogether, these studies suggest and important role for ECM changes in migration and invasiveness of GBM, one of the main hallmarks of this type of tumour. We considered initial evidence for the role of Piezo1 in glioma, comes from the open access database developed by the Brain Tumour Group in CNIO (Spain), which shows an upregulation of Piezo1 mRNA compared to controls in gliomas, and mainly astrocytoma such GBM (gliovis.bioinfo.cnio.es). Although requiring experimental evidence, a working hypothesis is that Piezo1 modulates the migratory capacity of GBM.

6. Alexander disease and glial scar formation: could Piezo1 be involved?

Glial cells comprise around 90% of the cells of the CNS, and amongst them, astrocytes are the most abundant. Amongst their many functions, astrocytes are involved in synaptic transmission, and can release gliotransmitters themselves, as well as communicate by the second messenger Ca^{2+} through Ca^{2+} waves (Fiacco & McCarthy, 2006; Verkhratsky & Zorec, 2018). Astrocytes are highly mechanosensitive cells, and express MSC such as TREK1 (Zhou et al., 2009), TREK2 (Gnatenco, Han, Snyder, & Kim, 2002) or TRPV4 (Benfenati et al., 2011) amongst others. Indeed, mechanical stimulation of one single astrocyte in a confluent culture can lead to a propagation of this signal through Ca^{2+} waves through the astrocyte cell network (Charles, Merrill, Dirksen, & Sanderson, 1991; Paemeleire & Leybaert, 2000). Alexander disease is a rare but severe disorder caused by astrocyte dysfunction due to a gain-of-function mutation in the *GFAP* gene on astrocytes (Messing, Brenner, Feany, Nedergaard, & Goldman, 2012). The pathology is caused to an upregulation of GFAP, as mice lacking the GFAP gene are viable (Pekny et al., 1995) while knock-in mice with human mutations associated to Alexander disease display part of the spectrum of the pathology (Hagemann, Connor, & Messing, 2006). The principal hallmark of this condition is the formation of Rosenthal fibres, aggregates of GFAP, vimentin and heat-shock proteins in the cytoplasm of astrocytes (Alexander, 1949). Notably, we observed expression of Piezo1 in the ER during exposure to inflammatory stimuli, which might resemble protein aggregates of Piezo1, although admittedly we have not shown such Piezo1 expression in Alexander disease. It might also be possible that fibrinous aggregates of GFAP and/or vimentin (as well as other aggregated proteins) could alter mechanical properties of brain tissue in Alexander disease. In agreement, studies on a mouse model of this pathology have shown increased stiffness in the brain compared to WT mice (L. Wang et al., 2018). Moreover, genetic screening in a *Drosophila* model of Alexander disease has also revealed a contribution of multiple proteins involved in mechanotransduction pathways, such as the Hippo pathway or focal adhesion. In addition, the expression of laminin and the nuclear mechanotransducer yes-associated protein (YAP) were found upregulated in this model (L. Wang et al., 2018).

Another feature of astrocytes is their contribution to wound healing. Brain injury leads to the formation of glial scar tissue, comprised of astrocytes, microglia, pericytes, meningeal cells and extracellular matrix (Burda, Bernstein, & Sofroniew, 2016; Fernandez-Klett & Priller, 2014). Glial scars are commonly regarded as barriers to axon regrowth and regeneration, therefore constituting a target for the treatment of neuropathies (Anderson et al., 2016; Windle,

Clemente, & Chambers, 1952). However, research in different models of glial scar shows that attenuation or prevention of the glial scar does not lead to axon regrowth (Anderson et al., 2016; Moon & Fawcett, 2001). Furthermore, studies have shown the beneficial role of the glial scar in the injured area, for instance by attracting olfactory ensheathing cells (OECs) which are crucial for axon regrowth beyond the injury site (Z. Su et al., 2009). By forming glial scars, astrocytes also isolate the area of damage, preventing toxic factors originating from the injury site to propagate to the surrounding areas, such as ROS, free radicals or pro-inflammatory factors (Reier & Houle, 1988; Roitbak & Sykova, 1999). Notably, scar tissue in the body is generally stiffer than the uninjured tissue; however, in the brain, glial scar tissue appears relatively softer than normal brain tissue (Moeendarbary et al., 2017). Glial scars are rich in proteoglycans and almost lack collagen-1 (Bradbury et al., 2002; Stichel & Muller, 1998), while scars outside the CNS are rich in collagen-1 (Swift et al., 2013), which might explain the softening of brain scar tissue. The implications of this shift in mechanical properties can be important. For instance, axons tend to direct their growth towards softer areas of the brain (Koser et al., 2016). and the environmental stiffness also contributes to the lineage choice of the NSC, where a softer environment leads towards to a neuronal or oligodendroglia lineage (Lourenco et al., 2016). The ECM scaffold of the glial scar can also contribute to angiogenesis and revascularization (Rolls, Shechter, & Schwartz, 2009), which could contribute to set up the conditions for regeneration, even if in acute or sub-acute timepoints the glial scar subsequently becomes a barrier for axonal regrowth.

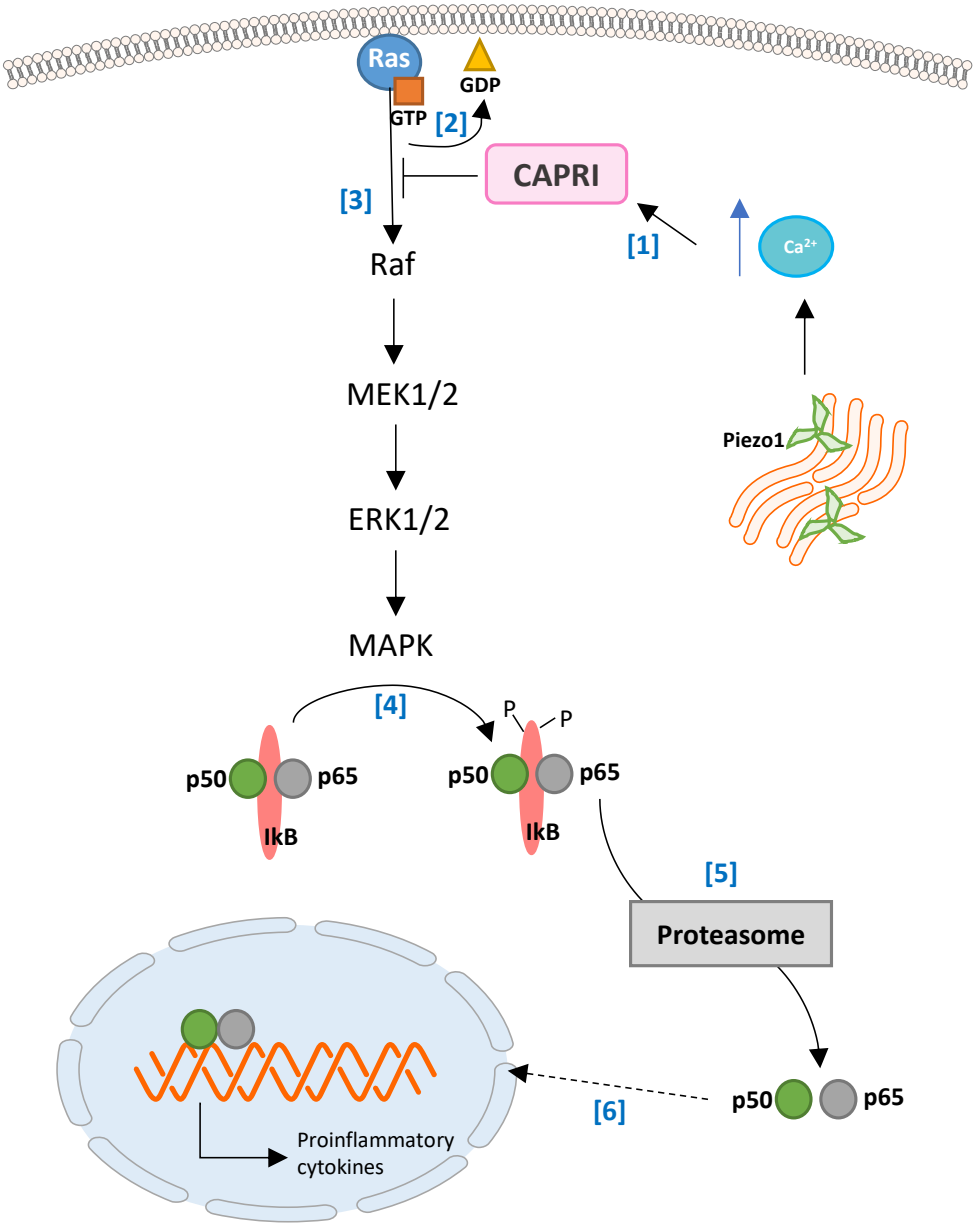

Figure 6. 1: Transcription of proinflammatory cytokines via activation of NFκB

The transcription factor NFκB is a common route for the induction of proinflammatory cytokines. **[3]** The small G protein Ras is active when bound to GTP, activating Raf and the subsequent ERK/MAPK cascade via MEK1/2, ERK1/2 and MAPK. **[4]** MAPK can phosphorylate the inhibitory subunit IκB, which is sequestering NFκB in the cytosol. **[5]** When phosphorylated, IκB is proteolyzed in the proteasome, and the remaining subunits p50 and p65 (NFκB complex) can then enter the nucleus and induce the transcription of genes involved in many processes, such as proinflammatory cytokines. **[1]** However, an increase of intracellular calcium can lead to the activation of the CAPRI protein, which is a GTPase that hydrolyses GTP to GDP, inactivating Ras and the subsequent signalling cascade.

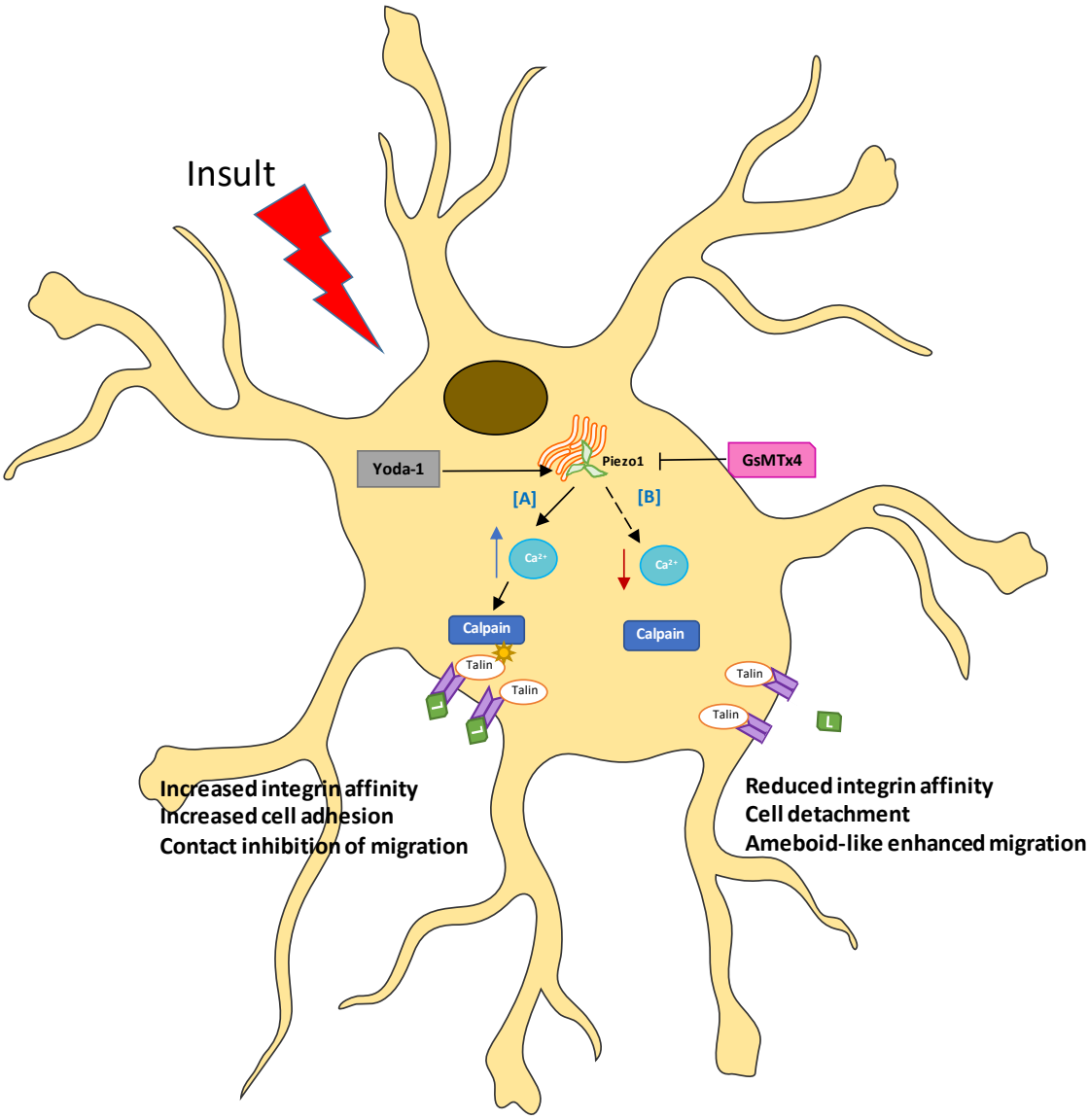

Figure 6. 2: Proposed mechanism of action of Piezo1 as modulator of astrocytic migration

Following certain pathological or inflammatory insults, astrocytes can turn into a reactive phenotype and induce the expression of Piezo1 in the endoplasmic reticulum. **[A]** When Piezo1 is activated, as with a mechanical stimulus or sensing an increased stiffness of the environment (such as when the glial scar is resolved), intracellular Ca^{2+} levels are increased, calpain activated and it causes an increased integrin affinity, followed by ligand binding and increased cell adhesion. This would inhibit the migratory capacity of astrocytes. **[B]** If Piezo1 is blocked, as with GsMTx4 or sensing a drop in the stiffness of the environment (such as in the glial scar or demyelination), the release of Ca^{2+} from intracellular stores is inhibit, leading to inactivation of calpain and a reduced integrin affinity, which results in cell detachment and transition to an ameboid-like type of migration.

7. Inflammation contributes to neurodegeneration

It is well known that AD is characterised by progressive cognitive and behavioural impairment, with amyloid plaque formation, NFTs, tau hyperphosphorylation and neuronal and synaptic loss (Holtzman et al., 2011). Historically, the amyloid cascade hypothesis has been associated with the etiopathology of AD (Amemori et al., 2015; Lukiw, 2012). The importance of chronic inflammation towards the onset and development of AD has also become more evident, where both acute bacterial and chronic inflammation worsen this disease (Holmes et al., 2009; Kempuraj et al., 2016; Sy et al., 2011). For instance, bacteria and their debris can induce chronic inflammation, via TLR signalling and enhance the amyloid deposition in AD brains (Bibi et al., 2014). These factors become more important when accounting for most AD patients being elderly, many of which have co-morbidities, including periodontal disease (Seymour, Ford, Cullinan, Leishman, & Yamazaki, 2007), pneumonia (Kamer et al., 2008) and urinary tract infection (Rowe & Juthani-Mehta, 2013), all known to be associated with AD. This disproportionate inflammatory response to a peripheral condition is a key player in the cognitive decline, due to the crosstalk between the brain and the peripheral immune system. There are several proposed mechanisms by which chronic inflammation can trigger and exacerbate the AD pathology. On the one hand, prior to AD onset, a severe or prolonged systemic inflammation (either caused by external pathogens or by chronic inflammatory conditions such as obesity or diabetes) can activate microglia and increase the risk of dementia (Cunningham & Hennessy, 2015; Lim et al., 2015). Normally, the activation of microglia is self-contained and resolved when the insult is cleared. However, exacerbated inflammatory response can cause irreversible damage to neuron and synaptic function and leading to a sustained inflammatory response that can induce or aggravate neurological pathologies such as AD (Bibi et al., 2014; Leyns & Holtzman, 2017). In AD patients, these 'primed' microglia can release proinflammatory cytokines and chemokines that can, in turn, activate astrocytes and induce the infiltration of peripheral monocytes through the blood-brain barrier (Simard, Soulet, Gowing, Julien, & Rivest, 2006).

Astrocytes can become activated in response to the amyloid plaques (Johnstone et al., 1999) where initial activation seems beneficial, as these cells cluster around the plaques and phagocytose and degrade Aβ deposits (Wyss-Coray et al., 2003). However, chronic activation of astrocytes in AD brains becomes detrimental, where these cells secrete proinflammatory cytokines, ROS and nitric oxide (NO), resulting in neuronal damage (Johnstone et al., 1999; Kempuraj et al., 2016; C. Liu et al., 2014; Smits et al., 2002). In this study, we observed astrocytes to be associated with amyloid plaques in the Alzheimer's rat model TgF344-AD and noted these

cells undergo a change towards a reactive phenotype **(Chapter 4)**. Furthermore, we observed that repeated peripheral infection with *E.coli* in the TgF344-AD rats enhanced plaque deposition, demyelination and reactive phenotype of the astrocytes, corroborating studies in the literature suggesting that peripheral infection exacerbates AD pathology. In agreement with our findings *in vitro*, we observed that Piezo1 was also upregulated *in vivo* in the astrocytes around amyloid plaques of the TgF344-AD rats. This Aβ-induced expression of Piezo1 was further enhanced by peripheral infections of the TgF344-AD, suggesting that both infection and AD pathology, triggers astrocytic expression of Piezo1. While the exact roles of Piezo1 in astrocytes in AD brain are unclear, we propose Piezo1 could represent a marker of inflammatory response of astrocytes as well as provide mechanical cues for glial cells, which might be disrupted in disease.

8. Astrocytic Ca^{2+} dysregulations in AD

Glial cells are affected by physiological ageing (Rodriguez-Arellano et al., 2016), where oligodendrocytes decline in an 34% with age (Fabricius, Jacobsen, & Pakkenberg, 2013) and microglia undergo morphological atrophy and decreased defensive capabilities (Streit, Braak, Xue, & Bechmann, 2009). The number of astrocytes in ageing, however, does not seem to change, although senescent astrocytes present atrophy and hypertrophy (Fabricius et al., 2013). A dysfunction in astrocytic Ca^{2+} homeostasis with age may also contribute to degenerative pathologies (Gomez-Gonzalo et al., 2017). Astrocytes actively communicate with neurons and other cell types via Ca^{2+} waves (Perea, Sur, & Araque, 2014). Dysfunction or dyshomeostasis of the astrocytic Ca^{2+} responses has been associated to neurological pathologies in general, like Huntington's disease (Tong et al., 2014), Multiple Sclerosis (Vardjan, Verkhratsky, & Zorec, 2017), and specially to AD (Magi et al., 2016; Ronco et al., 2014). *In vitro* studies have demonstrated that Aβ oligomers loaded on cultures astrocytes evoke changes in astrocytic Ca^{2+} signalling (Grolla et al., 2013). These effects have been corroborated *ex vivo*, where higher frequency Ca^{2+} spiking is found in astrocytes of acute brain slices obtained from AD mouse model Tg2576 (Riera, Hatanaka, Uchida, Ozaki, & Kawashima, 2011). Studies on APP/PS1 mice have also shown abnormal Ca^{2+} oscillation in the reactive astrocytes associated to the amyloid plaques (Kuchibhotla, Lattarulo, Hyman, & Bacskai, 2009), as well as in astrocytes on healthy WT animals that were injected in β-amyloid, proving that this dysregulation in Ca^{2+} signalling may be due to the amyloidosis (Takano, Han, Deane, Zlokovic, & Nedergaard, 2007). Elegant studies performed in the senescence mouse model SAMP8 and in the Alzheimer mouse model

APP/PS1 show that senescence healthy astrocytes present a reduced number of intrinsic Ca^{2+} oscillations compared to juvenile or adults, but that neurotransmitter-dependent Ca^{2+} signals were maintained. However, hippocampal and cortical recordings from the APP/PS1 mice showed increased Ca^{2+} responses in basal conditions, suggesting an increased tone of glutamatergic gliotransmission. This gliotransmission was also enhanced in the senescence model SAMP8, which presents amyloidosis as well as cognitive decline, endorsing that these alterations in Ca^{2+} signalling on senile astrocytes are not due to age, but to AD pathology (Gomez-Gonzalo et al., 2017). Based on these studies proving an enhanced basal Ca^{2+} signalling on astrocytes around the amyloid plaques as well as in our previous findings on the induced expression of Piezo1 in reactive astrocytes, we suggest that this increment in the gliotransmission could be due to Piezo1 activity, activated by the mechanical properties of the amyloid plaques. Although it has been shown that pathological AD brains are softer than healthy brain (Murphy et al., 2012; Murphy et al., 2011; Murphy et al., 2016), the specific intricated fibrillar structure of the amyloid plaques is stiffer (Y. B. Lu et al., 2006). This could cause the mechanical activation of Piezo1 in the astrocytes surrounding the amyloid plaques, leading to a basal increment in the spontaneous Ca^{2+} oscillations, and thus altering the gliotransmission which may contribute to the progression of disease.

9. Myelin state associated to AD

Because of the physiological process of ageing, white matter in the CNS is reduced by approximately 11% in volume (Haug & Eggers, 1991) as well as a significant decrease in the number of oligodendrocytes (Fabricius et al., 2013). This myelin loss contributes to neuronal dysfunction and cognitive decline associated to age (P. H. Lu et al., 2011). Parallel to myelin alterations in healthy ageing, the AD brain also displays myelin disruption and intracellular deposits (X. Zhan et al., 2014). Of interest, initial amyloid deposits start developing in the poorly myelinated areas of the cortex, suggesting that myelin injury is not only a cause, but it is involved in the development of the pathology (Braak & Braak, 1997). This is supported by the evidence that myelin alterations and oligodendrocyte dysfunction can be observed in AD models before the appearance of some other hallmarks of AD, such as a high load of amyloid plaques or tau hyperphosphorylation (Desai et al., 2010; Desai et al., 2009). It has been suggested that the myelin debris promotes the accumulation of Aβ, therefore contributing to its later deposition and formation of the amyloid plaques (Bartzokis et al., 2007; X. Zhan et al., 2015).

The mechanisms underlying myelin disruption in AD are not fully understood. Studies have reported Aβ toxicity of oligodendrocytes. In vivo, stereotaxic injection of Aβ in the corpus callosum of mice induces oligodendrocyte cell death and disruption of myelination (Jantaratnotai, Ryu, Kim, & McLarnon, 2003). Treatment with Aβ *in vitro* also induces apoptosis in matured oligodendrocytes, while OPC appear relatively resistant to Aβ toxicity (Horiuchi et al., 2012). In early stages of AD, an increased level of OPC proliferation and differentiation is observed, perhaps in an attempt to restore myelin breakdown at this stage (Behrendt et al., 2013). However, when differentiated, the OPC capacity of myelin formation was impaired in the presence of Aβ (Horiuchi et al., 2012). Mechanisms through which Aβ induced apoptosis in OLs appears to involve ceramide-dependent apoptosis, where Aβ induces neutral sphingomyelinase, producing ceramide and mediating apoptosis cascades in oligodendrocytes (J. T. Lee et al., 2004). Interestingly, AD brains present focal demyelination in areas with amyloid plaque deposits, where demyelination is pronounced in the core of the Aβ plaque. In these areas, there is a loss of oligodendrocytes, myelin disruption and an increase of myelin debris, whilst areas with a lower density of plaques, or plaque-free areas, do not show significant demyelination (Mitew et al., 2010). This suggest that Aβ toxicity to oligodendrocytes could trigger focal demyelination to occur. We have also observed that the repeated peripheral infections with *E.Coli* enhanced myelin loss, in TgF344-AD rats. Many studies have correlated abnormal immune response to demyelination, mostly in the pathology of MS (Gilden, 2005; Libbey & Fujinami, 2010; O'Brien et al., 2008; Steelman, 2015). Because of their low levels of glutathione and their high iron content, oligodendrocytes are more susceptible to oxidative damage, which is increased in inflammatory state (Juurlink, 1997). This, combined with a detrimental role of chronic reactivity of glia to myelin levels, could contribute to the exacerbated myelin loss in TgF344-AD animals with peripheral infection.

An interesting component that could contribute to demyelination in AD is the mechanical properties of the plaques. AD brains have lower stiffness than healthy brains (Murphy et al., 2012; Murphy et al., 2011; Murphy et al., 2016) which may be due to a combination of (I) the myelin loss in AD, as white matter is stiffer than grey matter (Budday et al., 2015; Weickenmeier et al., 2016) and (II) the changes in the mechanical properties of the cellular membranes caused by Aβ, which leads to a loss of stiffness (Ungureanu et al., 2016). Contrarily to this, Aβ plaques themselves are stiffer, as the fibrillary structure of the tangle has harder mechanical properties than healthy ECM (Y. B. Lu et al., 2006). OPCs and oligodendrocytes have been shown to be highly sensitive to mechanical stimuli. For instance, it has been demonstrated that rigid matrices inhibit the oligodendrocytic branching and the maturation of OPC (Urbanski et al., 2016), and

that mechanical strain to OPC inhibit their maturation and differentiation into myelinating oligodendrocytes (Jagielska et al., 2017). This may, in part, explain how Aβ produces focal demyelination not only by causing oligodendrocytes apoptosis, but by also inhibiting the maturation and differentiation of OPC by mechanical activation.

10. Role of mechanotransduction in myelination

Myelination has traditionally been studied as a process regulated by the crosstalk between neuronal and glial cells and by the chemical signals that lead to differentiation and maturation of oligodendrocytes and Schwann cells (Fancy et al., 2009; Hu et al., 2013; Ishii et al., 2014). Several studies have supported the idea of mechanotransduction being a modulator of myelination and remyelination. It is now known that OPCs and oligodendrocytes are mechanosensitive, and that physical properties of the ECM regulate their survival, differentiation, migration and myelinating capacities (Jagielska et al., 2017; Jagielska et al., 2012; Lourenco et al., 2016). *In vitro* studies with OPC in matrices with different stiffnesses have shown that survival, migration and proliferation of OPC are higher in softer and intermediate substrata, whilst differentiation of OPC increases in stiffer matrices (Jagielska et al., 2012). These changes are likely due to genetic regulation, as mechanical strains applied to cultures OPC induced changes in chromatin organization, histone deacetylation and nuclear shape, inhibiting the proliferation of OPC but inducing the differentiation in oligodendrocytes (Jagielska et al., 2017). In addition, despite oligodendrocyte maturation being favoured on intermediate to stiff matrices, oligodendrocyte grown on hard substrata, mimicking a lesion-like matrix, present impaired maturation (Urbanski et al., 2016) suggesting there is a certain range in which each cellular process is optimal.

Of interest, elegant studies have suggested that physical cues may have a bigger contribution in the initiation of myelination, than previously thought, as oligodendrocytes can myelinate electro-spun nanofibers when their diameters are similar to neural axons (S. Lee et al., 2012). In addition, it has been demonstrated that OPCs seeded onto PFA-fixed axons can differentiate and myelinate those axons in the same timing and consistency as they do on live axons (S. S. Rosenberg et al., 2008). These findings show a mechanical component important for myelination that does not require cellular signalling between the axon and oligodendrocytes, although there is likely a crosstalk between mechanical cues and chemical signalling, as oligodendrocytes do not myelinate nanofibers to the same extent as axons (S. Lee et al., 2012).

For an efficient conduction, the myelinated axon should have a specific g-ratio, defined as the diameter of the axon divided by the diameter of the axon plus myelin (Domingues et al., 2018). It was observed that nanofibers do not show the typical g-ratios (S. Lee et al., 2012), which suggests a need for crosstalk with neurons for efficient myelination.

11. Piezo1 as regulator of myelination

In this study, we have shown that Piezo1 alters myelination in rodent brain tissue. Piezo1 is largely expressed in neurons of highly myelinated tracts of CNS, in an age-dependent manner (unpublished data) **(Supplemental Figure 5.1)**. Our results showed that inhibition of mechanosensation by GsMTx4 increased the myelin markers MOG, MBP and PLP, in ex vivo mouse organotypic cerebellar slice cultures. In contrast, activation of Piezo1 by its specific activator Yoda-1, decreased these myelin markers, supporting a hypothesis that Piezo1 activation negatively regulates myelination. GsMTx4 also induced an increase in the neural marker NFH, suggesting that it might have a neurotrophic role too. Psychosine, the toxin that accumulates in the pathology of Krabbe's disease due to the lack of the enzyme galactosylceramidase (Davenport et al., 2011), can be used as an tool to cause demyelination *ex vivo* (Misslin et al., 2017; C. O'Sullivan & Dev, 2015). We showed that GsMTx4 treatment attenuated the psychosine-induced demyelination in slices, as well as the axonal damage as seen in the expression of SMI-32 in axons. These effects were observed at a 48h time point, suggesting that this attenuation is caused by a prevention in demyelination rather than remyelination.

These findings were supported *in vivo*, where stereotaxic injections of GsMTx4 prevented the LPC-induced focal demyelination in young adult mice. LPC is an endogenous lysophospholipid that disrupt myelin lipids in a nonspecific way (Plemel et al., 2018) leading to focal demyelination. In this *in vivo* model, GsMTx4 prevented demyelination and neuronal loss four days post-injection, with no apparent changes in the number of oligodendrocytes. This supports our hypothesis that blockade of mechanosensation prevents myelin disruption. Interestingly, in accordance with our findings *in vitro*, GsMTx4 increased the hallmarks of reactive astrocytes, such as astrocyte hypertrophy, increased levels of GFAP and an increased number of astrocytes per area in the injury region. Although we did not examine the expression of Piezo1 after LPC injection, it might be the case that LPC increases Piezo1 in the ER of astrocytes, similar to Aβ, psychosine or LPS, allowing GsMTx4 to be effective.

Based on our findings and previous studies we hypothesize that Piezo1 acts as a mechanotransductor between oligodendrocytes and neurons, playing a role in efficient myelination and generating appropriate g-ratio. Interestingly, OPC in soft matrices express low levels of the Yes-associated protein (YAP) (Shimizu et al., 2017). YAP is a component of the Hippo pathway, and its translocation to the nucleus promotes gene expression (Low et al., 2014). Piezo1 has been suggested to activate YAP/TAZ signalling by transients in Ca^{2+}, as it has been shown that Piezo1 knockdown reduced the nuclear translocation of YAP, suppressing neurogenesis in neural stem cells and promoting astrogenesis (Pathak et al., 2014). Thus, Piezo1 could mediate oligodendrocyte differentiation and maturation via YAP/TAZ. Activation of Piezo1 by mechanical stiffening of the environment could activate the Hippo cascade and promote genetic changes in OPCs that lead to differentiation and oligodendrocyte maturation, explaining why OPC differentiation occurs in stiffer substrata (Jagielska et al., 2017).

Demyelination triggers changes in the distribution of ion channels along the axon, especially around the nodes of Ranvier, which can lead to this alteration of the ionic homeostasis (Alizadeh et al., 2015). Dysregulation of the ion homeostasis in axons, mainly when caused by increase of Ca^{2+}, leads to axonal injury (Wojda, Salinska, & Kuznicki, 2008). Based upon our findings, we suggest that the protective effects of GsMTx4 can be due to the dampening of this Ca^{2+} dysregulation in both axons and oligodendrocytes, explaining why GsMTx4 protects from demyelination and stabilizes the axons leading to higher NFH levels. We hypothesize that the Yoda-1 mediated demyelination could be due to an increase of Ca^{2+} in the axons by activation of Piezo1 both on the basal membrane and the axoplasmic reticulum. Activation of Piezo1 also induced the production of ATP (T. Miyamoto et al., 2014), that could in turn activate the IP3 receptors in the reticulum further enhancing this Ca^{2+} upregulation. High levels of Ca^{2+} cause excitotoxicity (Wojda et al., 2008) and can cause the activation of calpain, altering the integrin signalling and disrupting the axonal cytoskeleton stability. However, GsMTx4 can inhibit this Ca^{2+} in the axon, leading to a stabilization of the actin cytoskeleton in neurons, and we suggest that GsMTx4 can also block SACs in the membrane of oligodendrocytes, inhibiting the influx of Ca^{2+} and subsequent activation of calpain and PLA_2, the enzyme responsible of lipid degradation and subsequent demyelination. Studies using CARS microscopy have shown that LPC-induced demyelination of axons requires an increase of intracellular Ca^{2+} level in the oligodendrocytes, and that in absence of extracellular Ca^{2+}, LPC does not mediate demyelination (Fu et al., 2007). Previous studies in our group have also demonstrate that PLA_2 plays a role in demyelination,

especially in psychosine-induced demyelination, as inhibition of PLA_2 in organotypic slices prevented this demyelination (Misslin et al., 2017).

In summary, we suggest, for the first time, a role for Piezo1 in modulating myelination, and propose that inhibitors of Piezo1 and other mechanoreceptors, using for example GsMTx4, could protect from demyelinating insults via a dual effect on both axons and oligodendrocytes. Our findings suggest that Piezo1 may be considered a target for new drug development for demyelinating conditions

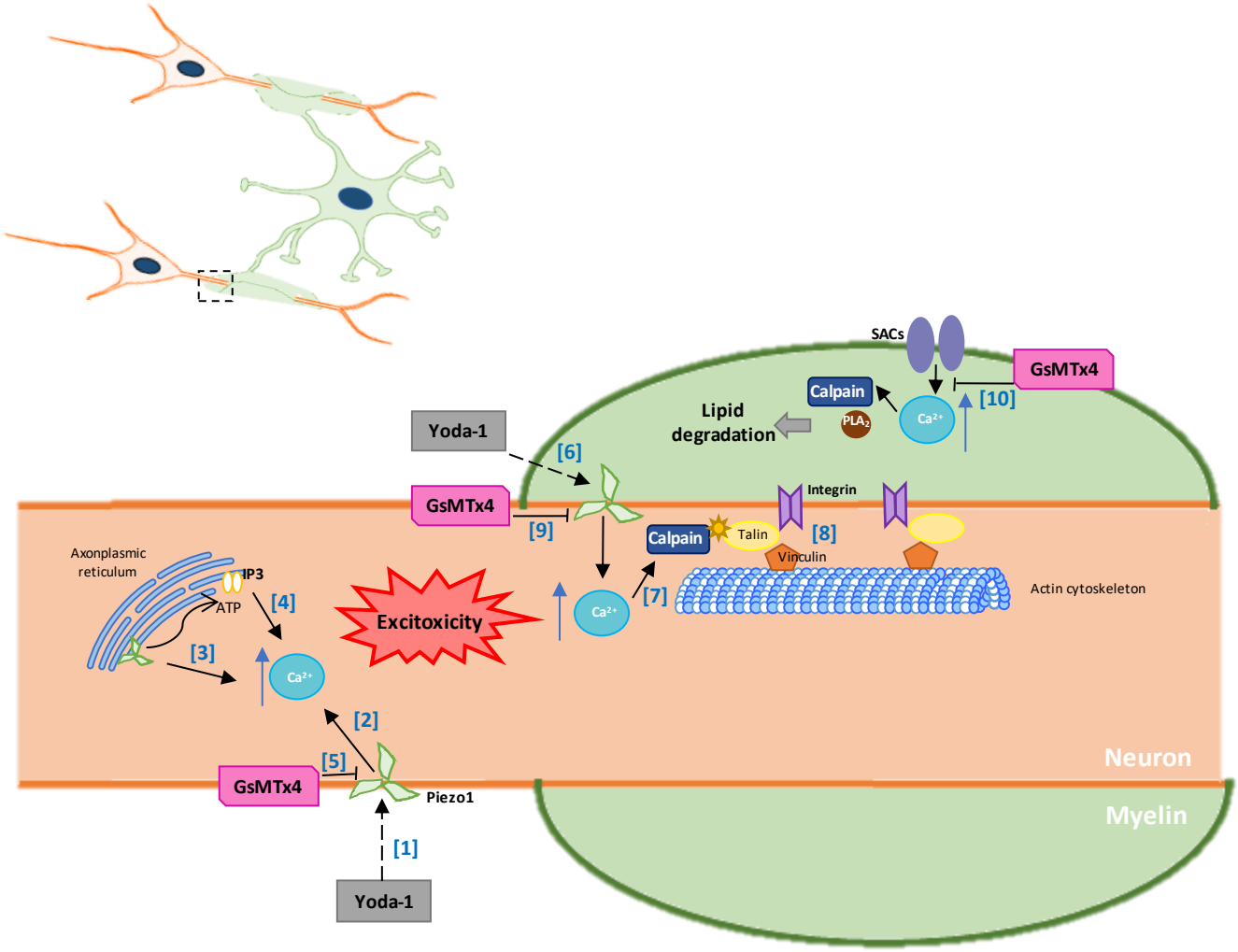

Figure 6. 3: Putative mechanism of action of the role of Piezo1 in the modulation of myelination. **[1, 2]** Yoda-1 activates Piezo1, which causes an influx of Ca^{2+} inside the axons. **[3]** Piezo1 located in the axoplasmic reticulum can also be activated and release Ca^{2+} from the intracellular stores. Furthermore, the activation of Piezo1 leads to a release of ATP through Ca^{2+}-regulated vesicular exocytosis, and **[4]** ATP can act as allosteric agonist for IP_3Rs, which would contribute to the further release of Ca^{2+} to the cytoplasm. This high load of Ca^{2+} inside the cell can have an excitotoxicity effect, as well as **[7]** activate calpain, which would disrupt the integrin signalling between axonal cytoskeleton and oligodendrocyte through talin and vinculin **[8]**. **[5, 9]** However, these effects can be inhibited by blockage of SACs as Piezo1 in the axons by GsMTx4. **[10]** Furthermore, GsMTx4 seems to have a protecting effect from demyelination by acting through blockage of SACs in oligodendrocytes. It has been shown that an increase in Ca^{2+} inside the oligodendrocytes can cause the activation of calpain and PLA_2, causing lipid degradation and demyelination. GsMTx4 could act blocking SACs and preventing this influx of Ca^{2+} inhibiting this effect.

12. Limitations of the study.

There are a number of limitations of the study which are listed below:

1. Antibodies for Piezo1:

We characterised the expression of Piezo1 with immunofluorescent techniques. We note these results are dependent on the quality of the antibodies used and especially the commercially available antibodies against Piezo1. Admittedly, only one of the Piezo1 antibodies commercially available has been tested in knockout tissue (X. F. Li, Zhang, Chen, Cui, & Zhang, 2017). In our studies, we synthesized the epitope against sc-164319, confirming the specificity of the antibody, although we would need similar blocking studies to test the ab128245 from Abcam.

2. Function of surface expressed Piezo1:

At present, we cannot be certain that Piezo1 is not expressed in the basal membrane, as it could be below detection levels using standard immunolabelling. Other methods such as GFP-tagged Piezo1 could be developed to further understand the function of Piezo1 at the cell surface.

3. Culture Conditions:

Another limitation of this study involved further understanding and better control of the mechanical properties of the environment used in our *in vitro* studies. Our experiments in stimulated astrocytes were performed on well plates and/or glass coverslips. Piezo1 is a mechanoreceptor, therefore being susceptible to the mechanical stiffness of the matrix. Both plastic and mostly glass coverslips have a much higher stiffness (100kPa) than the physiological brain conditions (0.1 to 1kPa). This might, then, affect the functionality of Piezo1, as astrocytes might not act as they would *in vivo*, sensing a rigid extracellular environment. While our slice culture and *in vivo* experiments may have been better models to study Piezo1, the use of astrocytes grown in 3D matrix may also allow better analysis of the functionality of Piezo1.

4. Lack of vehicle control conditions

Yoda-1 was dissolved in DMSO. However, no vehicle control was done to investigate whether the amount of DMSO inherent to the Yoda-1 treatment (regardless of how little this could be) was performed.

5. Animal Numbers:

We also note that our studies using the in vivo LPC-induced focal demyelination model were performed on a small number of animals. Furthermore, we only analysed the brain at 4 days post-injection

6. Investigating myelin g-ratios

We also note that here we present findings on the levels of different myelin components, but we do not investigate the myelin structure or the g-ratios of the axons, which would be advisable to ensure that the myelin sheath under GsMTx4-treament is not aberrant. This study provides an analysis on the expression of myelin markers at a protein level, which is not fully translatable to myelination levels. Colocalization between myelin markers and neuronal markers, such as the tM2 values between the expression of MBP and NFH, are a more accurate measure for myelination, however it should be corroborated with other techniques such as electron microscopy to fully assess the myelination of the axons.

13. Future directions of the study

Our findings on the expression of Piezo1 in astrocytes suggest its role in the modulation of reactivity of astrocytes through cytokine release and migration. Recent studies have shown a phenotype for activated astrocytes, termed A1 astrocytes, that differentiates under inflammatory conditions such as LPS and that have neurotoxic effects (Liddelow et al., 2017). In order to assess whether the expression of Piezo1 is linked to reactive astrocytes, studies of co-localization of Piezo1 and the A1 phenotype marker C3 are suggested. If Piezo1 were expressed in reactive astrocytes, the decrease in the levels of IL-6, IL-1β and TNF-α after Piezo1 activation might be linked to a change in the astrocytes' reactive phenotype and likely on their neurotoxic effects as well, maybe then proposing Piezo1 as a target to treat detrimental neuroinflammation derived from astrocytes. We have also hypothesized the mechanisms of action through which Piezo1 could modulate the cytokine release and migration of astrocytes. However, to corroborate the biochemical pathways underlying these processes, different approaches could be considered. Western-Blot analysis could help define the cascades involved in the regulation of the astrocytic reactivity. In addition, immunoprecipitation followed Liquid Chromatography-Mass Spectrometry analysis would help elucidate any binding partners of Piezo1. As we previously mentioned, our *in vitro* studies have been performed in hard surfaces, with higher stiffnesses than the physiological conditions on the brain. We suggest that further studies using different 3D matrices with different physical properties are advisable.

We are aware that, although we have shown that inhibition of Piezo1 attenuates the decrease of myelin markers caused by psychosine, we cannot know whether this attenuation is due to an increase of the remyelination process, or due to protection against demyelination. In order to examine how Piezo1 attenuates the psychosine-induced demyelinating effect, we propose the analysis of the axonal damage marker SMI-32. This marker is constitutively expressed in the soma and dendrites of the neurons, but when there is damage of axons or demyelination, it starts to be expressed in the axons (Milosevic & Zecevic, 1998). Expression of SMI-32 in the axons of psychosine plus GsMTx4 treated organotypic slices would indicate that GsMTx4 promotes remyelination of these axons, which would have previously undergone demyelination. Also, in order to examine whether Piezo1 has a regulatory effect on the maturation of oligodendrocytes, analysis of the mature oligodendrocytes marker NOGO-A would be advisable. We also note that this study measures fluorescence intensity of myelin markers, which is not necessarily corresponding to the levels of myelination, as these markers are also detected in the non-myelinating oligodendrocytes and in myelin debris. Moreover, we note that the increase in myelin caused by GsMTx4 can be non-functional or aberrant. Therefore, EM studies showing the thickness and structure of the myelin sheath would corroborate and support our findings.

We note that our study has only analysed the levels of myelin marker by immunolabelling, without assessing the functionality of the myelin sheath. Therefore, electron microscopy (EM) should be performed to analyse the structure of the myelin and the g-ratios of the myelinating axons, to corroborate whether the inhibition of Piezo1 leads to thicker or aberrant forms of myelin in the neural axons instead of prevent demyelination. In addition, longer studies with a higher number of animals should be performed, where we could analyse the myelin state at 7- and 15-days post-injury to investigate the effects of GsMTx4 on myelination at longer times. Furthermore, we are aware that GsMTx4 is a non-specific blocker of Piezo1. We suggest that Piezo1 plays an actual role in the process of myelination, as specific activation by Yoda-1 leads to demyelination *ex vivo*. However, we cannot assure that the effects observed with GsMTx4 are solely due to Piezo1 activity, and not due to other SACs. Thus, in other to corroborate whether GsMTx4 exerts its protective effects through Piezo1 or through several SACs, experiments in which Piezo1 is knockout or specifically blocked would be needed.

Finally, we proposed that GsMTx4 could be used as a potential treatment in other demyelinating animal models. Our lab has ongoing studies on the Krabbe's disease model, twitcher mouse. We hypothesize that co-treatment of GsMTx4 with FTY720 could be a potential efficient approach to prevent demyelination in the twitcher model, and thus the progression of the pathology. Because of the peptidic nature of GsMTx4, the development of an efficient, and preferably non-invasive, method of delivery would be ideal. For example, development of nasal delivery nanoparticles that would encapsulate GsMTx4 could, in theory, deliver GsMTx4 to the brain, crossing the blood-brain barrier without previous breakdown and clearance of the peptide.

14. Conclusions

This is a novel study investigating the potential role of the mechanoreceptor Piezo1 in the Central Nervous System. Here, we have shown that Piezo1 is expressed in the endoplasmic reticulum of astrocytes under certain pathological conditions (i.e. infection and Alzheimer's disease) and that this expression of Piezo1 could constitute a mechanism to define the reactive state of astrocytes, by regulating intracellular Ca^{2+} signalling. Moreover, we have shown that activation of Piezo1 with Yoda-1 leads to lower levels of myelin protein expression without affecting neuronal markers. On the contrary, blockage of mechanoreceptors with GsMTx4 led to higher level of myelin proteins and, more interestingly, it prevented the demyelination associated to the toxin psychosine *ex vivo*, using organotypic slice cultures. These results were also observed in an *in vivo* model of LPC-induced focal demyelination, where GsMTx4 prevented the demyelination, neuronal loss, astrocytic death and microglial activation associated to LPC injections. Thus, this study shows, for the first time in the literature, the potential of Piezo1 in regulating the neuroinflammatory state of glia and regulating the myelination process in the Central Nervous System.

Bibliography

Abad-Rodriguez, J., Ledesma, M. D., Craessaerts, K., Perga, S., Medina, M., Delacourte, A., . . . Dotti, C. G. (2004). Neuronal membrane cholesterol loss enhances amyloid peptide generation. *J Cell Biol, 167*(5), 953-960. doi:10.1083/jcb.200404149

Akira, S., & Takeda, K. (2004). Toll-like receptor signalling. *Nat Rev Immunol, 4*(7), 499-511. doi:10.1038/nri1391

Akiyama, H., Schwab, C., Kondo, H., Mori, H., Kametani, F., Ikeda, K., & McGeer, P. L. (1996). Granules in glial cells of patients with Alzheimer's disease are immunopositive for C-terminal sequences of beta-amyloid protein. *Neurosci Lett, 206*(2-3), 169-172.

Albuisson, J., Murthy, S. E., Bandell, M., Coste, B., Louis-Dit-Picard, H., Mathur, J., . . . Patapoutian, A. (2013). Dehydrated hereditary stomatocytosis linked to gain-of-function mutations in mechanically activated PIEZO1 ion channels. *Nat Commun, 4*, 1884. doi:10.1038/ncomms2899

Alexander, W. S. (1949). Progressive fibrinoid degeneration of fibrillary astrocytes associated with mental retardation in a hydrocephalic infant. *Brain, 72*(3), 373-381, 373 pl.

Alizadeh, A., Dyck, S. M., & Karimi-Abdolrezaee, S. (2015). Myelin damage and repair in pathologic CNS: challenges and prospects. *Front Mol Neurosci, 8*, 35. doi:10.3389/fnmol.2015.00035

Allan, S. M., Tyrrell, P. J., & Rothwell, N. J. (2005). Interleukin-1 and neuronal injury. *Nat Rev Immunol, 5*(8), 629-640. doi:10.1038/nri1664

Alper, S. L. (2017). Genetic Diseases of PIEZO1 and PIEZO2 Dysfunction. *Curr Top Membr, 79*, 97-134. doi:10.1016/bs.ctm.2017.01.001

Alvarez-Garcia, O., Vega-Naredo, I., Sierra, V., Caballero, B., Tomas-Zapico, C., Camins, A., . . . Coto-Montes, A. (2006). Elevated oxidative stress in the brain of senescence-accelerated mice at 5 months of age. *Biogerontology, 7*(1), 43-52. doi:10.1007/s10522-005-6041-2

Amemori, T., Jendelova, P., Ruzicka, J., Urdzikova, L. M., & Sykova, E. (2015). Alzheimer's Disease: Mechanism and Approach to Cell Therapy. *Int J Mol Sci, 16*(11), 26417-26451. doi:10.3390/ijms161125961

Amor, V., Feinberg, K., Eshed-Eisenbach, Y., Vainshtein, A., Frechter, S., Grumet, M., . . . Peles, E. (2014). Long-term maintenance of Na+ channels at nodes of Ranvier depends on glial contact mediated by gliomedin and NrCAM. *J Neurosci, 34*(15), 5089-5098. doi:10.1523/jneurosci.4752-13.2014

Anandh, K. R., Sujatha, C. M., & Ramakrishnan, S. (2014). Atrophy analysis of corpus callosum in Alzheimer brain MR images using anisotropic diffusion filtering and level sets. *Conf Proc IEEE Eng Med Biol Soc, 2014*, 1945-1948. doi:10.1109/embc.2014.6943993

Anderson, M. A., Burda, J. E., Ren, Y., Ao, Y., O'Shea, T. M., Kawaguchi, R., . . . Sofroniew, M. V. (2016). Astrocyte scar formation aids central nervous system axon regeneration. *Nature, 532*(7598), 195-200. doi:10.1038/nature17623

Andolfo, I., Alper, S. L., De Franceschi, L., Auriemma, C., Russo, R., De Falco, L., . . . Iolascon, A. (2013). Multiple clinical forms of dehydrated hereditary stomatocytosis arise from mutations in PIEZO1. *Blood, 121*(19), 3925-3935, s3921-3912. doi:10.1182/blood-2013-02-482489

Andolfo, I., Russo, R., Gambale, A., & Iolascon, A. (2016). New insights on hereditary erythrocyte membrane defects. *Haematologica, 101*(11), 1284-1294. doi:10.3324/haematol.2016.142463

Archer, N. M., Shmukler, B. E., Andolfo, I., Vandorpe, D. H., Gnanasambandam, R., Higgins, J. M., . . . Nathan, D. G. (2014). Hereditary xerocytosis

revisited. *Am J Hematol, 89*(12), 1142-1146. doi:10.1002/ajh.23799

Arnadottir, J., & Chalfie, M. (2010). Eukaryotic mechanosensitive channels. *Annu Rev Biophys, 39*, 111-137. doi:10.1146/annurev.biophys.37.032807.125836

Arulmoli, J., Pathak, M. M., McDonnell, L. P., Nourse, J. L., Tombola, F., Earthman, J. C., & Flanagan, L. A. (2015). Static stretch affects neural stem cell differentiation in an extracellular matrix-dependent manner. *Sci Rep, 5*, 8499. doi:10.1038/srep08499

Azuma, M., & Shearer, T. R. (2008). The role of calcium-activated protease calpain in experimental retinal pathology. *Surv Ophthalmol, 53*(2), 150-163. doi:10.1016/j.survophthal.2007.12.006

Backes, C., Harz, C., Fischer, U., Schmitt, J., Ludwig, N., Petersen, B. S., . . . Meese, E. (2015). New insights into the genetics of glioblastoma multiforme by familial exome sequencing. *Oncotarget, 6*(8), 5918-5931. doi:10.18632/oncotarget.2950

Bae, C., Sachs, F., & Gottlieb, P. A. (2011). The mechanosensitive ion channel Piezo1 is inhibited by the peptide GsMTx4. *Biochemistry, 50*(29), 6295-6300. doi:10.1021/bi200770q

Baloh, R. H. (2008). Mitochondrial dynamics and peripheral neuropathy. *Neuroscientist, 14*(1), 12-18. doi:10.1177/1073858407307354

Bansal, R., Warrington, A. E., Gard, A. L., Ranscht, B., & Pfeiffer, S. E. (1989). Multiple and novel specificities of monoclonal antibodies O1, O4, and R-mAb used in the analysis of oligodendrocyte development. *J Neurosci Res, 24*(4), 548-557. doi:10.1002/jnr.490240413

Baradaran, S., Hajizadeh Moghaddam, A., & Ghasemi-Kasman, M. (2018). Hesperetin reduces myelin damage and ameliorates glial activation in lysolecithin-induced focal demyelination model of rat optic chiasm. *Life Sci, 207*, 471-479. doi:10.1016/j.lfs.2018.07.001

Barichello, T., dos Santos, I., Savi, G. D., Florentino, A. F., Silvestre, C., Comim, C. M., . . . Quevedo, J. (2009). Tumor necrosis factor alpha (TNF-alpha) levels in the brain and cerebrospinal fluid after meningitis induced by Streptococcus pneumoniae. *Neurosci Lett, 467*(3), 217-219. doi:10.1016/j.neulet.2009.10.039

Barnes, J. M., Przybyla, L., & Weaver, V. M. (2017). Tissue mechanics regulate brain development, homeostasis and disease. *J Cell Sci, 130*(1), 71-82. doi:10.1242/jcs.191742

Barsukova, A. G., Forte, M., & Bourdette, D. (2012). Focal increases of axoplasmic Ca2+, aggregation of sodium-calcium exchanger, N-type Ca2+ channel, and actin define the sites of spheroids in axons undergoing oxidative stress. *J Neurosci, 32*(35), 12028-12037. doi:10.1523/jneurosci.0408-12.2012

Bartzokis, G., Lu, P. H., & Mintz, J. (2007). Human brain myelination and amyloid beta deposition in Alzheimer's disease. *Alzheimers Dement, 3*(2), 122-125. doi:10.1016/j.jalz.2007.01.019

Bavi, N., Nikolaev, Y. A., Bavi, O., Ridone, P., Martinac, A. D., Nakayama, Y., . . . Martinac, B. (2017). Principles of mechanosensing at membrane interface. In J.-M. R. R.M. Epand (Ed.), *The biophysics of cell membranes* (19 ed., pp. 85-119): Springer.

Beck, A., Nieden, R. Z., Schneider, H. P., & Deitmer, J. W. (2004). Calcium release from intracellular stores in rodent astrocytes and neurons in situ. *Cell Calcium, 35*(1), 47-58.

Beedle, A. E., Williams, A., Relat-Goberna, J., & Garcia-Manyes, S. (2015). Mechanobiology - chemical origin of membrane mechanical resistance and force-dependent signaling. *Curr Opin Chem Biol, 29*, 87-93. doi:10.1016/j.cbpa.2015.09.019

Behrendt, G., Baer, K., Buffo, A., Curtis, M. A., Faull, R. L., Rees, M. I., . . . Dimou, L. (2013). Dynamic changes in myelin aberrations and oligodendrocyte generation in chronic amyloidosis in

mice and men. *Glia, 61*(2), 273-286. doi:10.1002/glia.22432

Benfenati, V., Caprini, M., Dovizio, M., Mylonakou, M. N., Ferroni, S., Ottersen, O. P., & Amiry-Moghaddam, M. (2011). An aquaporin-4/transient receptor potential vanilloid 4 (AQP4/TRPV4) complex is essential for cell-volume control in astrocytes. *Proc Natl Acad Sci U S A, 108*(6), 2563-2568. doi:10.1073/pnas.1012867108

Bibi, F., Yasir, M., Sohrab, S. S., Azhar, E. I., Al-Qahtani, M. H., Abuzenadah, A. M., . . . Naseer, M. I. (2014). Link between chronic bacterial inflammation and Alzheimer disease. *CNS Neurol Disord Drug Targets, 13*(7), 1140-1147.

Biessels, G. J., & Kappelle, L. J. (2005). Increased risk of Alzheimer's disease in Type II diabetes: insulin resistance of the brain or insulin-induced amyloid pathology? *Biochem Soc Trans, 33*(Pt 5), 1041-1044. doi:10.1042/bst20051041

Bitsch, A., Schuchardt, J., Bunkowski, S., Kuhlmann, T., & Bruck, W. (2000). Acute axonal injury in multiple sclerosis. Correlation with demyelination and inflammation. *Brain, 123 (Pt 6)*, 1174-1183.

Blumenthal, N. R., Hermanson, O., Heimrich, B., & Shastri, V. P. (2014). Stochastic nanoroughness modulates neuron-astrocyte interactions and function via mechanosensing cation channels. *Proc Natl Acad Sci U S A, 111*(45), 16124-16129. doi:10.1073/pnas.1412740111

Boche, D., Perry, V. H., & Nicoll, J. A. (2013). Review: activation patterns of microglia and their identification in the human brain. *Neuropathol Appl Neurobiol, 39*(1), 3-18. doi:10.1111/nan.12011

Boggs, J. M. (2006). Myelin basic protein: a multifunctional protein. *Cell Mol Life Sci, 63*(17), 1945-1961. doi:10.1007/s00018-006-6094-7

Bogler, O., Wren, D., Barnett, S. C., Land, H., & Noble, M. (1990). Cooperation between two growth factors promotes extended self-renewal and inhibits differentiation of oligodendrocyte-type-2 astrocyte (O-2A) progenitor cells. *Proc Natl Acad Sci U S A, 87*(16), 6368-6372. doi:10.1073/pnas.87.16.6368

Boka, G., Anglade, P., Wallach, D., Javoy-Agid, F., Agid, Y., & Hirsch, E. C. (1994). Immunocytochemical analysis of tumor necrosis factor and its receptors in Parkinson's disease. *Neurosci Lett, 172*(1-2), 151-154.

Bollmann, L., Koser, D. E., Shahapure, R., Gautier, H. O., Holzapfel, G. A., Scarcelli, G., . . . Franze, K. (2015). Microglia mechanics: immune activation alters traction forces and durotaxis. *Front Cell Neurosci, 9*, 363. doi:10.3389/fncel.2015.00363

Borbiro, I., Badheka, D., & Rohacs, T. (2015). Activation of TRPV1 channels inhibits mechanosensitive Piezo channel activity by depleting membrane phosphoinositides. *Sci Signal, 8*(363), ra15. doi:10.1126/scisignal.2005667

Bosmans, F., & Swartz, K. J. (2010). Targeting voltage sensors in sodium channels with spider toxins. *Trends Pharmacol Sci, 31*(4), 175-182. doi:10.1016/j.tips.2009.12.007

Bowman, C. L., Gottlieb, P. A., Suchyna, T. M., Murphy, Y. K., & Sachs, F. (2007). Mechanosensitive ion channels and the peptide inhibitor GsMTx-4: history, properties, mechanisms and pharmacology. *Toxicon, 49*(2), 249-270. doi:10.1016/j.toxicon.2006.09.030

Braak, H., & Braak, E. (1997). Frequency of stages of Alzheimer-related lesions in different age categories. *Neurobiol Aging, 18*(4), 351-357.

Braak, H., Braak, E., & Kalus, P. (1989). Alzheimer's disease: areal and laminar pathology in the occipital isocortex. *Acta Neuropathol, 77*(5), 494-506.

Bradbury, E. J., Moon, L. D., Popat, R. J., King, V. R., Bennett, G. S., Patel, P. N., . . . McMahon, S. B. (2002). Chondroitinase ABC promotes functional recovery after spinal cord injury. *Nature,*

416(6881), 636-640. doi:10.1038/416636a

Brinkmann, V., Billich, A., Baumruker, T., Heining, P., Schmouder, R., Francis, G., . . . Burtin, P. (2010). Fingolimod (FTY720): discovery and development of an oral drug to treat multiple sclerosis. *Nat Rev Drug Discov, 9*(11), 883-897. doi:10.1038/nrd3248

Bruunsgaard, H., Andersen-Ranberg, K., Jeune, B., Pedersen, A. N., Skinhoj, P., & Pedersen, B. K. (1999). A high plasma concentration of TNF-alpha is associated with dementia in centenarians. *J Gerontol A Biol Sci Med Sci, 54*(7), M357-364.

Bryan, A. M., & Del Poeta, M. (2018). Sphingosine-1-phosphate receptors and innate immunity. *Cell Microbiol, 20*(5), e12836. doi:10.1111/cmi.12836

Budday, S., Nay, R., de Rooij, R., Steinmann, P., Wyrobek, T., Ovaert, T. C., & Kuhl, E. (2015). Mechanical properties of gray and white matter brain tissue by indentation. *J Mech Behav Biomed Mater, 46*, 318-330. doi:10.1016/j.jmbbm.2015.02.024

Buffo, A., Rolando, C., & Ceruti, S. (2010). Astrocytes in the damaged brain: molecular and cellular insights into their reactive response and healing potential. *Biochem Pharmacol, 79*(2), 77-89. doi:10.1016/j.bcp.2009.09.014

Buki, A., & Povlishock, J. T. (2006). All roads lead to disconnection?--Traumatic axonal injury revisited. *Acta Neurochir (Wien), 148*(2), 181-193; discussion 193-184. doi:10.1007/s00701-005-0674-4

Burda, J. E., Bernstein, A. M., & Sofroniew, M. V. (2016). Astrocyte roles in traumatic brain injury. *Exp Neurol, 275 Pt 3*, 305-315. doi:10.1016/j.expneurol.2015.03.020

Cahalan, S. M., Lukacs, V., Ranade, S. S., Chien, S., Bandell, M., & Patapoutian, A. (2015). Piezo1 links mechanical forces to red blood cell volume. *Elife, 4*. doi:10.7554/eLife.07370

Cai, Z., & Xiao, M. (2016). Oligodendrocytes and Alzheimer's disease. *Int J Neurosci, 126*(2), 97-104. doi:10.3109/00207454.2015.1025778

Carragher, N. O., Walker, S. M., Scott Carragher, L. A., Harris, F., Sawyer, T. K., Brunton, V. G., . . . Frame, M. C. (2006). Calpain 2 and Src dependence distinguishes mesenchymal and amoeboid modes of tumour cell invasion: a link to integrin function. *Oncogene, 25*(42), 5726-5740. doi:10.1038/sj.onc.1209582

Carson, J. A., & Turner, A. J. (2002). Beta-amyloid catabolism: roles for neprilysin (NEP) and other metallopeptidases? *J Neurochem, 81*(1), 1-8.

Casserly, I. P., & Topol, E. J. (2004). Convergence of atherosclerosis and alzheimer's disease: Cholesterol, inflammation, and misfolded proteins. *Discov Med, 4*(22), 149-156.

Chalfie, M. (2009). Neurosensory mechanotransduction. *Nat Rev Mol Cell Biol, 10*(1), 44-52. doi:10.1038/nrm2595

Chao, C. C., & Hu, S. (1994). Tumor necrosis factor-alpha potentiates glutamate neurotoxicity in human fetal brain cell cultures. *Dev Neurosci, 16*(3-4), 172-179.

Charles, A. C., Merrill, J. E., Dirksen, E. R., & Sanderson, M. J. (1991). Intercellular signaling in glial cells: calcium waves and oscillations in response to mechanical stimulation and glutamate. *Neuron, 6*(6), 983-992.

Chatelin, S., Constantinesco, A., & Willinger, R. (2010). Fifty years of brain tissue mechanical testing: from in vitro to in vivo investigations. *Biorheology, 47*(5-6), 255-276. doi:10.3233/bir-2010-0576

Chauvet, D., Imbault, M., Capelle, L., Demene, C., Mossad, M., Karachi, C., . . . Tanter, M. (2016). In Vivo Measurement of Brain Tumor Elasticity Using Intraoperative Shear Wave Elastography. *Ultraschall Med, 37*(6), 584-590. doi:10.1055/s-0034-1399152

Chen, B. M., & Grinnell, A. D. (1995). Integrins and modulation of transmitter release

from motor nerve terminals by stretch. *Science, 269*(5230), 1578-1580.

Chen, W. W., Zhang, X., & Huang, W. J. (2016). Role of neuroinflammation in neurodegenerative diseases (Review). *Mol Med Rep, 13*(4), 3391-3396. doi:10.3892/mmr.2016.4948

Choi, H. J., Sun, D., & Jakobs, T. C. (2015). Astrocytes in the optic nerve head express putative mechanosensitive channels. *Mol Vis, 21*, 749-766.

Cinar, E., Zhou, S., DeCourcey, J., Wang, Y., Waugh, R. E., & Wan, J. (2015). Piezo1 regulates mechanotransductive release of ATP from human RBCs. *Proc Natl Acad Sci U S A, 112*(38), 11783-11788. doi:10.1073/pnas.1507309112

Clodomiro, A., Gareri, P., Puccio, G., Frangipane, F., Lacava, R., Castagna, A., . . . Bruni, A. C. (2013). Somatic comorbidities and Alzheimer's disease treatment. *Neurol Sci, 34*(9), 1581-1589. doi:10.1007/s10072-013-1290-3

Cohen, R. M., Rezai-Zadeh, K., Weitz, T. M., Rentsendorj, A., Gate, D., Spivak, I., . . . Town, T. (2013). A transgenic Alzheimer rat with plaques, tau pathology, behavioral impairment, oligomeric abeta, and frank neuronal loss. *J Neurosci, 33*(15), 6245-6256. doi:10.1523/jneurosci.3672-12.2013

Comi, G., O'Connor, P., Montalban, X., Antel, J., Radue, E. W., Karlsson, G., . . . Kappos, L. (2010). Phase II study of oral fingolimod (FTY720) in multiple sclerosis: 3-year results. *Mult Scler, 16*(2), 197-207. doi:10.1177/1352458509357065

Corey, D. P., & Hudspeth, A. J. (1979). Ionic basis of the receptor potential in a vertebrate hair cell. *Nature, 281*(5733), 675-677.

Coste, B., Mathur, J., Schmidt, M., Earley, T. J., Ranade, S., Petrus, M. J., . . . Patapoutian, A. (2010). Piezo1 and Piezo2 are essential components of distinct mechanically activated cation channels. *Science, 330*(6000), 55-60. doi:10.1126/science.1193270

Coste, B., Xiao, B., Santos, J. S., Syeda, R., Grandl, J., Spencer, K. S., . . . Patapoutian, A. (2012). Piezo proteins are pore-forming subunits of mechanically activated channels. *Nature, 483*(7388), 176-181. doi:10.1038/nature10812

Cox, C. D., Bae, C., Ziegler, L., Hartley, S., Nikolova-Krstevski, V., Rohde, P. R., . . . Martinac, B. (2016). Removal of the mechanoprotective influence of the cytoskeleton reveals PIEZO1 is gated by bilayer tension. *Nat Commun, 7*, 10366. doi:10.1038/ncomms10366

Cullen, P. J., & Lockyer, P. J. (2002). Integration of calcium and Ras signalling. *Nat Rev Mol Cell Biol, 3*(5), 339-348. doi:10.1038/nrm808

Cunningham, C., & Hennessy, E. (2015). Co-morbidity and systemic inflammation as drivers of cognitive decline: new experimental models adopting a broader paradigm in dementia research. *Alzheimers Res Ther, 7*(1), 33. doi:10.1186/s13195-015-0117-2

Dansokho, C., & Heneka, M. T. (2018). Neuroinflammatory responses in Alzheimer's disease. *J Neural Transm (Vienna), 125*(5), 771-779. doi:10.1007/s00702-017-1831-7

Davenport, A., Williamson, P., & Taylor, R. (2011). Pathophysiology of Krabbe disease. *Orbit: The University of Sydney undergraduate research journal, 2*(1), 1-20.

de la Monte, S. M. (1989). Quantitation of cerebral atrophy in preclinical and end-stage Alzheimer's disease. *Ann Neurol, 25*(5), 450-459. doi:10.1002/ana.410250506

De Strooper, B. (2010). Proteases and proteolysis in Alzheimer disease: a multifactorial view on the disease process. *Physiol Rev, 90*(2), 465-494. doi:10.1152/physrev.00023.2009

Demolombe, S., Duprat, F., Honore, E., & Patel, A. (2013). Slower Piezo1 inactivation in dehydrated hereditary stomatocytosis (xerocytosis). *Biophys J, 105*(4), 833-834. doi:10.1016/j.bpj.2013.07.018

Denes, A., Wilkinson, F., Bigger, B., Chu, M., Rothwell, N. J., & Allan, S. M. (2013). Central and haematopoietic

interleukin-1 both contribute to ischaemic brain injury in mice. *Dis Model Mech, 6*(4), 1043-1048. doi:10.1242/dmm.011601

Desai, M. K., Mastrangelo, M. A., Ryan, D. A., Sudol, K. L., Narrow, W. C., & Bowers, W. J. (2010). Early oligodendrocyte/myelin pathology in Alzheimer's disease mice constitutes a novel therapeutic target. *Am J Pathol, 177*(3), 1422-1435. doi:10.2353/ajpath.2010.100087

Desai, M. K., Sudol, K. L., Janelsins, M. C., Mastrangelo, M. A., Frazer, M. E., & Bowers, W. J. (2009). Triple-transgenic Alzheimer's disease mice exhibit region-specific abnormalities in brain myelination patterns prior to appearance of amyloid and tau pathology. *Glia, 57*(1), 54-65. doi:10.1002/glia.20734

Discher, D. E., Mohandas, N., & Evans, E. A. (1994). Molecular maps of red cell deformation: hidden elasticity and in situ connectivity. *Science, 266*(5187), 1032-1035.

Doens, D., & Fernandez, P. L. (2014). Microglia receptors and their implications in the response to amyloid beta for Alzheimer's disease pathogenesis. *J Neuroinflammation, 11*, 48. doi:10.1186/1742-2094-11-48

Domingues, H. S., Cruz, A., Chan, J. R., Relvas, J. B., Rubinstein, B., & Pinto, I. M. (2018). Mechanical plasticity during oligodendrocyte differentiation and myelination. *Glia, 66*(1), 5-14. doi:10.1002/glia.23206

Duthie, A., Chew, D., & Soiza, R. L. (2011). Non-psychiatric comorbidity associated with Alzheimer's disease. *Qjm, 104*(11), 913-920. doi:10.1093/qjmed/hcr118

Eijkelkamp, N., Quick, K., & Wood, J. N. (2013). Transient receptor potential channels and mechanosensation. *Annu Rev Neurosci, 36*, 519-546. doi:10.1146/annurev-neuro-062012-170412

Eisenhoffer, G. T., Loftus, P. D., Yoshigi, M., Otsuna, H., Chien, C. B., Morcos, P. A., & Rosenblatt, J. (2012). Crowding induces live cell extrusion to maintain homeostatic cell numbers in epithelia. *Nature, 484*(7395), 546-549. doi:10.1038/nature10999

Ernstrom, G. G., & Chalfie, M. (2002). Genetics of sensory mechanotransduction. *Annu Rev Genet, 36*, 411-453. doi:10.1146/annurev.genet.36.061802.101708

Evans, E. L., Cuthbertson, K., Endesh, N., Rode, B., Blythe, N. M., Hyman, A. J., . . . Beech, D. J. (2018). Yoda1 analogue (Dooku1) which antagonizes Yoda1-evoked activation of Piezo1 and aortic relaxation. *Br J Pharmacol, 175*(10), 1744-1759. doi:10.1111/bph.14188

Fabricius, K., Jacobsen, J. S., & Pakkenberg, B. (2013). Effect of age on neocortical brain cells in 90+ year old human females--a cell counting study. *Neurobiol Aging, 34*(1), 91-99. doi:10.1016/j.neurobiolaging.2012.06.009

Fancy, S. P., Baranzini, S. E., Zhao, C., Yuk, D. I., Irvine, K. A., Kaing, S., . . . Rowitch, D. H. (2009). Dysregulation of the Wnt pathway inhibits timely myelination and remyelination in the mammalian CNS. *Genes Dev, 23*(13), 1571-1585. doi:10.1101/gad.1806309

Faucherre, A., Kissa, K., Nargeot, J., Mangoni, M. E., & Jopling, C. (2014). Piezo1 plays a role in erythrocyte volume homeostasis. *Haematologica, 99*(1), 70-75. doi:10.3324/haematol.2013.086090

Fernandez-Klett, F., & Priller, J. (2014). The fibrotic scar in neurological disorders. *Brain Pathol, 24*(4), 404-413. doi:10.1111/bpa.12162

Fiacco, T. A., & McCarthy, K. D. (2006). Astrocyte calcium elevations: properties, propagation, and effects on brain signaling. *Glia, 54*(7), 676-690. doi:10.1002/glia.20396

Fotiou, E., Martin-Almedina, S., Simpson, M. A., Lin, S., Gordon, K., Brice, G., . . . Ostergaard, P. (2015). Novel mutations in PIEZO1 cause an autosomal recessive generalized lymphatic

dysplasia with non-immune hydrops fetalis. *Nat Commun, 6*, 8085. doi:10.1038/ncomms9085

Frati, A., Cerretani, D., Fiaschi, A. I., Frati, P., Gatto, V., La Russa, R., . . . Fineschi, V. (2017). Diffuse Axonal Injury and Oxidative Stress: A Comprehensive Review. *Int J Mol Sci, 18*(12). doi:10.3390/ijms18122600

Friede, R. L. (1972). Control of myelin formation by axon caliber (with a model of the control mechanism). *J Comp Neurol, 144*(2), 233-252. doi:10.1002/cne.901440207

Friedl, P., & Brocker, E. B. (2000). The biology of cell locomotion within three-dimensional extracellular matrix. *Cell Mol Life Sci, 57*(1), 41-64. doi:10.1007/s000180050498

Friedrich, O., Schneidereit, D., Nikolaev, Y. A., Nikolova-Krstevski, V., Schurmann, S., Wirth-Hucking, A., . . . Martinac, B. (2017). Adding dimension to cellular mechanotransduction: Advances in biomedical engineering of multiaxial cell-stretch systems and their application to cardiovascular biomechanics and mechano-signaling. *Prog Biophys Mol Biol*. doi:10.1016/j.pbiomolbio.2017.06.011

Fu, Y., Wang, H., Huff, T. B., Shi, R., & Cheng, J. X. (2007). Coherent anti-Stokes Raman scattering imaging of myelin degradation reveals a calcium-dependent pathway in lyso-PtdCho-induced demyelination. *J Neurosci Res, 85*(13), 2870-2881. doi:10.1002/jnr.21403

Garcia, M. L., & Cleveland, D. W. (2001). Going new places using an old MAP: tau, microtubules and human neurodegenerative disease. *Curr Opin Cell Biol, 13*(1), 41-48.

Gard, A. L., Burrell, M. R., Pfeiffer, S. E., Rudge, J. S., & Williams, W. C., 2nd. (1995). Astroglial control of oligodendrocyte survival mediated by PDGF and leukemia inhibitory factor-like protein. *Development, 121*(7), 2187-2197.

Garzon-Rodriguez, W., Yatsimirsky, A. K., & Glabe, C. G. (1999). Binding of Zn(II), Cu(II), and Fe(II) ions to Alzheimer's A beta peptide studied by fluorescence. *Bioorg Med Chem Lett, 9*(15), 2243-2248.

Ge, J., Li, W., Zhao, Q., Li, N., Chen, M., Zhi, P., . . . Yang, M. (2015). Architecture of the mammalian mechanosensitive Piezo1 channel. *Nature, 527*(7576), 64-69. doi:10.1038/nature15247

Gilden, D. H. (2005). Infectious causes of multiple sclerosis. *Lancet Neurol, 4*(3), 195-202. doi:10.1016/s1474-4422(05)01017-3

Giri, S., Jatana, M., Rattan, R., Won, J. S., Singh, I., & Singh, A. K. (2002). Galactosylsphingosine (psychosine)-induced expression of cytokine-mediated inducible nitric oxide synthases via AP-1 and C/EBP: implications for Krabbe disease. *Faseb j, 16*(7), 661-672. doi:10.1096/fj.01-0798com

Giri, S., Khan, M., Nath, N., Singh, I., & Singh, A. K. (2008). The role of AMPK in psychosine mediated effects on oligodendrocytes and astrocytes: implication for Krabbe disease. *J Neurochem, 105*(5), 1820-1833. doi:10.1111/j.1471-4159.2008.05279.x

Gnanasambandam, R., Bae, C., Gottlieb, P. A., & Sachs, F. (2015). Ionic Selectivity and Permeation Properties of Human PIEZO1 Channels. *PLoS One, 10*(5), e0125503. doi:10.1371/journal.pone.0125503

Gnanasambandam, R., Ghatak, C., Yasmann, A., Nishizawa, K., Sachs, F., Ladokhin, A. S., . . . Suchyna, T. M. (2017). GsMTx4: Mechanism of Inhibiting Mechanosensitive Ion Channels. *Biophys J, 112*(1), 31-45. doi:10.1016/j.bpj.2016.11.013

Gnatenco, C., Han, J., Snyder, A. K., & Kim, D. (2002). Functional expression of TREK-2 K+ channel in cultured rat brain astrocytes. *Brain Res, 931*(1), 56-67.

Goldman, J. E., Zerlin, M., Newman, S., Zhang, L., & Gensert, J. (1997). Fate determination and migration of progenitors in the postnatal

mammalian CNS. *Dev Neurosci, 19*(1), 42-48. doi:10.1159/000111184

Gomez-Gonzalo, M., Martin-Fernandez, M., Martinez-Murillo, R., Mederos, S., Hernandez-Vivanco, A., Jamison, S., . . . Araque, A. (2017). Neuron-astrocyte signaling is preserved in the aging brain. *Glia, 65*(4), 569-580. doi:10.1002/glia.23112

Gottlieb, P. A., & Sachs, F. (2012). Piezo1: properties of a cation selective mechanical channel. *Channels (Austin), 6*(4), 214-219. doi:10.4161/chan.21050

Grigoriadis, N., & Hadjigeorgiou, G. M. (2006). Virus-mediated autoimmunity in Multiple Sclerosis. *J Autoimmune Dis, 3*, 1. doi:10.1186/1740-2557-3-1

Grolla, A. A., Fakhfouri, G., Balzaretti, G., Marcello, E., Gardoni, F., Canonico, P. L., . . . Lim, D. (2013). Abeta leads to Ca(2)(+) signaling alterations and transcriptional changes in glial cells. *Neurobiol Aging, 34*(2), 511-522. doi:10.1016/j.neurobiolaging.2012.05.005

Gu, Y., & Gu, C. (2014). Physiological and pathological functions of mechanosensitive ion channels. *Mol Neurobiol, 50*(2), 339-347. doi:10.1007/s12035-014-8654-4

Gudi, V., Gingele, S., Skripuletz, T., & Stangel, M. (2014). Glial response during cuprizone-induced de- and remyelination in the CNS: lessons learned. *Front Cell Neurosci, 8*, 73. doi:10.3389/fncel.2014.00073

Gudipaty, S. A., & Rosenblatt, J. (2016). Epithelial cell extrusion: Pathways and pathologies. *Semin Cell Dev Biol*. doi:10.1016/j.semcdb.2016.05.010

Guthrie, P. B., Knappenberger, J., Segal, M., Bennett, M. V., Charles, A. C., & Kater, S. B. (1999). ATP released from astrocytes mediates glial calcium waves. *J Neurosci, 19*(2), 520-528.

Hagemann, T. L., Connor, J. X., & Messing, A. (2006). Alexander disease-associated glial fibrillary acidic protein mutations in mice induce Rosenthal fiber formation and a white matter stress response. *J Neurosci, 26*(43), 11162-11173. doi:10.1523/jneurosci.3260-06.2006

Haile, W. B., Echeverry, R., Wu, F., Guzman, J., An, J., Wu, J., & Yepes, M. (2010). Tumor necrosis factor-like weak inducer of apoptosis and fibroblast growth factor-inducible 14 mediate cerebral ischemia-induced poly(ADP-ribose) polymerase-1 activation and neuronal death. *Neuroscience, 171*(4), 1256-1264. doi:10.1016/j.neuroscience.2010.10.029

Hamill, O. P., & Martinac, B. (2001). Molecular basis of mechanotransduction in living cells. *Physiol Rev, 81*(2), 685-740.

Han, B., & Logsdon, C. D. (2000). CCK stimulates mob-1 expression and NF-kappaB activation via protein kinase C and intracellular Ca(2+). *Am J Physiol Cell Physiol, 278*(2), C344-351. doi:10.1152/ajpcell.2000.278.2.C344

Haq, E., Giri, S., Singh, I., & Singh, A. K. (2003). Molecular mechanism of psychosine-induced cell death in human oligodendrocyte cell line. *J Neurochem, 86*(6), 1428-1440.

Harbo, H. F., Gold, R., & Tintore, M. (2013). Sex and gender issues in multiple sclerosis. *Ther Adv Neurol Disord, 6*(4), 237-248. doi:10.1177/1756285613488434

Hardy, J., & Allsop, D. (1991). Amyloid deposition as the central event in the aetiology of Alzheimer's disease. *Trends Pharmacol Sci, 12*(10), 383-388.

Haseley, A., Boone, S., Wojton, J., Yu, L., Yoo, J. Y., Yu, J., . . . Kaur, B. (2012). Extracellular matrix protein CCN1 limits oncolytic efficacy in glioma. *Cancer Res, 72*(6), 1353-1362. doi:10.1158/0008-5472.can-11-2526

Haug, H., & Eggers, R. (1991). Morphometry of the human cortex cerebri and corpus striatum during aging. *Neurobiol Aging, 12*(4), 336-338; discussion 352-335.

Hauser, S. L., & Oksenberg, J. R. (2006). The neurobiology of multiple sclerosis: genes, inflammation, and neurodegeneration. *Neuron, 52*(1), 61-76. doi:10.1016/j.neuron.2006.09.011

Healy, L. M., Sheridan, G. K., Pritchard, A. J., Rutkowska, A., Mullershausen, F., & Dev, K. K. (2013). Pathway specific modulation of S1P1 receptor signalling in rat and human astrocytes. *Br J Pharmacol, 169*(5), 1114-1129. doi:10.1111/bph.12207

Heo, D. K., Lim, H. M., Nam, J. H., Lee, M. G., & Kim, J. Y. (2015). Regulation of phagocytosis and cytokine secretion by store-operated calcium entry in primary isolated murine microglia. *Cell Signal, 27*(1), 177-186. doi:10.1016/j.cellsig.2014.11.003

Hernandez, M., Patzig, J., Mayoral, S. R., Costa, K. D., Chan, J. R., & Casaccia, P. (2016). Mechanostimulation Promotes Nuclear and Epigenetic Changes in Oligodendrocytes. *J Neurosci, 36*(3), 806-813. doi:10.1523/jneurosci.2873-15.2016

Hinz, M., Schwegler, H., Chwieralski, C. E., Laube, G., Linke, R., Pohle, W., & Hoffmann, W. (2004). Trefoil factor family (TFF) expression in the mouse brain and pituitary: changes in the developing cerebellum. *Peptides, 25*(5), 827-832. doi:10.1016/j.peptides.2004.01.020

Holcomb, L., Gordon, M. N., McGowan, E., Yu, X., Benkovic, S., Jantzen, P., . . . Duff, K. (1998). Accelerated Alzheimer-type phenotype in transgenic mice carrying both mutant amyloid precursor protein and presenilin 1 transgenes. *Nat Med, 4*(1), 97-100.

Holmes, C., Cunningham, C., Zotova, E., Woolford, J., Dean, C., Kerr, S., . . . Perry, V. H. (2009). Systemic inflammation and disease progression in Alzheimer disease. *Neurology, 73*(10), 768-774. doi:10.1212/WNL.0b013e3181b6bb95

Holtzman, D. M., Morris, J. C., & Goate, A. M. (2011). Alzheimer's disease: the challenge of the second century. *Sci Transl Med, 3*(77), 77sr71. doi:10.1126/scitranslmed.3002369

Horiuchi, M., Maezawa, I., Itoh, A., Wakayama, K., Jin, L. W., Itoh, T., & Decarli, C. (2012). Amyloid beta1-42 oligomer inhibits myelin sheet formation in vitro. *Neurobiol Aging, 33*(3), 499-509. doi:10.1016/j.neurobiolaging.2010.05.007

Hsuan, S. L., Kannan, M. S., Jeyaseelan, S., Prakash, Y. S., Malazdrewich, C., Abrahamsen, M. S., . . . Maheswaran, S. K. (1999). Pasteurella haemolytica leukotoxin and endotoxin induced cytokine gene expression in bovine alveolar macrophages requires NF-kappaB activation and calcium elevation. *Microb Pathog, 26*(5), 263-273. doi:10.1006/mpat.1998.0271

Hu, X., Schlanger, R., He, W., Macklin, W. B., & Yan, R. (2013). Reversing hypomyelination in BACE1-null mice with Akt-DD overexpression. *Faseb j, 27*(5), 1868-1873. doi:10.1096/fj.12-224212

Hung, W. C., Yang, J. R., Yankaskas, C. L., Wong, B. S., Wu, P. H., Pardo-Pastor, C., . . . Konstantopoulos, K. (2016). Confinement Sensing and Signal Optimization via Piezo1/PKA and Myosin II Pathways. *Cell Rep, 15*(7), 1430-1441. doi:10.1016/j.celrep.2016.04.035

Hyman, B. T., Marzloff, K., & Arriagada, P. V. (1993). The lack of accumulation of senile plaques or amyloid burden in Alzheimer's disease suggests a dynamic balance between amyloid deposition and resolution. *J Neuropathol Exp Neurol, 52*(6), 594-600.

Irvine, K. A., & Blakemore, W. F. (2008). Remyelination protects axons from demyelination-associated axon degeneration. *Brain, 131*(Pt 6), 1464-1477. doi:10.1093/brain/awn080

Ishii, A., Furusho, M., Dupree, J. L., & Bansal, R. (2014). Role of ERK1/2 MAPK signaling in the maintenance of myelin and axonal integrity in the adult CNS. *J Neurosci, 34*(48), 16031-16045. doi:10.1523/jneurosci.3360-14.2014

Jacobs, L. D., Cookfair, D. L., Rudick, R. A., Herndon, R. M., Richert, J. R., Salazar, A. M., . . . et al. (1996). Intramuscular interferon beta-1a for disease

progression in relapsing multiple sclerosis. The Multiple Sclerosis Collaborative Research Group (MSCRG). *Ann Neurol, 39*(3), 285-294. doi:10.1002/ana.410390304

Jagielska, A., Lowe, A. L., Makhija, E., Wroblewska, L., Guck, J., Franklin, R. J. M., . . . Van Vliet, K. J. (2017). Mechanical Strain Promotes Oligodendrocyte Differentiation by Global Changes of Gene Expression. *Front Cell Neurosci, 11*, 93. doi:10.3389/fncel.2017.00093

Jagielska, A., Norman, A. L., Whyte, G., Vliet, K. J., Guck, J., & Franklin, R. J. (2012). Mechanical environment modulates biological properties of oligodendrocyte progenitor cells. *Stem Cells Dev, 21*(16), 2905-2914. doi:10.1089/scd.2012.0189

Jankowsky, J. L., Slunt, H. H., Ratovitski, T., Jenkins, N. A., Copeland, N. G., & Borchelt, D. R. (2001). Co-expression of multiple transgenes in mouse CNS: a comparison of strategies. *Biomol Eng, 17*(6), 157-165.

Jantaratnotai, N., Ryu, J. K., Kim, S. U., & McLarnon, J. G. (2003). Amyloid beta peptide-induced corpus callosum damage and glial activation in vivo. *Neuroreport, 14*(11), 1429-1433. doi:10.1097/01.wnr.0000086097.47480.a0

Jarjour, A. A., Zhang, H., Bauer, N., Ffrench-Constant, C., & Williams, A. (2012). In vitro modeling of central nervous system myelination and remyelination. *Glia, 60*(1), 1-12. doi:10.1002/glia.21231

Johnson, L. A., Gamboa, A., Vintimilla, R., Cheatwood, A. J., Grant, A., Trivedi, A., . . . O'Bryant, S. E. (2015). Comorbid Depression and Diabetes as a Risk for Mild Cognitive Impairment and Alzheimer's Disease in Elderly Mexican Americans. *J Alzheimers Dis, 47*(1), 129-136. doi:10.3233/jad-142907

Johnstone, M., Gearing, A. J., & Miller, K. M. (1999). A central role for astrocytes in the inflammatory response to beta-amyloid; chemokines, cytokines and reactive oxygen species are produced. *J Neuroimmunol, 93*(1-2), 182-193.

Jones, R. S., Minogue, A. M., Connor, T. J., & Lynch, M. A. (2013). Amyloid-beta-induced astrocytic phagocytosis is mediated by CD36, CD47 and RAGE. *J Neuroimmune Pharmacol, 8*(1), 301-311. doi:10.1007/s11481-012-9427-3

Joo, I. L., Lai, A. Y., Bazzigaluppi, P., Koletar, M. M., Dorr, A., Brown, M. E., . . . Stefanovic, B. (2017). Early neurovascular dysfunction in a transgenic rat model of Alzheimer's disease. *Sci Rep, 7*, 46427. doi:10.1038/srep46427

Juurlink, B. H. (1997). Response of glial cells to ischemia: roles of reactive oxygen species and glutathione. *Neurosci Biobehav Rev, 21*(2), 151-166.

Kamajaya, A., Kaiser, J. T., Lee, J., Reid, M., & Rees, D. C. (2014). The structure of a conserved piezo channel domain reveals a topologically distinct beta sandwich fold. *Structure, 22*(10), 1520-1527. doi:10.1016/j.str.2014.08.009

Kamenetz, F., Tomita, T., Hsieh, H., Seabrook, G., Borchelt, D., Iwatsubo, T., . . . Malinow, R. (2003). APP processing and synaptic function. *Neuron, 37*(6), 925-937.

Kamer, A. R., Dasanayake, A. P., Craig, R. G., Glodzik-Sobanska, L., Bry, M., & de Leon, M. J. (2008). Alzheimer's disease and peripheral infections: the possible contribution from periodontal infections, model and hypothesis. *J Alzheimers Dis, 13*(4), 437-449.

Kant, A., Bhandakkar, T. K., & Medhekar, N. V. (2017). Stress enhanced calcium kinetics in a neuron. *Biomech Model Mechanobiol*. doi:10.1007/s10237-017-0952-0

Kempuraj, D., Thangavel, R., Natteru, P. A., Selvakumar, G. P., Saeed, D., Zahoor, H., . . . Zaheer, A. (2016). Neuroinflammation Induces Neurodegeneration. *J Neurol Neurosurg Spine, 1*(1).

Kim, S. E., Coste, B., Chadha, A., Cook, B., & Patapoutian, A. (2012). The role of Drosophila Piezo in mechanical

nociception. *Nature, 483*(7388), 209-212. doi:10.1038/nature10801

Kippert, A., Fitzner, D., Helenius, J., & Simons, M. (2009). Actomyosin contractility controls cell surface area of oligodendrocytes. *BMC Cell Biol, 10*, 71. doi:10.1186/1471-2121-10-71

Kiray, H., Lindsay, S. L., Hosseinzadeh, S., & Barnett, S. C. (2016). The multifaceted role of astrocytes in regulating myelination. *Exp Neurol, 283*(Pt B), 541-549. doi:10.1016/j.expneurol.2016.03.009

Knupfer, M. M., Poppenborg, H., Hotfilder, M., Kuhnel, K., Wolff, J. E., & Domula, M. (1999). CD44 expression and hyaluronic acid binding of malignant glioma cells. *Clin Exp Metastasis, 17*(1), 71-76.

Kocer, A. (2015). Mechanisms of mechanosensing - mechanosensitive channels, function and re-engineering. *Curr Opin Chem Biol, 29*, 120-127. doi:10.1016/j.cbpa.2015.10.006

Koch, D., Rosoff, W. J., Jiang, J., Geller, H. M., & Urbach, J. S. (2012). Strength in the periphery: growth cone biomechanics and substrate rigidity response in peripheral and central nervous system neurons. *Biophys J, 102*(3), 452-460. doi:10.1016/j.bpj.2011.12.025

Kontush, A. (2001). Alzheimer's amyloid-beta as a preventive antioxidant for brain lipoproteins. *Cell Mol Neurobiol, 21*(4), 299-315.

Koser, D. E., Thompson, A. J., Foster, S. K., Dwivedy, A., Pillai, E. K., Sheridan, G. K., . . . Franze, K. (2016). Mechanosensing is critical for axon growth in the developing brain. *Nat Neurosci, 19*(12), 1592-1598. doi:10.1038/nn.4394

Koutsis, G., Lynch, D., Manole, A., Karadima, G., Reilly, M. M., Houlden, H., & Panas, M. (2015). Charcot-Marie-Tooth disease type 2C and scapuloperoneal muscular atrophy overlap syndrome in a patient with the R232C TRPV4 mutation. *J Neurol, 262*(8), 1972-1975. doi:10.1007/s00415-015-7800-x

Krstic, D., & Knuesel, I. (2013). Deciphering the mechanism underlying late-onset Alzheimer disease. *Nat Rev Neurol, 9*(1), 25-34. doi:10.1038/nrneurol.2012.236

Kuchibhotla, K. V., Lattarulo, C. R., Hyman, B. T., & Bacskai, B. J. (2009). Synchronous hyperactivity and intercellular calcium waves in astrocytes in Alzheimer mice. *Science, 323*(5918), 1211-1215. doi:10.1126/science.1169096

Kulkarni, O. P., Lichtnekert, J., Anders, H. J., & Mulay, S. R. (2016). The Immune System in Tissue Environments Regaining Homeostasis after Injury: Is "Inflammation" Always Inflammation? *Mediators Inflamm, 2016*, 2856213. doi:10.1155/2016/2856213

Lacroix, J. J., Botello-Smith, W. M., & Luo, Y. (2018). Probing the gating mechanism of the mechanosensitive channel Piezo1 with the small molecule Yoda1. *Nat Commun, 9*(1), 2029. doi:10.1038/s41467-018-04405-3

Lamontagne, C. A., & Grandbois, M. (2008). PKC-induced stiffening of hyaluronan/CD44 linkage; local force measurements on glioma cells. *Exp Cell Res, 314*(2), 227-236. doi:10.1016/j.yexcr.2007.07.013

Landoure, G., Zdebik, A. A., Martinez, T. L., Burnett, B. G., Stanescu, H. C., Inada, H., . . . Sumner, C. J. (2010). Mutations in TRPV4 cause Charcot-Marie-Tooth disease type 2C. *Nat Genet, 42*(2), 170-174. doi:10.1038/ng.512

Lee, D. W., Banquy, X., Kristiansen, K., Kaufman, Y., Boggs, J. M., & Israelachvili, J. N. (2014). Lipid domains control myelin basic protein adsorption and membrane interactions between model myelin lipid bilayers. *Proc Natl Acad Sci U S A, 111*(8), E768-775. doi:10.1073/pnas.1401165111

Lee, J. T., Xu, J., Lee, J. M., Ku, G., Han, X., Yang, D. I., . . . Hsu, C. Y. (2004). Amyloid-beta peptide induces oligodendrocyte death by activating the neutral sphingomyelinase-ceramide pathway. *J Cell Biol, 164*(1), 123-131. doi:10.1083/jcb.200307017

Lee, S., Leach, M. K., Redmond, S. A., Chong, S. Y., Mellon, S. H., Tuck, S. J., . . . Chan, J. R. (2012). A culture system to study oligodendrocyte myelination processes using engineered nanofibers. *Nat Methods, 9*(9), 917-922. doi:10.1038/nmeth.2105

Lee, S. Y., & O'Grady, S. M. (2003). Modulation of ion channel function by P2Y receptors. *Cell Biochem Biophys, 39*(1), 75-88. doi:10.1385/cbb:39:1:75

Leipzig, N. D., & Shoichet, M. S. (2009). The effect of substrate stiffness on adult neural stem cell behavior. *Biomaterials, 30*(36), 6867-6878. doi:10.1016/j.biomaterials.2009.09.002

Lepekhin, E. A., Eliasson, C., Berthold, C. H., Berezin, V., Bock, E., & Pekny, M. (2001). Intermediate filaments regulate astrocyte motility. *J Neurochem, 79*(3), 617-625.

Lesne, S., Ali, C., Gabriel, C., Croci, N., MacKenzie, E. T., Glabe, C. G., . . . Buisson, A. (2005). NMDA receptor activation inhibits alpha-secretase and promotes neuronal amyloid-beta production. *J Neurosci, 25*(41), 9367-9377. doi:10.1523/jneurosci.0849-05.2005

Lewis, A. H., & Grandl, J. (2015). Mechanical sensitivity of Piezo1 ion channels can be tuned by cellular membrane tension. *Elife, 4*. doi:10.7554/eLife.12088

Leyns, C. E. G., & Holtzman, D. M. (2017). Glial contributions to neurodegeneration in tauopathies. *Mol Neurodegener, 12*(1), 50. doi:10.1186/s13024-017-0192-x

Li, C., Rezania, S., Kammerer, S., Sokolowski, A., Devaney, T., Gorischek, A., . . . Schreibmayer, W. (2015). Piezo1 forms mechanosensitive ion channels in the human MCF-7 breast cancer cell line. *Sci Rep, 5*, 8364. doi:10.1038/srep08364

Li, C., Zhao, R., Gao, K., Wei, Z., Yin, M. Y., Lau, L. T., . . . Yu, A. C. (2011). Astrocytes: implications for neuroinflammatory pathogenesis of Alzheimer's disease. *Curr Alzheimer Res, 8*(1), 67-80.

Li, X. F., Zhang, Z., Chen, Z. K., Cui, Z. W., & Zhang, H. N. (2017). Piezo1 protein induces the apoptosis of human osteoarthritis-derived chondrocytes by activating caspase-12, the signaling marker of ER stress. *Int J Mol Med, 40*(3), 845-853. doi:10.3892/ijmm.2017.3075

Libbey, J. E., & Fujinami, R. S. (2010). Potential triggers of MS. *Results Probl Cell Differ, 51*, 21-42. doi:10.1007/400_2008_12

Licastro, F., & Porcellini, E. (2016). Persistent infections, immune-senescence and Alzheimer's disease. In *Oncoscience* (Vol. 3, pp. 135-142). United States.

Liddelow, S. A., Guttenplan, K. A., Clarke, L. E., Bennett, F. C., Bohlen, C. J., Schirmer, L., . . . Barres, B. A. (2017). Neurotoxic reactive astrocytes are induced by activated microglia. *Nature, 541*(7638), 481-487. doi:10.1038/nature21029

Lilienbaum, A., & Israel, A. (2003). From calcium to NF-kappa B signaling pathways in neurons. *Mol Cell Biol, 23*(8), 2680-2698.

Lim, S. L., Rodriguez-Ortiz, C. J., & Kitazawa, M. (2015). Infection, systemic inflammation, and Alzheimer's disease. *Microbes Infect, 17*(8), 549-556. doi:10.1016/j.micinf.2015.04.004

Lindwall, G., & Cole, R. D. (1984). Phosphorylation affects the ability of tau protein to promote microtubule assembly. *J Biol Chem, 259*(8), 5301-5305.

Liu, C., Cui, G., Zhu, M., Kang, X., & Guo, H. (2014). Neuroinflammation in Alzheimer's disease: chemokines produced by astrocytes and chemokine receptors. *Int J Clin Exp Pathol, 7*(12), 8342-8355.

Liu, Z., Pelfrey, C. M., Cotleur, A., Lee, J. C., & Rudick, R. A. (2001). Immunomodulatory effects of interferon beta-1a in multiple sclerosis. *J Neuroimmunol, 112*(1-2), 153-162.

Lockyer, P. J., Kupzig, S., & Cullen, P. J. (2001). CAPRI regulates Ca(2+)-dependent inactivation of the Ras-MAPK pathway. *Curr Biol, 11*(12), 981-986.

Loleit, V., Biberacher, V., & Hemmer, B. (2014). Current and future therapies targeting the immune system in multiple sclerosis. *Curr Pharm Biotechnol, 15*(3), 276-296.

Loma, I., & Heyman, R. (2011). Multiple sclerosis: pathogenesis and treatment. *Curr Neuropharmacol, 9*(3), 409-416. doi:10.2174/157015911796557911

Louis, E. D., Ma, K., Babij, R., Cortes, E., Liem, R. K., Vonsattel, J. P., & Faust, P. L. (2012). Neurofilament protein levels: quantitative analysis in essential tremor cerebellar cortex. *Neurosci Lett, 518*(1), 49-54. doi:10.1016/j.neulet.2012.04.054

Lourenco, T., & Graos, M. (2016). Modulation of Oligodendrocyte Differentiation by Mechanotransduction. *Front Cell Neurosci, 10*, 277. doi:10.3389/fncel.2016.00277

Lourenco, T., Paes de Faria, J., Bippes, C. A., Maia, J., Lopes-da-Silva, J. A., Relvas, J. B., & Graos, M. (2016). Modulation of oligodendrocyte differentiation and maturation by combined biochemical and mechanical cues. *Sci Rep, 6*, 21563. doi:10.1038/srep21563

Low, B. C., Pan, C. Q., Shivashankar, G. V., Bershadsky, A., Sudol, M., & Sheetz, M. (2014). YAP/TAZ as mechanosensors and mechanotransducers in regulating organ size and tumor growth. *FEBS Lett, 588*(16), 2663-2670. doi:10.1016/j.febslet.2014.04.012

Lu, P. H., Lee, G. J., Raven, E. P., Tingus, K., Khoo, T., Thompson, P. M., & Bartzokis, G. (2011). Age-related slowing in cognitive processing speed is associated with myelin integrity in a very healthy elderly sample. *J Clin Exp Neuropsychol, 33*(10), 1059-1068. doi:10.1080/13803395.2011.595397

Lu, Y. B., Franze, K., Seifert, G., Steinhauser, C., Kirchhoff, F., Wolburg, H., . . . Reichenbach, A. (2006). Viscoelastic properties of individual glial cells and neurons in the CNS. *Proc Natl Acad Sci U S A, 103*(47), 17759-17764. doi:10.1073/pnas.0606150103

Lublin, F., Miller, D. H., Freedman, M. S., Cree, B. A. C., Wolinsky, J. S., Weiner, H., . . . Kappos, L. (2016). Oral fingolimod in primary progressive multiple sclerosis (INFORMS): a phase 3, randomised, double-blind, placebo-controlled trial. *Lancet, 387*(10023), 1075-1084. doi:10.1016/s0140-6736(15)01314-8

Lukacs, V., Mathur, J., Mao, R., Bayrak-Toydemir, P., Procter, M., Cahalan, S. M., . . . Krock, B. L. (2015). Impaired PIEZO1 function in patients with a novel autosomal recessive congenital lymphatic dysplasia. *Nat Commun, 6*, 8329. doi:10.1038/ncomms9329

Lukiw, W. J. (2012). Amyloid beta (Abeta) peptide modulators and other current treatment strategies for Alzheimer's disease (AD). *Expert Opin Emerg Drugs*. doi:10.1517/14728214.2012.672559

Lulevich, V., Zimmer, C. C., Hong, H. S., Jin, L. W., & Liu, G. Y. (2010). Single-cell mechanics provides a sensitive and quantitative means for probing amyloid-beta peptide and neuronal cell interactions. *Proc Natl Acad Sci U S A, 107*(31), 13872-13877. doi:10.1073/pnas.1008341107

Luo, Q., Ding, L., Zhang, N., Jiang, Z., Gao, C., Xue, L., . . . Wang, G. (2018). A stable and easily reproducible model of focal white matter demyelination. *J Neurosci Methods, 307*, 230-239. doi:10.1016/j.jneumeth.2018.05.024

Magi, S., Castaldo, P., Macri, M. L., Maiolino, M., Matteucci, A., Bastioli, G., . . . Lariccia, V. (2016). Intracellular Calcium Dysregulation: Implications for Alzheimer's Disease. *Biomed Res Int, 2016*, 6701324. doi:10.1155/2016/6701324

Marchbank, T., & Playford, R. J. (2018). Trefoil factor family peptides enhance cell migration by increasing cellular osmotic permeability and aquaporin 3 levels. *Faseb j, 32*(2), 1017-1024. doi:10.1096/fj.201700799R

Marques, S., Zeisel, A., Codeluppi, S., van Bruggen, D., Mendanha Falcao, A., Xiao, L., . . . Castelo-Branco, G. (2016). Oligodendrocyte heterogeneity in the

mouse juvenile and adult central nervous system. *Science, 352*(6291), 1326-1329. doi:10.1126/science.aaf6463

Martin-Almedina, S., Mansour, S., & Ostergaard, P. (2018). Human phenotypes caused by PIEZO1 mutations; one gene, two overlapping phenotypes? *J Physiol, 596*(6), 985-992. doi:10.1113/jp275718

Martinac, B. (2004). Mechanosensitive ion channels: molecules of mechanotransduction. *J Cell Sci, 117*(Pt 12), 2449-2460. doi:10.1242/jcs.01232

Martins, J. R., Penton, D., Peyronnet, R., Arhatte, M., Moro, C., Picard, N., . . . Demolombe, S. (2016). Piezo1-dependent regulation of urinary osmolarity. *Pflugers Arch, 468*(7), 1197-1206. doi:10.1007/s00424-016-1811-z

Matloubian, M., Lo, C. G., Cinamon, G., Lesneski, M. J., Xu, Y., Brinkmann, V., . . . Cyster, J. G. (2004). Lymphocyte egress from thymus and peripheral lymphoid organs is dependent on S1P receptor 1. *Nature, 427*(6972), 355-360. doi:10.1038/nature02284

Maxwell, W. L. (2013). Damage to myelin and oligodendrocytes: a role in chronic outcomes following traumatic brain injury? *Brain Sci, 3*(3), 1374-1394. doi:10.3390/brainsci3031374

McHugh, B. J., Buttery, R., Lad, Y., Banks, S., Haslett, C., & Sethi, T. (2010). Integrin activation by Fam38A uses a novel mechanism of R-Ras targeting to the endoplasmic reticulum. *J Cell Sci, 123*(Pt 1), 51-61. doi:10.1242/jcs.056424

McHugh, B. J., Murdoch, A., Haslett, C., & Sethi, T. (2012). Loss of the integrin-activating transmembrane protein Fam38A (Piezo1) promotes a switch to a reduced integrin-dependent mode of cell migration. *PLoS One, 7*(7), e40346. doi:10.1371/journal.pone.0040346

McIntosh, T. J., & Simon, S. A. (1986). Hydration force and bilayer deformation: a reevaluation. *Biochemistry, 25*(14), 4058-4066.

Messing, A., Brenner, M., Feany, M. B., Nedergaard, M., & Goldman, J. E. (2012). Alexander disease. *J Neurosci, 32*(15), 5017-5023. doi:10.1523/jneurosci.5384-11.2012

Milosevic, A., & Zecevic, N. (1998). Developmental changes in human cerebellum: expression of intracellular calcium receptors, calcium-binding proteins, and phosphorylated and nonphosphorylated neurofilament protein. *J Comp Neurol, 396*(4), 442-460.

Misslin, C., Velasco-Estevez, M., Albert, M., O'Sullivan, S. A., & Dev, K. K. (2017). Phospholipase A2 is involved in galactosylsphingosine-induced astrocyte toxicity, neuronal damage and demyelination. *PLoS One, 12*(11), e0187217. doi:10.1371/journal.pone.0187217

Mitew, S., Kirkcaldie, M. T., Halliday, G. M., Shepherd, C. E., Vickers, J. C., & Dickson, T. C. (2010). Focal demyelination in Alzheimer's disease and transgenic mouse models. *Acta Neuropathol, 119*(5), 567-577. doi:10.1007/s00401-010-0657-2

Miyamoto, A., Miyauchi, H., Kogure, T., Miyawaki, A., Michikawa, T., & Mikoshiba, K. (2015). Apoptosis induction-related cytosolic calcium responses revealed by the dual FRET imaging of calcium signals and caspase-3 activation in a single cell. *Biochem Biophys Res Commun, 460*(1), 82-87. doi:10.1016/j.bbrc.2015.02.045

Miyamoto, T., Mochizuki, T., Nakagomi, H., Kira, S., Watanabe, M., Takayama, Y., . . . Tominaga, M. (2014). Functional role for Piezo1 in stretch-evoked Ca(2)(+) influx and ATP release in urothelial cell cultures. *J Biol Chem, 289*(23), 16565-16575. doi:10.1074/jbc.M113.528638

Moe, P., & Blount, P. (2005). Assessment of potential stimuli for mechano-dependent gating of MscL: effects of pressure, tension, and lipid headgroups. *Biochemistry, 44*(36), 12239-12244. doi:10.1021/bi0509649

Moeendarbary, E., Weber, I. P., Sheridan, G. K., Koser, D. E., Soleman, S., Haenzi, B., . . . Franze, K. (2017). The soft mechanical signature of glial scars in the central nervous system. *Nat Commun, 8*, 14787. doi:10.1038/ncomms14787

Mogi, M., Harada, M., Riederer, P., Narabayashi, H., Fujita, K., & Nagatsu, T. (1994). Tumor necrosis factor-alpha (TNF-alpha) increases both in the brain and in the cerebrospinal fluid from parkinsonian patients. *Neurosci Lett, 165*(1-2), 208-210.

Mohieldin, A. M., Zubayer, H. S., Al Omran, A. J., Saternos, H. C., Zarban, A. A., Nauli, S. M., & AbouAlaiwi, W. A. (2016). Vascular Endothelial Primary Cilia: Mechanosensation and Hypertension. *Curr Hypertens Rev, 12*(1), 57-67.

Moon, L. D., & Fawcett, J. W. (2001). Reduction in CNS scar formation without concomitant increase in axon regeneration following treatment of adult rat brain with a combination of antibodies to TGFbeta1 and beta2. *Eur J Neurosci, 14*(10), 1667-1677.

Morell, P., & Norton, W. T. (1980). Myelin. *Sci Am, 242*(5), 88-90, 92, 96 passim.

Morita, M., Higuchi, C., Moto, T., Kozuka, N., Susuki, J., Itofusa, R., . . . Kudo, Y. (2003). Dual regulation of calcium oscillation in astrocytes by growth factors and pro-inflammatory cytokines via the mitogen-activated protein kinase cascade. *J Neurosci, 23*(34), 10944-10952.

Morley, J. E., Farr, S. A., Kumar, V. B., & Armbrecht, H. J. (2012). The SAMP8 mouse: a model to develop therapeutic interventions for Alzheimer's disease. *Curr Pharm Des, 18*(8), 1123-1130.

Morris, G. P., Clark, I. A., & Vissel, B. (2014). Inconsistencies and controversies surrounding the amyloid hypothesis of Alzheimer's disease. *Acta Neuropathol Commun, 2*, 135. doi:10.1186/s40478-014-0135-5

Moshayedi, P., Ng, G., Kwok, J. C., Yeo, G. S., Bryant, C. E., Fawcett, J. W., . . . Guck, J. (2014). The relationship between glial cell mechanosensitivity and foreign body reactions in the central nervous system. *Biomaterials, 35*(13), 3919-3925. doi:10.1016/j.biomaterials.2014.01.038

Mucke, L., & Eddleston, M. (1993). Astrocytes in infectious and immune-mediated diseases of the central nervous system. *Faseb j, 7*(13), 1226-1232.

Munson, J. M., Bellamkonda, R. V., & Swartz, M. A. (2013). Interstitial flow in a 3D microenvironment increases glioma invasion by a CXCR4-dependent mechanism. *Cancer Res, 73*(5), 1536-1546. doi:10.1158/0008-5472.can-12-2838

Murphy, M. C., Curran, G. L., Glaser, K. J., Rossman, P. J., Huston, J., 3rd, Poduslo, J. F., . . . Ehman, R. L. (2012). Magnetic resonance elastography of the brain in a mouse model of Alzheimer's disease: initial results. *Magn Reson Imaging, 30*(4), 535-539. doi:10.1016/j.mri.2011.12.019

Murphy, M. C., Huston, J., 3rd, Jack, C. R., Jr., Glaser, K. J., Manduca, A., Felmlee, J. P., & Ehman, R. L. (2011). Decreased brain stiffness in Alzheimer's disease determined by magnetic resonance elastography. *J Magn Reson Imaging, 34*(3), 494-498. doi:10.1002/jmri.22707

Murphy, M. C., Jones, D. T., Jack, C. R., Jr., Glaser, K. J., Senjem, M. L., Manduca, A., . . . Huston, J., 3rd. (2016). Regional brain stiffness changes across the Alzheimer's disease spectrum. *Neuroimage Clin, 10*, 283-290. doi:10.1016/j.nicl.2015.12.007

Murray, K. N., Parry-Jones, A. R., & Allan, S. M. (2015). Interleukin-1 and acute brain injury. *Front Cell Neurosci, 9*, 18. doi:10.3389/fncel.2015.00018

Nagarajan, A., Ning, Y., Reisner, K., Buraei, Z., Larsen, J. P., Hobert, O., & Doitsidou, M. (2014). Progressive degeneration of dopaminergic neurons through TRP channel-induced cell death. *J Neurosci, 34*(17), 5738-5746. doi:10.1523/jneurosci.4540-13.2014

Nakagawa, T., Kubota, T., Kabuto, M., Fujimoto, N., & Okada, Y. (1996). Secretion of matrix metalloproteinase-2 (72 kD gelatinase/type IV collagenase = gelatinase A) by malignant human glioma cell lines: implications for the growth and cellular invasion of the extracellular matrix. *J Neurooncol, 28*(1), 13-24.

Nakano, Y., Furube, E., Morita, S., Wanaka, A., Nakashima, T., & Miyata, S. (2015). Astrocytic TLR4 expression and LPS-induced nuclear translocation of STAT3 in the sensory circumventricular organs of adult mouse brain. *J Neuroimmunol, 278*, 144-158. doi:10.1016/j.jneuroim.2014.12.013

Nilius, B., & Honore, E. (2012). Sensing pressure with ion channels. *Trends Neurosci, 35*(8), 477-486. doi:10.1016/j.tins.2012.04.002

Nishizawa, K., Nishizawa, M., Gnanasambandam, R., Sachs, F., Sukharev, S. I., & Suchyna, T. M. (2015). Effects of Lys to Glu mutations in GsMTx4 on membrane binding, peptide orientation, and self-association propensity, as analyzed by molecular dynamics simulations. *Biochim Biophys Acta, 1848*(11 Pt A), 2767-2778. doi:10.1016/j.bbamem.2015.09.003

Nomura, T., Cranfield, C. G., Deplazes, E., Owen, D. M., Macmillan, A., Battle, A. R., . . . Martinac, B. (2012). Differential effects of lipids and lyso-lipids on the mechanosensitivity of the mechanosensitive channels MscL and MscS. *Proc Natl Acad Sci U S A, 109*(22), 8770-8775. doi:10.1073/pnas.1200051109

Nourse, J. L., & Pathak, M. M. (2017). How cells channel their stress: Interplay between Piezo1 and the cytoskeleton. *Semin Cell Dev Biol, 71*, 3-12. doi:10.1016/j.semcdb.2017.06.018

O'Brien, K., Fitzgerald, D. C., Naiken, K., Alugupalli, K. R., Rostami, A. M., & Gran, B. (2008). Role of the innate immune system in autoimmune inflammatory demyelination. *Curr Med Chem, 15*(11), 1105-1115.

O'Sullivan, C., & Dev, K. K. (2015). Galactosylsphingosine (psychosine)-induced demyelination is attenuated by sphingosine 1-phosphate signalling. *J Cell Sci, 128*(21), 3878-3887. doi:10.1242/jcs.169342

O'Sullivan, S. A., Velasco-Estevez, M., & Dev, K. K. (2017). Demyelination induced by oxidative stress is regulated by sphingosine 1-phosphate receptors. *Glia, 65*(7), 1119-1136. doi:10.1002/glia.23148

Oakley, H., Cole, S. L., Logan, S., Maus, E., Shao, P., Craft, J., . . . Vassar, R. (2006). Intraneuronal beta-amyloid aggregates, neurodegeneration, and neuron loss in transgenic mice with five familial Alzheimer's disease mutations: potential factors in amyloid plaque formation. *J Neurosci, 26*(40), 10129-10140. doi:10.1523/jneurosci.1202-06.2006

Obradovic, D., Kataranovski, M., Dincic, E., Obradovic, S., & Colic, M. (2012). Tumor necrosis factor-alfa and interleukin-4 in cerbrospinal fluid and plasma in different clinical forms of multiple sclerosis. *Vojnosanit Pregl, 69*(2), 151-156.

Oddo, S., Caccamo, A., Kitazawa, M., Tseng, B. P., & LaFerla, F. M. (2003). Amyloid deposition precedes tangle formation in a triple transgenic model of Alzheimer's disease. *Neurobiol Aging, 24*(8), 1063-1070.

Ohno, N., Chiang, H., Mahad, D. J., Kidd, G. J., Liu, L., Ransohoff, R. M., . . . Trapp, B. D. (2014). Mitochondrial immobilization mediated by syntaphilin facilitates survival of demyelinated axons. *Proc Natl Acad Sci U S A, 111*(27), 9953-9958. doi:10.1073/pnas.1401155111

Ohno, N., Kidd, G. J., Mahad, D., Kiryu-Seo, S., Avishai, A., Komuro, H., & Trapp, B. D. (2011). Myelination and axonal electrical activity modulate the distribution and motility of mitochondria at CNS nodes of Ranvier.

J Neurosci, 31(20), 7249-7258. doi:10.1523/jneurosci.0095-11.2011

Oswald, R. E., Suchyna, T. M., McFeeters, R., Gottlieb, P., & Sachs, F. (2002). Solution structure of peptide toxins that block mechanosensitive ion channels. *J Biol Chem, 277*(37), 34443-34450. doi:10.1074/jbc.M202715200

Ousman, S. S., & David, S. (2000). Lysophosphatidylcholine induces rapid recruitment and activation of macrophages in the adult mouse spinal cord. *Glia, 30*(1), 92-104.

Paemeleire, K., & Leybaert, L. (2000). Ionic changes accompanying astrocytic intercellular calcium waves triggered by mechanical cell damaging stimulation. *Brain Res, 857*(1-2), 235-245.

Pahl, H. L., & Baeuerle, P. A. (1996). Activation of NF-kappa B by ER stress requires both Ca2+ and reactive oxygen intermediates as messengers. *FEBS Lett, 392*(2), 129-136.

Palsson-McDermott, E. M., & O'Neill, L. A. (2004). Signal transduction by the lipopolysaccharide receptor, Toll-like receptor-4. *Immunology, 113*(2), 153-162. doi:10.1111/j.1365-2567.2004.01976.x

Pathak, M. M., Nourse, J. L., Tran, T., Hwe, J., Arulmoli, J., Le, D. T., . . . Tombola, F. (2014). Stretch-activated ion channel Piezo1 directs lineage choice in human neural stem cells. *Proc Natl Acad Sci U S A, 111*(45), 16148-16153. doi:10.1073/pnas.1409802111

Patti, F., Amato, M. P., Bastianello, S., Caniatti, L., Di Monte, E., Ferrazza, P., . . . Trojano, M. (2010). Effects of immunomodulatory treatment with subcutaneous interferon beta-1a on cognitive decline in mildly disabled patients with relapsing-remitting multiple sclerosis. *Mult Scler, 16*(1), 68-77. doi:10.1177/1352458509350309

Pearson, H. A., & Peers, C. (2006). Physiological roles for amyloid beta peptides. *J Physiol, 575*(Pt 1), 5-10. doi:10.1113/jphysiol.2006.111203

Pekny, M., Leveen, P., Pekna, M., Eliasson, C., Berthold, C. H., Westermark, B., & Betsholtz, C. (1995). Mice lacking glial fibrillary acidic protein display astrocytes devoid of intermediate filaments but develop and reproduce normally. *Embo j, 14*(8), 1590-1598.

Pentkowski, N. S., Berkowitz, L. E., Thompson, S. M., Drake, E. N., Olguin, C. R., & Clark, B. J. (2018). Anxiety-like behavior as an early endophenotype in the TgF344-AD rat model of Alzheimer's disease. *Neurobiol Aging, 61*, 169-176. doi:10.1016/j.neurobiolaging.2017.09.024

Perea, G., Sur, M., & Araque, A. (2014). Neuron-glia networks: integral gear of brain function. *Front Cell Neurosci, 8*, 378. doi:10.3389/fncel.2014.00378

Perl, D. P. (2010). Neuropathology of Alzheimer's disease. *Mt Sinai J Med, 77*(1), 32-42. doi:10.1002/msj.20157

Perry, S. W., Dewhurst, S., Bellizzi, M. J., & Gelbard, H. A. (2002). Tumor necrosis factor-alpha in normal and diseased brain: Conflicting effects via intraneuronal receptor crosstalk? *J Neurovirol, 8*(6), 611-624. doi:10.1080/13550280290101021

Peyronnet, R., Martins, J. R., Duprat, F., Demolombe, S., Arhatte, M., Jodar, M., . . . Patel, A. (2013). Piezo1-dependent stretch-activated channels are inhibited by Polycystin-2 in renal tubular epithelial cells. *EMBO Rep, 14*(12), 1143-1148. doi:10.1038/embor.2013.170

Pfrieger, F. W., & Barres, B. A. (1996). New views on synapse-glia interactions. *Curr Opin Neurobiol, 6*(5), 615-621.

Phinney, A. L., Deller, T., Stalder, M., Calhoun, M. E., Frotscher, M., Sommer, B., . . . Jucker, M. (1999). Cerebral amyloid induces aberrant axonal sprouting and ectopic terminal formation in amyloid precursor protein transgenic mice. *J Neurosci, 19*(19), 8552-8559.

Platt, A., & Wetzler, L. (2013). Innate immunity and vaccines. *Curr Top Med Chem, 13*(20), 2597-2608.

Plemel, J. R., Keough, M. B., Duncan, G. J., Sparling, J. S., Yong, V. W., Stys, P. K., & Tetzlaff, W. (2014). Remyelination after spinal cord injury: is it a target for repair? *Prog Neurobiol, 117*, 54-72. doi:10.1016/j.pneurobio.2014.02.006

Plemel, J. R., Michaels, N. J., Weishaupt, N., Caprariello, A. V., Keough, M. B., Rogers, J. A., . . . Yong, V. W. (2018). Mechanisms of lysophosphatidylcholine-induced demyelination: A primary lipid disrupting myelinopathy. *Glia, 66*(2), 327-347. doi:10.1002/glia.23245

Pogoda, K., Chin, L., Georges, P. C., Byfield, F. J., Bucki, R., Kim, R., . . . Janmey, P. A. (2014). Compression stiffening of brain and its effect on mechanosensing by glioma cells. *New J Phys, 16*, 075002. doi:10.1088/1367-2630/16/7/075002

Poliak, S., Gollan, L., Martinez, R., Custer, A., Einheber, S., Salzer, J. L., . . . Peles, E. (1999). Caspr2, a new member of the neurexin superfamily, is localized at the juxtaparanodes of myelinated axons and associates with K+ channels. *Neuron, 24*(4), 1037-1047.

Poliak, S., Salomon, D., Elhanany, H., Sabanay, H., Kiernan, B., Pevny, L., . . . Peles, E. (2003). Juxtaparanodal clustering of Shaker-like K+ channels in myelinated axons depends on Caspr2 and TAG-1. *J Cell Biol, 162*(6), 1149-1160. doi:10.1083/jcb.200305018

Polman, C. H., O'Connor, P. W., Havrdova, E., Hutchinson, M., Kappos, L., Miller, D. H., . . . Sandrock, A. W. (2006). A randomized, placebo-controlled trial of natalizumab for relapsing multiple sclerosis. *N Engl J Med, 354*(9), 899-910. doi:10.1056/NEJMoa044397

Pope, W. B., Mirsadraei, L., Lai, A., Eskin, A., Qiao, J., Kim, H. J., . . . Cloughesy, T. F. (2012). Differential gene expression in glioblastoma defined by ADC histogram analysis: relationship to extracellular matrix molecules and survival. *AJNR Am J Neuroradiol, 33*(6), 1059-1064. doi:10.3174/ajnr.A2917

Potrovita, I., Zhang, W., Burkly, L., Hahm, K., Lincecum, J., Wang, M. Z., . . . Schwaninger, M. (2004). Tumor necrosis factor-like weak inducer of apoptosis-induced neurodegeneration. *J Neurosci, 24*(38), 8237-8244. doi:10.1523/jneurosci.1089-04.2004

Previtera, M. L., Langhammer, C. G., Langrana, N. A., & Firestein, B. L. (2010). Regulation of dendrite arborization by substrate stiffness is mediated by glutamate receptors. *Ann Biomed Eng, 38*(12), 3733-3743. doi:10.1007/s10439-010-0112-5

Qiu, W. Q., Ye, Z., Kholodenko, D., Seubert, P., & Selkoe, D. J. (1997). Degradation of amyloid beta-protein by a metalloprotease secreted by microglia and other neural and non-neural cells. *J Biol Chem, 272*(10), 6641-6646.

Ranade, S. S., Qiu, Z., Woo, S. H., Hur, S. S., Murthy, S. E., Cahalan, S. M., . . . Patapoutian, A. (2014). Piezo1, a mechanically activated ion channel, is required for vascular development in mice. *Proc Natl Acad Sci U S A, 111*(28), 10347-10352. doi:10.1073/pnas.1409233111

Ranade, S. S., Syeda, R., & Patapoutian, A. (2015). Mechanically Activated Ion Channels. *Neuron, 87*(6), 1162-1179. doi:10.1016/j.neuron.2015.08.032

Reier, P. J., & Houle, J. D. (1988). The glial scar: its bearing on axonal elongation and transplantation approaches to CNS repair. *Adv Neurol, 47*, 87-138.

Reilly, K. M. (2009). Brain tumor susceptibility: the role of genetic factors and uses of mouse models to unravel risk. *Brain Pathol, 19*(1), 121-131. doi:10.1111/j.1750-3639.2008.00236.x

Reiss-Zimmermann, M., Streitberger, K. J., Sack, I., Braun, J., Arlt, F., Fritzsch, D., & Hoffmann, K. T. (2015). High Resolution Imaging of Viscoelastic Properties of Intracranial Tumours by Multi-Frequency Magnetic Resonance Elastography. *Clin Neuroradiol, 25*(4), 371-378. doi:10.1007/s00062-014-0311-9

Remahl, S., & Hildebrand, C. (1982). Changing relation between onset of myelination and axon diameter range in developing

feline white matter. *J Neurol Sci, 54*(1), 33-45.

Retailleau, K., Duprat, F., Arhatte, M., Ranade, S. S., Peyronnet, R., Martins, J. R., . . . Honore, E. (2015). Piezo1 in Smooth Muscle Cells Is Involved in Hypertension-Dependent Arterial Remodeling. *Cell Rep, 13*(6), 1161-1171. doi:10.1016/j.celrep.2015.09.072

Riera, J., Hatanaka, R., Uchida, T., Ozaki, T., & Kawashima, R. (2011). Quantifying the uncertainty of spontaneous Ca2+ oscillations in astrocytes: particulars of Alzheimer's disease. *Biophys J, 101*(3), 554-564. doi:10.1016/j.bpj.2011.06.041

Ries, M., & Sastre, M. (2016). Mechanisms of Abeta Clearance and Degradation by Glial Cells. *Front Aging Neurosci, 8*, 160. doi:10.3389/fnagi.2016.00160

Robel, S., Mori, T., Zoubaa, S., Schlegel, J., Sirko, S., Faissner, A., . . . Gotz, M. (2009). Conditional deletion of beta1-integrin in astroglia causes partial reactive gliosis. *Glia, 57*(15), 1630-1647. doi:10.1002/glia.20876

Rodriguez-Arellano, J. J., Parpura, V., Zorec, R., & Verkhratsky, A. (2016). Astrocytes in physiological aging and Alzheimer's disease. *Neuroscience, 323*, 170-182. doi:10.1016/j.neuroscience.2015.01.007

Rohn, T. T., Vyas, V., Hernandez-Estrada, T., Nichol, K. E., Christie, L. A., & Head, E. (2008). Lack of pathology in a triple transgenic mouse model of Alzheimer's disease after overexpression of the anti-apoptotic protein Bcl-2. *J Neurosci, 28*(12), 3051-3059. doi:10.1523/jneurosci.5620-07.2008

Roitbak, T., & Sykova, E. (1999). Diffusion barriers evoked in the rat cortex by reactive astrogliosis. *Glia, 28*(1), 40-48.

Rolls, A., Shechter, R., & Schwartz, M. (2009). The bright side of the glial scar in CNS repair. *Nat Rev Neurosci, 10*(3), 235-241. doi:10.1038/nrn2591

Ronco, V., Grolla, A. A., Glasnov, T. N., Canonico, P. L., Verkhratsky, A., Genazzani, A. A., & Lim, D. (2014). Differential deregulation of astrocytic calcium signalling by amyloid-beta, TNFalpha, IL-1beta and LPS. *Cell Calcium, 55*(4), 219-229. doi:10.1016/j.ceca.2014.02.016

Rosenberg, G. A., Estrada, E. Y., Dencoff, J. E., & Stetler-Stevenson, W. G. (1995). Tumor necrosis factor-alpha-induced gelatinase B causes delayed opening of the blood-brain barrier: an expanded therapeutic window. *Brain Res, 703*(1-2), 151-155.

Rosenberg, S. S., Kelland, E. E., Tokar, E., De la Torre, A. R., & Chan, J. R. (2008). The geometric and spatial constraints of the microenvironment induce oligodendrocyte differentiation. *Proc Natl Acad Sci U S A, 105*(38), 14662-14667. doi:10.1073/pnas.0805640105

Rowe, T. A., & Juthani-Mehta, M. (2013). Urinary tract infection in older adults. *Aging health, 9*(5). doi:10.2217/ahe.13.38

Rudrabhatla, P. (2014). Regulation of neuronal cytoskeletal protein phosphorylation in neurodegenerative diseases. *J Alzheimers Dis, 41*(3), 671-684. doi:10.3233/jad-130794

Sack, I., Streitberger, K. J., Krefting, D., Paul, F., & Braun, J. (2011). The influence of physiological aging and atrophy on brain viscoelastic properties in humans. *PLoS One, 6*(9), e23451. doi:10.1371/journal.pone.0023451

Salman, M. M., Kitchen, P., Woodroofe, M. N., Brown, J. E., Bill, R. M., Conner, A. C., & Conner, M. T. (2017). Hypothermia increases aquaporin 4 (AQP4) plasma membrane abundance in human primary cortical astrocytes via a calcium/transient receptor potential vanilloid 4 (TRPV4)- and calmodulin-mediated mechanism. *Eur J Neurosci, 46*(9), 2542-2547. doi:10.1111/ejn.13723

Sasayama, D., Hattori, K., Wakabayashi, C., Teraishi, T., Hori, H., Ota, M., . . . Kunugi, H. (2013). Increased cerebrospinal fluid interleukin-6 levels in patients with schizophrenia and

those with major depressive disorder. *J Psychiatr Res, 47*(3), 401-406. doi:10.1016/j.jpsychires.2012.12.001

Satoh, K., Hata, M., Takahara, S., Tsuzaki, H., Yokota, H., Akatsu, H., . . . Yamada, T. (2006). A novel membrane protein, encoded by the gene covering KIAA0233, is transcriptionally induced in senile plaque-associated astrocytes. *Brain Res, 1108*(1), 19-27. doi:10.1016/j.brainres.2006.06.050

Saunders, A. M. (2001). Gene identification in Alzheimer's disease. *Pharmacogenomics, 2*(3), 239-249. doi:10.1517/14622416.2.3.239

Savchenko, V. L., McKanna, J. A., Nikonenko, I. R., & Skibo, G. G. (2000). Microglia and astrocytes in the adult rat brain: comparative immunocytochemical analysis demonstrates the efficacy of lipocortin 1 immunoreactivity. *Neuroscience, 96*(1), 195-203.

Schmued, L. C., Raymick, J., Paule, M. G., Dumas, M., & Sarkar, S. (2013). Characterization of myelin pathology in the hippocampal complex of a transgenic mouse model of Alzheimer's disease. *Curr Alzheimer Res, 10*(1), 30-37.

Schrader, J., Gordon-Walker, T. T., Aucott, R. L., van Deemter, M., Quaas, A., Walsh, S., . . . Iredale, J. P. (2011). Matrix stiffness modulates proliferation, chemotherapeutic response, and dormancy in hepatocellular carcinoma cells. *Hepatology, 53*(4), 1192-1205. doi:10.1002/hep.24108

Schulze-Osthoff, K., Ferrari, D., Riehemann, K., & Wesselborg, S. (1997). Regulation of NF-kappa B activation by MAP kinase cascades. *Immunobiology, 198*(1-3), 35-49.

Schulze-Topphoff, U., Varrin-Doyer, M., Pekarek, K., Spencer, C. M., Shetty, A., Sagan, S. A., . . . Zamvil, S. S. (2016). Dimethyl fumarate treatment induces adaptive and innate immune modulation independent of Nrf2. *Proc Natl Acad Sci U S A, 113*(17), 4777-4782. doi:10.1073/pnas.1603907113

Selkoe, D. J., & Schenk, D. (2003). Alzheimer's disease: molecular understanding predicts amyloid-based therapeutics. *Annu Rev Pharmacol Toxicol, 43*, 545-584. doi:10.1146/annurev.pharmtox.43.100901.140248

Seymour, G. J., Ford, P. J., Cullinan, M. P., Leishman, S., & Yamazaki, K. (2007). Relationship between periodontal infections and systemic disease. *Clin Microbiol Infect, 13 Suppl 4*, 3-10. doi:10.1111/j.1469-0691.2007.01798.x

Sheikh, A. M., Nagai, A., Ryu, J. K., McLarnon, J. G., Kim, S. U., & Masuda, J. (2009). Lysophosphatidylcholine induces glial cell activation: role of rho kinase. *Glia, 57*(8), 898-907. doi:10.1002/glia.20815

Sheridan, G. K., & Dev, K. K. (2012). S1P1 receptor subtype inhibits demyelination and regulates chemokine release in cerebellar slice cultures. *Glia, 60*(3), 382-392. doi:10.1002/glia.22272

Shi, J., Badri, K. R., Choudhury, R., & Schuger, L. (2006). P311-induced myofibroblasts exhibit ameboid-like migration through RalA activation. *Exp Cell Res, 312*(17), 3432-3442. doi:10.1016/j.yexcr.2006.07.016

Shimizu, T., Osanai, Y., Tanaka, K. F., Abe, M., Natsume, R., Sakimura, K., & Ikenaka, K. (2017). YAP functions as a mechanotransducer in oligodendrocyte morphogenesis and maturation. *Glia, 65*(2), 360-374. doi:10.1002/glia.23096

Shmukler, B. E., Huston, N. C., Thon, J. N., Ni, C. W., Kourkoulis, G., Lawson, N. D., . . . Alper, S. L. (2015). Homozygous knockout of the piezo1 gene in the zebrafish is not associated with anemia. In *Haematologica* (Vol. 100, pp. e483-485). Italy.

Siechen, S., Yang, S., Chiba, A., & Saif, T. (2009). Mechanical tension contributes to clustering of neurotransmitter vesicles at presynaptic terminals. *Proc Natl Acad Sci U S A, 106*(31), 12611-12616. doi:10.1073/pnas.0901867106

Simard, A. R., Soulet, D., Gowing, G., Julien, J. P., & Rivest, S. (2006). Bone marrow-derived microglia play a critical role in restricting senile plaque formation in Alzheimer's disease. *Neuron, 49*(4), 489-502. doi:10.1016/j.neuron.2006.01.022

Simons, M., & Nave, K. A. (2015). Oligodendrocytes: Myelination and Axonal Support. *Cold Spring Harb Perspect Biol, 8*(1), a020479. doi:10.1101/cshperspect.a020479

Smith, S. J. (1994). Neural signalling. Neuromodulatory astrocytes. *Curr Biol, 4*(9), 807-810.

Smits, H. A., Rijsmus, A., van Loon, J. H., Wat, J. W., Verhoef, J., Boven, L. A., & Nottet, H. S. (2002). Amyloid-beta-induced chemokine production in primary human macrophages and astrocytes. *J Neuroimmunol, 127*(1-2), 160-168.

Snaidero, N., Mobius, W., Czopka, T., Hekking, L. H., Mathisen, C., Verkleij, D., . . . Simons, M. (2014). Myelin membrane wrapping of CNS axons by PI(3,4,5)P3-dependent polarized growth at the inner tongue. *Cell, 156*(1-2), 277-290. doi:10.1016/j.cell.2013.11.044

Sofroniew, M. V. (2009). Molecular dissection of reactive astrogliosis and glial scar formation. *Trends Neurosci, 32*(12), 638-647. doi:10.1016/j.tins.2009.08.002

Sofroniew, M. V., & Vinters, H. V. (2010). Astrocytes: biology and pathology. *Acta Neuropathol, 119*(1), 7-35. doi:10.1007/s00401-009-0619-8

Sospedra, M., & Martin, R. (2005). Immunology of multiple sclerosis. *Annu Rev Immunol, 23*, 683-747. doi:10.1146/annurev.immunol.23.021704.115707

Srinivasan, K. R., Kay, R. L., & Nagle, J. F. (1974). The pressure dependence of the lipid bilayer phase transition. *Biochemistry, 13*(17), 3494-3496.

Sriram, K., & O'Callaghan, J. P. (2007). Divergent roles for tumor necrosis factor-alpha in the brain. *J Neuroimmune Pharmacol, 2*(2), 140-153. doi:10.1007/s11481-007-9070-6

Steelman, A. J. (2015). Infection as an Environmental Trigger of Multiple Sclerosis Disease Exacerbation. *Front Immunol, 6*, 520. doi:10.3389/fimmu.2015.00520

Stichel, C. C., & Muller, H. W. (1998). The CNS lesion scar: new vistas on an old regeneration barrier. *Cell Tissue Res, 294*(1), 1-9.

Storr, S. J., Carragher, N. O., Frame, M. C., Parr, T., & Martin, S. G. (2011). The calpain system and cancer. *Nat Rev Cancer, 11*(5), 364-374. doi:10.1038/nrc3050

Strassburger-Krogias, K., Ellrichmann, G., Krogias, C., Altmeyer, P., Chan, A., & Gold, R. (2014). Fumarate treatment in progressive forms of multiple sclerosis: first results of a single-center observational study. *Ther Adv Neurol Disord, 7*(5), 232-238. doi:10.1177/1756285614544466

Streit, W. J., Braak, H., Xue, Q. S., & Bechmann, I. (2009). Dystrophic (senescent) rather than activated microglial cells are associated with tau pathology and likely precede neurodegeneration in Alzheimer's disease. *Acta Neuropathol, 118*(4), 475-485. doi:10.1007/s00401-009-0556-6

Su, Y., Wang, Y., Zhou, Y., Zhu, Z., Zhang, Q., Zhang, X., . . . Guo, A. (2017). Macrophage migration inhibitory factor activates inflammatory responses of astrocytes through interaction with CD74 receptor. *Oncotarget, 8*(2), 2719-2730. doi:10.18632/oncotarget.13739

Su, Z., Yuan, Y., Chen, J., Cao, L., Zhu, Y., Gao, L., . . . He, C. (2009). Reactive astrocytes in glial scar attract olfactory ensheathing cells migration by secreted TNF-alpha in spinal cord lesion of rat. *PLoS One, 4*(12), e8141. doi:10.1371/journal.pone.0008141

Suchyna, T. M., Johnson, J. H., Hamer, K., Leykam, J. F., Gage, D. A., Clemo, H. F., . . . Sachs, F. (2000). Identification of a peptide toxin from Grammostola spatulata spider venom that blocks cation-selective stretch-activated

channels. *J Gen Physiol, 115*(5), 583-598.

Suchyna, T. M., Tape, S. E., Koeppe, R. E., 2nd, Andersen, O. S., Sachs, F., & Gottlieb, P. A. (2004). Bilayer-dependent inhibition of mechanosensitive channels by neuroactive peptide enantiomers. *Nature, 430*(6996), 235-240. doi:10.1038/nature02743

Sukharev, S., & Anishkin, A. (2004). Mechanosensitive channels: what can we learn from 'simple' model systems? *Trends Neurosci, 27*(6), 345-351. doi:10.1016/j.tins.2004.04.006

Suzuki, K. (2003). Globoid cell leukodystrophy (Krabbe's disease): update. *J Child Neurol, 18*(9), 595-603. doi:10.1177/08830738030180090201

Swardfager, W., Lanctot, K., Rothenburg, L., Wong, A., Cappell, J., & Herrmann, N. (2010). A meta-analysis of cytokines in Alzheimer's disease. *Biol Psychiatry, 68*(10), 930-941. doi:10.1016/j.biopsych.2010.06.012

Swift, J., Ivanovska, I. L., Buxboim, A., Harada, T., Dingal, P. C., Pinter, J., . . . Discher, D. E. (2013). Nuclear lamin-A scales with tissue stiffness and enhances matrix-directed differentiation. *Science, 341*(6149), 1240104. doi:10.1126/science.1240104

Sy, M., Kitazawa, M., Medeiros, R., Whitman, L., Cheng, D., Lane, T. E., & Laferla, F. M. (2011). Inflammation induced by infection potentiates tau pathological features in transgenic mice. *Am J Pathol, 178*(6), 2811-2822. doi:10.1016/j.ajpath.2011.02.012

Syeda, R., Florendo, M. N., Cox, C. D., Kefauver, J. M., Santos, J. S., Martinac, B., & Patapoutian, A. (2016). Piezo1 Channels Are Inherently Mechanosensitive. *Cell Rep, 17*(7), 1739-1746. doi:10.1016/j.celrep.2016.10.033

Syeda, R., Xu, J., Dubin, A. E., Coste, B., Mathur, J., Huynh, T., . . . Patapoutian, A. (2015). Chemical activation of the mechanotransduction channel Piezo1. *Elife, 4*. doi:10.7554/eLife.07369

Sypecka, J., & Domanska-Janik, K. (1995). Expression of myelin-specific proteins during development of normal and hypomyelinated Paralytic tremor mutant rabbits. I. Studies on the brain homogenates. *Mol Chem Neuropathol, 26*(1), 53-66. doi:10.1007/bf02814941

Takano, T., Han, X., Deane, R., Zlokovic, B., & Nedergaard, M. (2007). Two-photon imaging of astrocytic Ca2+ signaling and the microvasculature in experimental mice models of Alzheimer's disease. *Ann N Y Acad Sci, 1097*, 40-50. doi:10.1196/annals.1379.004

Takeda, T. (2009). Senescence-accelerated mouse (SAM) with special references to neurodegeneration models, SAMP8 and SAMP10 mice. *Neurochem Res, 34*(4), 639-659. doi:10.1007/s11064-009-9922-y

Taniike, M., & Suzuki, K. (1995). Proliferative capacity of oligodendrocytes in the demyelinating twitcher spinal cord. *J Neurosci Res, 40*(3), 325-332. doi:10.1002/jnr.490400306

Tarbell, J. M., Simon, S. I., & Curry, F. R. (2014). Mechanosensing at the vascular interface. *Annu Rev Biomed Eng, 16*, 505-532. doi:10.1146/annurev-bioeng-071813-104908

Tasaki, I., Kusano, K., & Byrne, P. M. (1989). Rapid mechanical and thermal changes in the garfish olfactory nerve associated with a propagated impulse. *Biophys J, 55*(6), 1033-1040. doi:10.1016/s0006-3495(89)82902-9

Taupin, D., & Podolsky, D. K. (2003). Trefoil factors: initiators of mucosal healing. *Nat Rev Mol Cell Biol, 4*(9), 721-732. doi:10.1038/nrm1203

Thomas, W. E. (1992). Brain macrophages: evaluation of microglia and their functions. *Brain Res Brain Res Rev, 17*(1), 61-74.

Thone, J., & Linker, R. A. (2016). Laquinimod in the treatment of multiple sclerosis: a review of the data so far. *Drug Des Devel Ther, 10*, 1111-1118. doi:10.2147/dddt.s55308

Tong, X., Ao, Y., Faas, G. C., Nwaobi, S. E., Xu, J., Haustein, M. D., . . . Khakh, B. S. (2014). Astrocyte Kir4.1 ion channel deficits contribute to neuronal dysfunction in Huntington's disease model mice. *Nat Neurosci, 17*(5), 694-703. doi:10.1038/nn.3691

Tsai, Y., Lu, B., Ljubimov, A. V., Girman, S., Ross-Cisneros, F. N., Sadun, A. A., . . . Wang, S. (2014). Ocular changes in TgF344-AD rat model of Alzheimer's disease. *Invest Ophthalmol Vis Sci, 55*(1), 523-534. doi:10.1167/iovs.13-12888

Tu, H., Wang, Z., Nosyreva, E., De Smedt, H., & Bezprozvanny, I. (2005). Functional characterization of mammalian inositol 1,4,5-trisphosphate receptor isoforms. *Biophys J, 88*(2), 1046-1055. doi:10.1529/biophysj.104.049593

Ungureanu, A. A., Benilova, I., Krylychkina, O., Braeken, D., De Strooper, B., Van Haesendonck, C., . . . Bartic, C. (2016). Amyloid beta oligomers induce neuronal elasticity changes in age-dependent manner: a force spectroscopy study on living hippocampal neurons. *Sci Rep, 6*, 25841. doi:10.1038/srep25841

Urbanski, M. M., Kingsbury, L., Moussouros, D., Kassim, I., Mehjabeen, S., Paknejad, N., & Melendez-Vasquez, C. V. (2016). Myelinating glia differentiation is regulated by extracellular matrix elasticity. *Sci Rep, 6*, 33751. doi:10.1038/srep33751

Van Wagoner, N. J., & Benveniste, E. N. (1999). Interleukin-6 expression and regulation in astrocytes. *J Neuroimmunol, 100*(1-2), 124-139.

Vardjan, N., Verkhratsky, A., & Zorec, R. (2017). Astrocytic Pathological Calcium Homeostasis and Impaired Vesicle Trafficking in Neurodegeneration. *Int J Mol Sci, 18*(2). doi:10.3390/ijms18020358

Venkatachalam, K., & Montell, C. (2007). TRP channels. *Annu Rev Biochem, 76*, 387-417. doi:10.1146/annurev.biochem.75.103004.142819

Verkhratsky, A., & Zorec, R. (2018). Astroglial signalling in health and disease. *Neurosci Lett*. doi:10.1016/j.neulet.2018.07.026

Vishal, S., Sourabh, A., & Harkirat, S. (2011). Alois Alzheimer (1864-1915) and the Alzheimer syndrome. *J Med Biogr, 19*(1), 32-33. doi:10.1258/jmb.2010.010037

Wagner, S., Tagaya, M., Koziol, J. A., Quaranta, V., & del Zoppo, G. J. (1997). Rapid disruption of an astrocyte interaction with the extracellular matrix mediated by integrin alpha 6 beta 4 during focal cerebral ischemia/reperfusion. *Stroke, 28*(4), 858-865.

Wang, L., Xia, J., Li, J., Hagemann, T. L., Jones, J. R., Fraenkel, E., . . . Feany, M. B. (2018). Tissue and cellular rigidity and mechanosensitive signaling activation in Alexander disease. *Nat Commun, 9*(1), 1899. doi:10.1038/s41467-018-04269-7

Wang, S., Chennupati, R., Kaur, H., Iring, A., Wettschureck, N., & Offermanns, S. (2016). Endothelial cation channel PIEZO1 controls blood pressure by mediating flow-induced ATP release. *J Clin Invest, 126*(12), 4527-4536. doi:10.1172/jci87343

Wang, X., Liu, X., Chen, Y., Lin, G., Mei, W., Chen, J., . . . Zhang, S. (2015). Histopathological findings in the peritumoral edema area of human glioma. *Histol Histopathol, 30*(9), 1101-1109. doi:10.14670/hh-11-607

Wang, Y., Chi, S., Guo, H., Li, G., Wang, L., Zhao, Q., . . . Xiao, B. (2018). A lever-like transduction pathway for long-distance chemical- and mechano-gating of the mechanosensitive Piezo1 channel. *Nat Commun, 9*(1), 1300. doi:10.1038/s41467-018-03570-9

Warrington, A. E., Bieber, A. J., Ciric, B., Pease, L. R., Van Keulen, V., & Rodriguez, M. (2007). A recombinant human IgM promotes myelin repair after a single, very low dose. *J Neurosci Res, 85*(5), 967-976. doi:10.1002/jnr.21217

Webb, A., Clark, P., Skepper, J., Compston, A., & Wood, A. (1995). Guidance of

oligodendrocytes and their progenitors by substratum topography. *J Cell Sci, 108 (Pt 8)*, 2747-2760.

Weickenmeier, J., de Rooij, R., Budday, S., Steinmann, P., Ovaert, T. C., & Kuhl, E. (2016). Brain stiffness increases with myelin content. *Acta Biomater, 42*, 265-272. doi:10.1016/j.actbio.2016.07.040

Wen, J., Doerner, J., Weidenheim, K., Xia, Y., Stock, A., Michaelson, J. S., . . . Putterman, C. (2015). TNF-like weak inducer of apoptosis promotes blood brain barrier disruption and increases neuronal cell death in MRL/lpr mice. *J Autoimmun, 60*, 40-50. doi:10.1016/j.jaut.2015.03.005

Wiggins, P., & Phillips, R. (2004). Analytic models for mechanotransduction: gating a mechanosensitive channel. *Proc Natl Acad Sci U S A, 101*(12), 4071-4076. doi:10.1073/pnas.0307804101

Windle, W. F., Clemente, C. D., & Chambers, W. W. (1952). Inhibition of formation of a glial barrier as a means of permitting a peripheral nerve to grow into the brain. *J Comp Neurol, 96*(2), 359-369.

Wojda, U., Salinska, E., & Kuznicki, J. (2008). Calcium ions in neuronal degeneration. *IUBMB Life, 60*(9), 575-590. doi:10.1002/iub.91

Wujek, J. R., Dority, M. D., Frederickson, R. C., & Brunden, K. R. (1996). Deposits of A beta fibrils are not toxic to cortical and hippocampal neurons in vitro. *Neurobiol Aging, 17*(1), 107-113.

Wyss-Coray, T., Loike, J. D., Brionne, T. C., Lu, E., Anankov, R., Yan, F., . . . Husemann, J. (2003). Adult mouse astrocytes degrade amyloid-beta in vitro and in situ. *Nat Med, 9*(4), 453-457. doi:10.1038/nm838

Xu, L., Lin, Y., Han, J. C., Xi, Z. N., Shen, H., & Gao, P. Y. (2007). Magnetic resonance elastography of brain tumors: preliminary results. *Acta Radiol, 48*(3), 327-330. doi:10.1080/02841850701199967

Xu, X. Z. (2016). Demystifying Mechanosensitive Piezo Ion Channels. *Neurosci Bull, 32*(3), 307-309. doi:10.1007/s12264-016-0033-x

Xuan, A. G., Pan, X. B., Wei, P., Ji, W. D., Zhang, W. J., Liu, J. H., . . . Long, D. H. (2015). Valproic acid alleviates memory deficits and attenuates amyloid-beta deposition in transgenic mouse model of Alzheimer's disease. *Mol Neurobiol, 51*(1), 300-312. doi:10.1007/s12035-014-8751-4

Yang, M., & Teplow, D. B. (2008). Amyloid beta-protein monomer folding: free-energy surfaces reveal alloform-specific differences. *J Mol Biol, 384*(2), 450-464. doi:10.1016/j.jmb.2008.09.039

Yang, X. N., Lu, Y. P., Liu, J. J., Huang, J. K., Liu, Y. P., Xiao, C. X., . . . Guleng, B. (2014). Piezo1 is as a novel trefoil factor family 1 binding protein that promotes gastric cancer cell mobility in vitro. *Dig Dis Sci, 59*(7), 1428-1435. doi:10.1007/s10620-014-3044-3

Yednock, T. A., Cannon, C., Fritz, L. C., Sanchez-Madrid, F., Steinman, L., & Karin, N. (1992). Prevention of experimental autoimmune encephalomyelitis by antibodies against alpha 4 beta 1 integrin. *Nature, 356*(6364), 63-66. doi:10.1038/356063a0

Yuan, Y. M., & He, C. (2013). The glial scar in spinal cord injury and repair. *Neurosci Bull, 29*(4), 421-435. doi:10.1007/s12264-013-1358-3

Zanini, D., & Gopfert, M. C. (2014). TRPs in hearing. *Handb Exp Pharmacol, 223*, 899-916. doi:10.1007/978-3-319-05161-1_7

Zarychanski, R., Schulz, V. P., Houston, B. L., Maksimova, Y., Houston, D. S., Smith, B., . . . Gallagher, P. G. (2012). Mutations in the mechanotransduction protein PIEZO1 are associated with hereditary xerocytosis. *Blood, 120*(9), 1908-1915. doi:10.1182/blood-2012-04-422253

Zhan, J. S., Gao, K., Chai, R. C., Jia, X. H., Luo, D. P., Ge, G., . . . Yu, A. C. (2017). Astrocytes in Migration. *Neurochem*

Res, 42(1), 272-282. doi:10.1007/s11064-016-2089-4

Zhan, X., Jickling, G. C., Ander, B. P., Liu, D., Stamova, B., Cox, C., . . . Sharp, F. R. (2014). Myelin injury and degraded myelin vesicles in Alzheimer's disease. *Curr Alzheimer Res, 11*(3), 232-238.

Zhan, X., Jickling, G. C., Ander, B. P., Stamova, B., Liu, D., Kao, P. F., . . . Sharp, F. R. (2015). Myelin basic protein associates with AbetaPP, Abeta1-42, and amyloid plaques in cortex of Alzheimer's disease brain. *J Alzheimers Dis, 44*(4), 1213-1229. doi:10.3233/jad-142013

Zhang, Q. S., Heng, Y., Yuan, Y. H., & Chen, N. H. (2017). Pathological alpha-synuclein exacerbates the progression of Parkinson's disease through microglial activation. *Toxicol Lett, 265*, 30-37. doi:10.1016/j.toxlet.2016.11.002

Zhang, T., Chi, S., Jiang, F., Zhao, Q., & Xiao, B. (2017). A protein interaction mechanism for suppressing the mechanosensitive Piezo channels. *Nat Commun, 8*(1), 1797. doi:10.1038/s41467-017-01712-z

Zhang, Y., Zhu, T., Zhang, X., Chao, J., Hu, G., & Yao, H. (2015). Role of high-mobility group box 1 in methamphetamine-induced activation and migration of astrocytes. *J Neuroinflammation, 12*, 156. doi:10.1186/s12974-015-0374-9

Zhao, Q., Wu, K., Geng, J., Chi, S., Wang, Y., Zhi, P., . . . Xiao, B. (2016). Ion Permeation and Mechanotransduction Mechanisms of Mechanosensitive Piezo Channels. *Neuron, 89*(6), 1248-1263. doi:10.1016/j.neuron.2016.01.046

Zhao, Q., Zhou, H., Chi, S., Wang, Y., Wang, J., Geng, J., . . . Xiao, B. (2018). Structure and mechanogating mechanism of the Piezo1 channel. *Nature, 554*(7693), 487-492. doi:10.1038/nature25743

Zhao, Y., & Rempe, D. A. (2010). Targeting astrocytes for stroke therapy. *Neurotherapeutics, 7*(4), 439-451. doi:10.1016/j.nurt.2010.07.004

Zhou, M., Xu, G., Xie, M., Zhang, X., Schools, G. P., Ma, L., . . . Chen, H. (2009). TWIK-1 and TREK-1 are potassium channels contributing significantly to astrocyte passive conductance in rat hippocampal slices. *J Neurosci, 29*(26), 8551-8564. doi:10.1523/jneurosci.5784-08.2009

Zimmermann, D. R., & Dours-Zimmermann, M. T. (2008). Extracellular matrix of the central nervous system: from neglect to challenge. *Histochem Cell Biol, 130*(4), 635-653. doi:10.1007/s00418-008-0485-9